frontiers | Research Topics

Involvement of dendritic cells in gastrointestinal cancer

Edited by
Ling Ni, Haidong Tang, Mi Deng, Musheng Bao and Jingtao Chen

Published in
Frontiers in Immunology

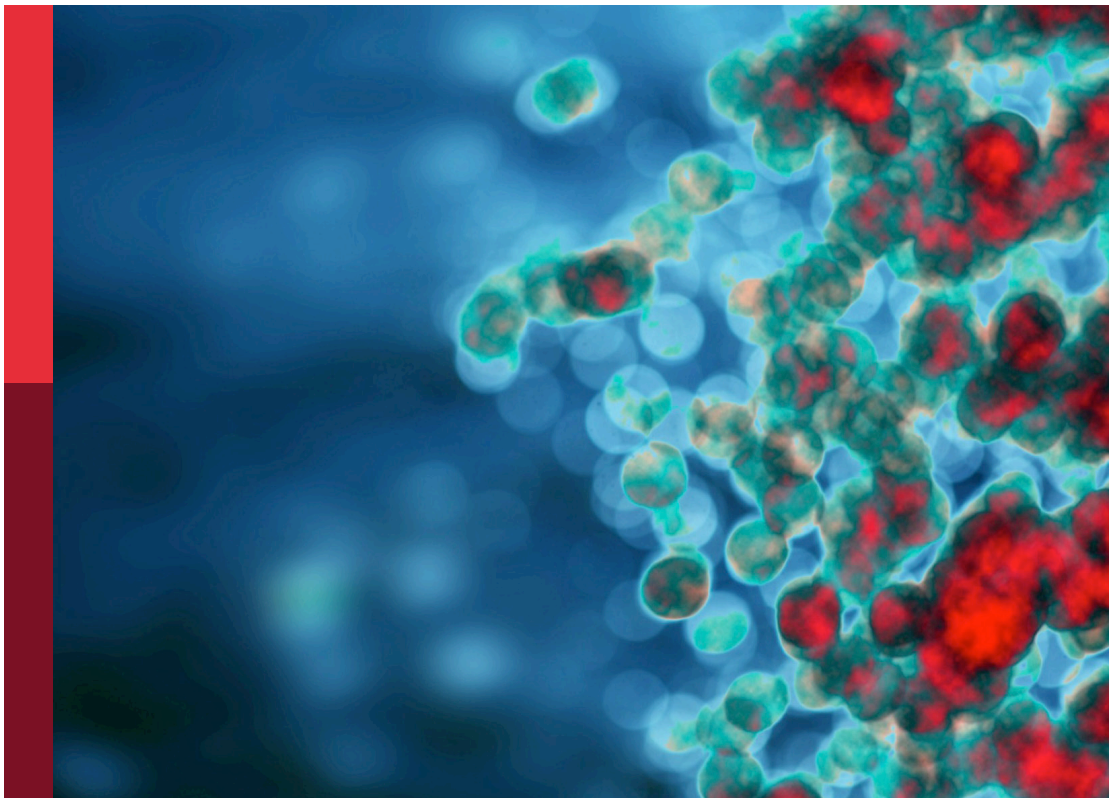

ISSN 1664-8714
ISBN 978-2-83252-069-7
DOI 10.3389/978-2-83252-069-7

About Frontiers

Frontiers is more than just an open access publisher of scholarly articles: it is a pioneering approach to the world of academia, radically improving the way scholarly research is managed. The grand vision of Frontiers is a world where all people have an equal opportunity to seek, share and generate knowledge. Frontiers provides immediate and permanent online open access to all its publications, but this alone is not enough to realize our grand goals.

Frontiers journal series

The Frontiers journal series is a multi-tier and interdisciplinary set of open-access, online journals, promising a paradigm shift from the current review, selection and dissemination processes in academic publishing. All Frontiers journals are driven by researchers for researchers; therefore, they constitute a service to the scholarly community. At the same time, the *Frontiers journal series* operates on a revolutionary invention, the tiered publishing system, initially addressing specific communities of scholars, and gradually climbing up to broader public understanding, thus serving the interests of the lay society, too.

Dedication to quality

Each Frontiers article is a landmark of the highest quality, thanks to genuinely collaborative interactions between authors and review editors, who include some of the world's best academicians. Research must be certified by peers before entering a stream of knowledge that may eventually reach the public - and shape society; therefore, Frontiers only applies the most rigorous and unbiased reviews. Frontiers revolutionizes research publishing by freely delivering the most outstanding research, evaluated with no bias from both the academic and social point of view. By applying the most advanced information technologies, Frontiers is catapulting scholarly publishing into a new generation.

What are Frontiers Research Topics?

Frontiers Research Topics are very popular trademarks of the *Frontiers journals series*: they are collections of at least ten articles, all centered on a particular subject. With their unique mix of varied contributions from Original Research to Review Articles, Frontiers Research Topics unify the most influential researchers, the latest key findings and historical advances in a hot research area.

Find out more on how to host your own Frontiers Research Topic or contribute to one as an author by contacting the Frontiers editorial office: frontiersin.org/about/contact

Involvement of dendritic cells in gastrointestinal cancer

Topic editors
Ling Ni — Tsinghua University, China
Haidong Tang — Tsinghua University, China
Mi Deng — Peking University, China
Musheng Bao — Harbour Antibodies US/Harbour BioMed, United States
Jingtao Chen — The First Hospital of Jilin University, China

Citation
Ni, L., Tang, H., Deng, M., Bao, M., Chen, J., eds. (2023). *Involvement of dendritic cells in gastrointestinal cancer*. Lausanne: Frontiers Media SA.
doi: 10.3389/978-2-83252-069-7

MB is an employee of Nona Biosciences.
The remaining authors declare that the research was conducted in the absence of any commercial or financial relationships that could be construed as a potential conflict of interest

Table of contents

frontiers | Frontiers in Immunology

TYPE Editorial
PUBLISHED 17 March 2023
DOI 10.3389/fimmu.2023.1178075

OPEN ACCESS

EDITED AND REVIEWED BY
Diane Bimczok,
Montana State University, United States

*CORRESPONDENCE
Ling Ni
lingni@tsinghua.edu.cn

†These authors have contributed equally to this work

SPECIALTY SECTION
This article was submitted to Cancer Immunity and Immunotherapy, a section of the journal Frontiers in Immunology

RECEIVED 02 March 2023
ACCEPTED 13 March 2023
PUBLISHED 17 March 2023

CITATION
Ni L, Chen J, Deng M, Tang H and Bao M (2023) Editorial: Involvement of dendritic cells in gastrointestinal cancer. *Front. Immunol.* 14:1178075. doi: 10.3389/fimmu.2023.1178075

Editorial: Involvement of dendritic cells in gastrointestinal cancer

Ling Ni[1*†], Jingtao Chen[2†], Mi Deng[3†], Haidong Tang[4†] and Musheng Bao[5†]

[1]Institute for Immunology and School of Medicine, Tsinghua University, Medical Research Building, Beijing, China, [2]Laboratory for Tumor Immunology, the First Hospital of Jilin University, Changchun, China, [3]Peking University International Cancer Institute, Peking University, Beijing, China, [4]School of Pharmaceutical Sciences, Tsinghua University, Beijing, China, [5]Biology Group, Nona Biosciences, Natick, MA, United States

KEYWORDS

dendritic cells, gastrointestinal cancer, DC differentiation, cancer immunotherapy, targeting DCs

Editorial on the Research Topic
Involvement of dendritic cells in gastrointestinal cancer

Immunotherapy has revolutionized cancer treatment over the past decade with remarkable results in terms of durable remission and extended survival in some patients. However, the response rate to current immunotherapy in patients with gastrointestinal (GI) cancer remains relatively low. For successful anti-cancer immune responses, the cancer-immunity cycle needs to be initiated to activate neoantigen-specific T cells and eliminate tumor cells. Dendritic cells (DCs) play a crucial role by processing neoantigens and presenting them to T cells. Therefore, targeting DCs has a significant potential for cancer immunotherapy. The current collection, "*Involvement of Dendritic Cells in Gastrointestinal Cancer*," covers recent studies on the involvement of DCs in GI cancer, including topics such as the differentiation of thymic DCs, immunological tolerance induced by DCs in tumors, the role of DCs in GI cancer, DC-based cancer immunotherapy, and strategies for targeting DCs in immunotherapy.

Tumor progression blocks the transition of double negative (DN) early T-cell progenitors in T cell maturation, instead leading to DN-T-cell differentiation into DCs (Guha et al.). Mechanistically, thymically-expressed IL-10 promotes the interaction between thymic stromal cells and Notch1(low) DN2-T cells, thus facilitating these DN2-T cells to differentiate toward thymic DCs, which thus limits the protective adaptive immune repertoire. The development of plasmacytoid DCs and their roles in a variety of malignancies, including GI cancers, have been summarized by Zhou et al.

Inhibitory immune checkpoint molecules on DCs have been shown to be involved in diminishing the efficacy of DC-mediated anti-tumor immune responses. Ghorbaninezhad et al. showed that silencing CTLA-4 using siRNA induces DC maturation, which leads to increased T cell proliferation and cytokine production. On the other hand, cancer-associated fibroblasts (CAFs) actively participate in tumor development and affect treatment responses. Berzaghi et al. showed that CAFs induce a tolerogenic phenotype in DCs, promoting the downregulation of the DC signature, activation markers, and

functions. Furthermore, certain radiation regimens can reverse the CAF-mediated immunosuppressive effects.

Subtil et al. established an organotypic 3-dimentions co-culture system to recapitulate and untangle interactions between DCs and patient-derived CRC organoids. They demonstrated high viability and extensive interactions between DCs and tumor organoids, which control the expression of activation markers on DCs and their ability to activate T-cells. In another study, by analyzing the data from a colon adenocarcinoma (COAD) cohort receiving immunotherapy, Zhou et al. found that the IL-1 signaling mutated-type group has higher infiltration levels of activated DCs, M1 macrophages, neutrophils, activated natural killer cells, activated $CD4^+$ memory T cells, and $CD8^+$ T cells than IL-1 signaling wild-type groups. These findings suggest that IL-1 mutation may be an independent biomarker for prognosis in patients with COAD receiving immunotherapy.

Advances in DC-based immunotherapy and clinical trials that indicate therapeutic efficacy and toxicity related to each vaccine have been reviewed by Ni et al. At the single-cell level, Wang et al. summarized the classification and development trajectory of DCs in GI cancer with a focus on the interaction of DCs with T cells and their effects on immunotherapy response. Newly identified tumor-infiltrating DCs and their potential functions in anti-tumor immunity have also been summarized. In order to offer more detailed evidence and novel opinions to enhance the development of a personalized neoantigen-based DC vaccines for pancreatic cancers (PCs), Zhang et al. summarized the advance of the neoantigen, neoantigen-based vaccines, and DC-based vaccine with the emphasis of the combination of the neoantigen and DC-based vaccine.

Rb9 is a cyclic VHCDR3-derived peptide from the RebMab200 antibody targeting a NaPi2B phosphate-transport protein. Rb9 showed anti-tumor activity in syngeneic mice, which was mainly due to increased $CD8^+$ T infiltration and decreased intratumoral $Foxp3^+$ T cells (Machado et al.). Human DCs showed increased expression of activation markers after exposure to Rb9.

Taken together, studies on DCs in GI cancer have achieved encouraging results. Nonetheless, a better understanding of the phenotypes and functions of DCs is required before we can properly target DCs and improve the overall response rate in GI cancer immunotherapy.

Author contributions

All authors listed have made a substantial, direct, and intellectual contribution to the work and approved it for publication.

Conflict of interest

MB is an employee of Nona Biosciences.

The remaining authors declare that the research was conducted in the absence of any commercial or financial relationships that could be construed as a potential conflict of interest.

Publisher's note

frontiers in Immunology

ORIGINAL RESEARCH
published: 15 January 2020
doi: 10.3389/fimmu.2019.03122

Immunomodulatory Protective Effects of Rb9 Cyclic-Peptide in a Metastatic Melanoma Setting and the Involvement of Dendritic Cells

Fabrício C. Machado[1,2†], *Natália Girola*[1,2†], *Vera S. C. Maia*[1,2†], *Patrícia C. Bergami-Santos*[1,3†], *Alice S. Morais*[1], *Ricardo A. Azevedo*[2], *Carlos R. Figueiredo*[2,4], *José A. M. Barbuto*[1,3] *and Luiz R. Travassos*[1,2*]

[1] Recepta Bio, São Paulo, Brazil, [2] Experimental Oncology Unit, Department of Microbiology, Immunology and Parasitology, Federal University of São Paulo, São Paulo, Brazil, [3] Tumor Immunology Laboratory, Department of Immunology, Biomedical Sciences Institute, University of São Paulo, São Paulo, Brazil, [4] MediCity, University of Turku, Turku, Finland

OPEN ACCESS

Edited by:
Fang-Ping Huang, Shenzhen University, China

Reviewed by:
Fermín E. González, University of Chile, Chile
Flavio Andres Salazar Onfray, University of Chile, Chile

***Correspondence:**
Luiz R. Travassos
luiztravassos@gmail.com

[†]*These authors have contributed equally to this work*

Specialty section:
This article was submitted to Cancer Immunity and Immunotherapy, a section of the journal Frontiers in Immunology

Received: *30 July 2019*
Accepted: *23 December 2019*
Published: *15 January 2020*

Citation:
Machado FC, Girola N, Maia VSC, Bergami-Santos PC, Morais AS, Azevedo RA, Figueiredo CR, Barbuto JAM and Travassos LR (2020) Immunomodulatory Protective Effects of Rb9 Cyclic-Peptide in a Metastatic Melanoma Setting and the Involvement of Dendritic Cells. Front. Immunol. 10:3122. doi: 10.3389/fimmu.2019.03122

The cyclic VHCDR3-derived peptide (Rb9) from RebMab200 antibody, directed to a NaPi2B phosphate-transport protein, displayed anti-metastatic melanoma activity at 50–300 μg intraperitoneally injected in syngeneic mice. Immune deficient mice failed to respond to the peptide protective effect. Rb9 induced increased CD8+ T and low Foxp3+ T cell infiltration in lung metastases and high IFN-γ and low TGF-β in lymphoid organs. The peptide co-localized with F-actin and a nuclear site in dendritic cells and specifically bound to MIF and CD74 in a dot-blot setting. Murine bone-marrow dendritic cells preincubated with Rb9 for 6 h were treated with MIF for short time periods. The modulated responses showed stimulation of CD74 and inhibition of pPI3K, pERK, and pNF-κB as compared to MIF alone. Rb9 in a melanoma-conditioned medium, stimulated the M1 type conversion in bone marrow-macrophages. Functional aspects of Rb9 *in vivo* were studied in therapeutic and prophylactic protocols using a melanoma metastatic model. In both protocols Rb9 exhibited a marked anti-melanoma protection. Human dendritic cells were also investigated showing increased expression of surface markers in response to Rb9 incubation. Rb9 either stimulated or slightly inhibited moDCs submitted to inhibitory (TGF-β and IL-10) or activating (LPS) conditions, respectively. Lymphocyte proliferation was obtained with moDCs stimulated by Rb9 and tumor cell lysate. In moDCs from cancer patients Rb9 exerted immunomodulatory activities depending on their functional status. The peptide may inhibit over-stimulated cells, stimulate poorly activated and suppressed cells, or cause instead, little phenotypic and functional alterations. Recently, the interaction MIF-CD74 has been associated to PD-L1 expression and IFN-γ, suggesting a target for melanoma treatment. The effects described for Rb9 and the protection against metastatic melanoma may suggest the possibility of a peptide reagent that could be relevant when associated to modern immunotherapeutic procedures.

Keywords: metastatic melanoma, cyclic-peptide, cytokines, MIF-CD74, dendritic cells, macrophage differentiation, lymphocyte proliferation

INTRODUCTION

Cancer is a leading cause of human death with high incidence in low, middle and high-income countries (1, 2). Malignant neoplasms derive from normal tissue with abnormal and excessive cellular growth, caused by genetic mutations and epigenetic modifications, leading to tumor masses formation. The progressive accumulation of cellular changes may give to the transformed cells the ability to invade adjacent tissues and spread to distant sites through the lymphatic and blood circulatory systems, forming metastases. Immune suppression can be induced at this stage and the untreated or treatment resistant cancers can be fatal (3, 4).

Monoclonal antibodies (mAbs) immunotherapy and chemotherapeutic agents may target tumor antigens and be effective because of their specificity and efficacy with acceptable side effects (5–7). The ability to modulate immune responses has become an important strategy in antibody cancer therapies (8–10). Recently, mAbs targeting immune checkpoints have been used to treat various solid tumors and lymphomas, but the low response rate and adverse events indicate the need for predictive biomarkers to improve the applicability of anti-PD-1/PD-L1 and anti-CTLA-4 agents (11).

Apart from mAbs specifically targeting tumor antigens, receptors and co-signaling molecules of the immune system, bioactive peptides from a number of sources have been studied with various specificities and affinities for microorganisms and eukaryotic cells (12, 13). For more than a decade, peptides derived from immunoglobulin (Ig) internal sequences have been shown to display differential anti-infective and anti-tumor activities *in vitro* and *in vivo* (14, 15). Different peptides can also be immunomodulatory by activating signaling pathways, stimulate, or regulate the expression of maturation markers on dendritic cells, stimulate antigen presentation, cytokine production, and lymphocyte interaction, phenotypes that will define the ultimate immune response (16, 17). High rates of resistance and relapse in anticancer treatment stimulate the search for additional agents, able to modulate dendritic cells and effector or regulatory T lymphocytes, memory T and B lymphocytes, which could improve the anti-infective or anti-tumor effectiveness of the immune response (18, 19).

In addition to the beneficial effects of delaying or arresting growth of certain types of neoplasms, current anticancer drugs may otherwise cause impairment of antibody synthesis, auto-immunity, and several side effects that altogether stimulate the research for new agents able to control the growth of neoplastic cells (20, 21). The present work focus on the anti-tumor effect of an immunologically bioactive synthetic peptide, Rb9, derived from the complementarity determining region-3 (CDR3) of V_H from a humanized monoclonal antibody (RebmAb 200) to NaPi2b transporter (22). The anti-tumor protective effects of Rb9 against metastatic melanoma, which depends on a healthy immune response and immune-modulatory activation of murine or human dendritic cells, and the possible molecular mechanism of this response were further investigated in the present work as an important step to the development of new anticancer drugs.

MATERIALS AND METHODS

Mice

Six- to eight-week-old male C57Bl/6, Balb/c, or NOD/Scid/IL-2R-γ^{null} mice were acquired from the Center for Development of Experimental Models (CEDEME) at Federal University of São Paulo (UNIFESP), Brazil. Mice were housed in ventilated racks in specific pathogen free conditions (SPF) for at least 1 week with *ad libitum* access to water and food in a light:dark cycle of 12 h each, before experimentation.

Ethics Statement

Animal experiments were carried out in accordance with the recommendations of the National Council for the Control of Animal Experimentation (CONCEA, Brazil) and approved by the Ethics Committee of Federal University of São Paulo, registered with the number CEUA 3521121217. All methods were performed in accordance with relevant guidelines and regulations approved by UNIFESP. Standard clinical symptoms that indicate deteriorating health conditions requiring euthanasia before the end of the experiment were followed.

The study with human donor and patient cells was carried out in accordance with the recommendations of Research Ethical Committee (CEP, Brazil) from the Faculty of Medicine, São Paulo University (FMUSP, Brazil). The protocol was approved ref. number 457.616 on Nov 13, 2013.

Peptides

Peptide Rb9 sequence is derived from V_H CDR3 of a humanized monoclonal antibody (RebmAb 200), which reacts with an epitope in the sodium-phosphate transporter NaPi2b (23–26). Synthetic Rb9, however, displays bio-reactivity independent of mAb specificity (22). The synthesis of Rb9 and other peptides was carried out by Peptide 2.0 (Chantilly, VA). Modifications included amidation at the C terminus (NH_2) and cyclization (C-C, disulfide bridge). A solution of Rb9 lyophilized material was prepared diluting the peptide in milli-Q water at 10–15 mM and further dilution for use, in RPMI 1640 medium or PBS. Linear sequences are shown below:

Peptide	Sequence	Modification
Rb9	CARGETARATFAYWGQGC	C-term NH_2, (C-C)
Scr-Rb9	TFAYWRAACACGQGRTEG	C-term NH_2
Rb10A1	AARGETARATFAYWGQG	C-term NH_2

Both scrambled (Scr-Rb9) and Rb10A1 peptides were derived from the linear form Rb10, analogous to RB9, without C-terminal QGC residues. Rb10A1 is a negative control for *in vitro* experiments replacing Cys in the N-terminal by Ala.

Tumor Cell Lines and Cell Cultures

B16F10-Nex2 subline of murine melanoma B16F10 (27), isolated and maintained at the Experimental Oncology Unit (UNONEX) of Federal University of São Paulo (UNIFESP) was deposited in the "Banco de Células do Rio de Janeiro" (BCRJ), no. 0342. The original B16F10 cell line was obtained

from the Ludwig Institute for Cancer Research (LICR), São Paulo Branch. Additional syngeneic tumor cells were kindly donated by Dr. G. Mazzolini from Gene therapy Laboratory, School of Medicine, Austral University; Buenos Aires, Argentina. The murine pancreatic carcinoma Panc02 cells, syngeneic in H-2^b C57Bl/6 and the colon-rectal carcinoma CT26 cells syngeneic in H-2^d Balb/c mice were tested *in vivo* via subcutaneous (s.c.) grafting (**Supplementary Figure 1**). Tumor cell lines and primary isolated cells were cultivated at 37°C, under humid atmosphere and 5% CO_2, in R10, which consisted in RPMI-1640 medium supplemented with 10 mM *N*-2-hydroxyethylpiperazine-*N*-2 ethane sulfonic acid (HEPES), 24 mM sodium bicarbonate, 40 mg/L gentamicin, 100 mg/L streptomycin, pH 7.2 and 10% fetal bovine serum (FBS). For some experiments, D10 medium was used (DMEM supplemented with 10% of FBS, 100 mM sodium pyruvate, 1x MEM-nonessential amino acids, 200 mM glutamine, 1x MEM vitamin solution, 0.05 M β-mercaptoethanol, 10,000 U penicillin and 10 mg/mL streptomycin). The protocol to obtain fresh isolated tissue cells is detailed below.

B16F10 melanoma cells were cultured in R10 until 70% confluence when the medium was harvested and fresh medium was added (v/v) to obtain a B16-conditioned medium (B16.CM). After three subculturings in the conditioned medium, B16.CM was collected, filtered, and used in functional assays.

Induced Melanoma Metastatic Model

In the lung metastatic-melanoma colonization model, 2–4 x 10^5 viable B16F10-Nex2 cells resuspended in 100 μL of serum-free RPMI medium, were intravenously (i.v.) injected in C57BL/6 or NOD/SCID/IL-2Rγ^{null} mice. Each inoculated mouse received 50–300 μg Rb9, Rb10A1 (a negative *in vitro* control), or Scr-Rb9 (a scrambled control version of Rb9) peptide diluted in 100 μL PBS via intraperitoneal (i.p.) administration or subcutaneous, in the interscapular area (s.c.). The peptide treatment occurred for 5–6 alternate days, starting 1 or 2 days after tumor cells injection. The control group (Veh) received a mock inoculation of PBS with the same volume. Anti-PD-1 (BioCell, InVivoPlus, clone J43) was used to treat mice at 6.25 mg/kg in 5 alternate days. Fifteen to twenty-two days later, mice were euthanized and their lungs were harvested. Macroscopic melanotic nodules were counted and images from the entire lung were captured with a stereomicroscope Nikon SMZ745T (magnification, 4x) coupled with Nikon Digital Sight DS-Fi2 and DS-U3 (Nikon Corporation, JA). The images were also used to measure the lung area with melanotic nodules. This quantification was obtained and measured by outlining the surface area covered by the black metastatic nodules in relation to the total organ area using Fiji/Image J version 1.52e software.

Pancreatic and Colorectal Subcutaneous Solid Tumor Model

In the subcutaneous tumor model, 5×10^5 syngeneic tumor cells resuspended in 100 μL of PBS were injected s.c. in the right flank of mice. C57Bl/6 mice were inoculated with Panc02 cells and Balb/c mice were inoculated with CT26 cells. Anti-tumor treatments with Rb9 or controls were performed as described before. Tumor longitudinal diameter (D) and transverse diameter (d) were measured by caliper rule every 2 days until the tumor volume reached 3,000 mm^3. Animals were euthanized when the allowed volume was reached. The tumor volume was calculated by the formula $V = D.d.2 \times 0.52$.

Lung Tissue Digestion and Flow Cytometry Analysis

Lungs with metastatic nodules were excised from metastatic B16F10-Nex2 melanoma-bearing mice and pooled for tissue digestion, using 40 U/mL DNAse (Sigma Aldrich), 125 U/mL Collagenase type IV (Sigma Aldrich), 100 U/mL Hyaluronidase (Sigma Aldrich), and 0.025 mg/mL Liberase™ (Sigma Aldrich) in PBS supplemented with 0.5% BSA. Pooled lung samples from each group were shaken for 2 h at 37°C and the digestion was interrupted by adding 1 mM EDTA. The liquid from digested samples was fully homogenized by softly pipetting and was then filtered through a 40-μM cell strainer (BD Falcon). Digested samples were kept at 4°C during centrifugation at 1,000 *g* for 5 min and incubated for 5 min in ACK buffer (NH_4Cl 150 mM, $KHCO_3$ 1 mM, and Na_2-EDTA 0.1 mM) for red cell lysis before another centrifugation for washing. Viable tissue cells from digested lung were counted in a Neubauer chamber using Trypan blue (Gibco™) and 1×10^6 cells were collected to analyze the following cell markers by flow cytometry.

The following antibodies were used in two combinations to analyze the collected tissue cells: 1 anti-CD3 (MACS, Miltenyi Biotec), anti-CD4 (MACS, Miltenyi Biotec), anti-CD8 (MACS, Miltenyi Biotec) and 2) anti-CD4 (MACS, Miltenyi Biotec), anti-CD25 (MACS, Miltenyi Biotec), anti-NKG2D (Invitrogen), and anti-Foxp3 (MACS, Miltenyi Biotec). In general, cells were stained in PBS, 0.5% BSA with 1 mM EDTA for 30 min using the appropriate antibody-fluorophore conjugate. Cells were washed in cold PBS with BSA and suspended in fixation buffer (PBS, BSA with 2% paraformaldehyde) before flow cytometry. For Foxp3 staining, cells were fixed and permeabilized using solutions from the MACS, Miltenyi Biotec kit before staining. Compensated multiparameter analysis was performed on a BD FACSCanto II analyzer (BD Biosciences, USA) with FlowJo X software (Tree Star Inc., USA).

ELISA for Cytokine Secretion

Mice challenged with B16F10-Nex2 tumor cells, received 300 μg i.p. of Rb9 or Rb10A1 and were euthanized after 17 days and their spleen and lymph nodes were collected, macerated, filtered through a cell strainer and washed 1x in PBS 1x. Splenocytes obtained after incubation in ACK hemolysis buffer were plated at 10^6 cells per well in 6-well plates with R10 medium. On the same day, splenocytes were further incubated for 72 h with or without tumor cell lysate obtained from freezing and thawing B16F10-Nex2 cells, adding the equivalent of 10^5 cells/well in triplicate. Lymph node cells were sorted for CD11c+ before incubation for 24 h with or without tumor cell lysate and supernatant collection. After incubation period, the supernatants were collected from both tissue cell culture and used to cytokine quantification by ELISA, following the manufacturer recommendations (BD Biosciences, USA). Briefly,

a 96-well opaque plate (Nunc, Roskilde, Denmark) was coated overnight at 4°C with IL-6, IL-10, IL-12, IFN-γ, TNF, and TGF-β capture antibody, following the manufacturer recommendations of respective kits. The plates were blocked for 2 h at room temperature and washed with 0.05% Tween 20-PBS (T-PBS) before incubation for 2 h with previously collected supernatants and respective recombinant proteins. After incubation, the plate was washed with T-PBS. Biotin-conjugated detection antibody were incubated for 1 h, with streptavidin-peroxidase to signal amplification. The evaluation of absorbance was performed by OPD (Sigma Aldrich) in a multiplate reader (SpectraMax M2e, Molecular Devices, USA) at 450 nm.

Immunohistochemistry

Tumor-bearing mice, received 200 μg i.p. of Rb9 or Scr-Rb9 and were euthanized after 15 days. Their lungs were surgically excised and cryopreserved in Tissue-Tek compound (Sakura Europe) at −80°C. Standard 5 μm sections were obtained from paraffin embedded lungs cuts laid on cleaned glass slides to immunohistochemistry preparation. Briefly, fixed sections were deparaffinized, rehydrated with graded xylene-ethanol series and endogenous peroxidases were inhibited by two washes of 3% hydrogen peroxide in methanol. Non-specific antigen-antibody reaction was blocked before staining with monoclonal anti-CD4 (Spring Biosciences Corp.) and monoclonal anti-granzyme B (Dako) antibodies. The immunohistochemical analysis was carried out using the peroxidase-conjugated Avidin-biotin complex and 3,3-diaminobenzidine (DAB) peroxidase substrate following standard procedures. The antigen-antibody reaction was visualized as a brown precipitate and stained tissue was counterstained with hematoxylin for 3 min. The slides were then rehydrated and mounted for observation under light microscopy. Photomicrographs were taken of each slide and the signal intensity was measured on images of several lung nodules using color deconvolution with Fiji/Image J version 1.52e software.

Bone Marrow Derived Dendritic Cells and Macrophages

Bone marrow-derived dendritic cells (bmDCs) were obtained from C57Bl/6 mice as previously described (28–30). Briefly, mice femura and tibiae were stripped out of muscles and tendons and bone ends were cut to flushed out the bone marrow using a 26-gauge needle and syringe with R10 medium. Cell clusters were dissociated by passing through a cell strainer and red cell lysis were carried out using ACK buffer. The bone marrow cells were cultured in 100-mm tissue culture dish with 10 ml of R10 medium supplemented with GM-CSF (50 ng/ml,) and IL-4 (50 ng/ml). Fresh medium (3 ml) with GM-CSF (100 ng/ml) and IL-4 (100 ng/ml) was added every 3 days. On day 7, non-adherent cells were collected and pooled with adherent cells, which were harvested by PBS with 2 mM EDTA. Bone marrow-derived macrophages (bmMΦs), were extracted from femura and tibiae incubated with M-CSF-1 (10 ng/mL) in complete D10 medium for 6 days.

Immunofluorescence

Murine bmDCs were plated on glass slides (Tekdon Inc.) inside 24 well plates at a concentration of 2.5×10^4 cells in 60 μL for 1 h. After adhesion, 300 μL R10 medium was added and the cells were incubated overnight. On the next day, bmDCs were incubated with 500 μM of Rb9 conjugated with biotin for 1, 3, 8, and 24 h. A negative control consisted of cells without peptide added. The culture medium was removed and the slides were washed 3x with PBS before fixation in PBS containing 3.7% of formaldehyde for 20 min. Cells were then washed 3x with PBS, permeabilized with PBS containing 0.01% Triton X-100 for 5 min and then incubated with PBS containing 0.25% BSA for 1 h at room temperature in order to block non-specific sites. Finally, cells were stained for 1 h at room temperature in the dark using the same blocking buffer supplement with phalloidin-rhodamine for actin cytoskeleton, 10 μg/mL 4',6-diamidino-2-phenylindole (DAPI) for nucleic acid and anti-biotin-FITC to localize the Rb9 peptide. Glass slides were washed 5x with PBS and prepared as glass covers using Vectashield (VectorLabs) and sealed with nail polish before visualization in TCS SP5 II Tandem Scanner (Leica) confocal microscope with a 63 × NA 1.40 PlanApo oil immersion objective.

Chemiluminescent Dot-Blotting

Rb9 and Rb10A1 peptides were diluted at 10 μg/10 μL in milli-Q water and applied on nitrocellulose membranes. Recombinant MIF and CD74 (Abcam, UK) were applied onto the nitrocellulose membranes at 50 nM and incubated overnight at 4°C. After washing, membranes were incubated with anti-MIF or anti-CD74 for 1 h at 37°C followed by several washes and anti-rabbit and anti-mouse IgG-HRP antibody incubation for 1 h at 37°C. Immunoreactivity was determined using the Luminata™ Forte solution (Millipore, Billerica, MA) and images were acquired by Uvitec Cambridge (Cambridge, UK). Some other peptides were also evaluated with negative reactivity (data not shown). This protocol was adapted from previous studies (31, 32).

Immunoblotting

Cultured bmDCs were treated with 200 μM Rb9 for 6 h and then incubated with 1 μg/mL recombinant MIF (rMIF) for 2, 5, 10, and 20 min before cells were lysed, centrifuged at 1,000 *g* for 5 min and washed 1x in TBS (50 mM Tris-HCl pH 7.5, 150 mM NaCl) before add Laemmli buffer (62.5 mM Tris-HCl, pH 6.8 at 25°C, 2% w/v SDS, 10% glycerol, 50 mM DTT, 0.01% w/v bromophenol blue) and heat denaturation at 95°C for 5 min. Electrophoresis in polyacrylamide gels containing SDS and transfer to PVDF Immobilon P membrane (Millipore, Darmstadt, Germany) were carried out by standard procedures. The membranes were stained with 0.5 % Ponceau S in 3% acetic acid and eventually cut separating proteins with mass above and below 50 kDa. All membranes were blocked with TBS (10 mM Tris-HCl, 150 mM NaCl, pH 8) containing 0.05% Tween 20 (TBS-T) and 5% BSA overnight. Membranes were incubated for 3 h with anti-Akt, anti-pAKT (S473), anti-ERK1/2, anti-pERK1/2, anti-NF-κB pr65, anti-pNF-κB pr65 (S536), anti-PI3K pr85, anti-pPI3K pr85 (T458), anti-IkBα, anti-pIkBα (S32),

anti-CD74, and anti-GAPDH, antibodies, purchased from Cell Signaling Technology (Beverly, MA) except for anti-GAPDH, acquired from Sigma-Aldrich (St. Louis, MO). The primary antibody was washed 3x in TBS-T for 10 min each and incubated for 1 h with anti-rabbit or anti-mouse IgG peroxidase-conjugated antibody (Thermo Fisher Scientific) diluted 1:20,000 in TBS. Membranes were washed 3x in TBS-T for 10 min. Immunoreactivity was determined using the Luminata™ Forte solution (Millipore, Billerica, MA) and images were acquired by Uvitec Cambridge (Cambridge, UK). Densitometry of bands was obtained using ImageJ software. pProtein/Protein ratios as in **Figures 6B–E** were normalized in relation to the ratios of unstimulated control cells (plotted = 1). For instance, sample 3 of pAkt: 9171.50/11358.86 = 0.8074 and CTR 1895.08/11373.45 = 0.1666; 0.8074/0.1666 = 4.84; or pAkt/Akt = 4.83/0.999 with CTR 1.00/1.00.

Adoptive Cell Transfer Treatment

Two different protocols of adoptive cell transfer (ACT) treatment were performed. To the therapeutic protocol, murine bmDCs obtained as described above were stimulated with 50 μg/mL of Rb9 or Rb10A1 for 24 h. Mice previously challenged with B16F10-Nex2 were inoculated with 5×10^5 bmDCs via i.p. per animal on the eighth day of tumor injection. The protective effect induced by Rb9 was evaluated after 15 days of tumor challenge by counting pulmonary melanotic nodules. In the prophylactic protocol of ACT, bmDCs were stimulated by Rb9 or Rb10A1, primed or not with tumor cell lysate (Lys, 1:10 v/v cell lysate from 5×10^4 tumor cells) for 24 h, before s.c. inoculation in naïve mice. Each naïve mouse received two inoculations of primed bmDCs, on the 2nd and 7th days before B16F10-Nex2 challenge. The protective effect induced by Rb9 was also evaluated after 15 days of tumor challenge by counting pulmonary melanotic nodules.

Human PBMC-Derived Dendritic Cell Obtention and Lymphocyte Proliferation

Blood samples from healthy donor and cancer patients (n = 22) were collected and peripheral blood mononuclear cells (PBMCs) were isolated by centrifugation over Ficoll-Paque Plus (GE Healthcare). After a 2 h-incubation in plastic 6-well plates, non-adherent cells were removed from culture and adherent cells (monocytes) were cultivated for 7 days in RPMI-1640 culture medium supplemented with 10% FCS, antibiotic-antimycotic agents (Gibco, Grand Island, NY, USA), in the presence of GM-CSF (50 ng/ml—Peprotech, Mexico) and IL-4 (50 ng/ml—Peprotech). At day 5 of culture TNF-α (50 ng/ml; Peprotech, Mexico) was added for monocyte derived DC maturation (mDCs). After maturation, mDCs received treatment with Rb9 or tumor cell lysate (Lys) before co-culture with allogeneic lymphocytes (DC:Ly = 1:30) to evaluate their ability to induce lymphocyte proliferation. Phytohemagglutinin (PHA) was also used as a control. The proliferation was measured by carboxyfluorescein succinimidyl ester (CFSE—Molecular Probes) dilution and activation was measured by correlation between CD4/CD25 and Foxp3 expression.

Flow Cytometry Analysis of Dendritic and Lymphocytic Cells

BmDCs from mice were stained for CD11c, CD11b, and CD74 after treatment with 50 μg/mL Rb9 for 48 h and 200 ng/mL LPS for 24 h, and bmMΦs were stained for F4/80, MHC-II, CD86, PD-L1, and CD206 in PBS, 0.5% BSA for 30 min using the different antibody-fluorophore conjugates from MACS, Miltenyi Biotec. Cells were washed in cold PBS with BSA and suspended in fixation buffer (PBS, BSA with 2% paraformaldehyde) before flow cytometry. Compensated multiparameter analysis was performed on a BD FACSCanto II analyzer (BD Biosciences, USA) with FlowJo X software (Tree Star Inc., USA).

Human cells were analyzed similarly to mice cells, but the staining was performed in BSA-PBS without EDTA. To flow cytometry analysis was used antibodies against CD11c, CD14, CD80, CD83, CD86, HLA-ABC, HLA-DR, CCR7, and PD-L1, conjugated with different fluorochromes, besideslive/dead labeling (Molecular Probes, Oregon, USA). Acquisition was performed in a FACSCanto II analyzer (BD Biosciences), analyzed with the FlowJo Software X.10.07r2 (Tree Star). The frequency of FoxP3+ human cells was analyzed using the e-Bioscience Foxp3/Transcription Factor Staining Buffer Set (Affymetrix, e-Bioscience, USA) as described in the manufacturer's protocol. Before intracellular staining, the cells were labeled with fluorescence labeled anti-CD4, anti-CD8, and anti-CD25 (BD Biosciences).

Statistics Analysis

The software GraphPad Prism version 7.0 (San Diego, CA) was used in all tests for significance analyses. Student, Welch, or Mann–Whitney t-test compared statistical differences between groups. One-Way ANOVA with Bonferroni correction; repeated measures ANOVA with Dunnett's correction, and two-way ANOVA were also applied. A difference in survival time was measured by Log-rank with Mantel-Cox test. P-values are indicated as $^{*}p < 0.05$, $^{**}p < 0.01$, and $^{***}p < 0.001$ indicating the significant difference. The X^2 (chi-squared) test was used to determine the statistical significance of different frequencies from flow cytometer data.

RESULTS

Anti-metastatic and Anti-tumor Activity of Rb9 Peptide

B16F10-Nex2 cells were intravenously inoculated in C57BL/6 mice to generate a syngeneic model of pulmonary metastatic melanoma (33, 34). The anti-tumor activity of Rb9 was quantified in tumor cell challenged mice treated with 300 μg of Rb9 peptide per animal via i.p., starting 1 day after tumor cell inoculation followed by 5 doses in alternate days (**Figure 1A**). The number of pulmonary tumor nodules reduced when mice were injected with Rb9 in relation to control groups (Veh), which received only PBS, indicating the protective role of the peptide against melanoma lung colonization (metastasis). Similar results were obtained using different numbers of melanoma cells and different peptide concentrations, ranging from 50 to 200 μg of Rb9 per animal

(**Figure 1B**). However, no protection was observed at 10 or 30 μg (not shown). Due to the variation of lung nodule size and the merge of individual nodules, the area of melanotic nodules over the lung surface was also measured (**Figure 1C**). In this experiment, mice received 6 inoculations of PBS, as a negative control group, or 200 μg of Rb9 per animal and equal amounts of Scr-Rb9 peptide i.p. and s.c. The tumor melanotic metastatic areas decreased significantly only after Rb9 treatment using both i.p. and s.c. administration routes. The lowest decrease was obtained with Rb9 s.c. treatment, as also observed in **Figure 1D**, which shows representative lung images from this experiment.

Although i.p. Rb9 treatment was efficient in the control of metastatic melanoma progression in immunocompetent mice, this peptide failed to promote a protective activity in immune-deficient mice (NOD/SCID/IL-2Rγ^{null}), i.v. challenged with B16F10-Nex2 cells (**Figure 1E**). In fact, the *in vivo* anti-tumor activity of Rb9 seems to be tightly depended on healthy, non-immune compromised syngeneic mice. To further verify an immune response induced by Rb9 inoculation in tumor-bearing mice, sera collected from mice that received Rb9 *via* i.p. or s.c were applied into melanoma cells adhered onto plastic plates blocked or not with BSA. Increased reactivity to plated B16F10-Nex2 cells was observed for both sera. The serum from mice inoculated s.c. with Rb9 was even more reactive with melanoma cells than the serum from animals inoculated i.p. with the peptide (not shown).

In addition to melanoma cells, Rb9 protective activity was also tested against syngeneic CT26 colon and Panc02 pancreatic cancer cells grafted subcutaneously in C57Bl/6 mice (**Supplementary Figure 1**). The peptide was administered in 3 μg/μL/animal, via i.p. for 6 times in alternate days, starting 1 day after tumor cell grafting. In both cases the subcutaneous tumor progression was delayed with full survival of Panc02 after 40 days treatment (**Supplementary Figure 1C**) and none of colon cancer challenged mice after 60 days (not shown).

Rb9 Modulates Cell Recruitment and Immune Activity in the Lung and Lymphoid Organs

As indicated above, the immune system is involved in the protective effect of Rb9 against metastatic melanoma. To further characterize this effect, the lung microenvironment and immune response in peptide-treated tumor-bearing mice were examined. The T lymphocyte population recruited in the lung microenvironment showed cells expressing CD3+, CD4+, CD8+, CD25+, and Foxp3+. We also evaluated NK cells by the expression of NKG2D marker in CD3- cells (**Figure 2**). After gating lymphocytes and measuring the cell population expressing both T-CD3+ and T-CD8+ an expressive increase of this population was observed in samples of s.c. Rb9-treated mice compared to Veh or Scr-Rb9 control groups (**Figure 2A**). Only a small increase of T-CD4+/T-CD3+ cells was observed in the same Rb9-treated samples (**Figure 2B**). Since the protective effect of Rb9 could be due to the modulation of lymphocyte recruitment and activation, the ratio of CD8+ T cells to CD4+ T cells was compared in lungs collected from different groups of treatment and it was increased only in the Rb9-treated group (**Figure 2C**). Inversely to T-CD4+ and T-CD8+ increased populations, the regulatory T lymphocytes expressing CD4+, CD25+, and Foxp3+ T lymphocytes were less expressed in Rb9-treated tissue samples (**Figure 2D**). Finally, NK cells defined with a similar size and granularity as T cells but without CD3 expression were evaluated using the activation marker NKG2D (**Figure 2E**) showing an increased recruitment of these cells similarly to the pulmonary recruitment of CD3-NKG2D+ cell after treatment with 6.25 mg/kg of murine anti-PD-1 therapy.

Immunohistochemistry of metastatic nodules in Rb9-treated mice showed that T-CD8+ and NK cells could be responsible for the secretion of granzyme B in the lung tumor tissue microenvironment from Rb9-treated mice (**Figures 3A,C**). The expression of T-CD4+ in metastatic nodules was only a little increased in Rb9-treated mice (**Figures 3B,D**).

Splenocytes isolated from Rb9-treated melanoma-bearing mice and thereafter stimulated with melanoma lysate were able to produce increased levels of IFN-γ as compared to splenocytes isolated from tumor-bearing mice treated with Veh or Rb10A1 control groups (**Figure 2F**). Axillary and cervical lymph node cells secreted low TGF-β under similar conditions (**Figure 2G**). Rb9 did not modify the melanoma lysate response in relation to IL-12, TNF, and IL-10 secretion but significantly reduced IL-6 (**Supplementary Figure 2**).

Altogether, these results suggest an immunomodulatory activity of Rb9 leading to anti-tumor response mediated by cytotoxic T-CD8+, NK cells, and IFN-γ with low TGF-β and Treg lymphocytes.

Rb9 Interacts With Murine Bone-Marrow Dendritic Cells (bmDCs)

Since Rb9 peptide requires the immune system participation to display anti-tumor response in a metastatic melanoma setting a direct interaction of the peptide with dendritic cells was looked for as a possible early step in this process. By using fluorescence microscopy we showed that murine bmDCs interact directly with biotinylated Rb9, as revealed with FITC-streptavidin (green staining in **Figure 4**, panels 2, 4, 5, and 6). Confocal microscopy showed colocalization points of FITC-complex-Rb9 signal and perinuclear regions, DAPI signal, within bmDC (panel 5), and also with actin cytoskeleton stained with red phalloidin (panels 3, 4, and 6). Presumably, after internalization Rb9 could be carried to the nuclear site via actin filaments to participate in a cell-signaling pathway.

Direct Binding of Rb9 Peptide to MIF and CD74 Proteins

The macrophage migration inhibitory factor (MIF) is synthesized by epithelial and endothelial cells, T lymphocytes, macrophages, and by several tumors, particularly melanoma (35, 36). MIF exerts its oncogenic effects through binding to CD74 receptor, CXCR4 chemokine receptor, and CD44, involved in MIF cell-signaling (37).

Rb9 peptide binds to MIF and CD74 as shown by dot blotting with the respective recombinant proteins (**Figure 5A**).

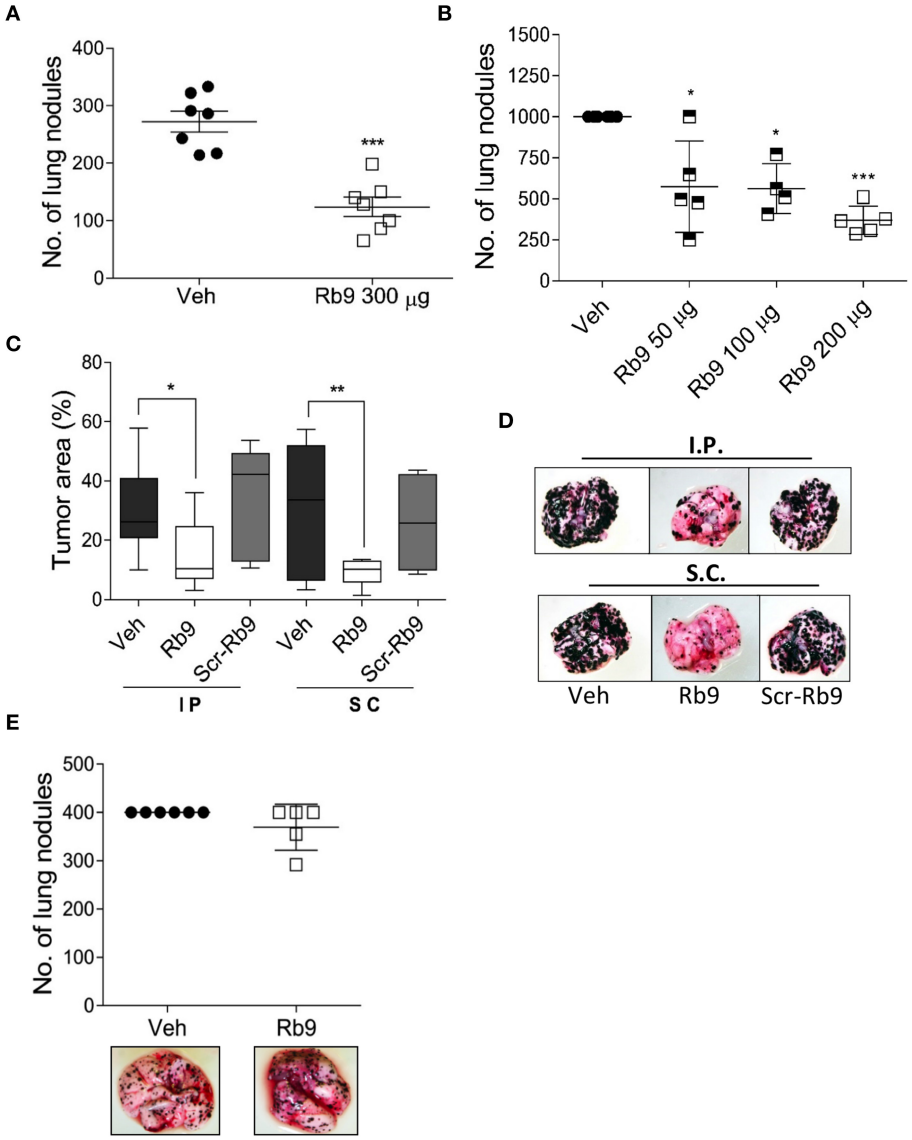

FIGURE 1 | Rb9 peptide inhibits *in vivo* development of melanoma metastasis in immunocompetent mice. **(A)** Rb9 intraperitoneal (i.p) administration of 300 μg per animal for 5 alternate days reduce the number of B16F10-Nex2 lung metastatic nodules as compared to vehicle (Veh, PBS); **(B)** Different doses of i.p. Rb9 administration, 15 days of tumor challenge. $^{*}p < 0.05$ and $^{***}p < 0.001$ calculated using Student's or Welch's *t*-test, respectively. Vehicle ($\geq 10^3$ counts); **(C)** Melanotic area on the lung surface, after 15-days tumor cell-challenge. Subcutaneously (s.c.) or intraperitoneally (i.p.) Rb9-treated mice, scrambled peptide (Scr-Rb9). Median, 25 and 75% quartiles, ± max and min values. $^{*}p < 0.05$ and $^{**}p < 0.01$. One-Way ANOVA with Bonferroni correction; **(D)** Representative panel of lungs after i.p. or s.c. Rb9 administration; **(E)** Immuno-compromised mice (NOD/Scid/IL-2Rγ^{null}) are not capable to arrest melanoma metastasis development after treatment with 300 μg of Rb9.

A peptide derived from linear Rb10 replacing the N-terminal cysteine by alanine, Rb10A1, Girola et al. (22) was unreactive and also used as a control for *in vitro* experiments. Rb9 also increased CD74 expression in immature dendritic cells (iDCs) expressing CD11b and CD11c, also reversing the negative effect in iDCs of treatment with 200 ng of LPS for 24 h as observed by flow cytometry (**Figure 5B**). MIF is commonly secreted by B16F10 in cultured melanoma cells, as detected in the conditioned medium (38). Another, previously studied, CDR peptide (C36L1) showed ability to bind to MIF's receptor CD74 and also interfere in the melanoma-secreted factor that regulates macrophage function (38). Based on these results, bone marrow-derived macrophages (bmMΦs) were evaluated in the presence of melanoma factors (B16F10 conditioned medium, B16.CM) with or without Rb9. M1 macrophages expressing CD86 and MHC II showed increased expression upon treatment with Rb9 (B16.CM, **Figure 5C**). In contrast, decreased expression of M2 macrophages expressing PD-L1 and CD206 was observed in response to Rb9 (**Figure 5D**).

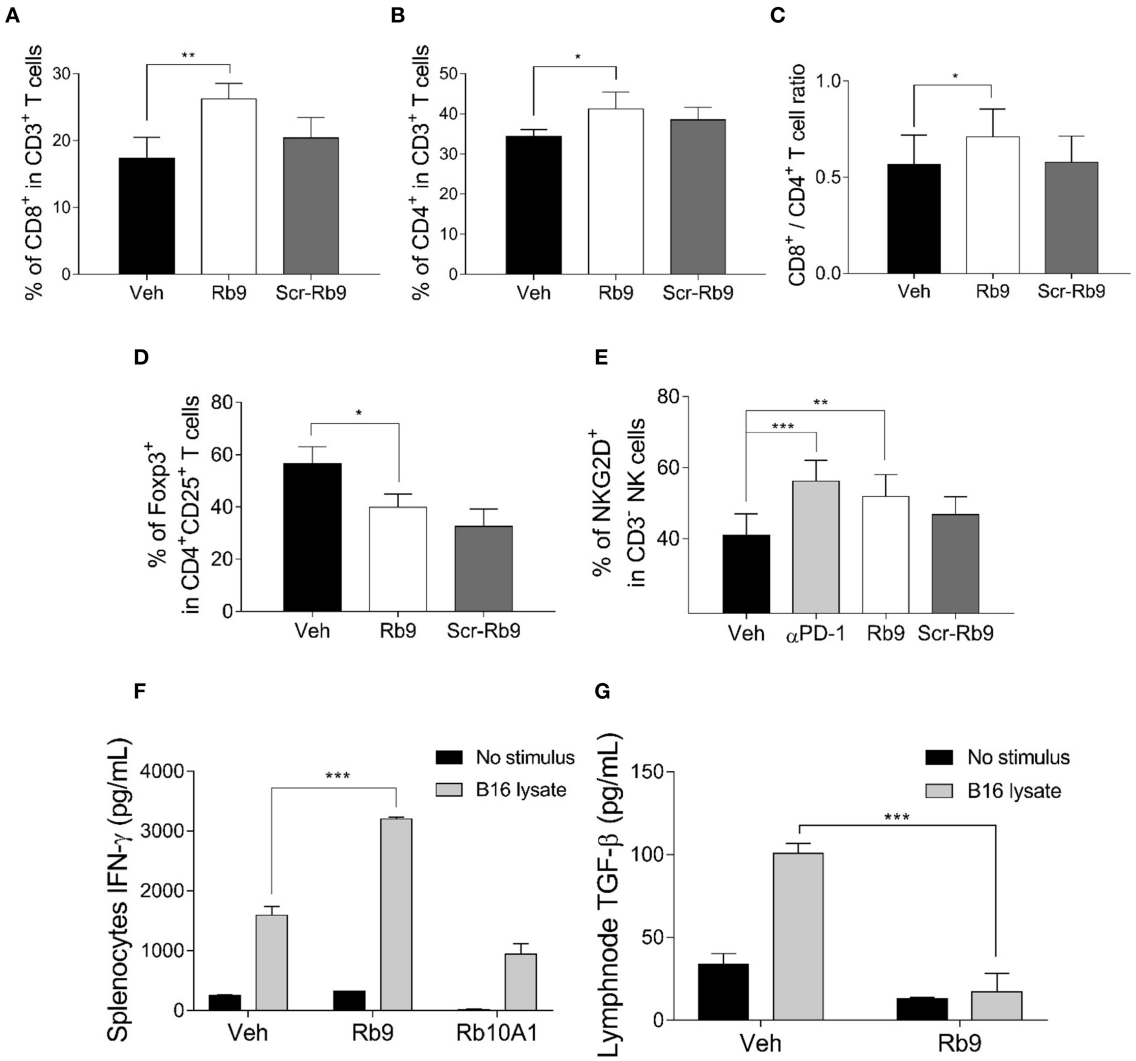

FIGURE 2 | Lung lymphocyte recruitment in Rb9-treated mice and specific cytokine expression in splenocytes and CD11+ lymph node cells. **(A)** Percent CD8+ T cells inside lungs collected after 15 days from mice receiving 200 μg of s.c. Rb9 or Scr-Rb9 for 6 alternate days starting on day 2 after challenge with B16F10-Nex2 cells; **(B)** Percent CD4+ T cells inside lungs as in **(A)**; **(C)** Ratio of CD8+ T and CD4+ T lung infiltrates significantly increased in s.c. Rb9-treated mice. Values are means ± SEM of the previous experiments; **(D)** Percent CD4+, CD25+, Foxp3+ T cells inside lungs and **(E)** Percent CD3–NKG2D+ natural killer cells inside lungs as in **(A,B)**. Values are ± SEM of three experiments with 4–5 pooled lungs; $^{**}p < 0.01$ and $^{*}p < 0.05$ with repeated measures (RM)-ANOVA and Dunnett's post-test compared to Veh. **(F)** Splenocytes from 17-day melanoma cell challenged mice and Rb9 or Rb10A1 i.p. treatment, for 5 alternate days, after challenge on the 1st day. The splenocytes cell culture supernatant was used to measure IFN-γ secretion after 72-h stimulus with B16F10-Nex2 lysate; **(G)** CD11c+ cells from cervical and axillary lymph nodes were used to measure TGF-β reduced expression on cells after 24 h with tumor lysate stimulus. Graphs from **(F)** to **(G)** represent means ± SD of triplicate experiments quantified by ELISA using standard controls. $^{***}p < 0.001$.

Rb9 Interferes With MIF Signaling Pathways in Murine bmDCs

As Rb9 was shown to interact with bmDCs and, at molecular level, with MIF and CD74 proteins, intracellular signaling pathways were evaluated in DCs in response to rMIF incubation and Rb9 modulatory effects (**Figure 6** and **Supplementary Figure 4**). In **Figure 6A**, signaling proteins in bmDCs, previously incubated for 6 h with Rb9 at 200 μM, and then treated with 1 μg/mL of rMIF for 2, 5, 10, and 20 min are shown. Cellular extracts at each time-point of rMIF treatment of Rb9-pretreated DCs, were collected and the total and phosphorylated protein levels of Akt, ERK1/2, NF-κB p65, and CD74 were quantified by immunoblotting methods and band densitometry as shown in **Figures 6B–E**. Overall, Rb9 treatment alone did not significantly change intracellular signaling mediators in bmDC. Nevertheless, when Rb9-preincubated bmDCs were treated with rMIF, Akt phosphorylation at serine 473 (S473) was stimulated after 2 min and less so after 10 min incubation (**Figure 6B**). In contrast, phosphorylation of ERK1/2 (**Figure 6C**) in Rb9-bmDCs was

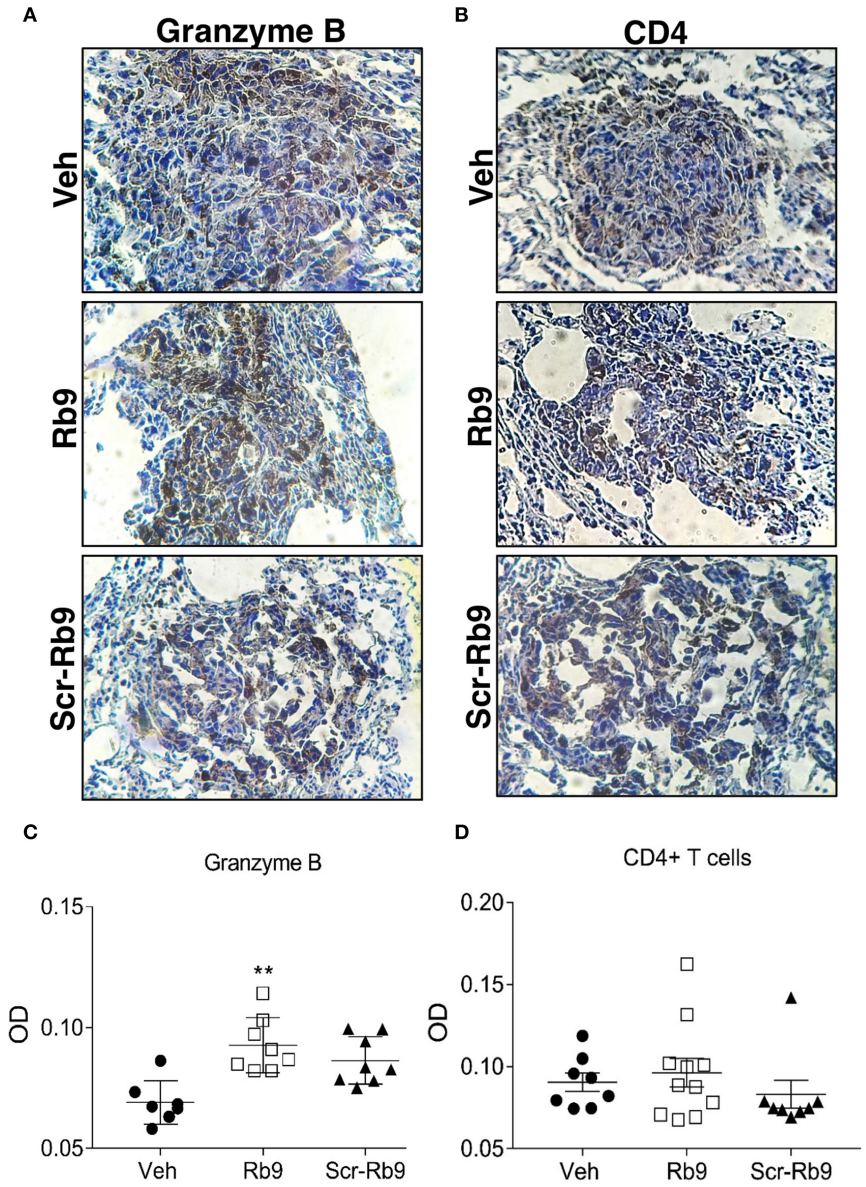

FIGURE 3 | Immunohistochemistry of increased granzyme B secretion around lung metastatic nodules in Rb9-treated mice. **(A,B)** Panels show lung tissue including B16F10-Nex2 metastatic nodules in Rb9-treated mice. Immunohistochemistry staining with 3,3-diaminobenzidine for granzyme B **(A)** and CD4+ T cells **(B)**. Counterstaining: hematoxylin, in blue. Magnification: x400. **(C,D)** Graphs represent individual nodule areas, means and ± SEM of optical densities (OD) calculated after color deconvolution on ImageJ software for at least 8 nodules on each experimental group. $^{**}p < 0.01$ Mann–Whitney *t*-test as compared to Veh.

significantly reduced by rMIF after 2–10 min incubation, as compared to bmDCs without pretreatment with Rb9. A similar reduction by rMIF in Rb9-bmDCs was observed after 5–10 min incubation, equally compared to bmDCs without Rb9 pre-treatment. For PI3K and IkBα signaling, Rb9 reduced by half the expression of pPI3k, without reversion by rMIF. As to pIkBα little or no difference of rMIF stimulation in bmDCs treated or not with Rb9 was seen (**Supplementary Figures 3A–C**). Finally, the MIF receptor CD74, showed increased expression when rMIF was added to Rb9-bmDCs for 2 min (**Figure 6E**) compared to the Rb9-untreated counterpart.

Therapeutic and Prophylactic Anti-tumor Protection by Adoptive Cell Transfer of Rb9-Stimulated Dendritic Cells

The immune system dependence of Rb9 anti-tumor protection *in vivo* was further explored testing bmDCs treated *ex vivo* with Rb9 and adoptively transferred into tumor-bearing mice (**Figure 7**). When syngeneic C57Bl/6 mice are i.v. challenged with B16F10-Nex2 cells, a predictable number of metastatic lung nodules in each animal can be represented as a cluster range after 7–8 days and then another after 12–15 days after tumor challenge injection (**Figure 7A**). Using this standard

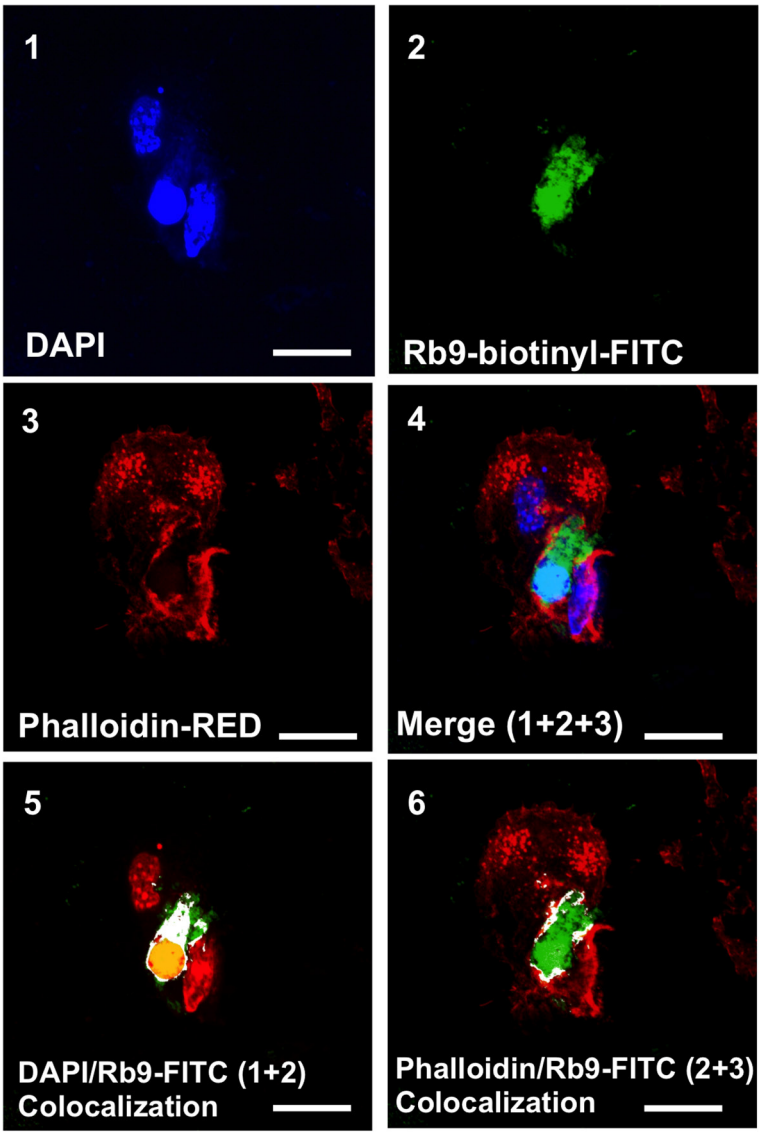

FIGURE 4 | Rb9 interacts with and is internalized by bone marrow derived dendritic cells (BMDCs). Panels are representative confocal images of bmDCs stained with DAPI (blue, panel 1) and phalloidin (red, panel 3) for nucleic acid and filamentous actin staining, respectively. Biotinyl-Rb9 is stained with FITC (green, panel 2). A merge of 1, 2, and 3 can be seen on panel 4. FITC-biotinyl-Rb9 colocalizes with DAPI in a nuclear region (panel 5) and peripherally with phalloidin (panel 6) as shown by white and yellow points/areas in the cellular cytosol on both colocalization panels. Bars = 10 μm.

response, the protective effect of adoptive bmDCs stimulated *ex vivo* with Rb9 or Rb10A1 (negative control) was shown using a therapeutic protocol in which DCs were subcutaneously transferred 8 days after tumor cell challenge (**Figures 7B,C**). Rb9-DCs suppressed metastatic melanoma progression at 15 days after tumor injection, with the number of metastatic nodules equivalent to that of untreated mice after 8 days of B16F10-Nex2 inoculation (**Figure 7A**). In a prophylactic protocol, bmDC were previously primed *ex vivo* with tumor cell lysate (Lys) and stimulated with Rb9 or Rb10A1 peptides. Primed cells were injected twice prior to a single B16F10-Nex2 challenge inoculation (**Figure 7D**). Mice receiving Rb9-stimulated DCs, with or without Lys-priming, were best protected against metastatic melanoma after 15 days of challenge (**Figure 7E**).

Rb9 Affects Human moDCs' Surface Phenotype and Enhances Their Ability to Stimulate Allogeneic Lymphocyte Proliferation

We evaluated the expression and activation of markers in human dendritic cells under Rb9 interference. The capacity of these DCs to stimulate allogeneic lymphocyte proliferation (**Figure 8**) was investigated with a healthy donor's dendritic cells differentiated *ex vivo* from blood monocytes and incubated with Rb9 alone

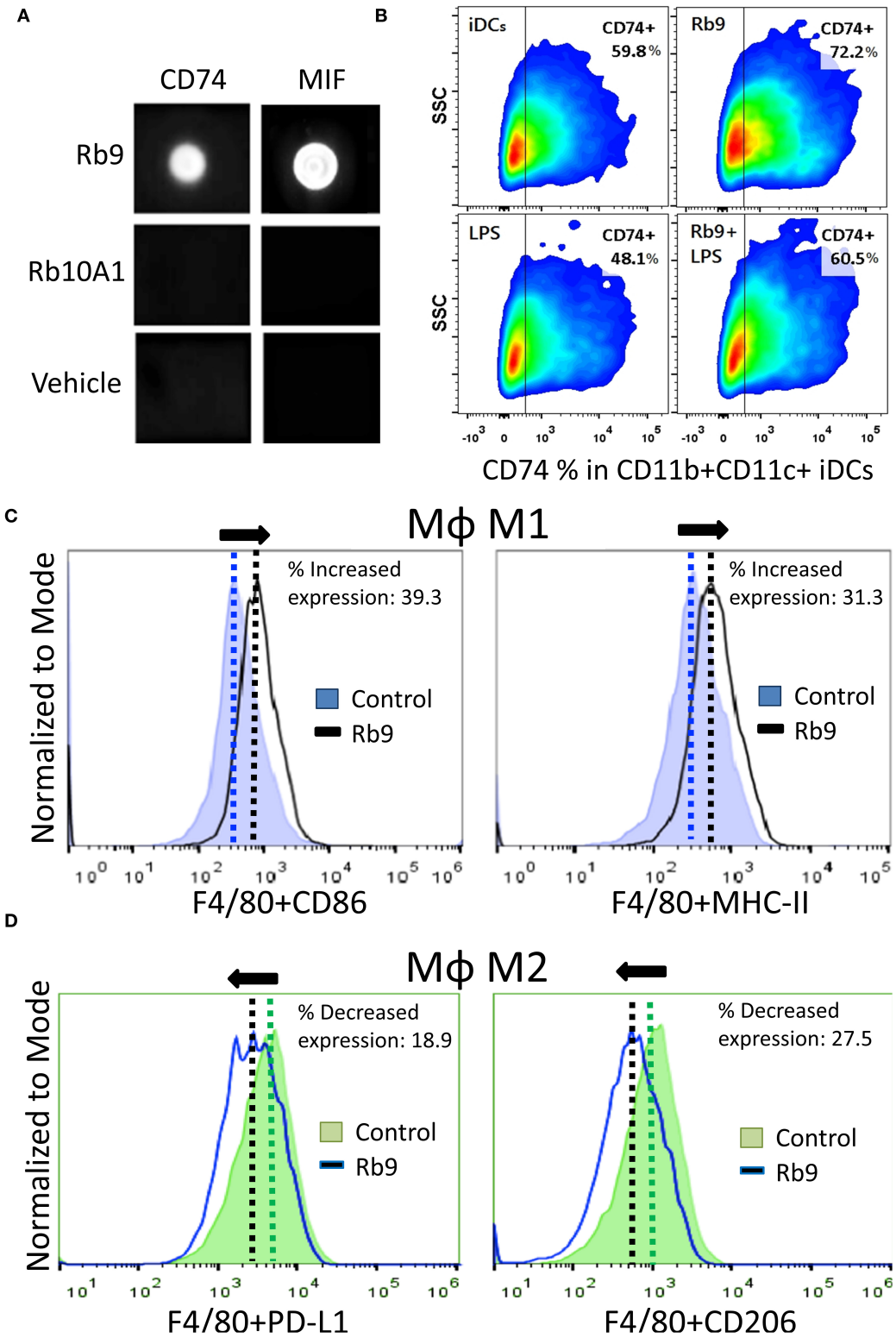

FIGURE 5 | Specific binding of Rb9 peptide to MIF or CD74 recombinant proteins. **(A)** Dot-blotting showing specific interaction of Rb9 peptide with rCD74 and rMIF proteins. No reaction was seen with Rb10A1 peptide or the peptide vehicle (Veh); **(B)** Rb9 increases the expression of CD74 in CD11b+CD11c+ iDCs; **(C)** Increased M1 MΦ marker expression (CD86+ and MHC-II+) in bmMΦs incubated with Rb9 in the presence of melanoma factors (B16F10 conditioned medium, B16.CM); **(D)** Decreased M2 MΦ marker expression (PD-L1+ and CD206+) in bmMΦs incubated with Rb9 in the presence of melanoma factors (B16.CM).

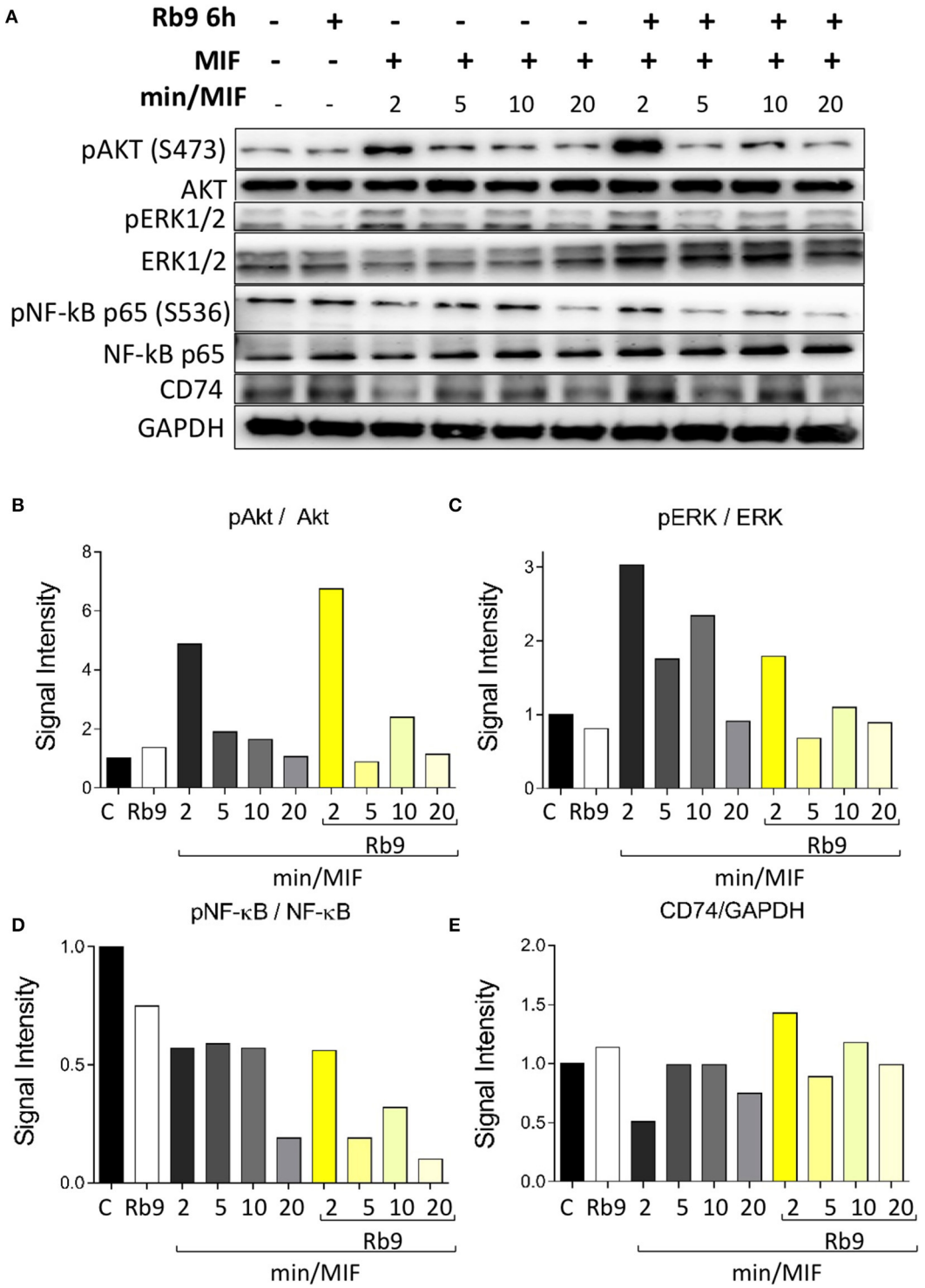

FIGURE 6 | Rb9 pre-incubation modifies the intracellular Akt, ERK, NF-κB signaling pathways and CD74 expression in MIF-stimulated murine bmDCs. **(A)** Western blotting bands of Akt, pAkt (Ser473), ERK1/2, pERK1/2, NF-κB pr65, pNF-κB pr65 (Ser536), CD74, and GAPDH (loading control) from bmDCs pre-incubated for 6 h with/without 200 μM of Rb9 and treated with 1 μg/mL of rMIF for 2, 5, 10, and 20 min; **(B)** Rb9-pretreated cells showed increased signal intensity of pAkt S473 on short incubation with rMIF; **(C)** pERK1/2 in relation to total ERK1/2 decreased in Rb9-pretreated cells in response to rMIF; **(D)** pNF-κB pr65 S536 showed a fast decrease in Rb9-pretreated cells at 5–10 min of rMIF incubation; **(E)** the expression of CD74 increased with Rb9 pre-incubation and combining Rb9 and rMIF.

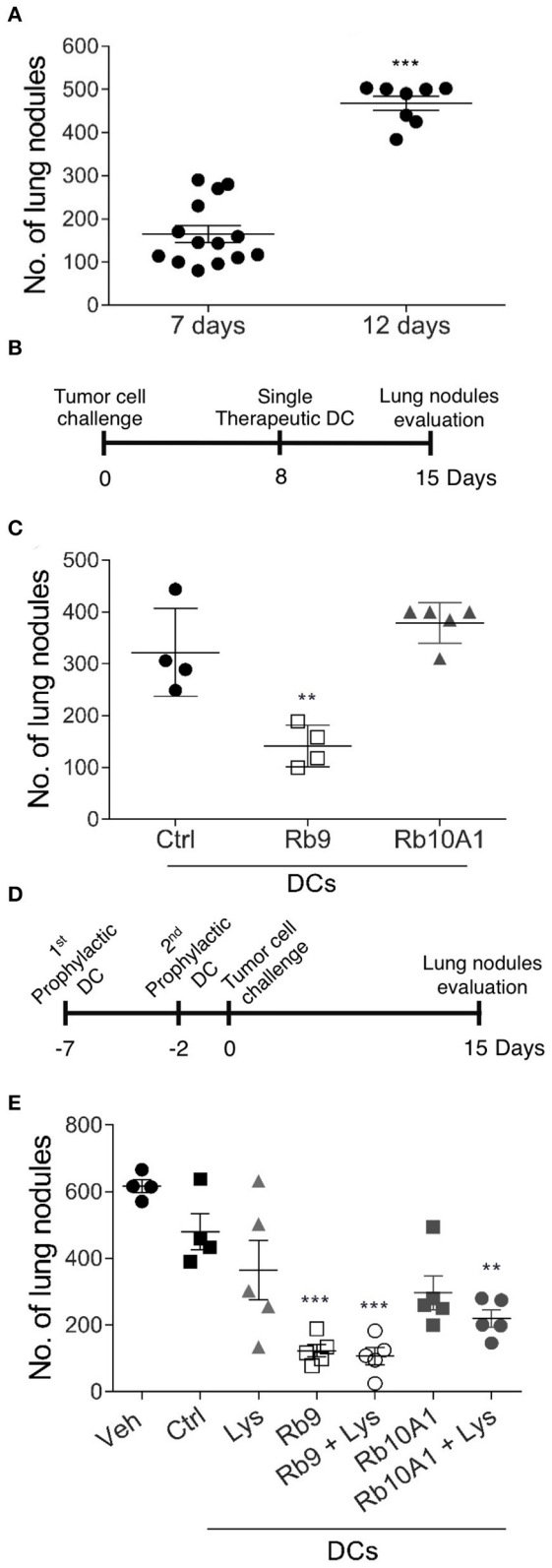

FIGURE 7 | Therapeutic and prophylactic adoptive cell transfer (ACT) using Rb9-stimulated dendritic cells (DCs). **(A)** Syngeneic mice injected i.v. with B16F10-Nex2 melanoma cells show increased number of lung metastatic nodules after 7 and 12 days of tumor cell challenge; **(B)** in a therapeutic protocol Rb9-stimulated bmDCs are injected once after 8 days of tumor cell i.v. challenge; **(C)** metastatic nodules have growth arrested even after 15 days as compared to Rb10A1 control peptide; **(D)** in the prophylactic protocol Rb9 alone or combined with tumor lysate, given *ex-vivo* to bmDCs, are injected twice before tumor cell challenge **(E)** and arrest metastatic growth of melanoma. For this protocol, bmDCs were stimulated with 50 μg/mL of Rb9, Rb10A1 with or without 5 x 10^4 B16F10-Nex2 cell lysate (Lys) for 24 h previously to s.c. inoculation of mice at 7 and 2 days before melanoma tumor cell challenge. Graphs **(C,E)** show individual values, with means ± SD. $^{**}p < 0.01$; $^{***}p < 0.001$ calculated using One-Way ANOVA and Bonferroni correction compared to bmDCs Ctrl groups.

(iDCs, **Figure 8A**) or incubated with Rb9 and TNFα (mDCs, **Figure 8B**). As both figures show, regardless of TNF stimulation, Rb9 treatment increased the expression of HLA-DR, CD11c, CD40, CD80, CD86, and PD-L1 human monocyte-derived DCs (hu-moDCs). Coherently, when hu-moDCs previously pulsed with tumor lysate and treated with Rb9 were co-cultured with allogeneic lymphocytes, the allostimulatory activity was higher than with hu-moDCs alone or combined with tumor lysate-pulsed condition, but without Rb9 treatment (**Figure 8C**).

Curiously, when hu-moDCs were submitted to stimuli that either over-activated them (LPS) or induced a tolerogenic phenotype (TGF-β + IL-10), Rb9 treatment had opposite effects. After tolerogenic stimuli with TGF-β and IL-10, RB9 treatment overcame the down-regulation of activation markers, increasing the expression of HLA-DR, CD80, CD83, and CD86. In contrast, hu-moDCs earlier hyperstimulated with the LPS treatment after receiving Rb9 showed a down-regulation of activation markers. The significance of these results was evaluated using a X^2 statistics (**Table 1**) on the flow cytometer data shown in **Supplementary Figure 4**. Interestingly, Rb9 treatment increased the expression of the MIF-receptor CD74 in LPS-activated cells, but not in tolerogenic hu-moDCs (**Figures 9A,B**). CD44 was downregulated in TGF-β + IL-10-treated hu-moDCs, with no alteration on CXCR4 expression (**Supplementary Figure 5**).

Further, hu-moDCs isolated from 22 cancer patients were treated with Rb9 before allostimulation with healthy donor lymphocytes (**Figures 9C,D**). Since hu-moDCs from cancer patients frequently show deficits in their allostimulatory ability (39, 40), the response in this experiment was evaluated against a positive control: the proliferative response induced by the mitogen, phytohemagglutinin A (PHA). Hu-moDCS from some patients, indeed, showed a "defective" activity (<35% of the response induced by PHA), while others had a "non-defective" activity (more than 35% of the response induced by PHA). Rb9 treatment in defective mDCs was able to slightly increase CD4 and CD8 T cell proliferation (**Figures 9C,D**) and, in contrast, decreased the response induced by "non-defective" cells.

Overall, these results suggest that Rb9 can modulate human monocyte-derived dendritic cells activity, especially in cancer patient cells, stimulating tolerogenic cells (biased either *in vitro*, by TGF-β with IL-10, or *in vivo* by the presence of cancer) and containing the activation of hyperstimulated cells (by LPS, for example).

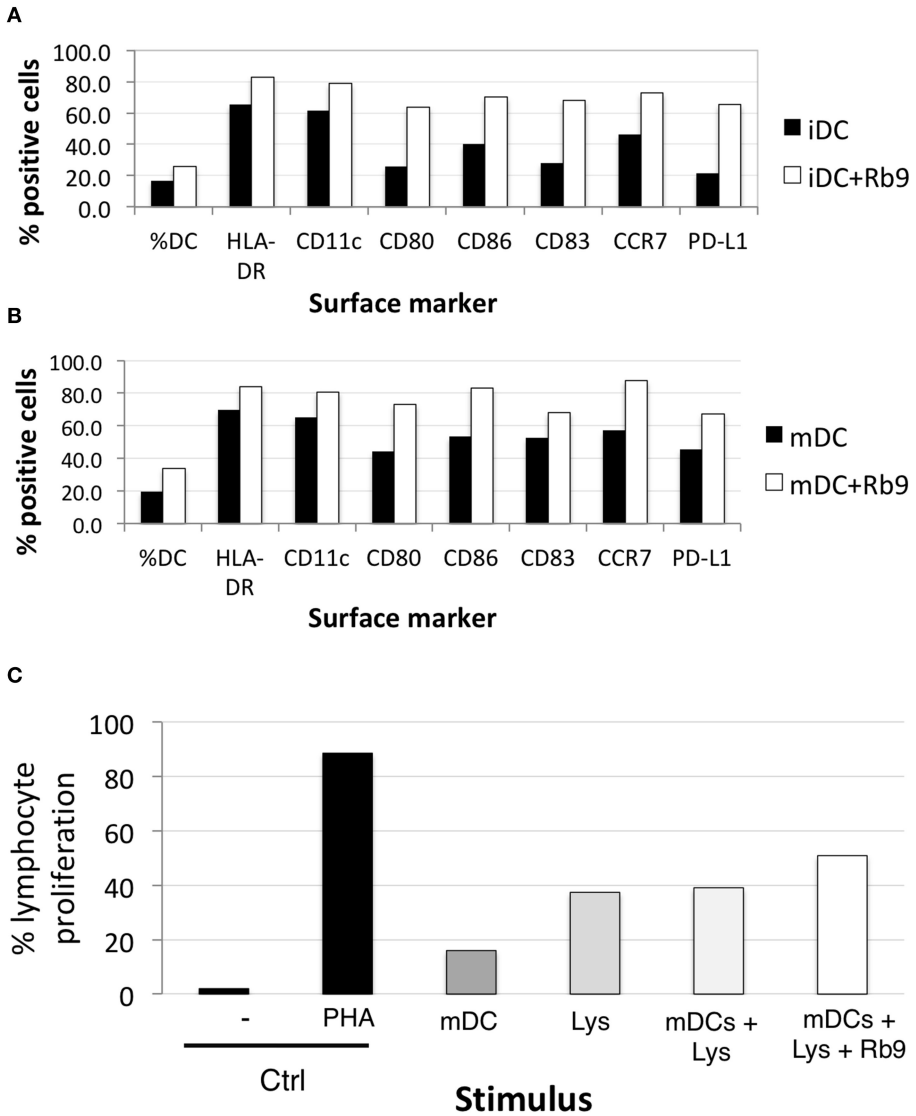

FIGURE 8 | Rb9 affects the phenotype of human monocyte-derived dendritic cells. PBMC from healthy human donor were differentiated into monocyte-dendritic cells and submitted to various treatments; **(A)** shows the increased expression of surface markers (HLA-DR, CD11c, CD80, CD86, CD83, CCR7, and PD-L1) after 48 h-treatment of immature DCs (iDCs) with Rb9 (50 μg/mL); **(B)** a similar effect is shown in TNF-stimulated (mDCs) submitted to Rb9-stimulation; **(C)** PBMC cells from healthy human donor were differentiated into mDCs, submitted to different treatments and used to stimulate CFSE-labeled allogeneic lymphocytes. Enhanced T cell proliferation was observed when mDCs were pulsed with tumor lysate (Lys) and treated with Rb9.

DISCUSSION

Synthetic peptides derived from Complementary Determining Regions (CDRs) of monoclonal antibodies frequently display anti-infective properties and anti-tumor effects (14, 32, 41–43).

Peptide AC1001-H3, derived from V_H CDR3 of anti-blood group A mAb showed apoptotic and autophagic effects in murine B16F10-Nex2 melanoma cells (44). The same peptide exerted anti-metastatic activity in C57Bl/6 syngeneic model as well as an immunomodulatory effect in macrophages (45). The PI3K-Akt signaling pathway and the increased expression of TLR-4 induced by TNF-α were characterized in this system.

Hypervariable complementarity determining regions (CDRs) from both light and heavy chains of immunoglobulins are sources of bioactive peptides, acting in many cases, such as V_HCDR3, as mini-antibodies (41). The immunoglobulin-superfamily (IgSF) carries the greatest number of domains with peptide sequences displaying biological activities including immunomodulatory ones. IgSF proteins make up over 2% of human genes, the largest family in the human genome (46).

As focused on in the present work, Rb9, derived from V_HCDR3 of RebmAb 200, has a configuration similar to that studied by Morea et al. (47), adding C-terminal amino acids QGC and a C-C disulfide bridge to make it cyclic. A stable structure

TABLE 1 | Significant effects of Rb9 (χ^2 statistics) on different populations of human neutral (TNF), activated (LPS), or suppressed (IL-10 + TGF-β) dendritic cells (DCs)[a].

mDC markers	Systems Rb9 and controls	Statistics of Rb9 effects	Stimuli
CD11c	LPS	C	
HLA-DR	LPS + Rb9	X^2 $p < 0.05$	*Neg
	TNF	C	
	TNF + Rb9	X^2 NS	0
	IL-10 + TGF-β	C	
	IL-10/TGF-β + Rb9	X^2 $p < 0.01$	**Pos
CD83	LPS	C	
HLA-DR	LPS + Rb9	X^2 NS	0
	TNF	C	
	TNF + Rb9	X^2 NS	0
	IL-10 + TGF-β	C	
	IL-10/TGF-β + Rb9	X^2 $p < 0.01$	**Pos
CD80	LPS	C	
CD86	LPS + Rb9	X^2 NS	0
	TNF	C	
	TNF + Rb9	X^2 NS	0
	IL-10 + TGF-β	C	
	IL-10/TGF-β + Rb9	X^2 $p < 0.01$	**Pos

[a] *Results obtained in a flow cytometer (see* ***Supplementary Figure 4****). C, control system; X^2, Chi- squared statistics; *Neg, significant inhibitory effect; **Pos, significant activation; NS, not significant effect.*

with numerous H-bonds, internal α-helix, and the disulfide in a hairpin were described in this peptide (22). *In vitro*, Rb9 interacts with HSP90, an adhesion G protein, and surface peroxiredoxin 1, the result being inhibition of melanoma cells migration and invasion (22). As presently shown, Rb9 is protective against metastatic melanoma but the results *in vivo* depend instead on an uncompromised immune system. In fact, dendritic cells (DCs) appear to be involved in the immune response induced by the peptide, since this protective activity of the latter could be reproduced by adoptive transference of DCs, treated *ex vivo* with the peptide, in melanoma-challenged susceptible animals. Therapeutic and prophylactic protocols were effective. With the prophylactic protocol, we observed that pre-treatment of DCs with melanoma lysate did not increase the efficiency compared to Rb9 alone, suggesting that the most important priming occurred *in vivo* after challenge with B16F10 cells, possibly resulting in extensive cell lysis due to NK activity, perforins, and IFN-γ dependent and independent mechanisms (48). Subcutaneous administration of Rb9 seems to be the preferred one, but it seems clear that whatever is the route of inoculation in a tumor-bearing experimental animal, the peptide reacts with local and recruited DCs, modulating their activity in a way that leads to anti-tumor effect and prolonged survival of the host. In the protocols used, depending on the possibility of low supply of tumor antigens, a melanoma cell lysate was used as a primer for cross-presentation by DCs. It is clear, however, that the nature of Rb9 activity is an immune modulatory one. Intraperitoneal administration of Rb9 was also effective in delaying s.c. growth of syngeneic pancreatic and colon cancer cells rather than s.c. B16F10-Nex2 melanoma.

The interaction of biotinyl-Rb9 with DCs was explored using confocal microscopy. Co-localization points were seen with actin-reacting phalloidin and condensed nuclear material, suggesting that the peptide could be carried to the nucleus via F-actin, eventually to mediate a signaling pathway. The discovery that Rb9 binds to rCD74 and rMIF, and the fact that melanoma cells *in vitro* and metastatic tumors secrete MIF (38), prompted us to functionally compare Rb9 with peptide C36L1. This peptide was shown to restore M2 macrophages and DC's immunogenic functions so as to inhibit metastatic tumor growth in lungs. M2 cells characterized by IL-12^{lo}IL-23^{lo}IL-10^{hi}TGF-β^{hi}, mediate Th2 responses, immune regulation, and tumor promotion (49). M1 macrophages, with IL-12^{hi}IL-23^{hi}IL-10^{lo} phenotype, are effector cells in Th1 responses and mediate resistance against tumors. They efficiently produce ROS and NO and inflammatory cytokines, IL-1β, TNF, IL- 6 (50).

Rb9 increased the expression of CD74 in CD11b+CD11c+ dendritic cells and this effect was less intense in iDCs activated by LPS. It was found that a combination of poly(I:C) and LPS with IFNα + γ downregulated the expression of CD74 (51). This effect could be reversed by the immunomodulatory action of Rb9, raising the question of the complex protection mechanism of the peptide against tumors. In fact, CD74 has been shown to negatively regulate DC migration. On the other hand, Rb9 increased M1 markers (CD86 and MHC II) in bmMΦs in the presence of B16F10 conditioned medium (B16.CM) and decreased M2 CD206 marker and PD-L1 in IL-4 polarized M2 bmMΦs also in B16.CM. rMIF signaling in bmDCs was modified by Rb9 pretreatment, particularly increasing the expression of CD74 and decreasing that of pERK and pNF-κB. All these effects pointed to a protective effect of Rb9 in face of the immune suppressive and tumor promoting activities of MIF. This cytokine, abundantly produced by melanoma cells, preferentially stimulates M2-macrophage differentiation. The CD74 receptor is also constitutively expressed on melanoma cells and the MIF-CD74 pathway is correlated with increased PD-L1 expression in cancerous cells (52). Interfering in the MIF-CD74 axis may affect signaling in macrophages and dendritic cells (DCs) that can downregulate immunosuppressive factors and activate cytotoxic T cells (38).

Granzyme B+ and T-CD4+ were examined by IHC in the lung nodules of metastatic melanoma treated with Rb9. Both cytotoxic T lymphocyte (CTLs) and NK cells use the serine protease granzymes as their major death effectors (53, 54). Staining of granzyme B reflected the significant presence of CTLs and NK cells in the tumor nodules, in response to Rb9, and represents the signature of immune effector cells infiltrating the lung tissue (55, 56). In the NK cell population, PD-1 blockade immunotherapy can activate those cells to infiltrate melanoma and lung tumors to elicit anti-tumor responses (57, 58). In the case of NKG2D, increased NKG2D ligand in the tumor cells enhances NK cell cytotoxicity (59). The significant difference in T-CD4+ cells was detected only by flow cytometry in the

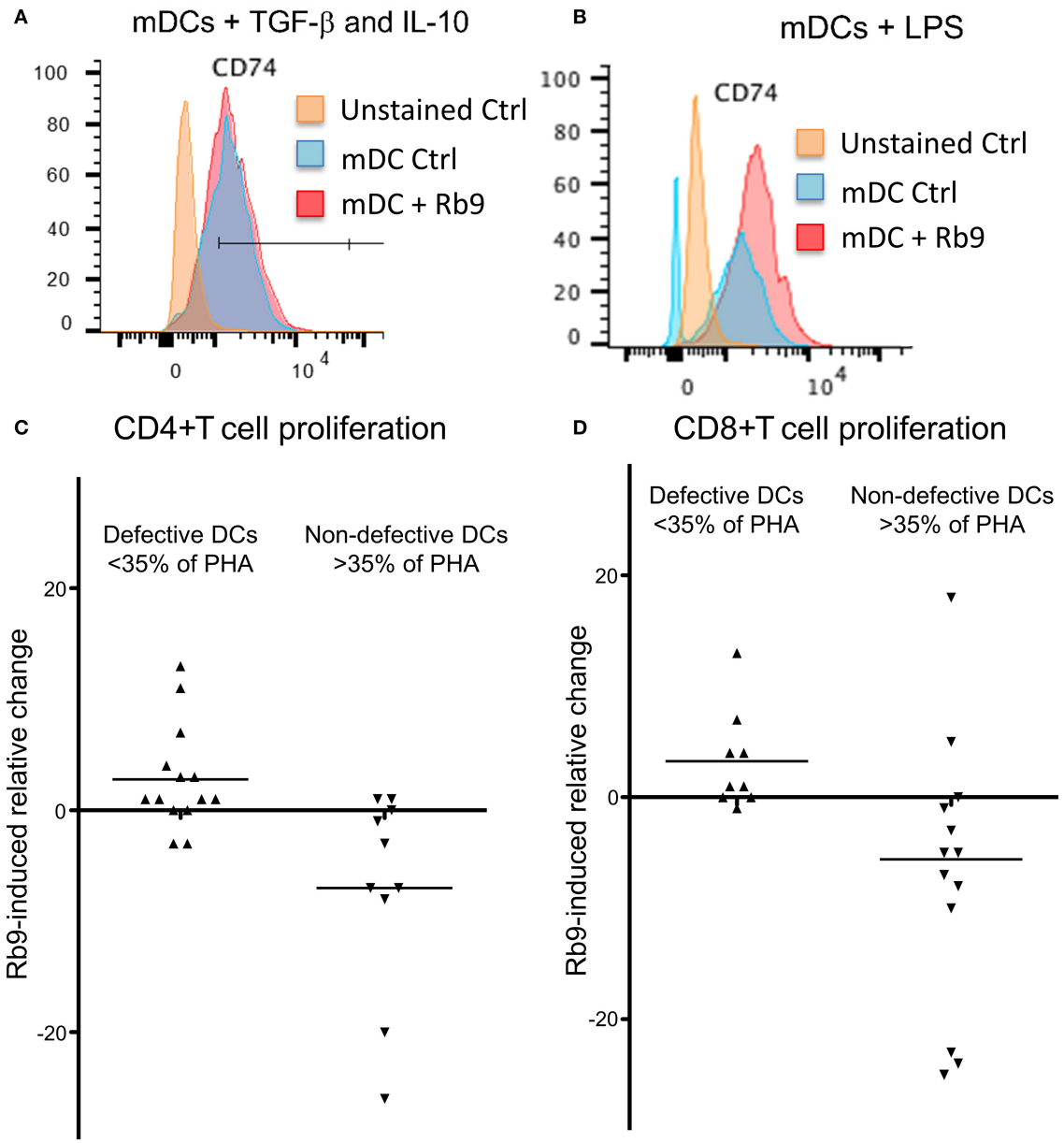

FIGURE 9 | Rb9 treatment of mDCs, from healthy donor and from 22 cancer patients. Ability to stimulate allogeneic lymphocytes' proliferation. Healthy donor' iDCs were stimulated to mDCs with TNF. They were also **(A)** simultaneously treated with TGF-β (10 ng/ml) and IL-10 (1 ng/ml) and further stimulated with Rb9 showing no change in CD74, the MIF receptor; **(B)** treatment with LPS and stimulation with Rb9, caused increased expression of CD74. Allogeneic CD4+ T cell **(C)** and CD8+ T cell **(D)** proliferative responses, were induced by Rb9-treatment of mDC differentiated from 22 cancer patients' PBMC. This depended on the ability of non-treated cancer patients' mDCs to stimulate T cells to proliferate: some had a poor allo-stimulatory activity (<35% the proliferation induced by phytohaemagglutinin, PHA), while others had not this same defective functional phenotype, for both CD4+ and CD8+ T cells. Rb9 treatment increased the lympho-stimulatory proliferation of "defective" mDCs, but decreased the same ability in non-defective mDCs.

lung nodules. As to human monocyte-derived dendritic cells (hu-moDC), Rb9 generally increased the expression of maturation markers and other surface molecules, with or without TNF activation of DCs. Rb9 stimulated lymphocyte proliferation associated to mDCs, further confirmed an immune modulatory activity of the peptide.

Hu-moDC represent an effective alternative for naturally occurring DCs, which due to their scarceness are not suitable for use in clinical protocols, but can be replaced by hu-moDC, that can be generated *in vitro* from easily obtainable precursors (60, 61). Dendritic cell-based vaccines still fail to reach the theoretical potential attributed to them (62), probably because DCs within tumors (39) and from circulating precursors in cancer patients (40) are functionally biased and frequently unable to induce effective anti-tumor T lymphocytes. The correction of this bias is an attractive way to develop cancer immunotherapy.

Presently, the Rb9 effects were analyzed in mDCs from 22 cancer patients' monocytes. These mDCs can be functionally biased; therefore, two groups were set apart, according to their ability to induce allogeneic T cell proliferation. Patients' mDCs, which induced <35% the response to phytohemagglutinin A (PHA) were considered as "defective" and those that induced a response higher than 35% that of PHA, as "normal." Rb9 clearly affected the phenotype of the cells from the "defective" mDC group, but had little effect upon "normal" mDCs. Such variation in Rb9 effects was more significant when the ability to induce allogeneic T cell proliferation was focused on. In this sense, Rb9 showed contrasting effects: it enhanced the ability of "defective" mDC to induce T cell proliferation, whereas it inhibited the lymphostimulatory activity of "normal" mDC. Rb9 was not a simple activator of DCs but, actually, a molecule that induced restoration of function in these cells on both directions. To test this hypothesis, hu-moDCs were generated in conditions that lead to the generation of immune response-inducing DCs or to the generation of tolerance-inducing DCs. For the response-inducing DCs, two different stimuli were used, TNF and LPS. TNF is a stimulus that induces a "mild" activation of the cells, thus resembling a close-to-homeostasis condition, while LPS is a stronger stimulus, signaling a more disturbed environment. For the tolerance-inducing DCs, TGF-beta and IL-10 were used (63). When Rb9 was added to these three different hu-moDCs, all in the presence of GM-CSF and IL-4 both at 50 ng/mL, the immune modulatory effects were evident. While Rb9 little affected the phenotype of TNF-stimulated hu-moDCs, it induced a decreased expression of maturation markers in LPS-stimulated hu-moDCs and an increase in the same markers on [TGF-β+IL-10]-stimulated hu-moDCs. A similar contrasting effect of Rb9 was noticed when the frequency of mature, HLA-DR+CD83+cells was determined, and when cells double positive for the co-stimulatory molecules, CD80 and CD86 were evaluated.

The effects of Rb9 peptide in nature and particularly those that play a role in the defense against tumors are complex, involving a great number of interacting molecules, strictly dependent on the experimental system set up for their investigation. Starting from the peptide protective activity against metastatic melanoma in susceptible mice, we evolved to immunological responses that have a counterpart in human immune mechanisms including cells from human cancers. Some interactions were found relevant to suggest predominant mechanisms of action *in vivo*, quite different from those previously described *in vitro* for the same melanoma cell line, acting directly on the cultured tumor cells without participation of the immune system (22). The anti-tumor protective effect *in vivo* by Rb9 involved mainly dendritic cells, T cell effector lymphocytes, cytokines, and several regulatory mechanisms of which the MIF-CD74 interaction appears to be most relevant. In fact, Rb9 binds to CD74 and to MIF, increases the expression of CD74, modify both the macrophage phenotype, increasing type M1, and bmDC signaling, decreasing pERK, pNF-kB, and pPI3K (alone or with MIF). Rb9 in the murine system also increases IFN-γ, which upregulates CD74, and decreases IL-6 (64) and TGF-β. In human moDCs Rb9 increases CD74 when activated by LPS but not when treated with TGF-β + IL-10. In the latter condition Rb9 decreased the expression of CD44 but not on LPS-activated mo-DCs (**Supplementary Figure 5**). Recently, MIF-CD74 interaction was identified as a regulator of PD-L1 expression, being therefore a target for melanoma treatment (52). In our laboratory, the subcutaneous immunization with shRNA-SOCS1-transduced viable B16F10-Nex2 tumor cells, which inhibited the expression of PD-L1 rendered significant protection against melanoma in the syngeneic model used (65). Whereas, the most aggressive WT B16F10 strain highly expressed PD-L1, the SOCS1 silenced variant, which lacked PD-L1, significantly lost its virulence suggesting a possible cross-interaction. The effects described for Rb9 and the protection against metastatic melanoma may suggest a potential for this peptide to be associated to modern cancer immunotherapeutic procedures.

DATA AVAILABILITY STATEMENT

The raw data supporting the conclusions of this article will be made available by the authors, without undue reservation, to any qualified researcher.

ETHICS STATEMENT

The studies involving human participants were reviewed and approved by Research Ethical Committee (CEP, Brazil) from the Faculty of Medicine, São Paulo University (FMUSP, Brazil). The protocol was approved ref. number 457.616 on Nov 13, 2013. The patients/participants provided their written informed consent to participate in this study. The animal study was reviewed and approved by National Council for the Control of Animal Experimentation (CONCEA, Brazil) and approved by the Ethics Committee of Federal University of São Paulo, registered with the number CEUA 3521121217.

AUTHOR CONTRIBUTIONS

LT, JB, FM, NG, VM, and PB-S conceived and designed the experiments. FM, VM, NG, PB-S, CF, and RA performed the experiments. LT, FM, and JB organized figures and wrote the manuscript. AM and the above authors helped with analysis and interpretation of results and approved the manuscript.

FUNDING

This work was supported by Financiadora de Estudos e Projetos (FINEP) grant 03.14.0198.00 and by Fundação de Amparo à Pesquisa do Estado de São Paulo (FAPESP) grants 2010/51423-0 and 2009/54599-5.

ACKNOWLEDGMENTS

LT was a career fellow of Brazilian National Research Council (CNPq).

SUPPLEMENTARY MATERIAL

The Supplementary Material for this article can be found online at: https://www.frontiersin.org/articles/10.3389/fimmu.2019.03122/full#supplementary-material

Supplementary Figure 1 | Rb9 decreased both colorectal and pancreatic syngeneic s.c. grafted tumors in mice. **(A)** Tumor volume of CT26 cell syngeneic colorectal cancer was measured in i.p. Rb9-treated mice with 300 μg/dose for five alternate days, starting on the first day after tumor cell challenge. The values are means ± SEM and $^{***}p < 0.001$ calculated using a ratio paired Student's *t*-test compared to Vehicle (Veh) treatment; **(B)** Tumor volume of Panc02 cell syngeneic pancreatic cancer was measured in i.p. Rb9-treated mice with 300 μg/dose for 5 alternate days, starting on the first day after tumor cell challenge. Graph represent means ± SD and $^{***}p < 0.001$ calculated using a ratio paired Student's *t*-test compared to Veh treatment. **(C)** Survival curve of mice from previous experiment **(B)**, Panc02 SC tumor model. $^{*}p < 0.01$ calculated using Log-rank (Mantel-Cox) test.

Supplementary Figure 2 | IL-12, TNF, IL-10, and IL-6 secretion in splenocytes from Rb9-treated mice. **(A)** Splenocytes were collected from 17-day tumor-cell challenged mice, treated with i.p Rb9 or Rb10A1 for five alternate days after melanoma cells inoculation. The splenocyte cell culture supernatants were used to measure cytokine secretion after 72 h stimulus with B16F10-Nex2 lysate **(A–D)**. All panels represent means ± SD of triplicate experiments quantified in ELISA assays using cytokine controls.

Supplementary Figure 3 | Effects of Rb9 and MIF treatment on PI3K and IkBα signaling pathways in bmDCs. **(A)** Panels showing Western blotting bands of PI3K p85, pPI3K pr85 (Tyr458), and IkBα, pIkBα (Ser32) from bmDCs, after preincubation or not with 200 μM Rb9 for 6 h, and treated with 1 μg/mL of rMIF for 2, 5, 10, and 20 min; **(B)** Signal intensity of pPI3K p85 T458 showed half decrease in all samples treated with Rb9 or rMIF; **(C)** Signal intensity of pIkBα showed a slight decrease in Rb9-pretreated bmDCs in response to rMIF.

Supplementary Figure 4 | Rb9 treatment of different mDC populations. iDCs obtained from human donor PBMC were stimulated to mDCs with TNF. They were also treated either with TGF-β (10 ng/ml) and IL-10 (1 ng/ml) to raise suppressed DCs or with LPS for activated DCs. Control populations examined in a cytometer expressed DCs gated for: **(A)** CD11c/HLA-DR; **(B)** CD83/HLA-DR; and **(C)** CD80/CD86. These three DC populations were further stimulated with Rb9 and the differential response compared to controls treated with TNF; (TNF) + TGF-β/IL-10 or (TNF) + LPS for significance using $\mathbf{X^2}$ statistics, as shown in **Table 1**.

Supplementary Figure 5 | CD44 and CXCR4 expression in human mDCs induced by different treatments. PBMC from healthy human donors were differentiated into monocyte-derived dendritic cells, maturated with LPS did not respond to Rb9 **(A)**; with TNF and TGF-β and IL-10 stimulation, Rb9 treatment reduced CD44 but not CXCR4 expression **(B)**.

REFERENCES

1. Hanahan D, Weinberg RA. The hallmarks of cancer. *Cell.* (2000) 100:57–70. doi: 10.1016/S0092-8674(00)81683-9
2. Hanahan D, Weinberg RA. Hallmarks of cancer: the next generation. *Cell.* (2011) 144:646–74. doi: 10.1016/j.cell.2011.02.013
3. Lambert AW, Pattabiraman DR, Weinberg RA. Emerging biological principles of metastasis. *Cell.* (2017) 168:670–91. doi: 10.1016/j.cell.2016.11.037
4. Riggi N, Aguet M, Stamenkovic I. Cancer metastasis: a reappraisal of its underlying mechanisms and their relevance to treatment. *Annu Rev Pathol.* (2018) 13:117–40. doi: 10.1146/annurev-pathol-020117-044127
5. Majidi J, Barar J, Baradaran B, Abdolalizadeh J, Omidi Y. Target therapy of cancer: implementation of monoclonal antibodies and nanobodies. *Hum Antibodies.* (2009) 18:81–100. doi: 10.3233/HAB-2009-0204
6. Scott AM, Wolchok JD, Old LJ. Antibody therapy of cancer. *Nat Rev Cancer.* (2012) 12:278–87. doi: 10.1038/nrc3236
7. Yoon S, Kim Y-S, Shim H, Chung J. Current perspectives on therapeutic antibodies. *Biotechnol Bioprocess Eng.* (2010) 15:709–15. doi: 10.1007/s12257-009-3113-1
8. Scott AM, Allison JP, Wolchok JD. Monoclonal antibodies in cancer therapy. *Cancer Immun.* (2012) 12:14.
9. Vacchelli E, Eggermont A, Galon J, Sautès-Fridman C, Zitvogel L, Kroemer G, et al. Trial watch: monoclonal antibodies in cancer therapy. *Oncoimmunology.* (2013) 2:e22789. doi: 10.4161/onci.22789
10. Pento JT. Monoclonal antibodies for the treatment of cancer. *Anticancer Res.* (2017) 37:5935–9. doi: 10.21873/anticanres.12040
11. Darvin P, Toor SM, Sasidharan Nair V, Elkord E. Immune checkpoint inhibitors: recent progress and potential biomarkers. *Exp Mol Med.* (2018) 50:165. doi: 10.1038/s12276-018-0191-1
12. Khavinson VK, Solov'ev AY, Tarnovskaya SI, Lin'kova NS. Mechanism of biological activity of short peptides: cell penetration and epigenetic regulation of gene expression. *Biol Bull Rev.* (2013) 3:451–5. doi: 10.1134/S2079086413060042
13. Vaudry H, Tonon M-C, Vaudry D. Editorial: Trends in regulatory peptides. *Front Endocrinol.* (2018) 9:125. doi: 10.3389/fendo.2018.00125
14. Polonelli L, Pontón J, Elguezabal N, Moragues MD, Casoli C, Pilotti E, et al. Antibody complementarity-determining regions (CDRs) can display differential antimicrobial, antiviral and anti-tumor activities. *PLoS ONE.* (2008) 3:e2371. doi: 10.1371/journal.pone.0002371
15. Magliani W, Conti S, Cunha RLOR, Travassos LR, Polonelli L. Antibodies as crypts of antiinfective and anti-tumor peptides. *Curr Med Chem.* (2009) 16:2305–23. doi: 10.2174/092986709788453104
16. Lim S, Koo J-H, Choi J-M. Use of cell-penetrating peptides in dendritic cell-based vaccination. *Immune Netw.* (2016) 16:33–43. doi: 10.4110/in.2016.16.1.33
17. Richardson JR, Armbruster NS, Günter M, Henes J, Autenrieth SE. Staphylococcus aureus PSM peptides modulate human monocyte-derived dendritic cells to prime regulatory T cells. *Front Immunol.* (2018) 9:2603. doi: 10.3389/fimmu.2018.02603
18. O'Neill DW, Adams S, Bhardwaj N, Pickl WF, Majdic O, Lyman SD, et al. Manipulating dendritic cell biology for the active immunotherapy of cancer. *Blood.* (2004) 104:2235–46. doi: 10.1182/blood-2003-12-4392
19. Huber A, Dammeijer F, Aerts JGJV, Vroman H. Current state of dendritic cell-based immunotherapy: opportunities for *in vitro* antigen loading of different DC subsets? *Front Immunol.* (2018) 9:2804. doi: 10.3389/fimmu.2018.02804
20. Chakraborty S, Rahman T. The difficulties in cancer treatment. *Ecancermedicalscience.* (2012) 6:ed16. doi: 10.3332/ecancer.2012.ed16
21. Kroschinsky F, Stölze1l F, von Bonin S, Beutel G, Kochanek M, Kiehl M, et al. New drugs, new toxicities: severe side effects of modern targeted and immunotherapy of cancer and their management. *Crit Care.* (2017) 21:89. doi: 10.1186/s13054-017-1678-1
22. Girola N, Matsuo AL, Figueiredo CR, Massaoka MH, Farias CF, Arruda DC, et al. The Ig V H complementarity-determining region 3-containing Rb9 peptide, inhibits melanoma cells migration and invasion by interactions with Hsp90 and an adhesion G-protein coupled receptor. *Peptides.* (2016) 85:1–15. doi: 10.1016/j.peptides.2016.08.006
23. Yin BWT, Kiyamova R, Chua R, Caballero OL, Gout I, Gryshkova V, et al. Monoclonal antibody MX35 detects the membrane transporter NaPi2b (SLC34A2) in human carcinomas. *Cancer Immun.* (2008) 8:3.
24. Ritter G, Yin B, Murray A, Mark G, Old LJ, Lloyd K, et al. *Membrane Transporter Napi2b (scl34a2) Epitope for Antibody Therapy, Antibodies Directed Thereto, and Target for Cancer Therapy.* U.S. Patent No: 9,701,755 B2. Washington, DC: U.S. Patent and Trademark Office.
25. dos Santos ML, Yeda FP, Tsuruta LR, Horta BB, Pimenta AA, Degaki TL, et al. Rebmab200, a humanized monoclonal antibody targeting the sodium phosphate transporter NaPi2b displays strong immune mediated cytotoxicity against cancer: a novel reagent for targeted antibody therapy of cancer. *PLoS ONE.* (2013) 8:e70332. doi: 10.1371/journal.pone.0070332

26. Lindegren S, Andrade LNS, Bäck T, Machado CML, Horta BB, Buchpiguel C, et al. Binding affinity, specificity and comparative biodistribution of the parental murine monoclonal antibody MX35 (Anti-NaPi2b) and its humanized version Rebmab200. *PLoS ONE.* (2015) 10:e0126298. doi: 10.1371/journal.pone.0126298
27. Dobroff AS, Rodrigues EG, Moraes JZ, Travassos LR. Protective, anti-tumor monoclonal antibody recognizes a conformational epitope similar to melibiose at the surface of invasive murine melanoma cells. *Hybrid Hybridomics.* (2003) 21:321–31. doi: 10.1089/153685902761022661
28. Lutz MB, Kukutsch NA, Menges M, Rößner S, Schuler G. Culture of bone marrow cells in GM-CSF plus high doses of lipopolysaccharide generates exclusively immature dendritic cells which induce alloantigen-specific CD4 T cell energy *in vitro*. *Eur J Immunol.* (2000) 30:1048–52. doi: 10.1002/(SICI)1521-4141(200004)30:4<1048::AID-IMMU1048>3.0.CO;2-W
29. Lutz MB, Schuler G. Immature, semi-mature and fully mature dendritic cells: which signals induce tolerance or immunity? *Trends Immunol.* (2002) 23:445–9. doi: 10.1016/S1471-4906(02)02281-0
30. Xu Y, Zhan Y, Lew AM, Naik SH, Kershaw MH. Differential development of murine dendritic cells by GM-CSF versus Flt3 ligand has implications for inflammation and trafficking. *J Immunol.* (2007) 179:7577–84. doi: 10.4049/jimmunol.179.11.7577
31. Bolte G, Knauss M, Metzdorf I, Stern M. Dot blot chemiluminescence assay for studying food protein binding to small intestinal brush border membranes *in vitro*. *J Biochem Biophys Methods.* (1997) 34:189–203. doi: 10.1016/S0165-022X(97)01214-1
32. Figueiredo CR, Matsuo AL, Azevedo RA, Massaoka MH, Girola N, Polonelli L, et al. A novel microtubule de-stabilizing complementarity-determining region C36L1 peptide displays anti-tumor activity against melanoma *in vitro* and *in vivo*. *Sci Rep.* (2015) 5:14310. doi: 10.1038/srep14310
33. Rodrigues EG, Garofalo AS, Travassos LR. Endogenous accumulation of IFN-gamma in IFN-gamma-R(-/-) mice increases resistance to B16F10-Nex2 murine melanoma: a model for direct IFN-gamma anti-tumor cytotoxicity *in vitro* and *in vivo*. *Cytokines Cell Mol Ther.* (2002) 7:107–16. doi: 10.1080/13684730310000121
34. Figueiredo CR, Matsuo AL, Massaoka MH, Polonelli L, Travassos LR. Anti-tumor activities of peptides corresponding to conserved complementary determining regions from different immunoglobulins. *Peptides.* (2014) 59:14–9. doi: 10.1016/j.peptides.2014.06.007
35. Bloom BR, Bennett B. Mechanism of a reaction *in vitro* associated with delayed-type hypersensitivity. *Science.* (1966) 153:80–2. doi: 10.1126/science.153.3731.80
36. Conroy H, Mawhinney L, Donnelly SC. Inflammation and cancer: macrophage migration inhibitory factor (MIF)–the potential missing link. *QJM.* (2010) 103:831–6. doi: 10.1093/qjmed/hcq148
37. Soumoy L, Kindt N, Ghanem G, Saussez S, Journe F. Role of macrophage migration inhibitory factor (MIF) in melanoma. *Cancers.* (2019) 11:529. doi: 10.3390/cancers11040529
38. Figueiredo CR, Azevedo RA, Mousdell S, Resende-Lara PT, Ireland L, Santos A, et al. Blockade of MIF-CD74 signalling on macrophages and dendritic cells restores the antitumour immune response against metastatic melanoma. *Front Immunol.* (2018) 9:1132. doi: 10.3389/fimmu.2018.01132
39. Baleeiro RB, Anselmo LB, Soares FA, Pinto CAL, Ramos O, Gross JL, et al. High frequency of immature dendritic cells and altered *in situ* production of interleukin-4 and tumor necrosis factor-α in lung cancer. *Cancer Immunol Immunother.* (2008) 57:1335–45. doi: 10.1007/s00262-008-0468-7
40. Ramos RN, Chin LS, dos Santos APSA, Bergami-Santos PC, Laginha F, Barbuto JAM. Monocyte-derived dendritic cells from breast cancer patients are biased to induce CD4+CD25+Foxp3+ regulatory T cells. *J Leukoc Biol.* (2012) 92:673–82. doi: 10.1189/jlb.0112048
41. Dobroff AS, Rodrigues EG, Juliano MA, Friaça DM, Nakayasu ES, Almeida IC, et al. Differential anti-tumor effects of IgG and IgM monoclonal antibodies and their synthetic complementarity-determining regions directed to new targets of B16F10-Nex2 melanoma cells. *Transl Oncol.* (2010) 3:204–17. doi: 10.1593/tlo.09316
42. Magliani W, Conti S, Giovati L, Zanello PP, Sperindè M, Ciociola T, et al. Antibody Peptide based antifungal immunotherapy. *Front Microbiol.* (2012) 3:190. doi: 10.3389/fmicb.2012.00190
43. Arruda DC, Santos LCP, Melo FM, Pereira F V., Figueiredo CR, Matsuo AL, et al. β-Actin-binding complementarity-determining region 2 of variable heavy chain from monoclonal antibody C7 induces apoptosis in several human tumor cells and is protective against metastatic melanoma. *J Biol Chem.* (2012) 287:14912. doi: 10.1074/jbc.M111.322362
44. Rabaça AN, Arruda DC, Figueiredo CR, Massaoka MH, Farias CF, Tada DB, et al. AC-1001 H3 CDR peptide induces apoptosis and signs of autophagy *in vitro* and exhibits antimetastatic activity in a syngeneic melanoma model. *FEBS Open Biol.* (2016) 6:885–901. doi: 10.1002/2211-5463.12080
45. Gabrielli E, Pericolini E, Cenci E, Ortelli F, Magliani W, Ciociola T, et al. Antibody complementarity-determining regions (CDRs): a bridge between adaptive and innate immunity. *PLoS ONE.* (2009) 4:e8187. doi: 10.1371/journal.pone.0008187
46. Srinivasan M, Roeske R. Immunomodulatory peptides from IgSF proteins: a review. *Curr Protein Pept Sci.* (2005) 6:185–96. doi: 10.2174/1389203053545426
47. Morea V, Tramontano A, Rustici M, Chothia C, Lesk AM. Conformations of the third hypervariable region in the VH domain of immunoglobulins. *J Mol Biol.* (1998) 275:269–94. doi: 10.1006/jmbi.1997.1442
48. Grundy MA, Zhang T, Sentman CL. NK cells rapidly remove B16F10 tumor cells in a perforin and interferon-gamma independent manner *in vivo*. *Cancer Immunol Immunother.* (2007) 56:1153–61. doi: 10.1007/s00262-006-0264-1
49. Sica A, Mantovani A. Macrophage plasticity and polarization: *in vivo* veritas. *J Clin Invest.* (2012) 122:787–95. doi: 10.1172/JCI59643
50. Gordon S, Taylor PR. Monocyte and macrophage heterogeneity. *Nat Rev Immunol.* (2005) 5:953–64. doi: 10.1038/nri1733
51. Nguyen-Pham T-N, Lim M-S, Nguyen TAT, Lee Y-K, Jin C-J, Lee HJ, et al. Type I and II interferons enhance dendritic cell maturation and migration capacity by regulating CD38 and CD74 that have synergistic effects with TLR agonists. *Cell Mol Immunol.* (2011) 8:341–7. doi: 10.1038/cmi.2011.7
52. Imaoka M, Tanese K, Masugi Y, Hayashi M, Sakamoto M. Macrophage migration inhibitory factor- CD 74 interaction regulates the expression of programmed cell death ligand 1 in melanoma cells. *Cancer Sci.* (2019) 110:2273–83. doi: 10.1111/cas.14038
53. Lieberman J. Anatomy of a murder: how cytotoxic T cells and NK cells are activated, develop, and eliminate their targets. *Immunol Rev.* (2010) 235:5–9. doi: 10.1111/j.0105-2896.2010.00914.x
54. Grossman WJ, Verbsky JW, Tollefsen BL, Kemper C, Atkinson JP, Ley TJ. Differential expression of granzymes A and B in human cytotoxic lymphocyte subsets and T regulatory cells. *Blood.* (2004) 104:2840–8. doi: 10.1182/blood-2004-03-0859
55. Mellor-Heineke S, Villanueva J, Jordan MB, Marsh R, Zhang K, Bleesing JJ, et al. Elevated granzyme B in cytotoxic lymphocytes is a signature of immune activation in hemophagocytic lymphohistiocytosis. *Front Immunol.* (2013) 4:72. doi: 10.3389/fimmu.2013.00072
56. Hodge G, Barnawi J, Jurisevic C, Moffat D, Holmes M, Reynolds PN, et al. Lung cancer is associated with decreased expression of perforin, granzyme B and interferon (IFN)-γ by infiltrating lung tissue T cells, natural killer (NK) T-like and NK cells. *Clin Exp Immunol.* (2014) 178:79–85. doi: 10.1111/cei.12392
57. Hsu J, Hodgins JJ, Marathe M, Nicolai CJ, Bourgeois-Daigneault M-C, Trevino TN, et al. Contribution of NK cells to immunotherapy mediated by PD-1/PD-L1 blockade. *J Clin Invest.* (2018) 128:4654–68. doi: 10.1172/JCI99317
58. Chen Z, Yang Y, Liu LL, Lundqvist A. Strategies to augment natural killer (NK) cell activity against solid tumors. *Cancers.* (2019) 11:E1040. doi: 10.3390/cancers11071040
59. Shi L, Lin H, Li G, Sun Y, Shen J, Xu J, et al. Cisplatin enhances NK cells immunotherapy efficacy to suppress HCC progression via altering the androgen receptor (AR)-ULBP2 signals. *Cancer Lett.* (2016) 373:45–56. doi: 10.1016/j.canlet.2016.01.017
60. Inaba K, Steinman RM, Pack MW, Aya H, Inaba M, Sudo T, et al. Identification of proliferating dendritic cell precursors in mouse blood. *J Exp Med.* (1992) 175:1157–67. doi: 10.1084/jem.175.5.1157
61. Sallusto F, Lanzavecchia A. Efficient presentation of soluble antigen by cultured human dendritic cells is maintained by granulocyte/macrophage colony-stimulating factor plus interleukin 4 and downregulated

by tumor necrosis factor alpha. *J Exp Med.* (1994) 179:1109–18. doi: 10.1084/jem.179.4.1109
62. Barbuto JAM. Are dysfunctional monocyte-derived dendritic cells in cancer an explanation for cancer vaccine failures? *Immunotherapy.* (2013) 5:105–7. doi: 10.2217/imt.12.153
63. Rutella S, Danese S, Leone G. Tolerogenic dendritic cells: cytokine modulation comes of age. *Blood.* (2006) 108:1435–40. doi: 10.1182/blood-2006-03-006403
64. Kushiro K, Chu RA, Verma A, Núñez NP. Adipocytes promote B16BL6 melanoma cell invasion and the epithelial-to-mesenchymal transition. *Cancer Microenviron.* (2012) 5:73. doi: 10.1007/s12307-011-0087-2
65. Berzaghi R, Maia VSC, Pereira F V., Melo FM, Guedes MS, Origassa CST, et al. SOCS1 favors the epithelial-mesenchymal transition in melanoma, promotes tumor progression and prevents anti-tumor immunity by PD-L1 expression. *Sci Rep.* (2017) 7:40585. doi: 10.1038/srep40585

Conflict of Interest: LT and JB are scientific advisers for Recepta Bio. FM, NG, VM, and PB-S have been fellows via ProUniemp association in a FAP-UNIFESP Foundation and Recepta Bio sponsored project. AM was an R&D analyst for Recepta Bio.

The remaining authors declare that the research was conducted in the absence of any commercial or financial relationships that could be construed as a potential conflict of interest.

frontiers in Immunology

ORIGINAL RESEARCH
published: 05 June 2020
doi: 10.3389/fimmu.2020.00898

Tumor Arrests DN2 to DN3 Pro T Cell Transition and Promotes Its Conversion to Thymic Dendritic Cells by Reciprocally Regulating Notch1 and Ikaros Signaling

Ipsita Guha[1], Avishek Bhuniya[1], Divanshu Shukla[2†], Ashok Patidar[2†], Partha Nandi[1], Akata Saha[1], Shayani Dasgupta[1], Nilanjan Ganguly[1], Sweta Ghosh[3], Arathi Nair[2], Subrata Majumdar[3], Bhaskar Saha[2], Walter J. Storkus[4], Rathindranath Baral[1‡] and Anamika Bose[1‡]*

[1] Department of Immunoregulation and Immunodiagnostics, Chittaranjan National Cancer Institute (CNCI), Kolkata, India, [2] Department of Pathogenesis and Cell Responses, National Centre for Cell Sciences, Pune, India, [3] Department of Molecular Medicine, Bose Institute, Kolkata, India, [4] Department of Immunology, University of Pittsburgh School of Medicine, Pittsburgh, PA, United States

Tumor progression in the host leads to severe impairment of intrathymic T-cell differentiation/maturation, leading to the paralysis of cellular anti-tumor immunity. Such suppression manifests the erosion of $CD4^+CD8^+$ double-positive (DP) immature thymocytes and a gradual increase in $CD4^-CD8^-$ double negative (DN) early T-cell progenitors. The impact of such changes on the T-cell progenitor pool in the context of cancer remains poorly investigated. Here, we show that tumor progression blocks the transition of $Lin^-Thy1.2^+CD25^+CD44^+c\text{-}Kit^{low}DN2b$ to $Lin^-Thy1.2^+CD25^+CD44^-c\text{-}Kit^-DN3$ in T-cell maturation, instead leading to DN2-T-cell differentiation into dendritic cells (DC). We observed that thymic IL-10 expression is upregulated, particularly at cortico-medullary junctions (CMJ), under conditions of progressive disease, resulting in the termination of $IL\text{-}10R^{high}$ DN2-T-cell maturation due to dysregulated expression of Notch1 and its target, CCR7 (thus restricting these cells to the CMJ). Intrathymic differentiation of T-cell precursors in $IL\text{-}10^{-/-}$ mice and *in vitro* fetal thymic organ cultures revealed that IL-10 promotes the interaction between thymic stromal cells and $Notch1^{low}$ DN2-T cells, thus facilitating these DN2-T cells to differentiate toward $CD45^+CD11c^+MHC\text{-}II^+$ thymic DCs as a consequence of activating the Ikaros/IRF8 signaling axis. We conclude that a novel function of thymically-expressed IL-10 in the tumor-bearing host diverts T-cell differentiation toward a DC pathway, thus limiting the protective adaptive immune repertoire.

Keywords: thymus, T cell, IL-10, DN2b, DC, Cancer

OPEN ACCESS

Edited by:
Jose A. Garcia-Sanz, Consejo Superior de Investigaciones Científicas (CSIC), Spain

Reviewed by:
Rong Jin, Peking University, China
Soldevila Gloria, National Autonomous University of Mexico, Mexico

***Correspondence:**
Anamika Bose
anamikabose2@gmail.com

†These authors have contributed equally to this work

‡These authors share senior authorship

Specialty section:
This article was submitted to Cancer Immunity and Immunotherapy, a section of the journal Frontiers in Immunology

Received: *16 October 2019*
Accepted: *17 April 2020*
Published: *05 June 2020*

Citation:
Guha I, Bhuniya A, Shukla D, Patidar A, Nandi P, Saha A, Dasgupta S, Ganguly N, Ghosh S, Nair A, Majumdar S, Saha B, Storkus WJ, Baral R and Bose A (2020) Tumor Arrests DN2 to DN3 Pro T Cell Transition and Promotes Its Conversion to Thymic Dendritic Cells by Reciprocally Regulating Notch1 and Ikaros Signaling. Front. Immunol. 11:898. doi: 10.3389/fimmu.2020.00898

INTRODUCTION

Immune system decline, dysfunction, and senescence are commonly observed in the setting of cancer progression, with a pronounced restriction amongst $CD8^+$ T effector cells, which are known for their capacity to mediate tumor regression (1). T-cell development occurs primarily in the thymus, even in adults, despite the convention for thymic atrophy post-adolescence (2). Interestingly, several recent reports, including a study by Martinez et al., suggest the maintenance of essential thymopoiesis and T-cell neogenesis in adults, which supports the rejuvenation of the peripheral naïve T-cell pool under pro-inflammatory conditions (3, 4). Moreover, adult thymopoiesis has also been reported to increase after growth hormone therapy (4) and pharmacologic androgenic blockade (5). Furthermore, in HIV-infected patients, thymus-derived $CD4^+$ T cells are known to increase in frequency after antiretroviral therapy (6). In stark contrast, in tumor-bearing hosts, the thymus may contribute principally to the development of regulatory T cells at the expense of effector T cells (7) and/or to the interruption of $CD4^+CD8^+$ DP immature thymocyte programming (8, 9).

The process of T-cell development starts with the migration of CD4 and CD8 negative—the double negative (DN)-lymphoid progenitor cells—from bone marrow to thymus. During progressive differentiation of DN cells, these cells move from the cortico-medullary junction (CMJ) to the sub-capsular region under the direction of chemokine gradients, where they interact with distinct populations of cortical stromal cells (10). Defined by their differential surface expression of CD25, CD44, and c-Kit, DN cells mature through four stages: DN1 ($CD25^-CD44^+$), DN2 ($CD25^+CD44^+$), DN3 ($CD25^+CD44^-$), and DN4 ($CD25^-CD44^-$). During their migration within the thymic cortex, DN4 cells are converted into $CD4^+CD8^+$ double-positive (DP) thymocytes, which are subsequently positively selected for self-MHC restriction. Finally, after negative selection, mature $CD4^+$ or $CD8^+$ T cells in medulla [i.e., single-positive (SP) cells], exit the thymus and enter the peripheral circulation (11, 12). This entire T-cell developmental process occurring within the thymus is strictly regulated by thymic cytokines, chemokines, and a coordinated crosstalk between several transcription factors, including Notch1, TCF, Ikaros, and Pu.1, among others (13–19).

Progressive tumor manifests several immune dysfunctions, including thymic atrophy and cessation of effector T-cell functions. Particularly, $CD8^+$ T cells in tumor hosts show a broad spectrum of dysfunctional states, shaped by various systemic and intra-tumoral suppressive mechanisms. Among these mechanisms, upregulation of PD1, CTLA4, etc. (20, 21) on the T-cell surface and conversion of T cells to Tregs has emerged as an important contributor, which is reflected in decreased effector T cells in response to tumor antigens, thus causing failure of therapy and tumor progression. Moreover, the elicited insults to T-cell function have been found to be both quantitative and qualitative. In GBM patients, a significant deficiency in the production of mature T cells is observed along with thymic involution (22). Recent studies on lymphoma patients also revealed the existence of T-cell dysfunction, with reduced output of thymic emigrants from atrophied thymus (23, 24) suggesting that tumor cell-secreted factors might contribute to blocking intra-thymic T-cell development. In transplantable T-cell lymphoma, murine hosts show tumor growth-dependent immunosuppression, which is correlated well with a block in early T-cell development in atrophied thymus (25). However, a detailed understanding of the role of tumor burden on early T-cell development and the fate of these targeted pre-T cells is lacking.

Herein, we show that progressive growth of tumors in mice leads to a blockade in the transition from the $CD25^+CD44^+$c-Kit^+ DN2 stage to the $CD25^+CD44^-$c-Kit^- DN3 stage of the T-cell maturation program. The decision-making genes like *notch1* (essential for T-cell lineage commitment) become downregulated, and *ikaros/irf8/pu.1* (essential for DC commitment) become upregulated in DN2a, which instruct the conversion to DC instead of T-cell lineage commitment. This process is driven by increased thymic production of IL-10 under tumor condition, which acts on IL-$10R^{high}$ DN2 cells by promoting DC lineage commitment (with assistance from $CD45^-$keratin5^{high} thymic stromal cells). This process differentially regulates *notch1* and *ikaros/irf8* gene transcription in DN2a cells. Tumor-induced IL-10 promotes STAT3 phosphorylation, its subsequent nuclear translocation and binding to *notch1* promoter to silence *notch1* gene transcription. Furthermore, we show that physical contact of IL-10-educated stromal cells with T cells is essential for early T-cell differentiative arrest and the co-option of these precursor cells for differentiation into DC.

MATERIALS AND METHODS

Antibodies and Reagents

RPMI-1640, RF10 (RPMI-1640 + 20 mM HEPES), DMEM high-glucose, and fetal bovine serum (FBS) were purchased from Hi-Media (Mumbai, India). Anti-mouse biotin-conjugated antibodies (lineage cocktail–biotin, and Thy1.2-biotin), anti-mouse fluorescence conjugated antibodies (CD4-FITC, CD8-PE, CD44-FITC, CD25-PE, c-Kit- PE/cy5.5 MHCII-FITC, and CD11c-PE), purified anti-mouse antibodies (CD4, CD8, CD45, Ki67, STAT3, IKAROS, IRF8, IL-10, and IL-10R), and CytoFix/CytoPerm solutions were procured from BD-Pharmingen or Biolegend (San Diego, CA, USA). Anti-pSTAT3 antibody and rmIL-10 were purchased from BD Biosciences (San Jose, CA). Aminoethylcarbazole (AEC) chromogen solution, and aqueous mounting media were procured from VECTOR Laboratories Inc. (Burlingame, CA).

Mice and Tumor

Wild-type (Wt) female C57BL/6 and Swiss mice (age: 4–6 weeks, body weight: 20–25 g on average) were obtained from Animal

Abbreviations: DN, Double negative; DP, Double positive; SP, Single positive; DC, Dendritic cell; S180, Sarcoma 180; FTOC, Fetal thymic organ culture; IRF8, Interferon Regulatory Factor 8; Lin^-, Lineage negative; CMJ, Cortico medullary junction; dGuo-2′, deoxyguanosine; BrdU, 5′-Bromo-2′-deoxyuridine; TEC, Thymic epithelial cell.

Facilities of the National Institute of Nutrition (Hyderabad, India). IL-$10^{-/-}$ mice were procured from Jackson Laboratories (Bar Harber, ME) and subsequently bred at the National Center for Cell Science (Pune, India). The care of animals was carried out according to the guidelines established by the Institutional Animal Care and Ethics Committee (IAEC Approval No. IAEC-1774/RB-4/2015/6 and IAEC-1774/RB-19/2017/15). Autoclaved dry pellets and water were provided *ad libitum*.

Tumor Growth and Development

Tumor-bearing mice were euthanized by overdose of Ketamine HCl (160 mg/kg) + Xylazine (20 mg/Kg) by intraperitoneal injection. They were euthanized if tumor size reached 20 mm in either direction, if the animal looked sick, or if any necrosis of tumor was observed. The overall health of animals was monitored twice a day and once in holidays. Animal death and abnormal symptoms, if any, were recorded thoroughly. Mice were monitored and cared for according to the guidelines established by the Institutional Animal Care and Ethics committee, CNCI, Kolkata.

Tumor Growth Measurement

Swiss and C57BL/6 mice ($n = 10$ in each group; two groups; normal and tumor) were inoculated s.c. with syngenic sarcoma 180 (1×10^6 cells/mice), B16F10 melanoma (2×10^5 cells/mice), or Lewis lung carcinoma (LLC) (2×10^5 cells/mice) cells in the lower right flank to establish solid tumors. Tumor growth was then monitored bi-weekly using calipers. Tumor size was recorded in mm^2 (as the product of length × width), and mice were sacrificed after euthanasia when tumor had reached a size of 20 mm in any direction.

Fetal Thymic Organ Culture (FTOC)

Mice fetal thymic pieces (Gestation period E14.5) were dissected and cultured as previously described for a total of 7 days [(26), **Supplementary Figure 4**]. Dissected thymic lobes were placed on 0.8 μm membrane on an anti-wrap sponge at the liquid/air interface in six-well plates containing 2 ml of medium (DMEM high-glucose supplemented with 10% FBS, glutamine, and penicillin/streptomycin). Twenty-four hours later, GSI 953 (CPD11, 50 μM final concentration, delivered in DMSO) or the solvent DMSO alone was added at 12-h intervals over the next 3 days (27). After 3 days in culture, 10 ng/ml of rmIL-10 (BD Biosciences, San Diego, USA) was added to the FTOC medium to simulate tumor-induced thymic alterations. Three days later, single cells were prepared by collagenase (1 mg/ml) treatment for phenotypic analysis.

DN Thymocytes and Thymic Stromal Cell Co-culture

$CD4^-CD8^-$ DN T cells were isolated (>95% pure) from mouse thymus by negative selection using BD IMag Anti-Mouse CD4 and CD8 Particles-DM (BD Biosciences, San Diego, CA). DN-T cells were cultured in complete RPMI-1640 medium (Invitrogen, Camarillo, CA). Fetal thymic organs (FTOs) from wild-type and IL-$10^{-/-}$ were cultured in DMEM high-glucose with 2′-deoxyguanosine (dGuo, Sigma Aldrich, St. Louis, USA) to a final concentration of 1.35 mM for 5 days. After 5 days, fetal thymic lobes were treated with collagenase (1 mg/ml) for single-cell preparation to isolate stromal cells. DN-T cells and stromal cells (28) were pretreated with mrIL-10 (10 ng/ml) for 24 h before their subsequent co-culture for an additional 24 h.

RT-PCR and Quantitative Real-Time PCR

Cellular RNA was isolated using Trizol (Invitrogen, Camarillo, CA), and random hexamers were used to generate corresponding cDNA (First Strand cDNA Synthesis Kit; Fermentas, Hanover, MD). RT-PCR amplification was performed using 2X Go Taq Green Mix (Promega, Madison, USA), and quantitative real-time PCR was performed by SYBR green (Roche, Germany). PCR was done with the following program: 94°C for 5 min; 35 cycles of 94°C for 30 s, 54–57°C for 30 s, and 72°C for 1 min; 72°C for 5 min. PCR products were identified by image analysis software for gel documentation (Versadoc; BioRad Laboratories, Hercules, CA) after electrophoresis on 1.5% agarose gels and stained with ethidium bromide (Sigma-Aldrich, St Louis, USA). RT-PCR primers were designed and purchased from MWG-Biotech (Bangalore, India). In quantitative PCR, after calculating the Ct value, expression fold change was analyzed.

Flow-Cytometric Staining

Thymocytes were isolated from normal and tumor-bearing hosts. The lineage negative Thy1.2 positive population was obtained by removal of mature lineage positive cells using cocktails of biotinylated lineage antibodies: anti-B220, anti-TER119, anti-CD11b (Mac-1), anti-Gr-1, and anti-CD3ε (Biolegend, San Diego, CA), followed by negative selection using BD IMag streptavidin particles-DM (BD Biosciences, San Diego, CA); Thy1.2 positive cells were isolated by positive selection using BD IMag anti-mouse Thy1.2 (CD 90.2) biotin streptavidin particles-DM (Biolegend, San Diego, CA), then those cells were sorted based on CD44 and CD25 expression using a FACSAria cell sorter (Becton Dickinson, Mountainview, CA). Flow cytometry was used to determine cell-surface phenotypes after first staining cells (1×10^6) with fluorescently labeled antibodies (specific and isotype-matched controls). After incubation for 30 min at 4°C in the dark, labeled cells were washed twice with FACS buffer (0.1% BSA in PBS) before flow-cytometric analysis. Similarly, intracellular molecules (i.e., Notch1, Ikaros, and IRF8) were stained with anti-mouse fluorescence-labeled antibodies using Cytofix/Cytoperm reagents per the manufacturer's protocol (BD Biosciences, San Diego, CA). For Ki67 staining, 70–80% chilled ethanol was added to fix the pelleted cells (1.5×10^7 cells) with vortexing, followed by incubation at −20°C for 2 h. Fixed cells were then washed twice with staining buffer and centrifuged (10 min, 200 × g), then diluted to a concentration of 1×10^7 cells/ml for staining and corollary flow-cytometry analyses. Cells were then fixed with 1% paraformaldehyde in PBS; acquisition was performed using a FACS Calibur (Becton Dickinson, Mountainview, CA) along with suitable negative isotype controls. For assessment of cellular apoptosis, fixed cells were stained with AnnexinV and PI by FITC-AnnexinV apoptosis detection kit I (BD, Biosciences, San Jose, CA). The percentage of positively stained populations was determined

using quadrant statistics established using Cell Quest (Becton Dickinson, Mountainview, CA) and FlowJo software (Tree Star, Ashland, OR).

Immunohistochemistry of Thymus Section

Thymus tissue samples were prepared (paraffin-embedded and frozen sample), and 5-μm sections were stained, as previously reported (29), with anti-mouse IL-10 antibody (Biolegend, San Diego, USA). Imaging was done by ZEISS Primo Star microscope, Zeiss (Zena, Germany), and laser capture microdissection was done by ZIESS PALM/APOSTOME (Zena, Germany) laser capture microscope.

Fluorescence Imaging of Thymus Sections

Tumor tissue samples were prepared from frozen sections by cryostat sectioning, and 5-μm sections were stained as previously reported (30). FITC-conjugated anti-mouse CD44 and PE-conjugated anti-mouse CD25 or matching isotype controls (all from BD Biosciences, San Jose, CA) were used. Imaging was performed using a ZEISS LSM-710 confocal microscope (Zena, Germany). Images were analyzed by ImageJ software, https://imagej.net>Fiji. The co-localization index was expressed by Mander's coefficient. A value close to 1 indicates reliable co-localization.

BrdU Labeling-Based Proliferation Assay

For detection of the thymic T-cell proliferation in the presence of tumor conditioning, a BrdU Labeling and Detection Kit I (Roche Diagnostics, Mannheim, Germany) was used per the manufacturer's instructions. Mice were injected intravenously with the BrdU labeling reagent (concentration 10 μM, dose 300 μl/25 gm body weight; two doses with a 4-h interval), with animals euthanized 1 h after the final injection and organs harvested for further studies. BrdU was detected with primary monoclonal anti-BrdU and secondary anti-mouse Ig FITC antibodies. T-cell proliferation was analyzed by flow cytometry.

siRNA-Mediated STAT3 and Ikaros Silencing

STAT3 siRNA (Santacruz Biotechnology, Dallas, TX) was procured, and Ikaros siRNA was prepared with a Silencer® siRNA construction kit (Life Technologies, USA). For Ikaros siRNA preparation, first sense 5′AATGGGGAAGAATGTGCA GAGCCTGTCTC-3′ and antisense 5′-CTCTGCACATTTCTT CCCCATTCCTGTCTC-3′ primer were taken, and siRNA was prepared as per manufacturer protocol. Both the siRNAs were added in FTOC to a final concentration of 100 nM (50 μM/25 μl). In different experimental setups, siRNA and lipofectamine-2000 reagent (Invitrogen, USA) (6 μl) were added to two Opti-MEM aliquots (250 μl each) and incubated for 5 min at RT (31). The siRNA/Opti-MEM and the Lipofectamine/Opti-MEM (500 μl total volume) were mixed and allowed to incubate for 20 min at RT. siRNA-containing medium was then added to the FTO culture. IL-10 (10 ng/ml) was added to the FTOC medium to mimic the tumor-induced thymic alteration. Finally, STAT3 and Ikaros expression were checked both in untreated and siRNA-transfected FTOCs by FACS staining. In siRNA-treated cells, STAT3 expression was confirmed to be reduced to 30% and Ikaros expression to be reduced to 50% of the control siRNA-treated cells.

CD49d-Mediated Inhibition of Extra-Thymic DC Homing

CD49d (Integrin-4α) neutralizing antibody (Invitrogen, California, USA) was used to inhibit extra-thymic DC homing in tumor host. Tumor-bearing mice were injected intra-peritoneally with the CD49d neutralizing antibody (concentration 1 mg/ml, dose 62.5 μg/25 gm body weight; 4 doses with 48 h interval over a period of 8 days), with animals euthanized the day after the final injection and organs harvested for further studies.

Statistical Analysis

All reported results represent the mean ± SE of data obtained in either 4–6 (for *in vivo* analysis) or 3–6 (*in vitro* assays) independent experiments. Statistical significance was determined using an unpaired *t*-test and one-way ANOVA followed by Tukey's multiple comparison in INSTAT3 Software (Graphpad, CA, USA). Differences between groups attaining a $p < 0.05$ are considered significant.

RESULTS

Tumor-Induced Thymic Atrophy Is Associated With the Early Arrest of T-Cell Differentiation

Immune suppression in the cancer-bearing host has previously been associated with involution or atrophy of the thymus, the primary site of T-cell development and education (32, 33). We confirmed thymic atrophy in the face of tumor progression in three mouse tumor models, including lung carcinoma (Lewis lung), sarcoma (S180), and melanoma (B16F10) (**Figures 1A1, A2**). Because T-cell development begins with $CD4^-CD8^-$DN pro-T cells that subsequently pass through four well-defined maturation stages, we next analyzed $Lin^-Thy1.2^+$DN subpopulations based on their differential expression of CD25 (IL-2Rβ), CD44 (pg1), and CD117 (c-Kit). Flow-cytometric analyses revealed significant alterations in the Lin-$Thy1.2^+$ DN2, DN3, and DN4 subpopulations ($CD25^-CD44^+$c-Kit^- DN1, $CD25^+CD44^+$c-Kit^+ DN2, $CD25^+CD44^-$c-Kit^- DN3, and $CD25^-CD44^-$c-Kit^- DN4) isolated from the thymi of tumor-bearing mice vs. control tumor-free mice (**Figures 1B,C**). As shown in **Figures 1B–D**, the proportions of early T-cell progenitors (DN1 to DN3 and particularly DN2) were markedly increased in tumor-bearing mice, while late-stage T-cell progenitors (DN4) were decreased, implying a blockade in T-cell precursor transition through normal differentiation programming. These alterations became more pronounced on day 25 of tumor growth (mean tumor size, 250–270 mm^2) when compared to day-11 tumors (mean tumor size, 70–80 mm^2) (**Figures 1C,D**). In order to identify the exact stage of the blockade in DN-T-cell transition, we next examined the status of the DN2a ($CD25^+CD44^+$c-Kit^{high}) and DN2b ($CD25^+CD44^+$c-Kit^{low}) subpopulations within the

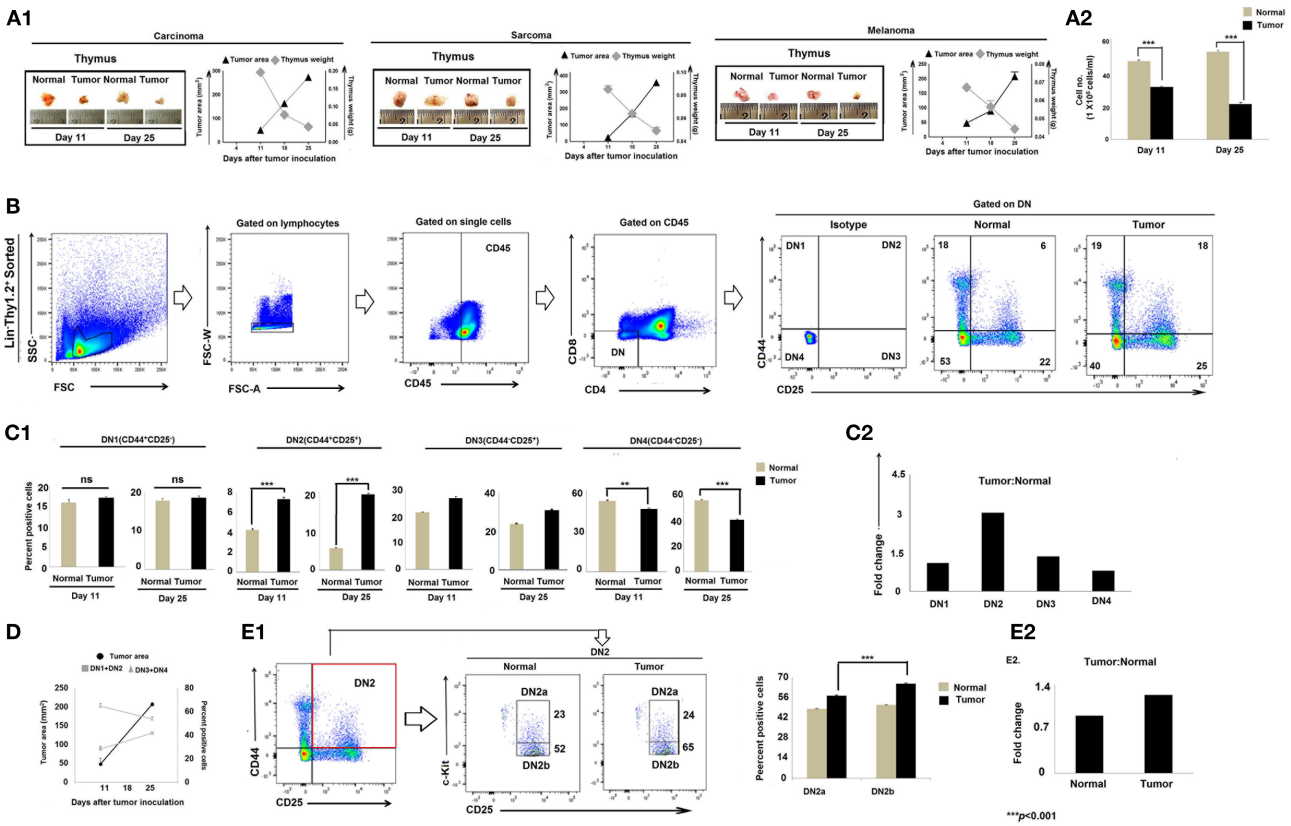

FIGURE 1 | Tumor-induced thymic atrophy is associated with arrest of DN pro-T cell maturation. **(A1)** Representative figures of thymi normal and tumor (carcinoma, melanoma, and sarcoma)-bearing mice on days 11 and 25 after tumor inoculation, along with line diagrams of tumor area (mm^2) vs. thymic weight (gm); $n = 12$ in each case. **(A2)** Bar diagram representing total thymocyte number from normal and tumor-bearing mice; $n = 12$ in each case. **(B)** Thymic T cells sorted based on Lin^- $Thy1.2^+$ phenotype and flow-cytometric analysis of CD25 and CD44 represent DN1 to DN4 T cells of normal and tumor-bearing mice. **(C1)** Bar diagrammatic representations of mean ± SE of positive percentage of $Lin^-Thy1.2^+$ DN1 ($CD25^-CD44^+$), DN2 ($CD25^+CD44^+$), DN3 ($CD25^+CD44^-$), and DN4 ($CD25^-CD44^-$) T cells, respectively, from normal and tumor-bearing mice; $n = 4$ in each case, $^{***}p < 0.001$. **(C2)** Bar diagrammatic representation of the fold change of the DN1 to DN4 population of tumor:normal, $n = 4$. **(D)** Line diagram of percentage positive T cells (DN1+DN2 vs. DN3+DN4) and tumor area (mm^2) of tumor-bearing mice on different days after tumor inoculation. **(E1)** Flow-cytometric representations of $Lin^-Thy1.2^+$-sorted T cells with CD25, CD44, and c-Kit staining, indicating the percentage of DN2a and DN2b cells. Bar diagrammatic representation of positive percentage of DN2a ($CD25^+CD44^+c\text{-}Kit^{high}$) and DN2b ($CD25^+CD44^+c\text{-}Kit^{low}$) cells from normal and tumor hosts; mean ± SE; $n = 4$ in each case, $^{***}p < 0.01$. **(E2)** Bar diagrammatic representation of the fold change of DN2a:DN2b expression from normal and tumor-bearing mice, $n = 4$.

tumor-conditioned thymi. We observed that, in tumor-bearing mice, the DN2-to-DN3 transition was arrested (**Figures 1E1,E2**). These results suggest that progressive tumor growth restricts the early stages of T-cell differentiation in the thymus at the DN2b-to-DN3 transition stage.

Accumulation of Early DN2 Pro-T Cells in Tumor-Bearing Mice Is Not Associated With Enhanced Proliferation of DN2 Cells or Enhanced Apoptosis of DN3 Cells

As numbers of $CD25^+CD44^+c\text{-}kit^+$ DN2 cells increase in tumor-bearing mice, we evaluated whether tumor progression led to enhanced DN2-cell proliferation. Control and tumor-bearing mice were injected twice with BrdU (300 µl/25 gm body weight at 4-h intervals), and thymi were harvested 1 h after the final injection. $CD25^+CD44^+$ DN2 cells stained with an anti-BrdU detection antibody indicated that there was a modest decrease in total $BrdU^+$ thymic cells in tumor progressors; however, proliferation amongst $BrdU^+$ DN2 cells remained unchanged in control vs. tumor-bearing mice (**Figure 2A**). As a confirmatory analysis, expression of the nuclear proliferation antigen Ki67 was used as an endpoint index in flow cytometry assay, which also revealed comparable DN2-cell proliferation in control vs. tumor-bearing mice (**Figure 2B**).

Since numbers of DN3 cells waned in tumor-bearing mice, we next examined whether the reduction in DN3 cells in tumor-conditioned mice was due to enhanced rates of apoptosis. We observed insignificant changes in Annexin-V^+ DN3 populations in the tumor-bearing mice when compared to tumor-free control mice (**Figure 2C**). These observations ruled out the possibility that heightened proliferation or enhanced apoptosis accounts for the observed increase in DN2 cells or the reduced count of DN3 cells, respectively, in the thymus of tumor-bearing mice.

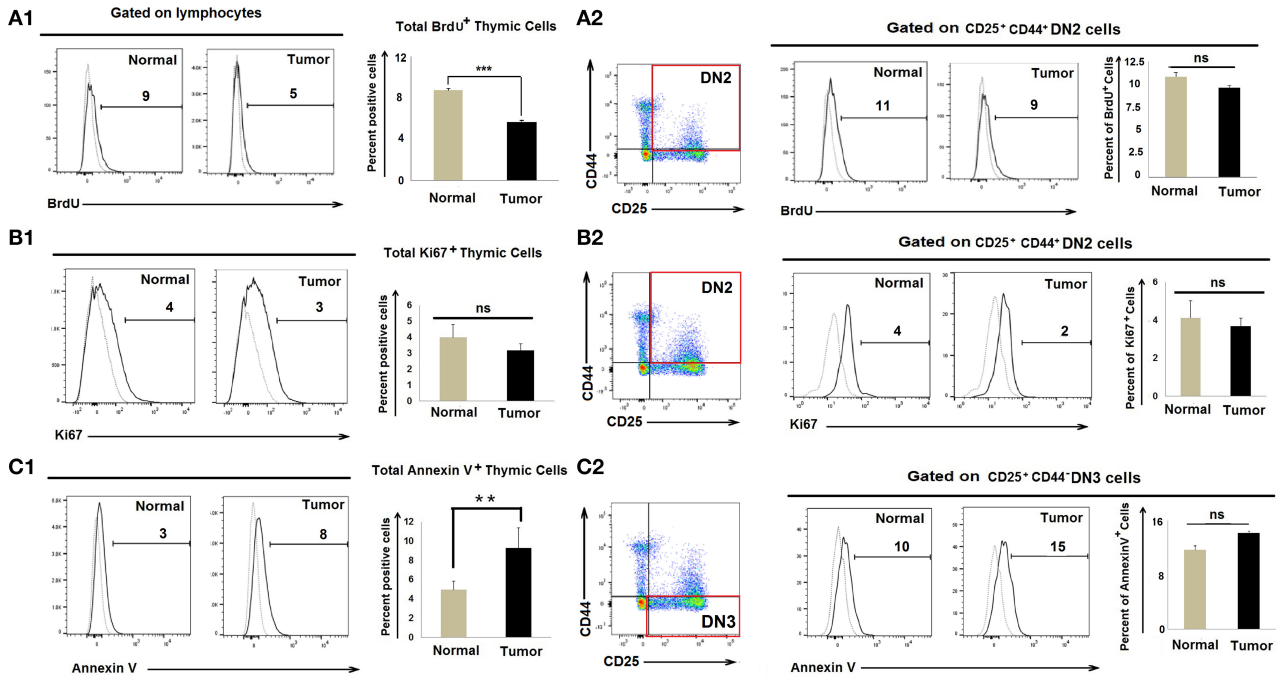

FIGURE 2 | Accumulation of DN2b T cells associated with neither proliferation nor apoptosis: Flow cytometric analysis as presented by histograms and bar diagrams of total BrdU **(A1)**, Ki67$^+$ **(B1)**, and AnnexinV$^+$ **(C1)** cells from thymi of normal and tumor-bearing mice. Dotted line represents isotype control. Similar analysis of CD25$^+$CD44$^+$BrdU$^+$ **(A2)**, CD25$^+$CD44$^+$Ki67$^+$ **(B2)**, and CD25$^+$CD44$^+$AnnexinV$^+$ **(C2)** cells from normal and tumor-bearing mice, where dotted line represents FMO; mean ± SE are shown in bar diagrams ($n = 3$ in each case); $^{**}p < 0.01$, $^{***}p < 0.001$.

CCR7 Downregulation Is Associated With Impaired DN2-to-DN3 Transition in Tumor-Bearing Mice

Migration of T-cell progenitors through a distinct stromal microenvironment is required for sequential interactions with cortical and medullary stromal cells that educate T cells during their development in the thymus (34). Given our findings for DN2→DN3 arrest in tumor-bearing mice, we next evaluated the expression of chemokines and their corresponding receptors associated with the trafficking of pro-T cells within the thymic microenvironment. Expressions of various CC, CXC chemokines and respective receptors like CCR4, CCR9, and CCR7, etc., were studied using RT-PCR or flow cytometry. Analysis of the total thymic cell population suggests insignificant changes in CCL17 (ligand for CCR4) and a modest decrease in CCL19 (ligands for CCR7) at day 25 but a drastic reduction in expression of CCL21 (ligands for CCR7) when comparing thymi harvested from tumor-bearing vs. control mice (**Figure 3A**). Expression of chemokine receptors also varied greatly among the different subpopulations of DN cells isolated from the thymus of tumor-bearing vs. control animals. Notably, the expression of CCR7 was strongly reduced in association with tumor progression in DN2 cells at both the transcript and protein levels (**Figures 3B,C**) while remaining unchanged in the DN1 and DN4 subsets (*data not shown*). Under normal conditions, *ccr7* expression was highest in the DN2 and DN3 subsets and lowest in the DN1 and DN4 subsets. Remarkably, immunofluorescence analyses revealed a more pronounced localization of CD25$^+$CD44$^+$ DN2 T cells at cortico-medullary junctions of thymus in tumor-bearing vs. tumor-free mice (**Figure 3D**). These data suggest significant alterations in CCR7 expression at the DN2 stage and expression of CCR7 ligands (CCL19 and CCL21) in the thymus that may be associated with arrest in T-cell maturation in the tumor-bearing host.

DN2b Cells Are Diverted to DC Programming Based on Suppressed Expression of Notch1 and Increased Expression of Ikaros in DN2a Cells

CCR7 expression is regulated by Notch1, a known controller of thymic pro-T-cell development (35, 36). Given our finding of reduced expression of *ccr7* in the tumor-conditioned DN2 subpopulation and the arrest of these cells for further T-cell lineage commitment and maturation, we next examined *notch1* expression amongst the various DN subpopulations. RT-PCR analysis of sorted DN2 cells revealed a significant loss of *notch1* gene expression in thymus on days 11 and 25 in tumor-bearing mice vs. control mice (**Figure 4A**). These DN2 cells also expressed significantly higher levels of *ikaros, irf8*, and Pu.1 (**Figure 4A**). Given the increased expressions of *ikaros, irf8*, and *pu.*1 along with decreased expression of *notch1* in the thymic DN2 population of the tumor host, we further analyzed these genes within the flow-sorted-DN2a and DN2b population by quantitative real-time PCR. Expressions of *ikaros* and *pu.1*

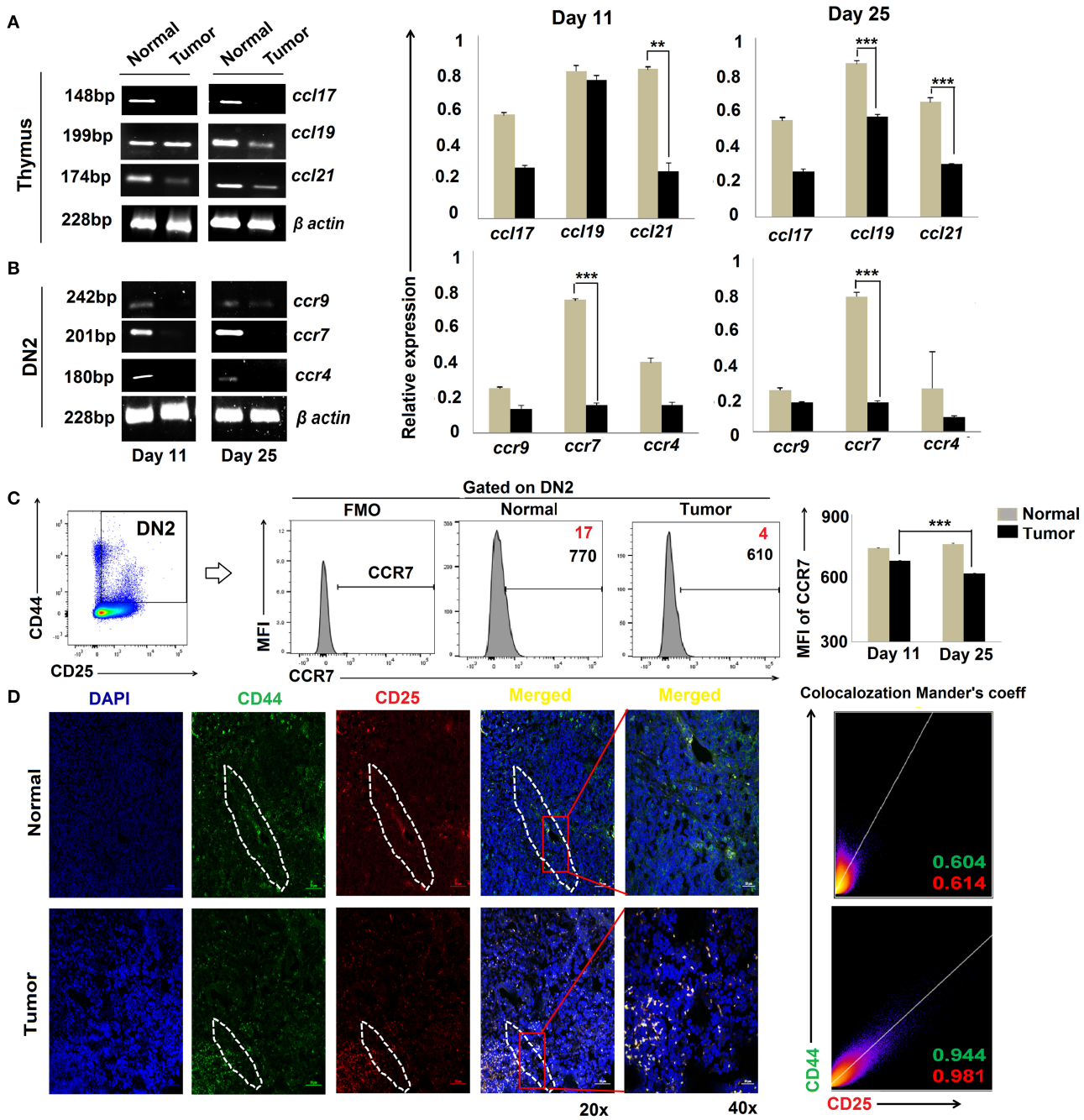

FIGURE 3 | Altered chemokine and chemokine ligand expressions are associated with tumor induced-arrest of DN2-to-DN3 transition: **(A)** Total thymic cells from normal and tumor hosts on days 11 and 25 ($n = 4$ in each group) were isolated to purify mRNA, and expressions of different chemokine ligands (*ccl17*, *ccl19*, and *ccl21)* were assessed by RT-PCR, keeping β-actin as a loading control. Bar diagrams show the mean ± SE of expression of *ccl17*, *ccl19,* and *ccl21* from normal and tumor host on days 11 and 25, respectively ($n = 3$); $^{**}p < 0.01$, $^{***}p < 0.001$. **(B)** Total thymic sorted DN2 ($CD25^+CD44^+$) cells were used to isolate mRNAs and analyzed by RT-PCR for different chemokine genes, e.g., *ccr9*, *ccr7*, and *ccr4*, from normal and tumor hosts on days 11 and 25 ($n = 4$ in each group), keeping β-actin as a loading control. Representative gene expression pattern is shown in panels. Bar diagrams show the mean ± SE of expression of *ccr9*, *ccr7*, and *ccr4* from normal and tumor host on days 11 and 25 ($n = 4$); $^{**}p < 0.01$, $^{***}p < 0.001$. **(C)** Flow-cytometric analysis of $CD25^+CD44^+CCR7^+$ thymic cells from normal and tumor-bearing mice. Representative histograms for CCR7 on $CD25^+CD44^+$(DN2) gated cells, and bar diagrammatic representation shows the mean ± SE of percentage positive $CD25^+CD44^+CCR7^+$ cells, where positive percentages of cells are shown in red, and bar diagram represents the mean ± SE of MFI of $CD25^+CD44^+CCR7^+$ cells; $n = 4$ in each group; $^{***}p < 0.001$. **(D)** Immunofluorescence staining was performed with CD25-PE and CD44-FITC on thymuses from normal and tumor hosts. Representative DAPI, CD44-FITC, CD25-PE, and merged figures of stained tissues show single staining and the co-localization of CD25 and CD44 in tissues from normal and tumor hosts. Dotted regions indicate the $CD44^+CD25^+$-localized CMJ regions in both cohorts. Representative 2D intensity histogram represents co-localization of CD25 and CD44; Manders' co-efficient represents the intensity and index of co-localization. Value close to 1 indicates reliable co-localization.

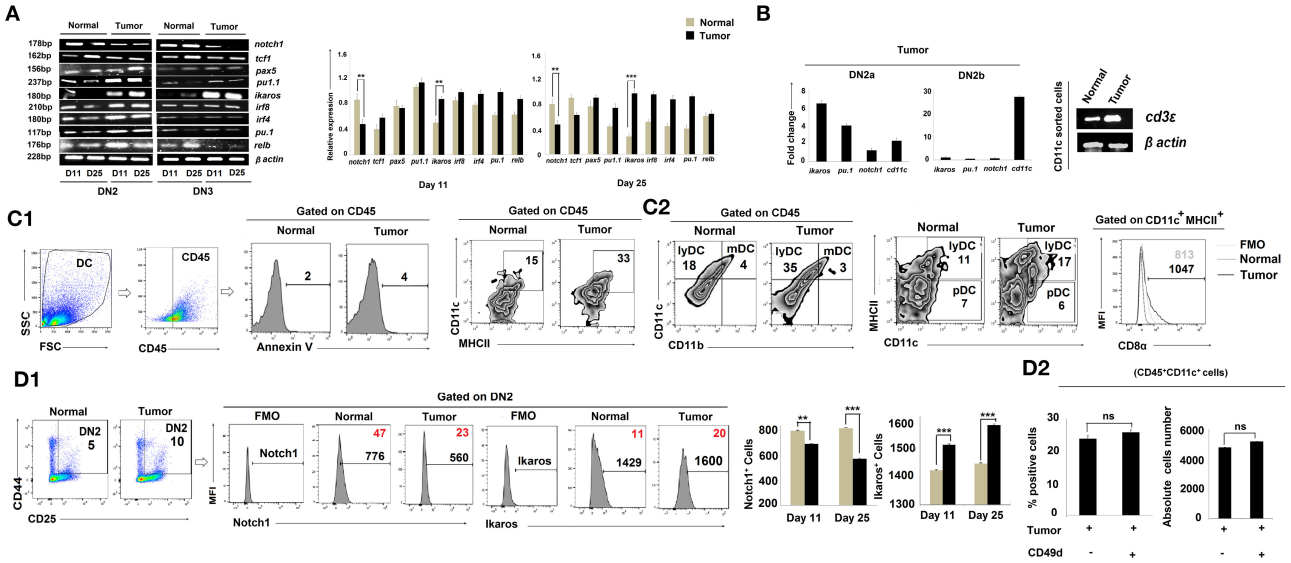

FIGURE 4 | Tumor microenvironment induces DC lineage commitment of DN2 pro-T cells. **(A)** Thymic T cells from normal and tumor hosts were sorted for $CD25^+CD44^+$ and $CD25^+CD44^-$ cells as DN2 and DN3 by flow cytometry on days 11 and 25 after tumor inoculation. Different gene expressions for different transcription factors were checked by RT-PCR using mRNA from thymic T cells, keeping β-actin as a loading control. *notch1* and *tcf1* were checked for T cells, *pax5* for B cells, *pu1.1* for macrophages, and *ikaros*, *irf8*, *irf4*, *pu.1*, and *relb* for myeloid lineage commitment. Representative expression patterns of genes are presented in the left panel along with bar diagrams showing mean ± SE of expression of mentioned transcription factors from normal and tumor hosts on days 11 and 25, respectively ($n = 4$); $^{**}p < 0.01$, $^{***}p < 0.001$. **(B)** Thymic T cells from normal and tumor hosts were sorted for $CD25^+CD44^+$c-Kit^{high} and $CD25^+CD44^+$c-Kit^{low} cells as DN2a and DN2b by flow-cytometry on day 25 after tumor inoculation. From the mRNA, different gene expressions were checked by quantitative real-time PCR, keeping β-actin as a housekeeping gene. Ct values were calculated, and fold change of Ct value against experimental control was represented by mean ± SE in a bar diagram ($n = 3$). The right panel shows the gene expression pattern of *cd3ε* from $CD11c^+$-sorted thymic cells from normal and tumor hosts using β-actin as a loading control. **(C1,C2)** The total percentages of dendritic cells of normal and tumor-bearing mice were checked by flow cytometry. Thymic cells were stained with CD45, Annexin V, CD11c, MHCII, CD11b, and CD8α. Gating strategies of staining are shown, and flow-cytometric representations of $CD45^+CD11c^+MHCII^+$, $CD45^+CD11b^-CD11c^+$ (lymphoid DC), $CD45^+CD11b^+CD11c^+$ (myeloid DC), $CD11c^+MHCII^{high}CD8\alpha^+$ (lymphoid DC), and $CD11c^+MHCII^{low}CD8\alpha^+$ (Plasmocytoid DC) cells reveal the number of total dendritic cells. **(D1)** Further validation of Notch1 and Ikaros expression was performed by flow cytometry along with DN2 (CD25, c-Kit) markers from thymic T cells. In histograms, positive percentages of cells are in red. Bar diagrams represent mean ± SE of percentage of $DN2^+Notch1^+$and $DN2^+Ikaros^+$ ($n = 4$) cells, respectively; $^{**}p < 0.01$, $^{***}p < 0.001$. **(D2)** Increased population of thymus from tumor host was checked after CD49d treatment (4 doses with 48 h interval over a period of 8 days). $CD45^+CD11c^+$ dendritic-cell population of thymus from B16 tumor host with or without CD49d treatment was checked by flow cytometry. Bar diagrams represent mean ± SE of percentage positive $CD45^+CD11c^+$ dendritic-cell population (left panel) and absolute cell numbers (right panel) of $CD45^+CD11c^+$ thymic cells from tumor host.

were significantly elevated and that of *notch1* was decreased in the DN2a population isolated from tumor host compared to the same from normal host, while expression of *cd11c* became upregulated in the DN2b population isolated from tumor host (**Figure 4B**). Since pu.1 serves a critical role in intrathymic DC development, and both Ikaros and IRF8 are critically associated with extra-thymic lineage commitment of DC, we next surveyed for the composition of lymphoid, myeloid, and plasmacytoid DC subsets within thymus. Flow-cytometric analysis suggested that tumor progression (from days 11 to 25) results in increased frequencies of $CD45^+CD11c^{high}CD11b^-MHCII^{high}$ lymphoid-DC, with the majority of DCs exhibiting a $CD8\alpha^+$ phenotype and expressed a significant amount of *cd3*ε (**Figures 4B,C1,C2**). Likewise, flow-cytometric analysis also suggested an increased percentage of $CD4^-CD8^-CD25^+CD44^+Ikaros^+$ cells and a downregulation in $CD4^-CD8^-CD25^+CD44^+Notch1^+$ cells within the thymus of tumor-bearing vs. control mice (**Figure 4D1**). We also checked for expression of other crucial transcription factors required for B-cell, macrophage, and T-cell lineage commitment in the various DN subpopulations. We observed no significant alterations in expression of *pax5* (B cells) and *pu1.1* (macrophages) in the tumor-bearing vs. control cohorts (**Figure 4A**). Furthermore, there were no significant alterations in the percentages of B cells and macrophages within the thymus, regardless of tumor status in the animals (*data not shown*). However, as shown in **Figure 4A**, expression of the T-cell lineage commitment marker *tcf1* was decreased in DN2 and DN3 cells sorted from the thymus of day-25 tumor-bearing mice compared to normal control mice. To check the possible contribution of extra-thymic/circulating DC in the enhanced DC pool in the thymus of tumor host, we next treated tumor-bearing mice with a neutralizing antibody for CD49d (37) for 8 days (4 times over a period of 8 days). Although such treatment increases the thymus volume, it failed to affect the number of $CD11c^+$ cells within the CD45 gated population (**Figure 4D2**), thereby excluding the possibility of homing of extrathymic DC. These aggregate data suggest that the reciprocal regulation of Notch1 and Ikaros in DN2 subpopulations in the thymus of

tumor-bearing mice instigates early arrest of T-cell development at the DN2a stage and its diversion toward the DC lineage.

Reciprocal Notch1 and Ikaros Regulation by IL-10 Impacts DN2b T-Cell Arrest

As the cytokine microenvironment within the thymus critically regulates T-cell development (38) and is perturbed by tumor conditioning (39), we assessed cytokines for their role(s) in reciprocally regulating Notch1 and Ikaros/IRF8 expression in arrested T cells. Cytokines relevant to thymic regulation such as *il-2, il-4, il-6, il-7, il-10, il-15*, and *tgfβ* were monitored amongst total thymic cell populations using RT-PCR. Our results suggest that tumor-induced arrest of DN2 T cells in the thymus is correlated with a significant increase in *il-10* transcription and a coordinated reduction in *il-7* and *il-15* transcription (**Figure 5A**).

To critically understand the role of upregulated IL-10, we next studied thymic early T-cell development in IL-$10^{-/-}$ mice. Although the thymus was atrophied in all IL-$10^{-/-}$ mice (regardless of tumor status), percentages of DN2 were reduced, and DN3 and DN4 subpopulations increased, in IL-$10^{-/-}$ vs. control tumor-bearing animals (**Figure 5B1**). Flow-cytometric analysis supported increased Notch1 protein expression but decreased Ikaros and IRF8 protein expression by DN2a and DN2b cells isolated from tumor-bearing IL-$10^{-/-}$ mice (**Figures 5B2,B3**, **Supplementary Figure 1**), suggesting a pivotal role of IL-10 in the reciprocal regulation of Notch1 and Ikaros signaling, leading to the arrest of T-cell maturation at the DN2 stage. *Notch1* expression was also increased and Ikaros/IRF8 expression decreased in the DN2 population isolated from tumor-bearing IL-$10^{-/-}$ mice as compared to wild-type tumor-bearing mice (**Figure 5C**).

Increased Dendritic-Cell Population and Lineage Commitment Regulated by the IL-10-Dependent Notch1/Ikaros Signaling Pathway

To further understand the regulatory network formed between Notch1, Ikaros, and IL-10, we turned to analyses of *in vitro* fetal thymus organ cultures (FTOC). Fetal thymus lobes from pregnant mice (E 14.5) were cultured for 3 days (22) and treated with rIL-10 to mimic *in vivo* tumor-conditioning (**Figure 6A1**). In the total thymocyte population, we first checked the Annexin V expression to exclude dead cells (**Figure 6A2**). Corollary analyses of $CD45^+CD11c^+MHCII^+$ cells revealed an increase in DC frequencies in IL-10-treated cultures (**Figure 6A3**). DN subpopulations were then analyzed based on differential expression of CD25, CD44, and c-kit. Flow-cytometric analyses revealed higher percentages of the DN2 subpopulation in IL-10-treated FTOC than in control cultures (**Figure 6A4**). These analyses also suggested an increased percentage of $CD4^-CD8^-CD25^+$ c-$kit^+Ikaros^+$ cells in IL-10-treated groups, with a significant decrease in Notch1 expression by DN2 cells (**Figure 6A4**). Since Notch1 expression was reduced in IL-10-conditioned early arrest of T cells in FTOC, we next evaluated the impact of adding gamma secretase inhibitor-953 (Cpd11) to FTOC to block Notch1 downstream signaling (**Figure 6A4**) (40). Consistent with our evolving operational paradigm, inhibition of Notch1 signaling resulted in arrest in DN2 populations while increasing Ikaros expression and promoting the accumulation of $CD45^+CD11c^+MHCII^+$ DCs in FTOC (**Figure 6A5**). Next, to validate the association between upregulated expression of Ikaros and termination in T-cell lineage commitment and its differentiation to DC, we performed knockdown of *ikaros* by ikaros-specific siRNA. A significant absence of ikaros (by 50%) results in a decrease in the DC population with a simultaneous release in the arrest of the DN2 population, which normalizes lineage commitment (**Figure 6A5**, **Supplementary Figure 2**).

Since STAT3 is essential in IL-10 signaling, we further decided to assess the impact of silencing STAT3 using specific siRNA in FTOC (**Figures 6B1,B2**). Silencing of STAT3 was determined to significantly ameliorate the regulatory effects of IL-10, leading to the rescue of (normal) DN2→DN3 transition in concert with normalized Notch1 and Ikaros expression (**Figure 6B3**).

As IL-10 failed to induce DN2→DN3 arrest in the absence of STAT3 (in concert with upregulated Notch1 expression), we next investigated the nucleotide sequence of the mouse *notch1* gene for the presence of putative STAT3 binding sites. In the nucleus, activated and tyrosine-phosphorylated STAT3 binds to the DNA-response elements (i.e., interferon-γ-activated sequence; GAS) found in the promoter regions of target genes (41). GAS is a nine-base-pair palindrome, having the consensus sequence TTCCGGGAA. Interestingly, we found four sites within introns just after the promoter region having the sequence 5′-TTCACAGAA-3′ from 991 to 999 bp (first site), 5′-TTCCCAGAA-3′ from 3,179 to 3,187 bp (second site), 5′-TTCCATGAA-3′ from 5,773 to 5,781 bp (third site), and 5′-TTCTAAGAA-3′ from 10,583 to 10,591 bp (fourth site) that were highly similar to the consensus GAS sequence (**Figure 6B4**). Accordingly, we performed ChIP assays to examine the binding of pSTAT3 to the *notch1* gene. Unstimulated control DN2 T cells show virtually no binding of pSTAT3 to the *notch1* gene at any site, while IL-10 pretreatment significantly augmented binding of pSTAT3 to the *notch1* gene at the second site, i.e., from 3,179 to 3,187 bp (**Figure 6B4**). These data suggest that IL-10-conditioning promotes direct binding of pSTAT3 to the GAS motif of the *notch1* gene, leading to reduced *notch1* gene expression and the differentiative arrest of DN2 T cells.

IL-10-Treated Stromal Cells Reprogram IL-$10R^{High}$ DN2 Cells Toward DC Differentiation in the Tumor-Bearing Host

Since IL-10 controlled early arrest of DN2 T cells, we profiled IL-10 receptor expression on DN1-DN4 cells. Flow-cytometric analysis revealed an increase in the expression of IL-10R (CD210) in Lin-$thy1.2^+CD25^+CD44^+$ DN2 T-cells isolated from the thymus of tumor-bearing vs. control, tumor-free mice (**Figure 7A**). An immunohistochemical analysis of the IL-10 protein expression pattern in thymus suggested focused expression in cortico-medullary junctions (**Figure 7B**), where accumulation of early T cells is commonly observed. Laser capture micro-dissection of the IL-10^{high} region followed by mRNA analysis suggested $keratin5^+$ thymic cortical epithelial

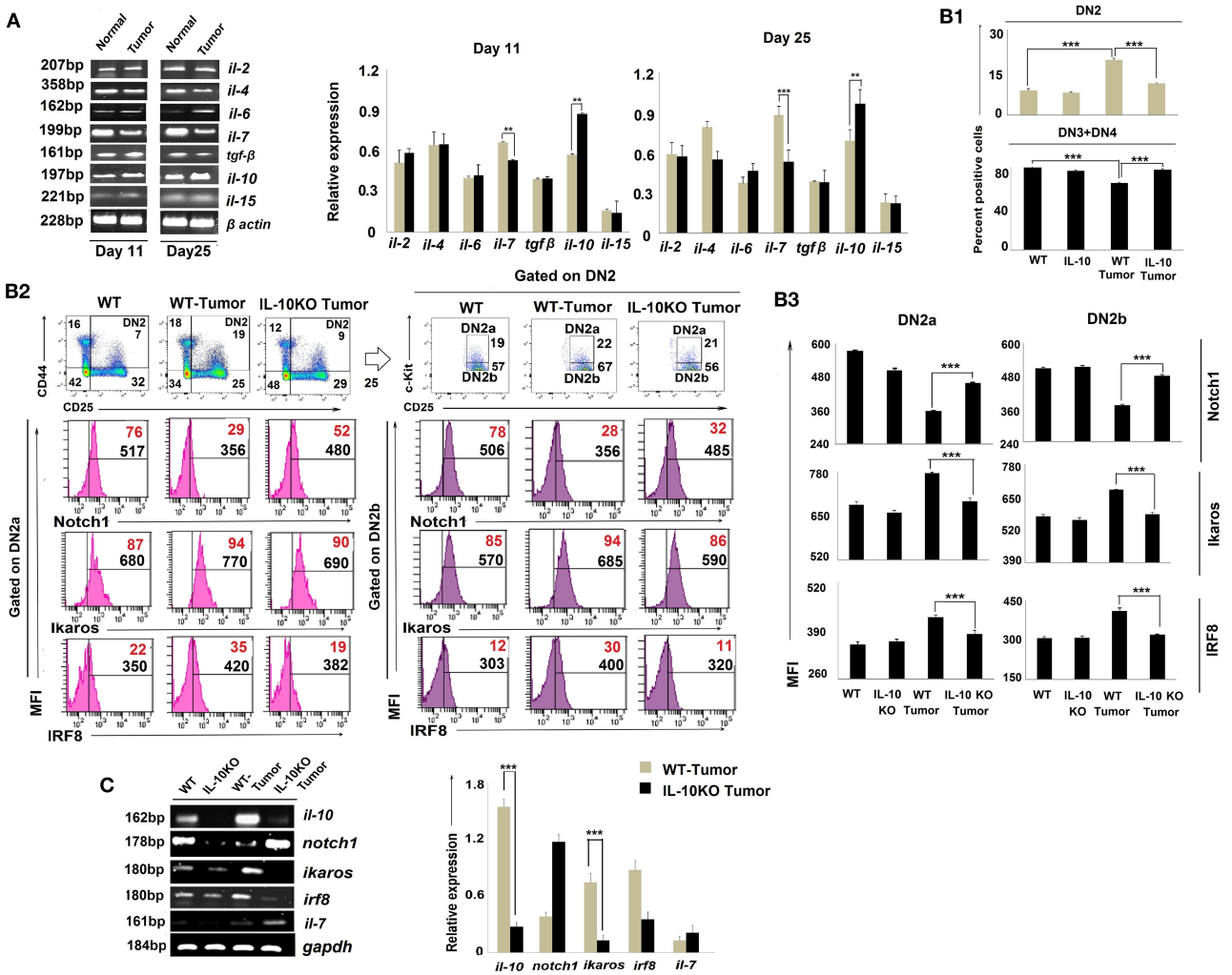

FIGURE 5 | IL-10 promotes tumor-induced early arrest of DN2 pro-T cells by reciprocal regulation of Notch1 and Ikaros signaling. **(A)** mRNA was isolated from thymi of normal and tumor hosts, and cytokine (*il-2, il-4, il-6, il-7, il-10, il-15*, and *tgfβ*) profiles were assessed by RT-PCR, keeping β-actin as a loading control. Representative figures of gene expression profile are shown in the left panel and bar diagrammatic representations of mean ± SE of relative expression of above-mentioned cytokines from normal and tumor hosts on days 11 and 25 following tumor inoculation, respectively, are shown in the right panel, $n = 3$; $^{**}p < 0.01$, $^{***}p < 0.001$. **(B1)** Thymic T cells were isolated from non-tumor (wild-type and IL-$10^{-/-}$) and tumor (wild-type and IL-$10^{-/-}$) mice. DN2, DN3, and DN4 cells were stained with CD45, CD4, CD8, CD25, CD44, and c-Kit. Gating strategies are shown in **Supplementary Figure 1**. Bar diagrams represent the mean ± SE percentage of DN2 and DN3+DN4 positive cells from the above-mentioned mice, respectively. **(B2)** Representative figures of flow cytometric analysis performed with CD45, CD4, CD8, CD44, CD25, c-Kit, Ikaros, IRF8, and Notch1 in thymic T cells from wild-type and IL-$10^{-/-}$ tumor-bearing mice. Histograms show MFI and positive percentages of cells of DN2a$^+$Notch1$^+$, DN2a$^+$ Ikaros$^+$, DN2a$^+$IRF8$^+$ DN2b$^+$Notch1$^+$, DN2b$^+$ Ikaros$^+$ and DN2b$^+$IRF8$^+$. **(B3)** Bar diagrams showing mean ± SE of MFI values of Notch1$^+$, Ikaros$^+$, and IRF8$^+$ within DN2a and DN2b cells, respectively, from the mice mentioned in B2. **(C)** Cytokine and transcription factor profiles were assessed in sorted DN2 cells from non-tumor (wild-type and IL-$10^{-/-}$) and tumor (wild-type and IL-$10^{-/-}$) mice by analyzing *il-10, notch1, ikaros, irf8*, and *il-7* gene expressions by RT-PCR, keeping gapdh as a loading control. Representative figures along with bar diagram show mean ± SE of different gene expressions from the above-mentioned mice. $n = 4$ in each group; *p*-values are mentioned in figure.

cells as a major source of IL-10, along with CD11c$^+$ thymic DCs (**Figure 7B**).

In order to examine whether thymic epithelial cell (TEC)-secreted IL-10 was sufficient to induce both blockade and lineage-switching in early T-cell developmental programming, we established *in vitro* co-culture trans-well assays using purified populations of DN2 cells and stromal cells in the presence and absence of rmIL-10 (**Figure 7C1**, **Supplementary Figure 3**). We observed that while rmIL-10 alone was moderately effective in promoting the arrest of DN2 cells (**Figure 7C2**), it failed to promote the T-DC differentiative switching. Maximum DN2 arrest and coordinate T-DC differentiation were observed only when IL-10 was used to pretreat stromal cells that were then co-cultured with IL-10-pretreated DN T cells. Physical separation of DN T cells from stromal cells had no effect on T-cell maturation or in early T-cell arrest (**Figure 7C2**). Therefore,

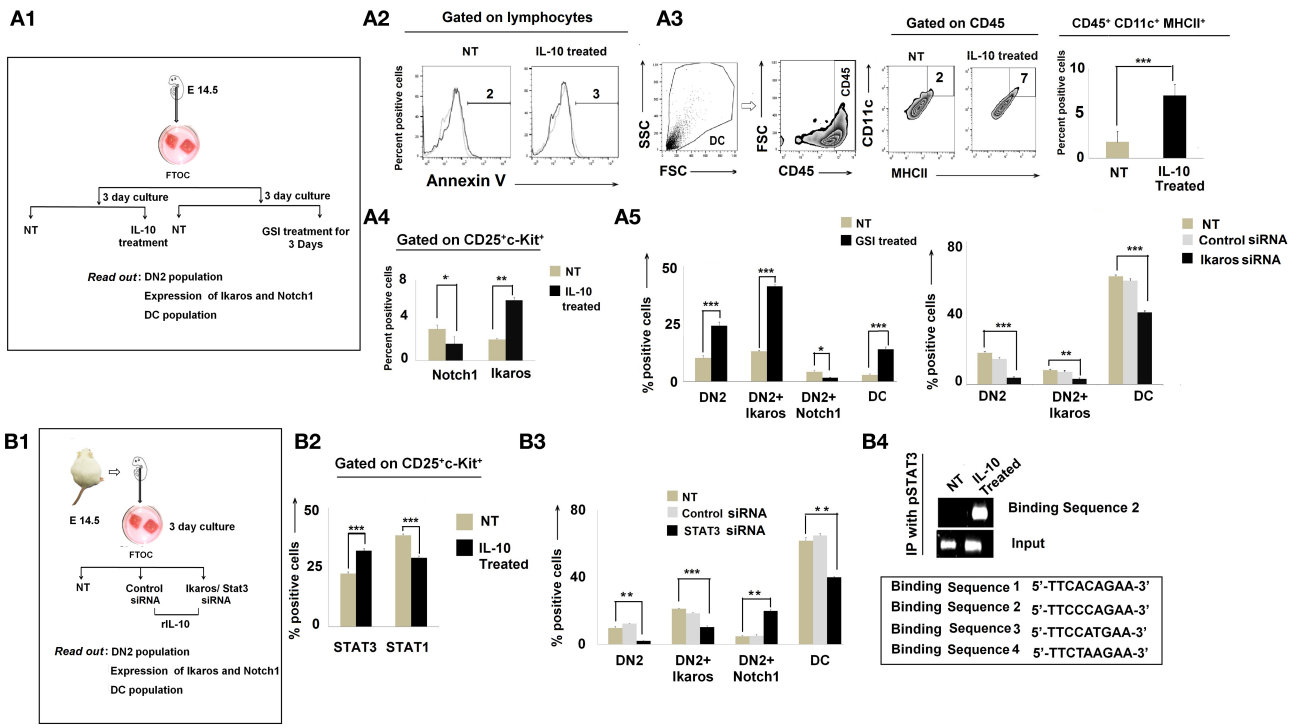

FIGURE 6 | IL-10 promotes DN2-to-dendritic cell lineage differentiation by Notch1/Ikaros signaling. **(A1)** Workflow diagram of the experimental design of fetal thymic organ culture (FTOC) using the fetuses of E14.5 pregnant mice. **(A2)** Total lymphocyte populations of FTOC were analyzed by Annexin V. Histograms of Annexin V^+ flow-cytometry results. Dotted line represents the isotype control. **(A3)** Total dendritic-cell population was checked in FTOC ± IL-10 treatment cohort. Representations of flow-cytometry results of $CD11c^+MHCII^+$ cells, gated on $CD45^+$ cells, and a bar diagram showing mean ± SE of percentage positive $CD45^+CD11c^+MHCII^+$ cells from either untreated or IL-10-treated FTOC. $n = 3$; $^{***}p<0.001$. **(A4)** Bar diagram to represent $DN2^+Notch1^+$ and $DN2^+Ikaros^+$ cells from ± IL-10-treated FTOC, $n = 3$; $^*p < 0.05$, $^{**}p < 0.01$ **(A5)** Bar diagrammatic representations of the mean ± SE of $DN2^+$, $DN2^+Ikaros^+$, and $DN2^+Notch1^+$ cells and DC population from untreated and GSI-treated cohorts in left panel along with mean ± SE of $DN2^+$, $DN2^+Ikaros^+$ cells, and $CD45^+CD11c^+MHCII^+$ DC population from untreated, control siRNA-treated, and Ikaros siRNA-treated cohorts in right panel, $n = 3$; $^{***}p < 0.001$, $^{**}p < 0.01$, $^*p < 0.05$. **(B1)** Workflow representing STAT3 and Ikaros silencing experiments with FTOC. **(B2)** Bar diagrammatic representation of mean ± SE of percentage of $DN2^+STAT3^+$ and $DN2^+STAT1^+$ cells in ± IL-10-treated cohort, $n = 3$; $^{***}p<0.001$ **(B3)** Flow-cytometric analysis was performed; bar diagram showing mean ± SE of percentage of $DN2^+$, $DN2^+Ikaros^+$, $DN2^+Notch1^+$ and $CD45^+CD11c^+MHCII^+$ DC population from untreated, control siRNA-treated and STAT3 siRNA-treated cohorts, $n = 3$; $^{***}p < 0.001$, $^{**}p<0.01$. **(B4)** ChIP assay for pSTAT3 recruitment to the putative binding site downstream of the Notch1 promoter. Gene expression patterns of different binding sites show that upon IL-10 treatment, a specific binding site (binding sequence 2) of the downstream region of Notch1 promoter sequenced 5′ TTCCCAGAA 3′ becomes bound by pSTAT3 and Notch1 becomes downregulated.

physical interaction between IL-10-conditioned stromal cells and DN T cells is required for DN2→DN3 arrest and the redirection of DN2→DC differentiation programming.

DISCUSSION

Progressively growing tumors in both human and mice are associated with host thymic atrophy, leading to alterations in T-cell proliferation, apoptosis, and/or differentiation programming, yielding paralysis in adaptive anti-tumor immunity (8, 42). Although the thymus undergoes age-related senescence after puberty, recent data suggest that extraneous stimuli, including inflammation, can reinvigorate thymopoiesis (6). One caveat in such thymic reactivation is that resultant T cells may be predominantly regulatory (Treg) vs. effector (T_{eff}) in nature, a detriment to effective host protection against cancer. In the present study, our major findings include the following. (i) Tumor progression is associated with an early arrest in transition between the DN2 to DN3 stages of T-cell maturation in the thymus. (ii) Tumor-induced IL-10 interferes with the interaction between thymic stromal cells and IL-$10R^{high}$ DN2 T cells to arrest their development. (iii) IL-10 counter-regulates Notch1 and Ikaros/IRF8 signaling while suppressing the expression of Notch1 target gene *ccr7* on DN2 T cells. (iv) This process instead shunts DN2b T-cell commitment toward DC differentiation (**Figure 8**).

T-cell maturation in the thymus is initiated from $Lin^-CD4^-CD8^-CD25^-CD44^+c\text{-}Kit^+DN1$ precursor cells, which subsequently pass through an ordered series of developmental stages, namely DN1-DN2-DN3-DN4-DP-SP, to maintain the supply of mature T cells circulating in the periphery of the host. Thymic T-cell output is drastically reduced in the vast majority of malignant diseases (43). In line with this observation, we noted an accumulation of $CD4^-CD8^-$(DN) thymocytes in tumor-bearing host in total thymocytes and in the lineage negative and thy1.2 positive population (**Supplementary Figure 5**). Consistent with previous

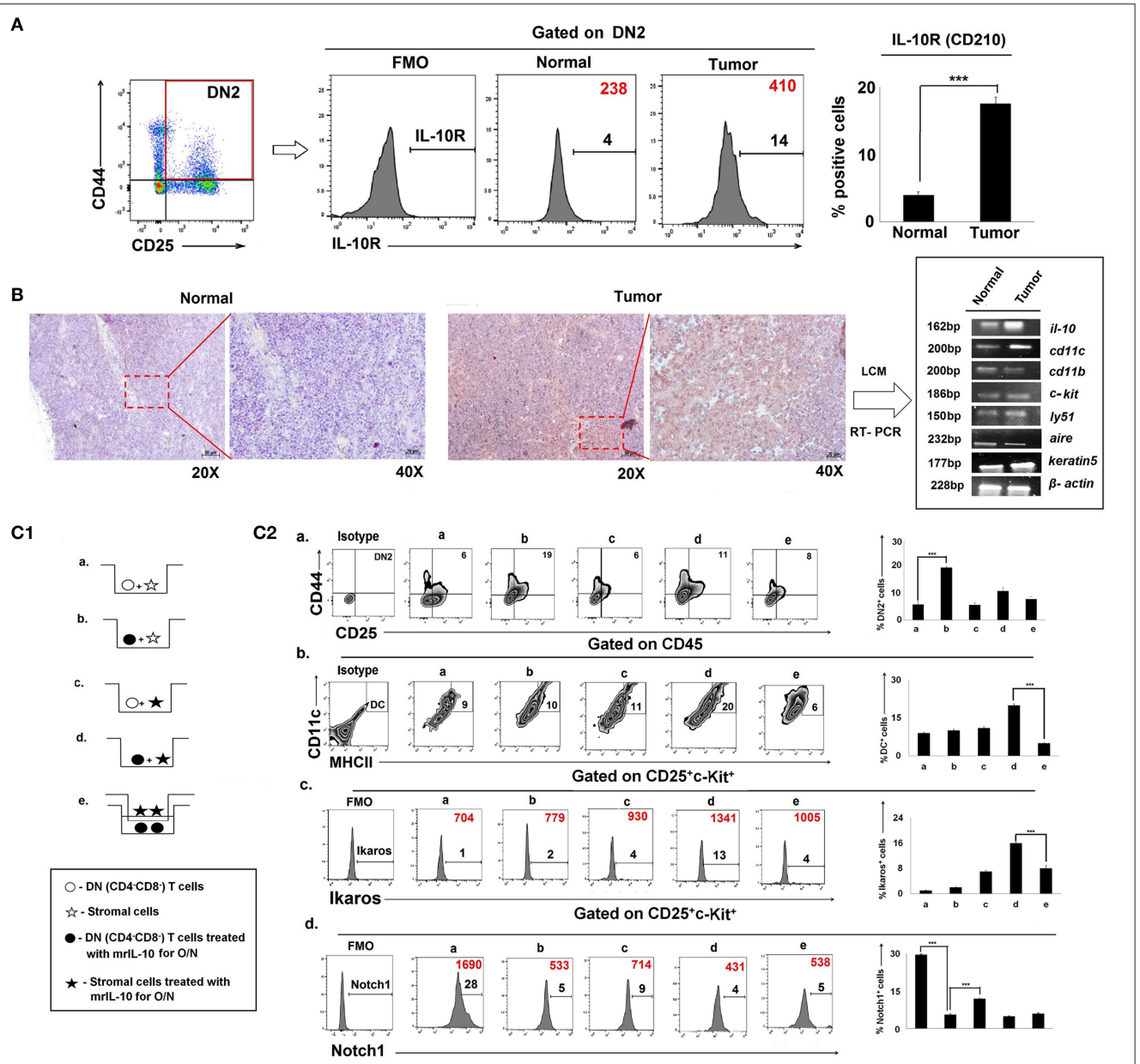

FIGURE 7 | Physical interaction between IL-10R^{high} T cells and stromal cells is required in tumor-induced early arrest and switching of DN2 pro-T cells toward DCs: **(A)** IL-10 receptors in thymic DN2 T cells are represented by flow-cytometric histograms (positive percentages are written in black, and MFI values are written in red). Bar diagram represents mean of positive percentages ± SE; $n = 3$, $^{***}p < 0.001$. **(B)** IL-10-rich zone in thymi of normal and tumor hosts was identified immunohistochemically. IL-10-rich regions, i.e., cortico-medullary region of thymus, are shown in 20× and 40× magnification, and these zones were isolated using a laser capture microscope to analyze the gene expression using mRNA by RT-PCR, keeping β-actin as a loading control. Genes include *il-10*, *cd11c*, *cd11b*, *c-kit*, *ly51*, *aire*, and *keratin5* in samples from normal and tumor cohorts ($n = 3$ in each case). **(C1)** Pictorial diagram of experimental set up of T-cell and stromal-cell interaction. DN T cells were isolated by BD Imag, and stromal cells were isolated by 2-deoxyguanosine treatment in FTOC culture for 3 days. DN-T cells and stromal cells were then co-cultured in transwell with or without trans-membrane and IL-10 treatment. Different conditions are: (a) DN T cells were co-cultured with stromal cells, (b) DN T cells were pre-treated with mrIL-10 overnight and co-cultured with stromal cells, (c) stromal cells were pre-treated with mrIL-10 overnight and co-cultured with DN T cells, (d) stromal cells and DN T cells were pre-treated with mrIL-10 overnight and then co-cultured, (e) stromal cells and DN T cells pre-treated with mrIL-10 overnight, and then DN T cells co-cultured with stromal cells were separated with 0.8-μm trans-membrane in trans-well. **(C2)** Flow cytometric representations of thymic cells for (a) CD25$^+$CD44$^+$, (b) CD45$^+$CD11c$^+$MHCII$^+$, (c) CD25$^+$c-Kit$^+$Ikaros$^+$ (d) CD25$^+$c-Kit$^+$Notch1$^+$ from (a–e) culture conditions as mentioned. In histograms, MFI values are represented in red, and positive percentages of cells are presented in black. Bar diagrams in each figure show the mean ± SE of 3 individual observations; $^{***}p < 0.001$.

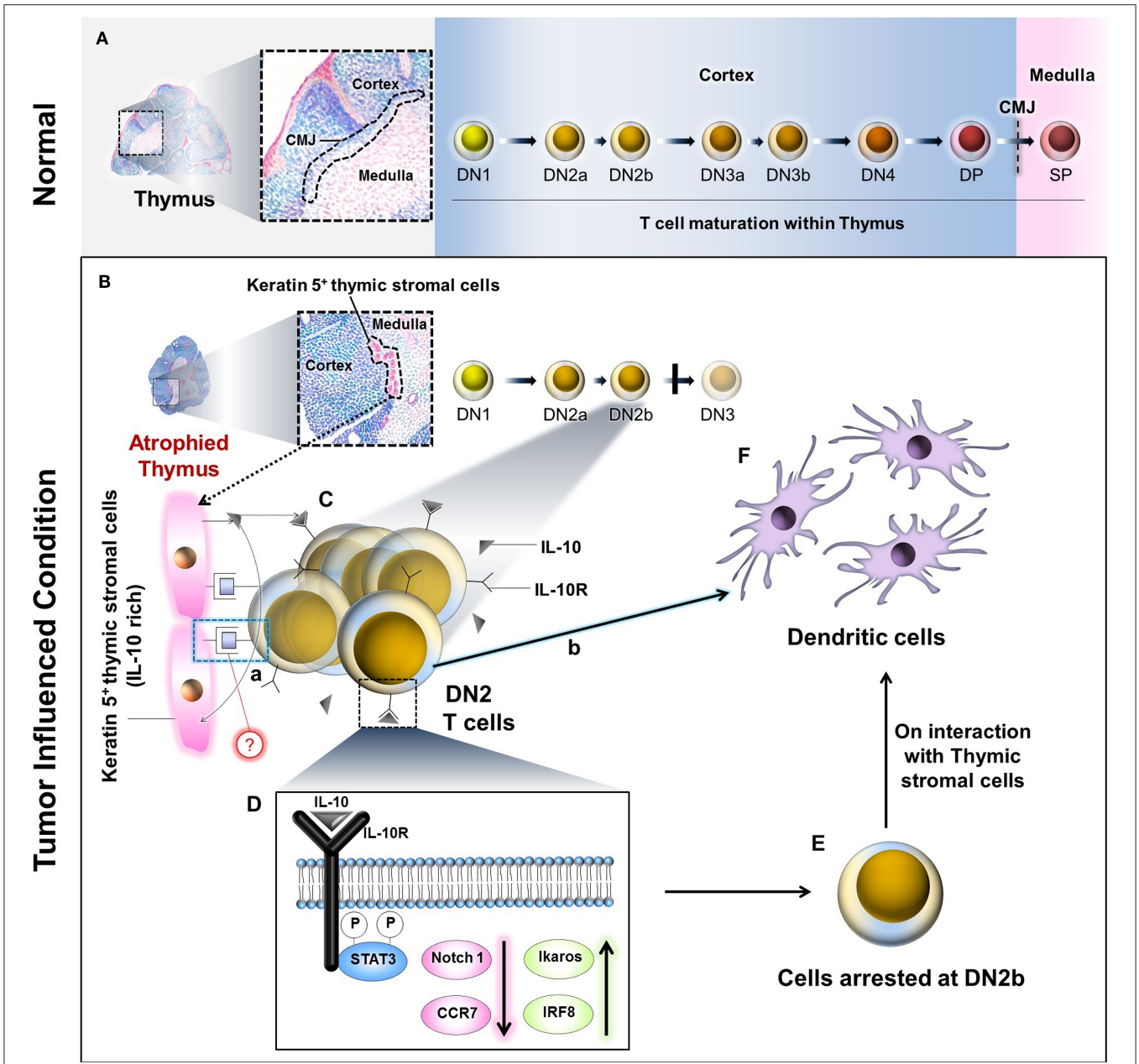

FIGURE 8 | Schematic diagram and probable mechanism of arrest of DN2 pro-T cell-to-DN3 transition and promotion of its conversion to thymic dendritic cells by reciprocal regulation of Ikaros/Notch1 signaling: **(A)** During maturation, the T lymphocytes progress through the DN1, DN2a, DN2b, DN3a, DN3b, and DN4 to DP stages within the thymic cortex. These DP cells pass the cortico-medullary junction (CMJ) to enter the medulla as they further mature to SP (DN, Double negative; DP, Double positive; SP, Single positive). **(B)** Under the influence of tumor, thymus becomes atrophied, and Keratin-5 expressing IL-10-rich stromal cells tend to accumulate at the CMJ. **(C)** IL-10 molecules secreted from these cells interact with DN2b T cells via IL-10 receptors (IL-10R). **(D)** However, following IL-10–IL-10R interaction(s), STAT3-mediated intracellular signaling events occur within the DN2 T cells, which ultimately bring down Notch1 expression. As a consequence, the T cells are arrested at the DN2b stage. **(E)** Other than Notch1, downregulation of CCR7 and upregulation of Ikaros and IRF8 has also been observed due to these signaling events. A few of these arrested DN2b T cells somehow interact physically with the Keratin 5^+ thymic stromal cells at the CMJ (C.a**)** and differentiate into dendritic cells (C.b, **F**) instead of staying at DN2b or progressing to DN3. The precise mode of the physical interaction(s) between the DN2b T cells and the Keratin-5^+ stromal cells (C.a) is yet to be elucidated.

reports (27), we observed severe thymic atrophy across a range of murine tumor models. Indeed, Adkins et al. (44) previously reported thymic T-cell arrest at an early stage ($CD25^+CD44^+$ DN2) in breast carcinoma-bearing mice. Here, we refined such analyses by the inclusion of an additional marker, c-Kit, providing evidence for prominent arrest occurring between

the DN2b and DN3 stages of pro-T-cell development, resulting in the accumulation of $CD25^{+}CD44^{+}$c-Kit^{low} DN2b cells within the cortico-medullary junction and depletion of more mature DN3 and DN4 T cells. During tumor progression, the thymic T-cell differentiation process appears to be negatively impacted by the silencing of Notch1 signaling (45) and corollary expression of Notch1-downstream target *ccr7* (19, 46), along with its two ligands CCL19 and CCL21 within thymus. In this light, previous reports have suggested an indispensable role of CCR7 in facilitating the migration of the $CD25^{+}CD44^{+}$ DN2 population to the outer thymic cortex (47), with CCR7 deficiency restricting these cells within the cortico-medullary junction (CMJ) and hampering their development beyond the DN2 stage (28, 48). In FTOC cultures, under conditions permissive for Notch1 signaling (i.e., with TNFα stimulation), DN2-to-DN3 transition was promoted. However, when Notch1 signaling was blocked by a gamma-secretase inhibitor, early T-cell differentiation was prevented.

In extended studies, we determined that another important contributor to tumor-induced T-cell developmental arrest is IL-10, whose expression was upregulated in the thymus, particularly that of the tumor-bearing host, particularly at the thymic CMJ where DN2 T cells tend to accumulate. Although previous reports suggest that tumor-associated IL-10 activity disrupts normal T-cell maturation (49), even in some SCID patients, overexpression of IL-10 appears to specifically interrupt T-cell maturation at an early stage (50). However, these studies failed to explain how tumor initiation and/or progression promoted intra-thymic IL-10 activity. Clearly, one cannot ignore the additional contributions of one or several tumor-induced systemic factor(s) including hormones (secreted from tumor-involved organs), neurotransmitters, galectins, and PGE2 in intra-thymic cytokine (including IL-10)-production by TEC. In our model, $keratin5^{+}$ medullary TEC seemed to be primarily responsible for IL-10 production in the tumor-bearing host, followed by $CD11c^{+}$ DCs. Not surprisingly, IL-10R expression was determined to be higher in the DN2 T-cell subset, likely making $IL\text{-}10R^{high}$ DN2 T cells more susceptible to IL-10-mediated lineage arrest. IL-10 was also likely responsible for suppressing the Notch1 expression in DN2a T cells, since *notch 1* expression in DN2 T cells and transition from DN2 to DN3 was normalized in tumor-bearing $IL\text{-}10^{-/-}$ mice. To support the notion that IL-10-mediated arrest at the DN2-to-DN3 transition involves STAT3, we showed that knockdown of STAT3 (using STAT3 specific siRNA) ameliorates IL-10-induced arrest at the DN2 stages in concert with normalization in *notch1* expression. In contrast to our observations, Garner et al. (51), reported that constitutively activated STAT3 along with activated NF-κB promotes Notch expression in glioblastoma cancer stem cells. In our hands, however, we failed to see any activation in NFκB-associated molecules, which may simply be related to the different cell systems being evaluated in each case. Therefore, to better understand the regulatory effects of IL-10 on *notch1* more precisely, we designed four primers based on the putative *p*STAT3 binding site downstream of *notch1* promoter. ChIP assays performed on sorted DN2 T cells supported the direct binding of pSTAT3 at a 5′-XXX-TTCCAGAA-XX-3′ site downstream of the *notch1* promoter (among the four putative stat3 binding regions) of *notch1* gene after IL-10 stimulation. Interestingly, unlike Notch1, Ikaros and IRF8 expressions were found to be significantly elevated in the "stunted" DN2-T cells isolated from the thymi of tumor-bearing mice. Moreover, FTOC experiments suggested that the reciprocal regulation of Notch1 and Ikaros/IRF8 is IL-10 dependent. In the normal thymus, Ikaros expression was restricted primarily to DN3 and DN4 T cells, where it is believed to play a critical role as a checkpoint regulator during DN3 to DN4 transition and again during subsequent DN4 to DP transition. Furthermore, loss of Ikaros in the face of intact Notch1 signaling allows for T-cell maturation programming to occur between the DN-DP and DP-SP transition stages without appropriate pre-TCR and TCR signaling (52). In contrast, in a tumor-conditioning model, enhanced *Ikaros* in the absence of *notch1* along with *tcf1* and *bcl11b* (18, 53, 54), leads to aborted T-cell maturation beyond DN2a. Accordingly, knockdown of Ikaros promotes pro-T-cell maturation beyond the DN2 stage and a reduction of the DC population, like in a tumor-free host.

Strikingly, we observed a significant rise in lymphoid DC frequencies in thymus of tumor-bearing mice without discernable alterations in other immune cell subpopulations. Thymic pro-T cells, through many generations, retain the differentiative potential for alternate cell lineages, such as monocytes or DC (39), Such latent myeloid differentiative potential in committed T cells is also promoted by ectopic anti-inflammatory cytokine production (55) and by the dysregulation of transcription factors such as Notch1 (39, 56, 57). Therefore, loss of Notch1 induced by IL-10, yields a conditional state conducive for DN2 T cell→lymphoid DC differentiation [i.e., coordinated expression of Pu.1 (58), Cebpalpha (59), Ikaros, and IRF8 along with CD3ε] within the thymus of the cancer-bearing host. This inter-lineage conversion of DN2 T cells is consistent with a report from Feyerabend et al.; however, unlike their observation, notch1 reduction in a tumor-induced model only resulted in the generation of lymphoid DCs but not B cells, and the involvement of Ikaros and IRF8 was not demonstrated. Notably, the role of Ikaros and IRF8 in promoting DC commitment in the extra-thymic environment has been reported previously (60–62). DC lineage potential is clearly present in ETPs and DN2a cells (63–65), and when we specifically checked the DN2a and DN2b populations, we found that *ikaros* and *pu.1* expression became elevated in the DN2a stage, which may serve as a preparatory phase for initiation of arrest in T cell-lineage commitment and switching to DC, which drives DN2b to DC commitment in tumor host. Moreover, we also checked the contribution of homing of circulating DC via CD49d; however, neutralization of CD49d ruled out such a possibility.

Additionally, in this trans-differentiation process, direct cell-to-cell interactions between DN2 thymocytes and IL-10-pretreated thymic epithelial cells are required (66), as IL-10 treatment of DN-T cells only partially restricts DN T-cell maturation at the DN2 stage, and it failed in DN2→DC differentiation. This observation again strongly supports the influence of lymphoid-stromal cell interactions as a major determinant for lineage commitment (67); which stromal

cells are responsible for this effect will be determined in future studies.

In conclusion, we have identified a novel mechanism through which (tumor-induced) IL-10 paralyzes host anti-tumor immunity by blocking thymic DN2a cells along a T-cell fate pathway and altering the T-cell fate pathway by promoting the commitment of pro-T (DN2) toward DC lineage. This mechanism of lineage re-registry is unique to the cancer setting and distinct from age-induced thymic involution. Finally, the role(s) of thymic DC evolved from DN2 T-cell progenitors in the evolving anti-tumor T-cell repertoire and tumor progression remain unknown, providing a major area of focus for future studies designed to advance our understanding of tumor-associated immune deviation and the development of target therapeutics for improved treatment outcomes in the cancer setting.

DATA AVAILABILITY STATEMENT

The data and materials related to the findings of this study are mentioned in the article, figures, and **Supplementary Material**. Raw data are available from the corresponding authors on reasonable request.

ETHICS STATEMENT

The animal study was reviewed and approved by Institutional Animal Care and Ethics Committee of CNCI, Kolkata, India. Ethics Committee Approval No. IAEC-1774/RB-4/2015/6 and IAEC-1774/RB-19/2017/15.

AUTHOR CONTRIBUTIONS

IG, ABo, and RB designed the study, analyzed the data, and wrote the manuscript. IG, ABh, DS, AP, PN, AS, and SD performed the research. SG, BS, and AN provide resources. SM, BS, and WS prepared the manuscript. ABo and RB supervised the project. ABo and RB acquired the funding. All authors approved the manuscript.

FUNDING

This study was supported by Chittaranjan National Cancer Institute, Kolkata, India, and the Department of Science and Technology, Govt. of India (Grant No. SR/WOS-A/LS-152/2017). These funding agencies had no role in study design, data collection and analysis, decision to publish, or the preparation of this manuscript.

ACKNOWLEDGMENTS

We acknowledge the Director of the Chittaranjan National Cancer Institute, Kolkata, for providing the facilities necessary for the performance of this study. We also wish to thank Dr. Parthasarahi Dasgupta for his critical comments on the manuscript and all members of our respective laboratories for their technical support of this work. Special thanks are extended to Dr. Abhijit Rakshit, Head, Animal Care and Maintenance Department, CNCI, Kolkata. We acknowledge Dr. Amit Pal, Dr. Santasabuj Das, and Dr. Moumita Bhaumik (Ghosh), NICED, Kolkata, for providing flow-cytometric and confocal microscope facilities.

SUPPLEMENTARY MATERIAL

The Supplementary Material for this article can be found online at: https://www.frontiersin.org/articles/10.3389/fimmu.2020.00898/full#supplementary-material

Supplementary Figure 1 | Overall gating strategy of CD45, CD4, CD8, CD25, CD44, c-Kit, Notch1, Ikaros, and IRF8 stained thymic T cells from non-tumor (wild-type and IL-$10^{-/-}$) and tumor (wild-type and IL-$10^{-/-}$) hosts. Dot plot representations for **(A)** lymphocytes, **(B)** doublet discrimination, **(C)** CD45 gating, with $CD45^+$ population selected on lymphocytes, **(D)** CD4/CD8 gating, **(E)** DN ($CD4^-CD8^-$) population was selected for DN1, DN2, DN3, and DN4 analysis based on CD25 CD44-staining. **(F)** DN2 population was sub-gated into DN2a and DN2b based on c-Kit, CD25 expression. **(G)** Histograms represent FMO of $Ikaros^+$, $IRF8^+$, and $Notch1^+$ cells within DN2a and DN2b cell populations, respectively, $n = 3$.

Supplementary Figure 2 | (A) Flow-cytometric analysis of Ikaros was performed in untreated and Ikaros siRNA-treated cohorts. Ikaros was analyzed on DN2 ($CD25^+CD44^+$) positive cells. Histograms represent percentage of positive cells of FMO, untreated, and Ikaros siRNA-treated cohorts, respectively, on $DN2^+$ cells.

Supplementary Figure 3 | (A) Workflow diagram on experimental design of 2-deoxy guanosine treatment on fetal thymic organ culture (FTOC) using E14.5 fetus from IL-$10^{-/-}$ pregnant mice and co-cultured with wild-type fetal thymocytes. **(B)** Bar diagram shows the percentage of DN2, DC, $DN2^+$Ikaros and $DN2^+$Notch1 positive cells of untreated and IL-10-treated cohorts; $n = 3$, $^{***}p < 0.001$.

Supplementary Figure 4 | (A) Flow-cytometric dot plot representations of thymic cells with CD4 and CD8 staining from Days 0, 1, 3–7 of FTOC culture. **(B)** Bar diagrams represent percentages of DN, DP, CD4SP, and CD8SP cells in total FTOC population at Days 4–6; $n = 4$, $p < 0.001$.

Supplementary Figure 5 | (A) Bar diagram represents the pre- and post-sorting percentages of DN, DP, CD4SP, and CD8SP thymocyte positive cells. **(B)** Bar diagram represents the pre- and post-sorting absolute cell numbers of DN, DP, CD4SP, and CD8SP thymocytes. In the case of pre-sorting, absolute numbers of thymocytes were counted from total cell population, and in the case of post-$lin^-Thy1.2^+$-sorting, absolute numbers were calculated from total sorted population for DN, DP, CD4SP, and CD8SP thymocytes; $n = 4$, $p < 0.001$.

REFERENCES

1. Zhang H, Chen J. Current status and future directions of cancer immunotherapy. *J Cancer*. (2018) 9:1773–81. doi: 10.7150/jca.24577
2. Hirokawa M, Shimizu M, Fukuya T, Manabe T, Sonoo H. Columnar cell carcinoma of the thyroid: MIB-1 immunoreactivity as a prognostic factor. *Endor Pathol*. (1998) 9:31–4. doi: 10.1007/BF02739949
3. Shiraishi J, Utsuyama M, Seki S, Akamatsu H, Sunamori M, Kasai M, et al. Essential Microenvironment for Thymopoiesis is preserved in human adult and Aged Thymus. *Clin Dev Immunol*. (2003) 10:53–9. doi: 10.1080/1044667031000159846 5
4. Ferrando-Martínez S, Franco JM, Hernandez A, Ordoñez A, Gutierrez E, Abad A, et al. Thymopoiesis in elderly human is associated with systemic inflammatory status. *Age*. (2009) 31:87–97. doi: 10.1007/s11357-008-9084-x

5. Goldberg GL, Alpdogan Ö, Muriglan SJ, Hammett MV, Milton MK, Eng JM, et al. Enhanced immune reconstitution by sex steroid ablation following allogeneic hemopoietic stem cell transplantation. *J Immunol*. (2007) 178:7473–84. doi: 10.4049/jimmunol.178.11.7473
6. Goldberg GL, Zakrzewski JL, Perales MA, van den Brink MR. Clinical strategies to enhance T cell reconstitution. *Semin Immunol*. (2007) 19:289–96. doi: 10.1016/j.smim.2007.08.001
7. De la Rosa R, Leal M. Thymic involvement in recovery of immunity among HIV-infected adults on highly active antiretroviral therapy. *J Antimicrob Chemother*. (2003) 52:155–8. doi: 10.1093/jac/dkg311
8. Laronne-Bar-On A, Zipori D, Haran-Ghera N. Increased regulatory versus effector T cell development is associated with thymus atrophy in mouse models of multiple myeloma. *J Immunol*. (2008) 181:3714–24. doi: 10.4049/jimmunol.181.5.3714
9. Hadden JW. Immunodeficiency and cancer: prospects for correction. *Int Immunopharmacol*. (2003) 3:1061–71. doi: 10.1016/S1567-5769(03)00060-2
10. Aspinall R, Pitts D, Lapenna A, Mitchell W. Immunity in the elderly: the role of the thymus. *J Comp Pathol*. (2010) 142:111–5. doi: 10.1016/j.jcpa.2009.10.022
11. Rothenberg EV, Moore JE. Launching the T-lineage developmental programme. *Nat Rev Immunol*. (2008) 8:9–21. doi: 10.1038/nri2232
12. Ciofani M, Zúñiga-Pflücker JC. The thymus as an inductive site for T lymphopoiesis. *Ann Rev Cell Dev Biol*. (2007) 23:463–93. doi: 10.1146/annurev.cellbio.23.090506.123547
13. Dzhagalov I, Phee H. How to find your way through the thymus: a practical guide for aspiring T cells. *Cell Mol Life Sci*. (2012) 69:663–82. doi: 10.1007/s00018-011-0791-6
14. Schwarz BA, Sambandam A, Maillard I, Harman BC, Love PE, Bhandoola A. Selective thymus settling regulated by cytokine and chemokine receptors. *J Immunol*. (2007) 178:2008–17. doi: 10.4049/jimmunol.178.4.2008
15. Seo W, Taniuchi I. Transcriptional regulation of early T-cell development in the thymus. *Eur J Immunol*. (2016) 46:531–8. doi: 10.1002/eji.201545821
16. Carpenter AC, Bosselut R. Decision checkpoints in the thymus. *Nat Immunol*. (2010) 11:666–73. doi: 10.1038/ni.1887
17. Rothenberg EV. T cell lineage commitment: identity and renunciation1. *J Immunol*. (2011) 186:6649–55. doi: 10.4049/jimmunol.1003703
18. Shah D, Flücker J. An overview of the intrathymic intricacies of T cell development. *J Immunol*. (2014) 192:4017–23. doi: 10.4049/jimmunol.1302259
19. Tan JB, Visan I, Yuan JS, Guidos CJ. Requirement signals at sequential early stages of intrathymic T cell development. *Nat Immunol*. (2005) 6:671–9. doi: 10.1038/ni1217
20. Wherry EJ. T cell exhaustion. *Nat Immunol*. (2011) 12:492–9. doi: 10.1038/ni.2035
21. Wang JC, Xu Y, Huang JM, Lu XJ. T cell exhaustion in cancer: mechanisms and clinical implications. *J Cell Biochem*. (2017) 119:4279–86. doi: 10.1002/jcb.26645
22. Prins RM, Graf MR, Merchant RE, Black KL, Wheeler CJ. Thymic function and output of recent thymic emigrant T cells during intracranial glioma progression. *J Neurooncol*. (2003) 64:45–54. doi: 10.1007/BF02700019
23. Li, Y, Yin, Q, Yang, L, Chen S, Geng S, Wu X, et al. Reduced levels of recent thymic emigrants in acute myeloid leukemia patients. *Cancer Immunol Immunother*. (2009) 58:1047–55. doi: 10.1007/s00262-008-0621-3
24. Driss V, Quesnel B, Brinster C. Monocyte chemoattractant protein 1 (MCP-1/CCL2) contributes to thymus atrophy in acute myeloid leukemia. *Eur J Immunol*. (2015) 45:396–406. doi: 10.1002/eji.201444736
25. Shanker A, Singh SM, Sodhi A. Ascitic growth of a spontaneous transplantable T cell lymphoma induces thymic involution. 1. Alterations in the CD4/CD8 distribution in thymocytes. *Tumor Biol*. (2000) 21:288–98. doi: 10.1159/000030134
26. Anderson G, Jenkinson EJ. Fetal thymus organ culture. *CSH Protoc*. (2007) 2007. doi: 10.1101/pdb.prot4808
27. Hadland BK, Manley NR, Su D, Longmore GD, Moore CL, Wolfe MS, et al. Gamma -secretase inhibitors repress thymocyte development. *Proc Natl Acad Sci USA*. (2001) 98:7487–91. doi: 10.1073/pnas.131202798
28. Jenkinson EJ, Franchi LL, Kingston R. Owen Effect of deoxyguanosine on lymphopoiesis in the developing thymus rudiment *in vitro*: application in the production of chimeric thymus rudiments. *Eur J Immunol*. (1982) 12:583–7. doi: 10.1002/eji.1830120710
29. Zhao X, Bose A, Komita H, Taylor JL, Kawabe M, Chi N, et al. Intratumoral IL-12 gene therapy results in the cross priming of Tc1 cells reactive against tumor-associated stromal antigens. *Mol Ther*. (2011) 19:805–14. doi: 10.1038/mt.2010.295
30. Bose A, Barik S, Banerjee S, Ghosh T, Mallick A, Bhattacharyya S, et al. Tumor-derived vascular pericytes anergize Th cells. *J Immunol*. (2013) 191:971–81. doi: 10.4049/jimmunol.1300280
31. Ghosh T, Barik S, Bhuniya A, Dhar J, Dasgupta S, Ghosh S, et al. Tumor-associated mesenchymal stem cells inhibit naïve T cell expansion by blocking cysteine export from dendritic cells. *Int J Cancer*. (2016). 139:2068–81. doi: 10.1002/ijc.30265
32. Lopez DM, Charyulu V, Adkins B. Influence of breast cancer on thymic function in mice. *J Mammary Gland Biol Neoplasia*. (2002) 7:191–9. doi: 10.1023/A:1020356020542
33. Carrio R, Torroella-Kouri M, Iragavarapu-Charyulu V, Lopez DM. Tumor-induced thymic atrophy: alteration in interferons and Jak/Stats signaling pathways. *Int J Oncol*. (2011) 38:547–53. doi: 10.3892/ijo.2010.870
34. Petrie HT. Cell migration and the control of post-natal T-cell lymphopoiesis in the thymus. *Nat Rev Immunol*. (2003) 3:859–66. doi: 10.1038/nri1223
35. Radtke F, Wilson A, Stark G, Bauer M, Van Meerwijk J, MacDonald HR, et al. Deficient T cell fate specification in mice with an induced inactivation of Notch1. *Immunity*. (1999) 10:547–8l. doi: 10.1016/S1074-7613(00)80054-0
36. Weaver AN, Burch MB, Cooper TS, Della Manna DL, Wei S, Ojesina AI, et al. Notch signaling activation is associated with patient mortality and increased FGF1-mediated invasion in squamous cell carcinoma of the oral cavity. *Mol Cancer Res*. (2016) 14:883–91. doi: 10.1158/1541-7786.MCR-16-0114
37. Bonasio R, Scimone ML, Schaerli P, Grabie N, Lichtman AH, Von Andrian UH. Clonal deletion of thymocytes by circulating dendritic cells homing to the thymus. *Nat Immunol*. (2006) 7:1092–100. doi: 10.1038/ni1385
38. Carding SR, Hayday AC, Bottomly K. Cytokines in T-cell development. *Immunol Today*. (1991) 12:239–45. doi: 10.1016/0167-5699(91)90037-T
39. Bubanovic IV. Failure of blood-thymus barrier as a mechanism of tumor and trophoblast escape. *Med Hypotheses*. (2003) 60:315–20. doi: 10.1016/S0306-9877(02)00450-4
40. Wolfe MS, Xia W, Moore CL, Leatherwood DD, Ostaszewski B, Rahmati T, et al. Peptidomimetic probes and molecular modeling suggest that Alzheimer's gamma-secretase is an intramembrane-cleaving aspartyl protease. *Biochemistry*. (1999) 38:4720–7. doi: 10.1021/bi982562p
41. Becker S, Groner B, Mu€ller CW. Three-dimen-sional structure of the Stat3b homodimer bound to DNA. *Nature*. (1998) 394:145–51. doi: 10.1038/28101
42. Heinzel K, Benz C, Martins VC, Haidl ID, Bleul CC. Bone marrow-derived hemopoietic precursors commit to the T cell lineage only after arrival in the thymic microenvironment. *J Immunol*. (2007) 178:858–68. doi: 10.4049/jimmunol.178.2.858
43. Lynch HE, Goldberg GL, Chidgey A, Van den Brink MR, Boyd R, Sempowski GD. Thymic involution and immune reconstitution. *Trends Immunol*. (2009) 30:366–73. doi: 10.1016/j.it.2009.04.003
44. Adkins B, Charyulu V, Sun QL, Lobo D, Lopez DM. Early block in maturation is associated with thymic involution in mammary tumor-bearing mice. *J Immunol*. (2000) 164:5635–40. doi: 10.4049/jimmunol.164.11.5635
45. Feyerabend TB, Terszowski G, Tietz A, Blum C, Luche H, Gossler A, et al. Deletion of Notch1 converts pro-T cells to dendritic cells and promotes thymic B cells by cell-extrinsic and cell-intrinsic mechanisms. *Immunity*. (2009) 30:67–79. doi: 10.1016/j.immuni.2008.10.016
46. Pui JC, Allman D, Xu L, Rocco SD, Karnell FG, Bakkour S, et al. Notch1 expression in early lymphopoiesis influences B versus T lineage determination. *Immunity*. (1999) 11:299–308. doi: 10.1016/S1074-7613(00)80105-3
47. Ueno T, Saito F, Gray DH, Kuse S, Hieshima K, Nakano H, et al. CCR7 signals are essential for cortex-medulla migration of developing thymocytes. *J Exp Med*. (2004) 200:493–505. doi: 10.1084/jem.20040643
48. Davalos-Misslitz AC, Worbs T, Willenzon S, Bernhardt G, Förster R. Impaired responsiveness to T-cell receptor stimulation and defective negative selection of thymocytes in CCR7-deficient mice. *Blood*. (2007) 110:4351–9. doi: 10.1182/blood-2007-01-070284

49. Hassuneh MR, Nagarkatti M, Nagarkatti PS. Role of interleukin-10 in the regulation of tumorigenicity of a T cell lymphoma. *Leuk Lymphoma*. (2013) 54:827–34. doi: 10.3109/10428194.2012.726721
50. Rouleau M, Cottrez F, Bigler M, Antonenko S, Carballido JM, Zlotnik A, et al. IL-10 transgenic mice present a defect in T cell development reminiscent of SCID patients. *J Immunol*. (1999) 163:1420–7.
51. Garner JM, Fan M, Yang CH, Du Z, Sims M, Davidoff AM, et al. Constitutive activation of signal transducer and activator of transcription 3 (STAT3) and nuclear factor κB signaling in glioblastoma cancer stem cells regulates the Notch pathway. *J Biol Chem*. (2013) 288:26167–76. doi: 10.1074/jbc.M113.477950
52. Winandy S, Wu L, Wang JH, Georgopoulos K. Pre-T cell receptor (TCR) and TCR-controlled checkpoints in T cell differentiation are set by Ikaros. *J Exp Med*. (1999) 190:1039–48. doi: 10.1084/jem.190.8.1039
53. Weber BN, Chi AW, Chavez A, Yashiro-Ohtani Y, Yang Q, Shestova O, et al. A critical role for TCF-1 in T-lineage specification and differentiation. *Nature*. (2011) 476:63–78. doi: 10.1038/nature10279
54. Wakabayashi Y, Watanabe H, Inoue J, Takeda N, Sakata J, Mishima Y, et al. Bcl11b is required for differentiation and survival of alphabeta T lymphocytes. *Nat Immunol*. (2003) 4:533–9. doi: 10.1038/ni927
55. King AG, Kondo M, Scherer DC, Weissman IL. Lineage infidelity in myeloid cells with TCR gene rearrangement: a latent developmental potential of pro-T cells revealed by ectopic cytokine receptor signaling. *Proc Natl Acad Sci USA*. (2002) 99:4508–13. doi: 10.1073/pnas.072087899
56. Laiosa CV, Stadtfeld M, Xie H, de Andres-Aguayo L, Graf T. Reprogramming of committed T cell progenitors to macrophages and dendritic cells by C/EBP alpha and PU.1 transcription factors. *Immunity*. (2006) 25:731–44. doi: 10.1016/j.immuni.2006.09.011
57. Rothenberg EV. Cell lineage regulators in B and T cell development. *Nat Immunol*. (2007) 8:441–4. doi: 10.1038/ni1461
58. Rothenberg EV, Ungerbäck J, Champhekar A. Forging T-lymphocyte identity: intersecting networks of transcriptional control. *Adv Immunol*. (2016) 129:109–74. doi: 10.1016/bs.ai.2015.09.002
59. Wölfler A, Danen-van Oorschot AA, Haanstra JR, Valkhof M, Bodner C, Vroegindeweij E, et al. Lineage-instructive function of C/EBPα in multipotent hematopoietic cells and early thymic progenitors. *Blood*. (2010) 116:4116–25. doi: 10.1182/blood-2010-03-275404
60. Movassagh M, Laderach D, Galy A. Proteins of the Ikaros family control dendritic cell maturation required to induce optimal Th1 T cell differentiation. *Int Immunol*. (2004) 16:867–75. doi: 10.1093/intimm/dxh090
61. Chari S, Winandy S. Ikaros regulates Notch target gene expression in developing thymocytes. *J Immunol*. (2008) 181:6265–74. doi: 10.4049/jimmunol.181.9.6265
62. Tailor P, Tamura T, Ozato K. IRF family proteins and type I interferon induction in dendritic cells. *Cell Res*. (2006) 16:134–40. doi: 10.1038/sj.cr.7310018
63. Donskoy E, Goldschneider I. Two developmentally distinct populations of dendritic cells inhabit the adult mouse thymus: demonstration by differential importation of hematogenous precursors under steady state conditions. *J Immunol*. (2003) 170:3514–21. doi: 10.4049/jimmunol.170.7.3514
64. LiJ, Park J, Foss D, Goldschneider I. Thymus-homing peripheral dendritic cells constitute two of the three major subsets of dendritic cells in the steady-state thymus. *J Exp Med*. (2009) 206:607–22. doi: 10.1084/jem.20082232
65. Yui, MA, Feng N, Rothenberg EV. Fine-scale staging of T cell lineage commitment in adult mouse thymus. *J Immunol*. (2010) 185:284–93. doi: 10.4049/jimmunol.1000679
66. Prockop SE, Palencia S, Ryan CM, Gordon K, Gray D, Petrie HT. Stromal cells provide the matrix for migration of early lymphoid progenitors through the thymic cortex. *J Immunol*. (2002) 169:4354–61. doi: 10.4049/jimmunol.169.8.4354
67. Sano SL, Nowak J, Fallet M, Bajenoff M. Stromal cell networks regulate thymocyte migration and dendritic cell behavior in the thymus. *J Immunol*. (2011) 186:2835–41. doi: 10.4049/jimmunol.1003563

Conflict of Interest: The authors declare that the research was conducted in the absence of any commercial or financial relationships that could be construed as a potential conflict of interest.

frontiers in Immunology

ORIGINAL RESEARCH
published: 09 June 2021
doi: 10.3389/fimmu.2021.662594

Ionizing Radiation Curtails Immunosuppressive Effects From Cancer-Associated Fibroblasts on Dendritic Cells

Rodrigo Berzaghi[1]*, *Stian Tornaas*[1], *Kristin Lode*[1], *Turid Hellevik*[2] and *Inigo Martinez-Zubiaurre*[1]

[1] Department of Clinical Medicine, Faculty of Health Sciences, UiT-The Arctic University of Norway, Tromsø, Norway,
[2] Department of Radiation Oncology, University Hospital of Northern Norway, Tromsø, Norway

OPEN ACCESS

Edited by:
Udo S. Gaipl,
University Hospital Erlangen, Germany

Reviewed by:
Yona Keisari,
Tel Aviv University, Israel
Christina Janko,
University Hospital Erlangen, Germany

***Correspondence:**
Rodrigo Berzaghi
rodrigo.berzaghi@uit.no

Specialty section:
This article was submitted to Cancer Immunity and Immunotherapy, a section of the journal Frontiers in Immunology

Received: 17 February 2021
Accepted: 24 May 2021
Published: 09 June 2021

Citation:
Berzaghi R, Tornaas S, Lode K, Hellevik T and Martinez-Zubiaurre I (2021) Ionizing Radiation Curtails Immunosuppressive Effects From Cancer-Associated Fibroblasts on Dendritic Cells. Front. Immunol. 12:662594. doi: 10.3389/fimmu.2021.662594

Cancer-associated fibroblasts (CAFs) participate actively in tumor development and affect treatment responses, by among other mechanisms, promoting an immunosuppressive tumor microenvironment. In contrast to normal fibroblasts, reactive CAFs secrete a myriad of immunomodulatory soluble factors at high levels, i.e. growth factors, cytokines, and chemokines, which directly influence tumor immunity and inflammation. CAFs have been identified as important players in tumor radioresistance. However, knowledge on the immunomodulatory functions of CAFs during/after radiotherapy is still lacking. In this study, we investigated the effects of ionizing radiation on CAF-mediated regulation of dendritic cells (DCs). CAFs were obtained from freshly operated lung cancer tissues, while DCs were procured from peripheral blood of healthy donors. Experimental settings comprised both co-cultures and incubations with conditioned medium from control and irradiated CAFs. Functional assays to study DC differentiation/activation consisted on cytokine release, expression of cell-surface markers, antigen uptake, migration rates, T cell priming, and DC-signaling analysis. We demonstrate that CAFs induce a tolerogenic phenotype in DCs by promoting down-regulation of: i) signature DC markers (CD14, CD1a, CD209); ii) activation markers (CD80, CD86, CD40, and HLA-DR) and iii) functional properties (migration, antigen uptake, and $CD4^+$ T cell priming). Notably, some of these effects were lost in conditioned medium from CAFs irradiated at fractionated medium-dose regimens (3x6 Gy). However, the expression of relevant CAF-derived regulatory agents like thymic stromal lymphopoietin (TSLP) or tryptophan 2,3-dioxygenase (TDO2) was unchanged upon irradiation. This study demonstrates that CAFs interfere with DC immune functions and unveil that certain radiation regimens may reverse CAF-mediated immunosuppressive effects.

Keywords: cancer-associated fibroblasts (CAFs), monocyte-derived DC, immunosuppression, ionizing radiation, radiotherapy, non-small cell lung cancer, tumor microenvironment

INTRODUCTION

Recent studies in both pre-clinical and clinical settings have demonstrated that radiotherapy (RT) has the power to trigger immunological responses that can influence disease outcomes (1–3). By induction of immunogenic cell death (ICD) and the release of tumor-associated antigens and immune adjuvants, RT can trigger pro-inflammatory reactions, promote immune cells recruitment, and break the balance of tumor immune tolerance (4). Conversely, RT can also trigger immunosuppressive signals, which can lead to tumor radioresistance (5). Treatment outcomes will ultimately depend on the net effect of pro-immunogenic and anti-immunogenic signals. Understanding the effects of radiation on the multifactorial elements of the tumor microenvironment (TME) is becoming a subject of great interest (6–8). Recent studies have shown a correlation between cancer-associated fibroblasts (CAFs), a major component of the tumor stroma (9–11), and increased radiotherapy resistance in colorectal cancer (12) and non-small cell lung cancer (NSCLC) (13). Other studies have suggested a loss of pro-tumorigenic functions in CAFs after radiation (14). Besides, it is well established that CAFs play an important role in suppressing anti-tumor immune responses in the TME, with ability to negatively affect activation, trafficking, and state of differentiation of a vast population of immune cells (15–17). However, little is known about how RT is affecting the crosstalk between CAFs and immune cells.

In the context of immune responses triggered by RT, antigen-presenting cells, in particular, dendritic cells (DCs) (18), and the induction of immunogenic cell death (ICD) are key components for effective anti-tumor response (4, 19). DCs are professional antigen-presenting cells bridging innate and adaptive immunity and are broadly divided into two major phenotypes, immature and mature DCs (20). Immature DCs are defined by a high capacity for antigen uptake and processing, with MHC-II molecules sequestered in lysosomes and low levels of antigen presentation and T cell stimulation. In contrast, mature DCs have poor endocytic capacity, with peptide-MHC complexes localized at the cell surface, securing excellent T cell priming capacity (21). Exposure of tumor lesions to ionizing radiation (IR) provokes DNA damages and may trigger ICD. ICD is characterized by the generation of damage-associated molecular patterns (DAMPs) including extracellular exposure of calreticulin, and release of alarmins, such as high mobility group box 1 (HMGB1) and ATP (22–24). The presence of DAMPs engages receptors and ligands on dendritic cells, accelerates the engulfment of tumor-derived antigens, promotes the processing of phagocytic cargo, and activates immature DCs transition to a mature phenotype. Consequently, *via* antigen presentation, DCs stimulate specific T cell responses resulting in a robust adaptive anti-tumor immune response (20, 25). In the TME, both tumor and stromal cells can modulate infiltration, maturation, and function of DCs (18). In particular, some studies have indicated that CAFs may induce a tolerogenic phenotype on DCs. In a transplantable model of lung carcinoma, for instance, CAF-secreted tryptophan 2,3-dioxygenase (TDO2) was shown to inhibit DC differentiation and function, whereas inhibition of TDO2 improved DC function and T cell responses with decreased experimental metastasis (26). In hepatocellular carcinoma, IL-6 produced by CAFs induced a tolerogenic phenotype on DCs with decreased expression of co-stimulatory molecules and antigen-presenting receptors (CD1a, HLA-DR, CD80, CD86), and increased expression of immunosuppressive cytokines such as IL-10 and TGF-β. These CAF-educated DCs promoted tumor infiltration of immunosuppressive Tregs ($CD4^+CD25^+Foxp3^+$) cells and decreased production of IFN-γ from $CD8^+$ T cells (27). Interplay between CAFs and DCs has also been shown to affect the ability of DCs to induce the differentiation of T cells into a Th2 phenotype in pancreatic cancer, *via* CAF secretion of thymic stromal lymphopoietin (TSLP) (28).

In the RT context, CAFs are known to be highly radioresistant and may survive even ablative doses of ionizing radiation (1x18 Gy), largely reflecting their restricted tendency to proliferate, their capacity to mount solid cytoprotective responses to radiation and their high apoptotic threshold (29). In culture conditions, exposure to medium or high doses of IR does not trigger ICD in CAFs (30). However, single-high radiation doses provoke permanent DNA damage responses and the induction of premature senescence accompanied by functional changes including decreased proliferation, migration, and invasion rates (29). Radiation-induced changes have also been observed on CAF-mediated paracrine signaling. Conditioned medium (CM) from irradiated CAFs reduces the migratory capacity of endothelial cells and inhibits angiogenesis (29, 31). CAF-CM also inhibits pro-inflammatory features in M1-macrophages, and these effects are unchanged after exposing CAFs to single-high dose or fractionated-medium dose irradiation (32). In this context, levels of key CAF-secreted immunosuppressive factors such as interleukin (IL)-6, prostaglandin E_2 (PGE2), IL-10, and transforming growth factor-beta (TGF-β), remained unchanged after radiation exposure (30–32). To better understand and exploit the immunoregulatory power of RT, it is essential to unveil how radiation modifies CAF-mediated immunoregulatory proprieties towards immune cells. In this

Abbreviations: α-SMA, smooth muscle α-actin; CAFs, Cancer-associated fibroblasts; CAF-CM, Cancer-associated fibroblast-conditioned medium; DAMPs, Damage-associated molecular patterns; DCs, Dendritic cells; FAP-1, Fibroblast activation protein 1; GAPDH, Glyceraldehyde-3-phosphate dehydrogenase; GM-CSF, Granulocyte-macrophage colony-stimulating factor; Gy, Gray; HMGB1, High motility group box 1; iDCs, Immature dendritic cells; ICD, Immunogenic cell death; IR, Ionizing radiation; mDCs, Mature dendritic cells; NFκB, Nuclear factor kappa-light-chain-enhancer of activated B cells; NSCLC, Non-small cell lung cancer; PBMC, Peripheral blood mononuclear cells; PGE2, Prostaglandin E2; PI, Propidium iodide; RT, Radiotherapy; STAT3, Signal transducer and activator of transcription 3; TDO2, tryptophan 2,3-dioxygenase; TGF-β, Transforming growth factor-beta; TME, Tumor microenvironment; TNF-α, Tumor necrosis factor-alpha; TSLP, Thymic stromal lymphopoietin; UNN, University Hospital of Northern Norway; VEGF, Vascular endothelial growth factor.

study, we explore if CAF-mediated immunoregulatory effects on monocyte-derived DCs are changed after exposure to different radiation schemes.

MATERIALS AND METHODS

Human Material, CAF Isolation, and Cultures

Human lung CAFs were prepared from freshly resected NSCLC tumor tissue from patients undergoing surgery at the University Hospital of Northern Norway (UNN), Tromsø, as previously described (29). Lung tumor specimens from four different patients (**Table 1**) and blood (i.e. buffy-coats) from ten unrelated healthy donors, all collected under patient written informed consent, were included in this study. All methods involving human material were performed following proper ethical guidelines and regulations under the approval of the Regional Ethical Committee of Northern Norway (REK Nord 2014/401; 2016/714; 2016/2307). NSCLC-derived CAFs were isolated by enzymatic digestion of tissues and the outgrowth method and phenotypically characterized by the presence of specific markers smooth muscle α-actin (α-SMA) and fibroblast activation protein 1 (FAP1), as described previously (29). Isolated CAFs were cultivated in Dulbecco's modified Eagle's medium (DMEM) (Sigma-Aldrich, St Louis, MO, USA) supplemented with 10% fetal bovine serum (FBS) (Biochrom, Berlin, Germany) and used for experimentation after the third and fourth passage (3-4 week-old cultures). Human lung cancer cell line A549 (human lung adenocarcinoma) were purchased from LGC Standards AB (Borås, Sweden). Cells were cultivated in RPMI-1640 supplemented with 10% FBS and penicillin (1%) and streptomycin (1%) in a humidified incubator at 37°C, containing 5% CO_2 and 20% O_2.

Irradiation of Cells

Adherent CAFs cultured in DMEM (with 10% FBS) or A549 cultured in RPMI (with 10% FBS) and grown in T-175 flasks or 24 well culture plates were irradiated when 70–90% confluent with high-energy photons producing by a clinical Varian linear accelerator and delivered in two different radiation regimens, as single-high dose (1×18 Gy) or in fractionated schemes (3×6 Gy for CAFs and 3x8 Gy for A549 cells) at 24h intervals, as previously described (29). Standard parameters for dose delivery were depth 30 mm, beam quality 15 MV, dose-rate of 6 Gy/min, and field sizes of 20×20 cm.

TABLE 1 | Clinical and patient records corresponding to CAF donors used in this study.

Donors	Sex	Tumor type	T-size (mm)	Stage
1	Male	Squamous cell carcinoma	35	pT2aN0Mx
2	Male	Squamous cell carcinoma	22	pT1cN0Mx
3	Female	Adenocarcinoma	25	pT1cN0Mx
4	Male	Squamous cell carcinoma	30	pT2bN2Mx

Preparation of Conditioned Media

CAFs at early passages and A549 were seeded (separately) at a density of 4×10^5 cells in T-75 tissue culture flask and incubated for 24h in DMEM and RPMI (with 10% FBS), respectively. After cell attachment and spreading, cultures were gently washed with PBS (37°C) and 6 mL of new incubation medium was added, followed by irradiation of dishes, as previously described (29). Media from CAFs and A549 cells exposed to IR (3×6 Gy and 3×8 Gy, respectively) were conditioned for 48h, after the last radiation dose. For the group exposed to 1×18 Gy, CM was conditioned between day 3 and day 5 after irradiation. Supernatants were spun down by centrifugation (2000×g, 4°C, 10 min) and then filtrated (Ø = 0.45 μm) for elimination of potential cell debris. The resulting samples were either used immediately or frozen at −80°C for later use.

Isolation of Peripheral Blood Mononuclear Cells and Generation of Monocyte-Derived Dendritic Cells

Peripheral blood mononuclear cells (PBMCs) were isolated from human blood (i.e., buffy-coats) using Lymphoprep-TM (StemCell Technologies, Vancouver, BC, Canada) gradient centrifugation. CD14+ monocytes were isolated from the PBMCs pool using magnetic $CD14^+$ Microbeads (Cat. no. 130-050-201; Miltenyi Biotec, Bergisch Gladbach, Germany). Monocytes ($CD14^+$) purity and recovery were determined by CD14 antibody labeling (Cat. no. 130-113-708; Miltenyi Biotec), and cell viability by propidium iodide (PI) staining. Cells were analyzed by flow cytometry on a BD FACSAria III (BD Biosciences, San Jose, CA, USA). For the generation of immature DCs (iDCs), CD14+ monocytes were cultured in R10 medium (RPMI 1640 with 10% FBS, 1% streptomycin/penicillin, and 100 mM Sodium Pyruvate) supplemented with IL-4 (100 ng/mL; cat. no. 300-25; PrepoTech, Rocky Hill, NJ, USA) and GM-CSF (100 ng/mL; cat. no. 300-03; Prepotech) and kept in a humidified atmosphere (5% CO2, 37°C), for 5 days. The incubation medium was replaced after three days with new (pre-warmed) R10 medium supplemented with GM-CSF and IL-4. For maturation of DCs, iDCs were transferred to 6-well tissue culture plate and incubated (37°C, 48h.) in 5% CO2 humified atmosphere in the presence of the following cytokines (PrepoTech): IL-6 (15 ng/mL), IL-1β (10 ng/mL) TNF-α (50 ng/mL), and PGE2 (1 μg/mL). Absolute cell count of mature-DCs (mDCs) was determined by flow cytometry *via* light scatter signals and PI fluorescence.

Co-Cultures and Dendritic Cell Stimulation With CAF-Conditioned Medium

In co-culture experiments, control and irradiated CAFs were established in 24-well plates (2×10^5 cells per well). Monocytes or iDCs were thereafter added at a density of 4×10^5 live cells per well (ratio; 2:1). Cultures with mixed cell types were further incubated for 48h at 37°C in R10 medium. Parallel procedures were implemented for experiments with CAF-CMs, but instead of cells, CAFs culture supernatants were collected, diluted (1:1) with fresh pre-warmed R10 medium, and added to the DC

cultures. For differentiation studies, monocytes were exposed to GM-CSF and IL-4 immediately after initiation of co-cultures or incubations with CAF-CM. For maturation studies, iDCs were exposed to cytokine-maturation cocktail immediately after initiation of co-cultures or incubations with CAF-CM. Following treatments, DCs and supernatants were collected and used for further analysis.

Quantitative Cell Surface Markers Expression by Flow Cytometry

DCs surface markers were analyzed by flow cytometry on BD FACSAria III using the FlowJo software, Ver.7.2.4 (Tree Star, Ashland, OR, USA). Briefly, DC preparations (3×10^5 cells/condition) were labeled with panels of specific antibodies for each phenotype (Miltenyi Biotec). Maturation markers consisted of CD40, CD80, CD86, and HLA-DR (Cat. no. 130-099-385, 130-110-371, 130-113-571, and 130-111-943, respectively) whereas differentiation markers were identified by CD209 (DC-SIGN), CD1a, and CD14 (Cat. No. 130-101-239, 130-097-905, and, 130-113-708, respectively). Isotype controls consisted of REA control and IgG2a (Cat. no. 130-113-450 and 130-104-612, respectively). Data were obtained by flow cytometry using the following gating strategy: a) Differentiation markers: cells gated according to their scatter properties (FSC-A *vs* SSC-A), doublets exclusion (SSC-H *vs* SSC-W), and analyzed by the percentage of total cells expressing CD14, CD1a, and CD209; and b) Maturation markers: after cells were gated by scattering properties (described above), $CD14^+$cells were excluded by the inverted gate and then plotted for CD1a *versus* CD209 expression. Mean fluorescence intensity (MFI) of activation markers (CD40, CD80, CD86, and HLA-DR) were analyzed in the population gated for $CD1a^{med/hi}/CD209^{med/hi}$ cells.

Dendritic Cell Antigen Uptake

To assess DCs endocytic capacity, iDCs or mDCs (1×10^5), previously co-cultured with irradiated or non-irradiated CAFs or CAF-CM (as described above), were incubated with FITC-labeled dextran (1 mg/mL, Cat. no. FD40S; Sigma-Aldrich) in R10 medium prepared with RPMI without phenol red (ThermoFisher Scientific, Waltham, MA, USA) for 60 min at 37°C. Non-specific binding of FITC-dextran to the cell surface was checked by keeping a control sample on ice for 60 min. Then, all samples were washed twice (centrifugation at 300×g, 5 min, 4°C) with ice-cold PBS supplemented with 0.5% of BSA and ultimately resuspended in the same ice-cold buffer. The uptake of FITC-dextran was determined by measuring MFI of the probe in cells by flow cytometry. Dead cells were excluded from the analysis by PI fluorescence. For analyses, the specific uptake of FITC-dextran was calculated by subtracting MFI of the control sample (incubated on ice) from MFI of samples incubated at 37°C.

Dendritic Cell Migration

CCR7-dependent chemotactic responses of mDCs towards CCL19 was measured by a Boyden chamber assay. Briefly, iDCs or mDCs, previously exposed to control or irradiated CAFs/CAF-CMs (as described above), were resuspended in 200 µL of RPMI 1640 with 10% FBS at a density of 5×10^5 cells/mL and placed in the upper compartment of a 24-well Transwell Plates (Corning; pore size 5 µm). Bottom chambers were filled with fresh pre-warmed standard fibroblast growth medium in the presence or absence of the chemoattractant CCL19 (50 ng/mL) (Cat. # 130-105-744, Miltenyi Biotec). In experiments with CAF-CM, bottom chambers were filled with CM from irradiated and control CAF cultures diluted (1:1) with fresh pre-warmed growth medium. After incubation in a humidified atmosphere (5% CO2, 37°C, 3h), cells that had migrated into the lower compartment were harvested and counted in a hemocytometer under light microscopy.

Assessment of T Cell Priming Capacity of mDCs

Purified allogeneic naive $CD4^+$ T cells were isolated from PBMCs-pool using magnetic Naive $CD4^+$ T Cell Isolation Kit II (Cat. no. 130-094-131; Miltenyi Biotec) and labeled with carboxyfluorescein succinimidyl ester (CFSE) (Cayman Chemical, Ann Arbor, MI, USA) for 15 min at 37°C (1:400 dilution in PBS). The purity of isolated enriched naïve $CD4^+$ T cells was determined by CD4, CD45RO, and CD45RA antibody labeling (cat. no. 130-113-776, 130-109-507, and 130-098-187; Miltenyi Biotec). CSFE-stained $CD4^+$ T cells (5×10^5 cells/mL) were co-cultured with iDCs or mDCs (1×10^6 cells/mL, ratio 1:2), previously incubated with irradiated or control CAFs/CAF-CM for 48h (as described above), in MLR medium (RPMI 1640, 2 mM L-glutamine, non-essential amino acids, 0.1 mM sodium pyruvate, 5% AB serum) for 7 days at 37°C, 5% CO_2. Proliferation of $CD4^+$ T cells was determined by measuring CFSE fluorescence intensity by flow cytometry. Cell debris and dead cells were excluded from the analysis by scatter signals and PI fluorescence.

Quantitative Cytokine Release by ELISA

Quantitative determinations of IL-10 and IL-12 in supernatants (diluted 1:10) from co-cultures (DCs/CAFs) or DCs cultures stimulated with CAF-CM were determined using ELISA kits (R&D Systems, Minneapolis, MN, USA) according to the manufacturer's instructions. For TSLP quantification, CAFs were cultured at T-75 tissue culture flasks in DMEM (with 10% FBS) and exposed to fractionated medium-dose of IR (3×6 Gy) or stimulated with 10 ng/mL of TNF-α (PrepoTech) to induce TSLP secretion by CAFs (28). After 48h, CM were collected, spun down by centrifugation (2000x g, 4°C, 10 min), filtrated (Ø = 0.45 µm) and stored at -80 °C. Samples (diluted 1:2) were analyzed using Human TSLP ELISA Kit (Abcam, Cambridge, UK). Absorbance at 450 nm for each sample was analyzed by SpectraMax Plus 384 Microplate Reader (Molecular Devices, CA, USA).

Immunoblotting

Whole-cell extracts from DCs or CAFs were prepared in RIPA buffer (Cell Signaling, Boston, MA, USA) plus Complete Protease and Phosphatase Inhibitor Cocktail (ThermoFisher, cat.no. 78440). Total cell-associated proteins were separated on 10% SDS-polyacrylamide gel electrophoresis (PAGE) and

transferred onto a PVDF membrane. The membrane was blocked with 1% BSA in tris buffered saline, 0.1% Tween 20 (TBS-T) for 2h at room temperature, and then incubated (overnight, 4°C) with primary antibodies (anti-GAPGH, cat. no. 5174; anti-STAT3, cat. no. 4904; anti-p-STAT3 (S727), cat.no. 34911; anti-p-STAT3 (Y705), cat-no. 9145; anti-NF-κB/p65, cat.no. 8242; anti-p-NF-κB/p65, cat.no 3033; Cell Signaling; anti-TDO2, cat.no. ab76859) diluted 1:1000 (in TBS-T with 1% BSA). Subsequently, the membrane was washed 5x in TBS-T and then incubated with an anti-rabbit or anti-mouse HRP-conjugated secondary antibody (diluted 1:2000; Cell Signaling) for 1h at room temperature. Finally, proteins transferred to the membrane were visualized with Enhanced Chemiluminescence at ImageQuant LAS 4000 CCD (GE Healthcare Bio-Sciences, PA, USA). Relative intensity was assessed using ImageJ software.

Statistical Analysis

All statistical analyses were performed using GraphPad Prism (GraphPad Software, Inc, La Jolla, CA). Comparison of data between experimental groups was analyzed using the Brown-Forsythe and Welch ANOVA test, and significance values were adjusted by Dunnett's T3 correction for multiple comparisons. Outcomes of Western blot experiments were analyzed using the 2way ANOVA test, and significance values were adjusted by Dunnett correction for multiple comparisons. The level of significance was set at $p < 0.05$. Results were presented in graphs, where each donor was plotted as an individual dot in the dataset. In ELISAs, only readings above the detection limit of the assay are shown.

RESULTS

CAF-Mediated Effects on DC Phenotypic Differentiation and Maturation

To investigate the effects of IR on CAF-mediated regulation of monocyte-to-DC trans-differentiation, peripheral blood monocytes from health donors ($CD14^+$ cells – 89% purity) were cultured in medium containing DC differentiation cytokines (IL-4 and GM-CSF) in the absence or presence of conditioned medium from irradiated or non-irradiated CAFs (CAF-CM) or alternatively in (CAF-DC) co-cultures (CAF-CC). DCs were not differentiated from peripheral blood monocytes of cancer patients mainly because of an individual constitutional characteristic of the patients that reflects on phenotypic and functional alterations in mo-DC (33–35). Following incubation for 6 days, non-adherent cells were harvested and phenotyped by flow cytometry. Considering the potentially different effects triggered by different radiation schemes, we compared the effects of fractionated and single-high dose radiation. **Figure 1** shows the percentage of cells expressing signature DC surface marker molecules CD1a and CD209 (DC-SIGN), and the lipopolysaccharide co-receptor CD14, as determined by flow cytometry. Transformed monocytes presented the typical phenotypic profile of immature DCs (iDCs) defined by $CD1a^{high}$, $CD209^{high}$, and $CD14^{medium/low}$ (**Figure 1A**). As shown in **Figure 1B**, the presence of CAFs clearly interferes with monocyte-DC differentiation, especially in co-culture conditions. DCs in co-culture with CAFs expressed significantly lower levels of CD1a ($p \leq 0.001$) and CD209 ($p \leq 0.01$) and increased expression of CD14 ($p \leq 0.01$). In experiments with CAF-CM, only the expression of CD1a was slightly decreased when compared to iDCs controls. Of note, no statistically significant differences were observed in the expression of any of the receptors when comparing irradiated with non-irradiated CAF conditions, both in CC- or CM-conditions.

To induce DC maturation, iDCs were exposed for 2 days to a maturation-cocktail of cytokines comprising IL-6, IL-1β, TNF-α, and PGE2. Matured DCs (mDCs) cultured in the absence or presence of CM from irradiated or non-irradiated CAFs revealed differences in their morphology (**Figure 2**). Whereas conventional mDC presented abundant cellular protrusions and membrane ruffling, DCs maturated in the presence of CAF-CM appeared with a typical iDC morphology; large rounded cells with eccentrical nucleus location and few cellular protrusions. However, this effect was to some extent abolished in cells cultured in the presence of irradiated CAF-CM.

Next, we determined whether CAFs could affect DC maturation. Surface expression of antigen-presenting receptor HLA-DR and the co-stimulatory receptors CD40, CD80, and CD86 were analyzed following the gating strategy described in **Figure 3A**. As expected, stimulation of iDC with the cytokine maturation cocktail enhanced the expression of CD40, CD80, CD86, and HLA-DR as shown in **Figure 3B**. However, cells incubated with CAF-CM showed decreased expression of CD80 ($p = 0.4256$), CD86 ($p \leq 0.05$), and HLA-DR ($p = 0.8375$), with same tendency also for CD40. Similarly, in co-culture conditions, CAFs were exerting inhibitory effects on surface expression of CD40 ($p \leq 0.01$) and HLA-DR ($p \leq 0.01$), compared to mDCs controls. No statistical differences were observed when comparing DC phenotype cultured with both irradiated and non-irradiated CAF-CM or CAF-CC. Nevertheless, CAFs irradiated with fractionated medium-doses showed a tendency to reverse the paracrine effect on the expression of DC surface receptors exerted by control CAFs (**Figure 3C**).

Effects of CAFs on DC Cytokine Release

To explore further the immunoregulatory properties exerted by CAFs on DCs, we quantified protein levels of IL-10 and IL-12 in culture supernatants from DCs exposed to CAF-CM or in co-cultures under the stimulus of maturation cocktail. Of note, CAF exposed to DCs maturation cocktail did not secrete significant levels of IL-10 and IL-12 as shown in **Supplementary Figure 3**. Results from corresponding analyses of IL-10 and IL-12 are presented in **Figure 4**. The amount of IL-10 was very low in supernatants of iDCs and nearly undetectable in mDCs, treated or not with CAF-CM. However, levels of IL-10 were considerably increased ($p \leq 0.05$) in CAF-CC experiments, including both irradiated and non-irradiated CAFs. On the other hand, levels of IL-12 were undetectable in iDCs cultures but considerably increased in mDCs supernatants. Interestingly, a significant increase in secreted levels of IL-12 was observed in mDCs cultures in the presence of CM from the two irradiated-CAF

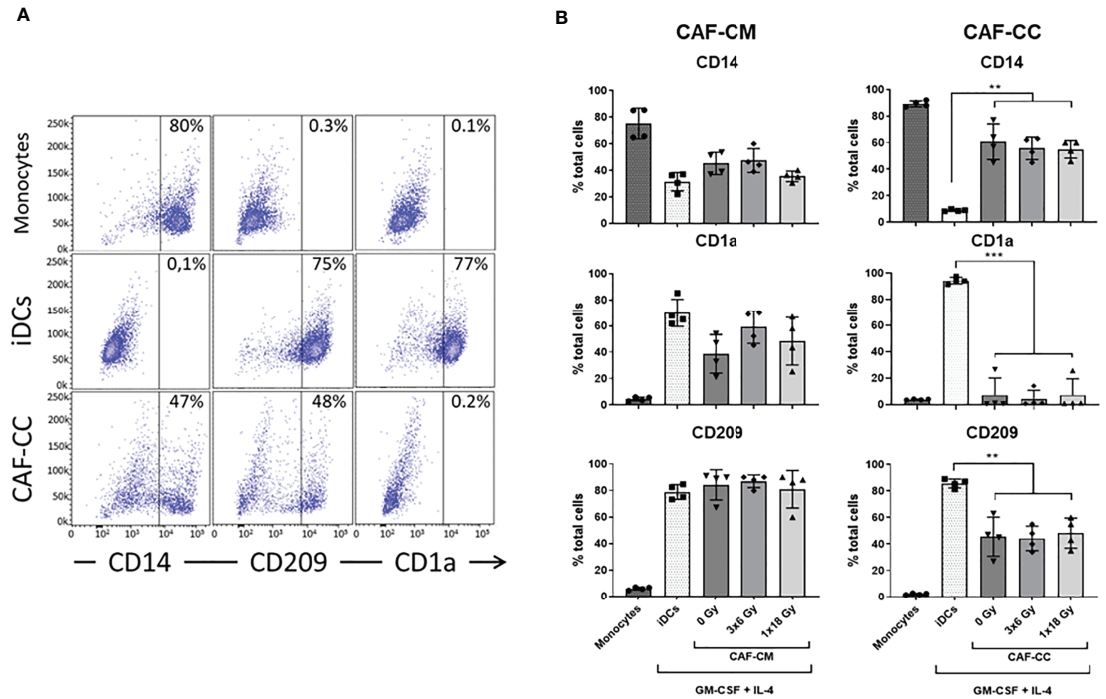

FIGURE 1 | Effects of CAFs on DC differentiation markers. Monocytes stimulated with GM-CSF and IL-4 were incubated for 6 days with conditioned medium from irradiated or non-irradiated CAFs (CAF-CM, left panels) or in co-cultures (CAF-CC, right panels). Resulting expression of iDC cell surface markers CD14, CD1a, and CD209 were evaluated by flow cytometry. **(A)** Representative dot plots of the percentage of expression of CD14, CD209, and CD1a in monocytes, iDCs, and monocytes stimulated with GM-CSF and IL-4 in co-culture with CAFs. **(B)** Bar graphs represent mean (± SD) values from flow cytometry analysis of 4 different CAF donors, measured independently. Pattern columns indicate surface levels in control monocytes and iDC cultures. Results are expressed as percentage of total cells. Brown-Forsythe and Welch ANOVA test and *p-values* were determined between iDCs and non-irradiated CAFs, iDCs, and the two irradiated CAF-groups separately. **p ≤ 0.01

groups (3x6 Gy, $p \leq 0.05$; 1x18 Gy, $p \leq 0.0001$). Moreover, increased IL-12 secretion was also observed when mDCs were co-cultured with CAFs irradiated at 3x6 Gy ($p \leq 0.05$), whereas minor differences were seen between mDC alone or co-cultured with non-irradiated or 1x18 Gy irradiated CAFs (**Figure 4**).

CAF-Mediated Effects on DC Functions

We sought to explore the capacity of CAFs to modulate key functional properties on DCs. First, we analyzed changes in the endocytic capacity of DCs by exposing DC cultures for 1h to soluble FITC-dextran by flow cytometry. iDCs had the highest antigen uptake capacity, reflected in an increased MFI, as compared to mDCs (**Figure 5A**). Of note, immature DCs exposed to CM from non-irradiated ($p \leq 0.01$) and high-dose irradiated ($p \leq 0.05$) CAFs presented a significant decrease in uptake capacity, as compared to untreated iDCs. Notably, DC uptake of FITC-Dextran in the (3x6 Gy) irradiated CAF-CM group was comparable to (high-uptake) iDCs controls. However, in CAF-CC, no significant differences were observed between iDCs control and CAF-treated groups (**Figure 5B** and **Supplementary Figure 4**).

Second, we assessed the capacity of CAFs to modulate the migratory capacity of mDCs. DC migration depends on the surface expression of C-C Motif Chemokine Receptor 7 (CCR7) (36). CCR7 expression increase during DC maturation, acting as a receptor for the constitutively expressed chemo-attractants CCL21 and CCL19 (37). As illustrated in **Figure 5C**, mDCs display much higher migration rates as compared to iDCs. Matured DCs exposed to any of the three different CAF-CMs resulted in decreased migratory capacity with significant values from both control CAF-CM ($p \leq 0.01$) and irradiated CAF-CM (3x6 Gy, $p \leq 0.05$; 1x18 Gy, $p \leq 0.01$), although DCs exposed to (3x6 Gy) irradiated CAF-CM displayed a significantly increased migration rates compared to other CAF-CM groups. In CAF-CC conditions, no significant differences in migration were observed between mDCs control and CAF-treated groups (**Figure 5C**).

Third, we tested how CAFs may influence the mDC capacity to induce T cell proliferation in a mixed lymphocyte reaction (MLR). To this end, we isolated and labeled allogeneic naive $CD45RA^+/CD4^+$ T cells (purity of 91%, **Figure 5D**) from whole blood with CFSE. The resulting fluorescent T cells were incubated with mDCs (2:1 ratio) that were previously conditioned with CAF-CM or CAF-CC for 48h. T cell proliferation rates were measured by CFSE dilution assay and analyzed by flow cytometry (**Figure 5D**). mDCs were able to stimulate T cells proliferation much more efficiently than iDCs. However, a significant decrease in T cell proliferation was observed when mDCs were pre-exposed to irradiated or non-irradiated CAF-CM ($p \leq 0.05$), or with CAF-CC ($p \leq 0.05$)

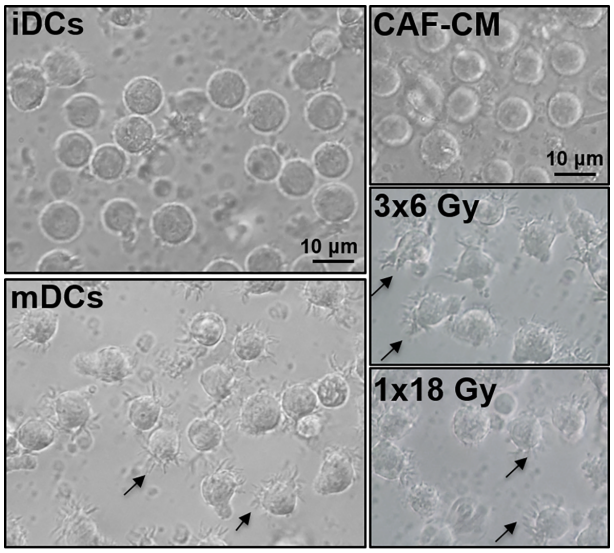

FIGURE 2 | Effects of CAF-CM on DC phenotype. Gross morphology of DC cultures by phase-contrast microscopy. Immature DCs show a classical round morphology whereas mature DCs present characteristic dendrites. Incubations with CAF-CM partially revert the phenotype of mDCs into iDCs (top-right panel), whereas this effect is lost in the conditioned medium from CAFs exposed to 3x6 Gy. Cells presenting dendrites in control mDCs and fractionated radiation (3x6 Gy) CAF-CM groups are shown by arrowheads. Scale Bars = 10 µm.

(**Figure 5E**). In both conditions, ionizing radiation, applied in single or fractionated doses, did not change the CAF-mediated suppressive effects on DC-mediated T cell proliferation.

Alterations on STAT3 Signaling and NF-κB/p65 Activation in CAF-Exposed DCs

To investigate CAF-mediated DC alterations in NF-κB/p65 and STAT3 signaling pathways, DCs were exposed to irradiated and non-irradiated CAF-CM (from 3 different donors) during DC maturation, and expression of total and phosphorylated NF-κB/p65 and STAT3 were analyzed by immunoblotting (**Figure 6A**). STAT3 signaling analysis showed that phosphorylation of STAT3 at Y705 was enhanced in DCs incubated with CAF-CM, and significantly increased in cells exposed to CM from irradiated groups as compared to non-irradiated (3x6 Gy, $p \leq 0.05$), but even more pronounced when compared to the group irradiated with a single high-dose ($p \leq 0.001$). No significant differences between irradiated and non-irradiated groups were observed on STAT3 phosphorylation at S727, although irradiated-CAF-CM showed a tendency to increase the phosphorylation at S727 (**Figure 6B**). Similar patterns were observed in the activation of NF-κB/p65; expression of total NF-κB/p65 were increased in DCs exposed to irradiated-CAF CM. However, phosphorylation at S536 was lower in DCs exposed to CM from CAFs irradiated with high-single dose ($p \leq 0.001$). Of note, CM from non-irradiated CAFs attenuated both total and phosphorylated NF-κB/p65 in DCs (**Figure 6B**). In summary, these data indicate that: 1) secreted factors from CAFs can interfere with cytokine-induced NF-κB/p65 and STAT3 signaling on DCs, and 2) ionizing radiation abrogates to some degree the CAF-mediated effects.

Effect of Radiation on CAFs Secretory Profile and Paracrine Signaling

Earlier studies on the crosstalk between CAFs and DCs in different cancer models suggest that CAF-mediated immunoregulation on DCs is achieved *via* release of the cytokine thymic stromal lymphopoietin (TSLP) or expression of the catalytic enzyme tryptophan 2,3 dioxygenase (TDO2). To investigate the possible effects of fractionated medium-dose radiation on the expression of TDO2 and TSLP, both CAFs and A549 lung tumor cells were irradiated (3x6 Gy and 3x8 Gy, respectively) and the expression of TDO2 was analyzed in cell lysates by immunoblotting (**Figure 7A**), whereas TSLP release was analyzed in supernatants by ELISA (**Figure 7C**). Lung tumor cells (A549) showed significantly higher expression of TDO2 than CAFs ($p \leq 0.01$) (**Figure 7B**). However, no significant differences were observed between irradiated and non-irradiated CAFs or A549 groups on TDO2 expression (**Figures 7A, B**). Positive controls, represented by A549 cells stimulated with poly (I:C) and CAFs stimulated with IFN-γ, showed a slight increase in TDO2 expression compared to untreated cells. Analysis by ELISA showed no differences in the secretion of TSLP between irradiated and non-irradiated CAFs whereas CAFs treated with TNF-α (positive controls) secreted significantly higher levels of TSLP as compared to the control group ($p \leq 0.001$) (**Figure 7C**). In summary, these data indicate that the depriving effects mediated by fractionated medium-dose radiation on CAF-induced DCs tolerogenic phenotype are not dependent on the regulation of TDO2 or TSLP expression.

Further, we characterized the effect of IR on IFN-β secretion by CAFs. Analysis by ELISA showed that IFN-β levels were not detectable in the CM from non-irradiated and irradiated CAFs (3x6 Gy and 1x18 Gy) after 48, 96, and 144h of IR exposure (**Figure 7D**). On the other hand, A549 tumor cells exposed to 3x8 Gy secreted increased levels of IFN-β ($p \leq 0.01$) 144h post-IR exposure, as compared to non-irradiated cells (**Figure 7E**). Next, we determined whether CM from fractionated irradiated CAFs (3x6 Gy) could induce DC maturation through the analysis of co-stimulatory receptors CD40 and CD86, and the induction of T cell proliferation in MLR. As shown in **Figure 7F**, no differences in the expression levels of CD40 and CD86 were observed in DC stimulated with CM from irradiated or non-irradiated CAFs (3x6 Gy) and A549 tumor cells (3x8 Gy). CAFs stimulated with IFN-γ (positive control) showed a slight increase in CD86 expression on DCs compared to cells cultured with CM from untreated CAFs (**Figure 7F**). Similar patterns were observed in the ability of DCs to stimulate T cell proliferation. We show that iDCs incubated with CM from non-irradiated and irradiated CAFs or A549 tumor cells were not able to induce $CD4^+$ T cell proliferation to the extent of mature DC controls (**Figure 7G**).

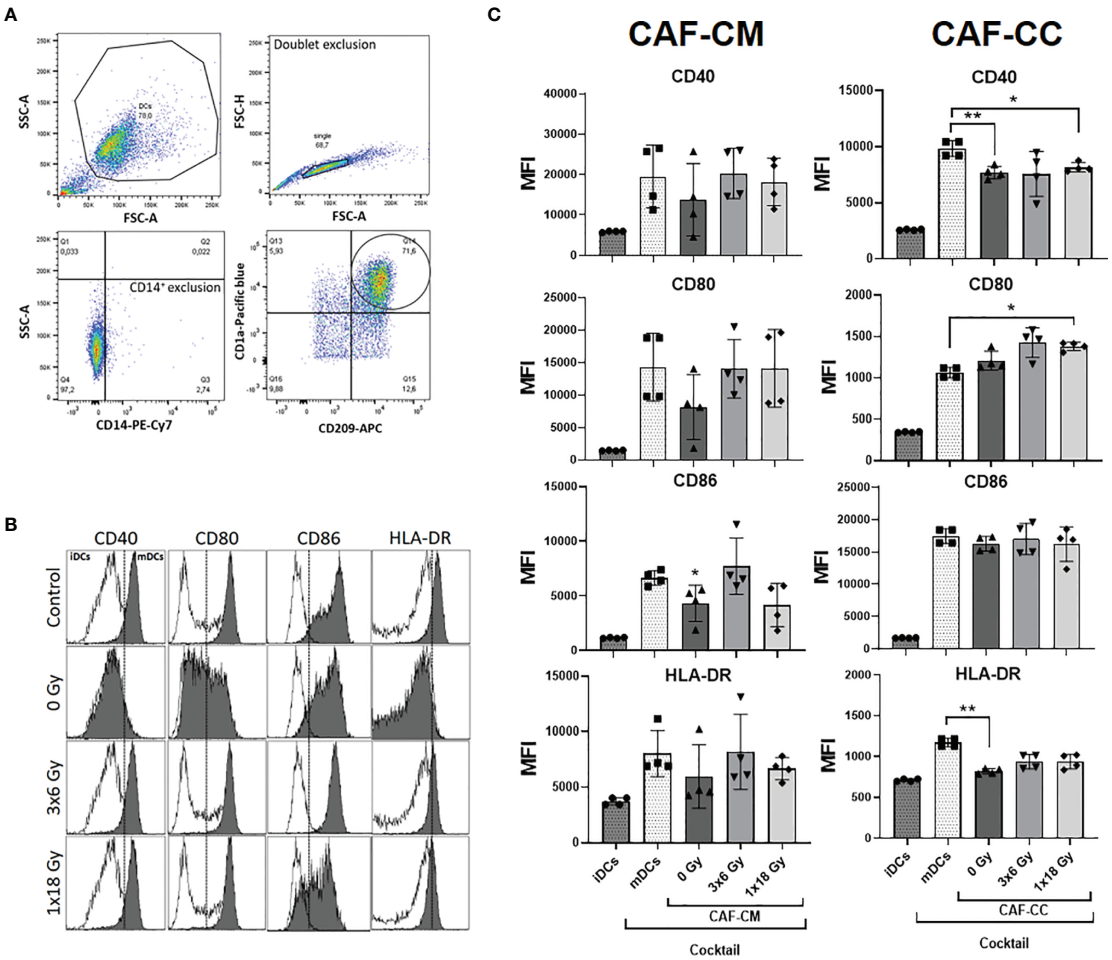

FIGURE 3 | Effects of CAFs on DC activation markers. Immature DC (iDCs) stimulated with a maturation cytokine cocktail were incubated for 48h with conditioned medium from irradiated or non-irradiated CAFs (CAF-CM, left panels) or in co-cultures (CAF-CC, right panels). Resulting expression of mDC cell surface markers CD40, CD80, CD86, and HLA-DR was evaluated by flow cytometry. **(A)** Gating strategy used to analyze the expression of activation markers in DCs. **(B)** Representative histograms of expression by mean fluorescence intensity (MFI) of CD40, CD80, CD86, and HLA-DR in DCs stimulated with maturation cocktail in culture with conditioned medium from non-irradiated and irradiated CAFs (1 donor). **(C)** Bar graphs represent mean (± SD) values from flow cytometry analysis of four-4 different CAF donors, measured independently. Pattern columns indicate protein surface levels in control iDC and mDC cultures. Results are expressed as percentage of total cells. Data represent mean (± SD) values from 4 different CAF donors measured independently. Brown-Forsythe and Welch ANOVA test and *p-values* were determined between control and non-irradiated CAFs, mDCs, and the two irradiated CAF-groups individually. *p ≤ 0.05, **p ≤ 0.01.

DISCUSSION

In the present study, we have investigated how CAFs from lung tumors influence monocyte-derived DC differentiation, maturation, and functions *in vitro*; and whether ionizing radiation is able to modify the CAF-mediated immunoregulatory features on DCs. We have observed that: (i) CAFs hamper monocytes differentiation into DCs; (ii) CAFs induce a tolerogenic phenotype on mature DCs, as evidenced by decreased expression of activation markers (CD80, CD86, CD40, and HLA-DR) and reduced functional properties (migration, antigen uptake, and $CD4^+$ T cell priming); (iii) IR applied in fractionated medium-doses (3x6 Gy) reverts some of the CAF-mediated effects on DCs; (iv) IR induces changes in CAF paracrine factors that modulate the activation of NF-κB/p65 and STAT3 signaling pathways on DCs; (v) neither TSLP nor TDO2 expression in CAFs is altered by radiation exposure.

Early on, we showed that cytokine-induced monocyte differentiation into DCs is hampered in the presence of CAFs. DCs exposed to both irradiated and non-irradiated CAFs showed increased levels of the monocyte marker CD14 and decreased expression of DC signature molecules CD1a and CD209 (DC-SIGN). Some authors consider residual $CD209^+$ cells as macrophages based on their morphology and co-expression of CD14 (38). However, we did not confirm whether CAF-educated monocytes were macrophages or not. The failure of those cells to downregulate CD14 could be attributed, in part, to the secretion

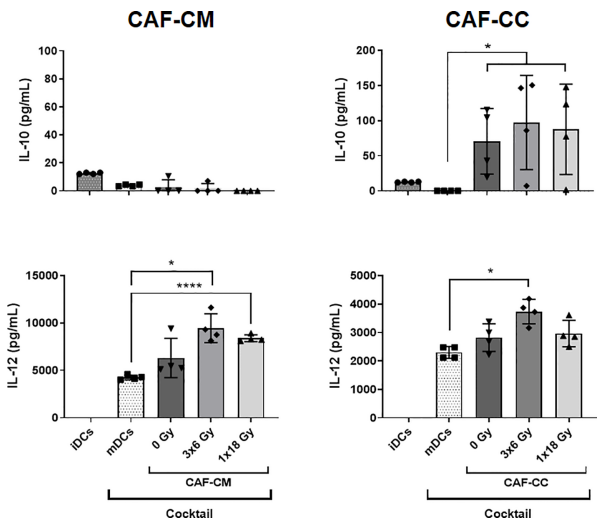

FIGURE 4 | CAF-induced cytokine secretion by DCs. Monocyte-derived dendritic cells in non-stimulated or stimulated conditions were incubated for 48h with irradiated or non-irradiated CAF conditioned medium (CAF-CM, left panels) or in co-cultures (CAF-CC, right panels). Resulting levels of IL-10 (top panels) and IL-12 (lower panels) found in supernatants were quantified by ELISA assays. Data represent the mean (± SD) values from 4 different CAF donors measured in duplicates. Brown-Forsythe and Welch ANOVA test and-values were determined between mDCs and non-irradiated CAF-CM, mDCs *vs* irradiated CAFs. *p ≤ 0.05, ****p ≤ 0.0001.

of IL-6 by CAFs. Fibroblast-derived IL-6 has previously been shown to affect differentiation of monocytes into macrophages rather than DCs, by inducing expression of functional M-CSF on monocytes (39). In a different study, Spary et al. (40) demonstrated that the high expression of IL-6 produced by stromal cells (α-SMA$^+$ cells), in prostate cancer tissue, is correlated with an induction of tolerogenic DCs phenotype, characterized by cells expressing high surface levels of CD14 and PD-L1. We have previously shown that lung CAFs represent an important source of IL-6 into the TME, however, exposure to IR does not seem to modify substantially IL-6 release from CAFs in cultures (31, 32). Likewise, Kalinski et al. (41) suggested that monocyte differentiation into DCs could be regulated by PGE2, with subsequent activation of cyclic nucleotide signaling pathways on DCs, blocking both down-regulation of CD14 and up-regulation of immature DC marker CD1a. In agreement with our observations, CAFs in cultures have been shown to produce PGE2, but its expression remains stable upon irradiation (30). Additionally, TGF-β and IFNs have been identified as negative regulators of CD209 expression and, consequently, inhibit CD209-dependent binding of HIV-1 to differentiated DCs (42). In the radiation context, we have previously shown that CAF-secreted TGF-β is not changed after exposure to single high-dose or fractionated medium-dose IR (30, 32) and in this study, we show that IFN-type I is undetectable in supernatants from irradiated or control CAFs (**Figure 7**). Collectively, knowledge generated on the irradiated CAF secretory profile, showing unchanged levels of relevant immunosuppressive signals, may explain to some extent the observation that CAF-induced effects on monocyte-to-DC differentiation is not changed after IR.

Moreover, we show that iDCs in the presence of CAF-CM display reduced antigen uptake capacity, which can be correlated with the down-regulation of CD209 expression in the target cells (43). Importantly, we showed that fractionated medium-dose radiation abrogates the CAF-mediated paracrine effect on DCs antigen uptake. However, we see no differences in the expression of CD209 in DCs exposed to irradiated or non-irradiated CAF-CM, suggesting that CAFs could regulate expression of different receptors involved in the uptake of dextran, e.g. mannose receptor (CD206), langerin receptor (CD207) or scavenger receptors (44, 45). Furthermore, iDCs were maturated with a cocktail of cytokines, including TNF-α, IL-1β, IL-6, and PGE2. The rationale for the use of this cocktail is to enhance the pro-inflammatory effects and to attempt mimicry of the RT-induced inflammatory tumor microenvironment. We found that both CAF paracrine factors and cell-contact mediated mechanisms were involved in the induction of a tolerogenic phenotype in DCs, characterized by lower expression of co-stimulatory markers, enhanced IL-10 release, along with reduced antigen capture, lower migratory capacity, and T cell priming capacity. Differences in DCs phenotype and function were observed between experiments conducted with CAF conditioned medium and in co-culture conditions. We hypothesize that the presence of concentrated soluble factors on CAF conditioned medium can significantly modulate the functions of DCs compared to those in DCs co-cultured with CAFs. On the other side, in co-culture conditions, we must consider effects coming from both soluble signals and cell-cell contacts, and effects exerted in two directions, whereas in CM conditions we only observe effects exerted by CAFs on DCs mediated by soluble factors. Previous studies demonstrated that both cell-cell interaction (fibroblasts/DCs) and soluble factors secreted from fibroblasts could act as potent regulators of DC differentiation and function (46–48). Collectively, our data are in line with previous studies that have demonstrated a direct connection between tumor-associated fibroblasts and induction of tolerogenic DCs in hepatocellular carcinoma (27), lung (26), and pancreatic (28) cancers. Some CAF-released suppressive soluble mediators, like TGF-β, IL-6, or PGE2, as well as VEGF, TDO, and TSLP, have been shown to impair DC maturation, co-stimulatory molecule expression, and antigen-presenting function (17, 26, 28, 42). We have shown in previous *in vitro* studies that protein levels of IL-6, TGF-β, VEGF, or PGE2, secreted by CAFs, are not significantly modified after direct radiation exposure (31, 32). In this study, we additionally show that CAF-derived TSLP and TDO2 levels are unchanged after exposing CAFs to fractionated medium-dose IR. The results suggest that the loss of CAF-mediated effects over DC following IR is not dependent on the modulation of previously highlighted soluble mediators.

Furthermore, we observed that IR applied as fractionated medium-doses, but not as single high-doses, promotes the loss of

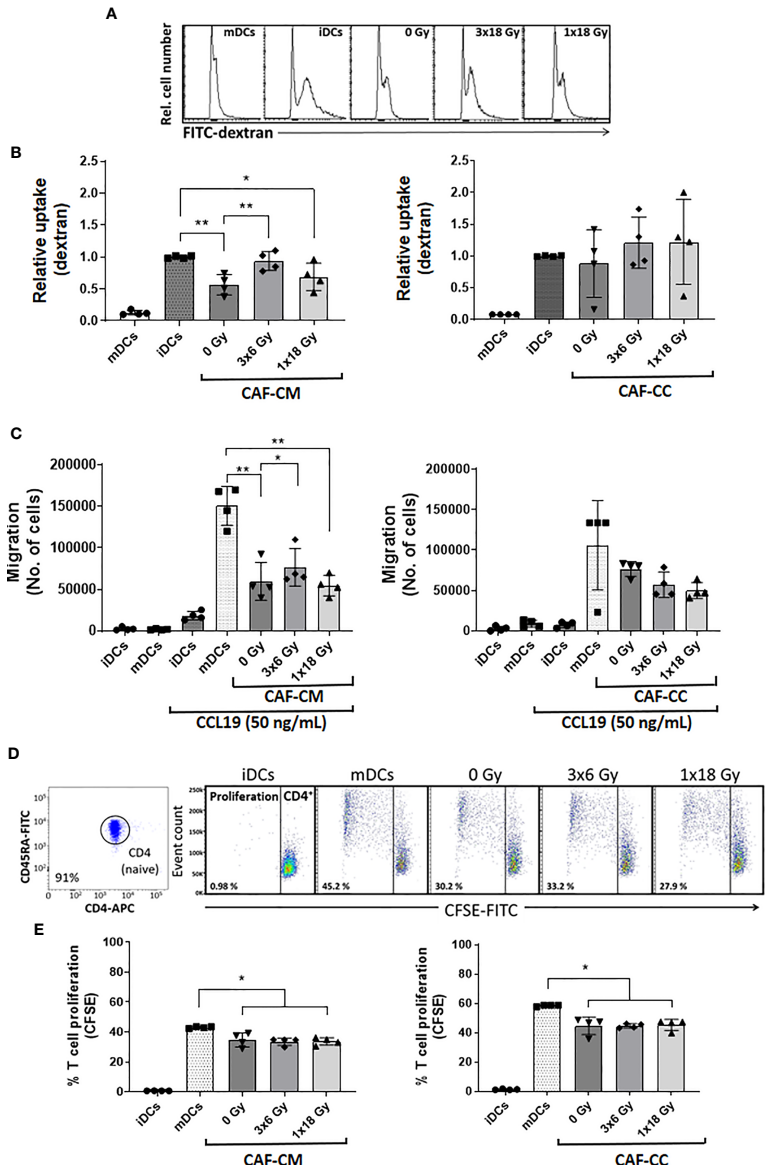

FIGURE 5 | CAF-mediated effects on DC functions. Antigen uptake capacity by DCs was analyzed by flow cytometry. After initial treatments, DCs were cultured for 60 min in the presence of FITC-dextran. Relative FITC-dextran uptake was calculated by subtracting MFI of cells incubated for 60 min on ice from MFI of cells allowed to internalize antigen during 60 min at 37°C. **(A)** Representative histograms indicating MFI of FITC-dextran uptake by mDCs. **(B)** Bar graphs represent mean (± SD) values from flow cytometry analysis of four-4 different CAF donors measured independently. **(C)** DC migration rates were measured by the Boyden chamber assay. The total number of cells that migrated towards a CCL19 gradient during 3h was determined for each experimental group. **(D, E)** DCs T cell priming capacity was analyzed by CFSE-dilution assay. Naive $CD4^+$ T cells were co-cultured with mDCs (ratio 2:1) in the presence of CAFs or CAF-CM for 7 days and the percentage of proliferating T cells was determined by flow cytometry. **(D)** Representative dot plots indicating the percentage of purity of CD4RA naive T cells and the percentage of the proliferation of CD4 cells co-cultured with mDCs. **(E)** The bar graphs represent mean (± SD) values from flow cytometry analysis of 4 different CAF donors measured independently. Dead cells were excluded from the analysis by PI fluorescence. Brown-Forsythe and Welch ANOVA test and *p-values* were determined between controls and non-irradiated CAFs, mDCs, and the two irradiated CAF-groups individually. *p ≤ 0.05, **p ≤ 0.01.

CAF-mediated immunosuppressive effects on DCs *via* paracrine signaling. In an earlier preclinical study by Dewan et al., it was demonstrated that interferon type-I responses and abscopal effects in combination with immune checkpoint inhibitors are only accomplished when radiation is given in fractionated medium-high doses (3x8Gy) (49). Later on, the same group has shown that repeated medium-high doses, below a threshold of 10-12 Gy, do not induce DNA exonuclease Trex1, and thus elevates interferon-β production in tumor cells, which promotes recruitment and activation of Batf3-dependent DCs (50). Importantly, on the opposite of what it is normally observed with tumor cells, we do not see type-I IFN responses induced by

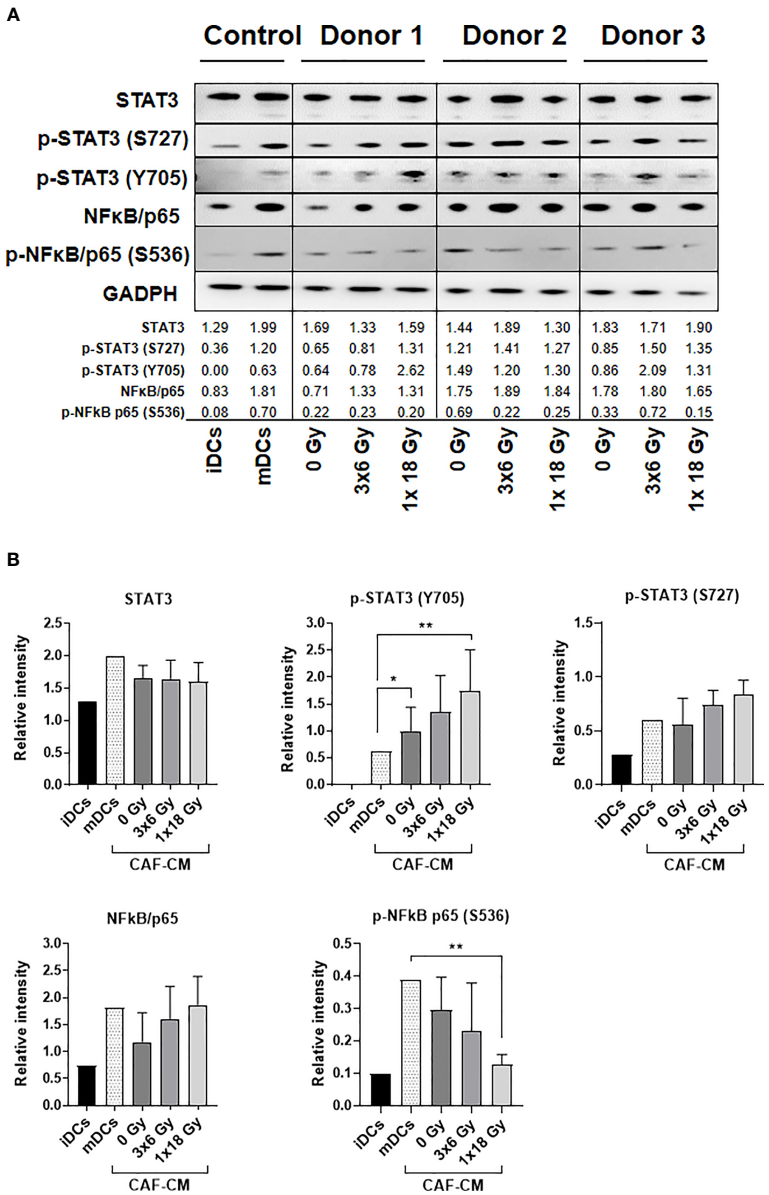

FIGURE 6 | Alterations on STAT3 signaling and NF-κB activation in DCs exposed to CAF-CM. **(A)** Western blot analysis, using anti-STAT3, p-STAT3 (S727), p-STAT3 (Y705), NF-κB/p65, and p-NF-κB/p65 (S536) on whole DC cell lysates stimulated with irradiated and non-irradiated CAF-CM. Results were normalized against GAPDH expression and the results of phosphorylated proteins were normalized against the respective total proteins. In **(B)**, the relative intensity of the bands corresponding to **(A)**, determined by densitometry, is shown as a bar graph. Data represent mean (± SD) values from 3 different CAF donors. Two-way ANOVA test and *p-values* were determined between non-irradiated CAFs, mDCs, and the two irradiated CAF-groups individually. *p ≤ 0.05, **p ≤ 0.01.

radiation in CAFs (**Figure 7D**). Accordingly, we do not observe activation of iDC by irradiated CAF supernatants. These outcomes are consistent with the highly radioresistant nature and the remarkable cytoprotective responses displayed by CAFs in stressful scenarios and suggest that CAFs do not contribute to the release of ICD signals and immune adjuvants following radiotherapy. Altogether, these observations indicate that radiotherapy, applied in hypofractionated medium-dose schemes to tumors, has the potential to achieve both induction of immune activation (from tumor cells) and reduction of immunosuppression (from CAFs) concomitantly.

To explore possible mechanisms behind the effects of irradiated CAF-CM on DCs, we investigated the activation of NF-κB and STAT3 signaling pathways on DCs. Activation of the NF-κB pathway is a central component of DC activation (51–53) and has also been implicated in the cellular response to radiation (54). During DC maturation, through pro-inflammatory stimulus (e.g., TNF-α, IL-1, IL-6, PGE2, between others), the

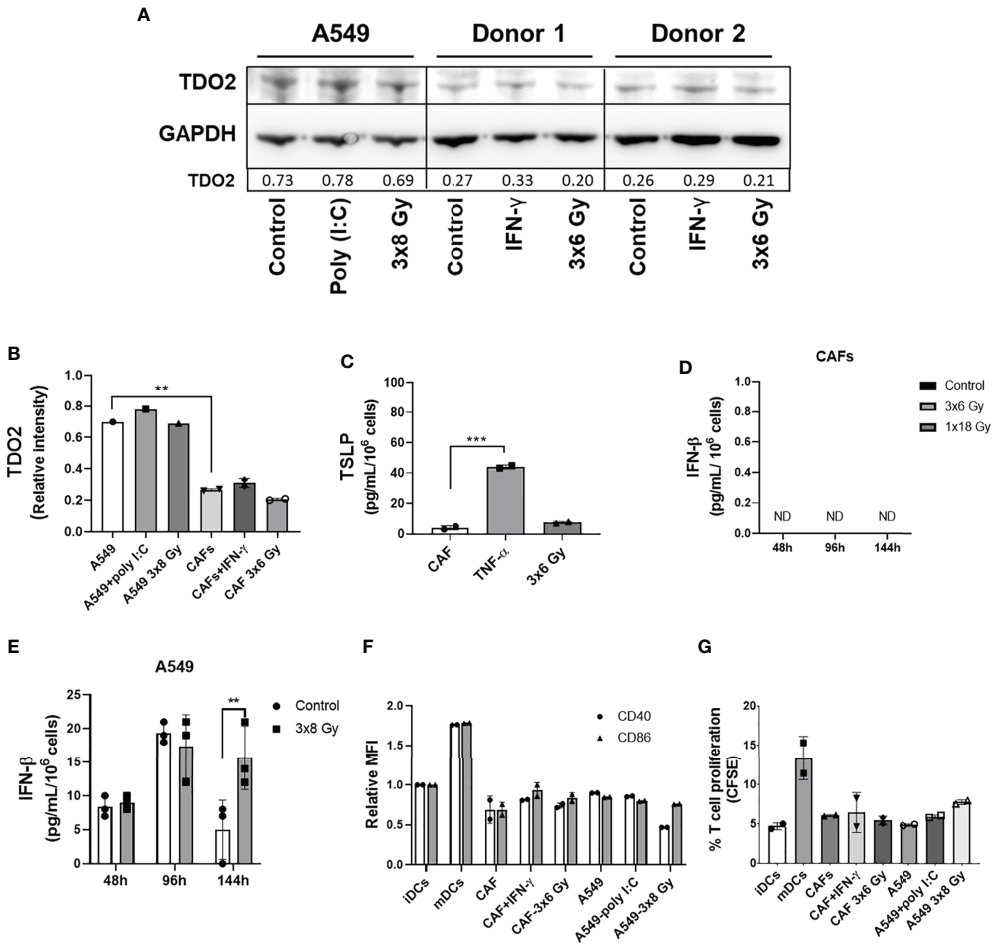

FIGURE 7 | Effect of radiation on expression of CAF immunomodulators and DC immunoregulation by irradiated CAFs supernatants. Cultures were irradiated with fractionated doses of 6 Gy (CAFs) and 8 Gy (A549) during three consecutive days. **(A)** Protein expression of TDO2 was determined by Western blotting and results were normalized against GAPDH expression. For positive controls, A549 cells were stimulated with 0.1 μg/mL of poly (I:C) and CAFs were stimulated with 10 ng/mL of IFN-γ. In **(B)**, relative intensity of the bands corresponding to panel A, determined by densitometry, is shown as a bar graph. Data represent mean (± SD) values from two different CAF donors. In **(C)**, the resulting levels of TSLP were quantified by ELISA. For positive controls, CAFs were stimulated with 10 ng/mL of TNF-α. Data represent mean (± SD) values from two different CAF donors measured in duplicates. The effect of radiation on the secretion of IFN-β by CAFs **(D)** and by A549 cells **(E)** was analyzed by ELISA assay. IFN-γ secretion in supernatants was determined 48, 96, and 144h post-irradiation. In **(F)**, the resulting expression of co-stimulatory markers CD40 and CD86 on DCs treated with CM from non-irradiated and irradiated CAFs (3x6 Gy) and A549 tumor cells (3x8 Gy) were evaluated by flow cytometry. In **(G)**, naive CD4+ T cells were co-cultured for 7 days with DCs (ratio 2:1) stimulated with CM from non-irradiated and irradiated CAFs (3x6 Gy) and A549 tumor cells (3x8 Gy), and percentage of proliferating T cells was determined by flow cytometry. Dead cells were excluded from the analysis by based on PI fluorescence. Data represent the mean (± SD) values from triplicates. Two-way ANOVA test and *p-values* were determined between non-irradiated *vs* irradiated cells. Brown-Forsythe and Welch ANOVA test and *p-values* were determined between control and TNF-α stimulated CAF-CM and control *vs* irradiated CAFs. ***p ≤ 0.001, ***p ≤ 0.001. ND, not detected.

canonical NF-κB signaling is activated (55). This signaling cascade involves phosphorylation and degradation of the inhibitory complex IκB, with release of NF-κB heterodimer p65/p50, followed by nuclear translocation and upregulated transcription of NF-κB (51, 52). On the other hand, induction of STAT3 signaling in immature myeloid cells may prevent DCs from differentiating into mature DCs (56). Several tumor-associated factors that are known to suppress DC maturation, including IL-6, IL-10, and VEGF, are activators of STAT3 (57). In this study, we observed that CM from irradiated and non-irradiated CAFs keeps NF-κB activation at lower levels during DC differentiation. However, CM from single high-dose irradiated CAFs (1x18 Gy) promoted a decreased activation of the canonical NF-κB signaling pathway. Li et al. (58) demonstrated that DCs stimulated with sera from patients with NSCLC had systematic functional deficiencies correlated with simultaneous repression of NF-κB and STAT3 signaling pathways. In our study, a slight decrease of phosphorylated p-STAT3 (S727) was observed in cells stimulated with CAF-CM. However, CM from both irradiated CAF-groups increased

expression levels of p-STAT3 (Y705) on DCs. Based on those shreds of evidence, we hypothesize that IR could modulate a pro-inflammatory CAF-secretome that regulates various downstream target genes, including cytokines, chemokines, receptors, and transcription factors that are relevant for DC functions.

Our study adds new knowledge to the important crosstalk between CAFs and dendritic cells in the irradiated tumor microenvironment. The results show that lung CAFs lower the expression of antigen-presenting molecules and co-stimulatory receptors in monocyte-derived DCs, thus inhibiting to some extent their antigen presentation capacity and their capability to activate cytotoxic T cell responses. Importantly, we have demonstrated that radiation, given as fractionated medium-dose regimens, can curtail some of the CAF-mediated inhibiting effects on DC functions. However, the radiation-induced effects were not observed when CAFs were irradiated with a single high-dose. These outcomes suggest that only certain radiation regimens may be able to modify favorably the inherent immunosuppressive functions of CAFs on DCs. The rationale behind these observations is still unknown, and the results presented in this study should also be confirmed in more complex *in vivo* models. Understanding the impact of IR on the multifactorial components in the TME will bring us closer to the ultimate goal of using radiotherapy effectively as an immunological adjuvant in the clinics.

DATA AVAILABILITY STATEMENT

The original contributions presented in the study are included in the article/**Supplementary Material**. Further inquiries can be directed to the corresponding author.

ETHICS STATEMENT

The Regional Ethical Committee of Northern Norway has approved the use of human material included in this study (REK Nord 2014/401; 2016/714; 2016/2307) and all patients provided informed written consent.

AUTHOR CONTRIBUTIONS

RB, ST, KL, and TH have been implicated in experimental work. TH established radiation protocols and conducted protocols for cell irradiation. RB, IM-Z, ST, and TH carried out evaluation and interpretation of data and drafted the manuscript. RB and IM-Z had the main role in the conception and design of the work. IM-Z has been the main coordinator of the study. All authors contributed to the article and approved the submitted version.

FUNDING

This work was supported by the Norwegian Regional Health Authorities under Grant (HNF1373-17 to RB and HNF1423-18 to TH); The Norwegian Cancer Society and the Aakre Foundation at UiT. Publication charges for this article have been funded by a grant from the publication fund at UiT, The Arctic University of Norway.

SUPPLEMENTARY MATERIAL

The Supplementary Material for this article can be found online at: https://www.frontiersin.org/articles/10.3389/fimmu.2021.662594/full#supplementary-material

Supplementary Figure 1 | Uncropped scans of Western blots found in **Figure 6**.

Supplementary Figure 2 | Uncropped scans of Western blots found in **Figure 7**.

Supplementary Figure 3 | Effects of DCs maturation cocktail on CAF-mediated secretion of IL-10 and IL-12. The release of IL-10 and IL-12 from CAFs was measured by ELISA in three different donors stimulated with IL-6, TNF-α, IL-1β, and PGE2, for 48 hrs.

Supplementary Figure 4 | Representative micrographs of uptake of FITC-Dextran by immature-DCs previously exposed to conditioned medium from irradiated or non-irradiated CAFs (Two different CAF donors) or in co-culture (CAF/DC).

REFERENCES

1. Demaria S, Golden EB, Formenti SC. Role of Local Radiation Therapy in Cancer Immunotherapy. *JAMA Oncol* (2015) 1(9):1325–32. doi: 10.1001/jamaoncol.2015.2756
2. Rodriguez-Ruiz ME, Vanpouille-Box C, Melero I, Formenti SC, Demaria S. Immunological Mechanisms Responsible for Radiation-Induced Abscopal Effect. *Trends Immunol* (2018) 39(8):644–55. doi: 10.1016/j.it.2018.06.001
3. Frey B, Ruckert M, Deloch L, Ruhle PF, Derer A, Fietkau R, et al. Immunomodulation by Ionizing Radiation-Impact for Design of Radio-Immunotherapies and for Treatment of Inflammatory Diseases. *Immunol Rev* (2017) 280(1):231–48. doi: 10.1111/imr.12572
4. Rodriguez-Ruiz ME, Vitale I, Harrington KJ, Melero I, Galluzzi L. Immunological Impact of Cell Death Signaling Driven by Radiation on the Tumor Microenvironment. *Nat Immunol* (2020) 21(2):120–34. doi: 10.1038/s41590-019-0561-4
5. Wennerberg E, Lhuillier C, Vanpouille-Box C, Pilones KA, Garcia-Martinez E, Rudqvist NP, et al. Barriers to Radiation-Induced in Situ Tumor Vaccination. *Front Immunol* (2017) 8:229. doi: 10.3389/fimmu.2017.00229
6. Hellevik T, Martinez-Zubiaurre I. Radiotherapy and the Tumor Stroma: The Importance of Dose and Fractionation. *Front Oncol* (2014) 4:1. doi: 10.3389/fonc.2014.00001
7. Barker HE, Paget JT, Khan AA, Harrington KJ. The Tumour Microenvironment After Radiotherapy: Mechanisms of Resistance and Recurrence. *Nat Rev Cancer* (2015) 15(7):409–25. doi: 10.1038/nrc3958
8. Martinez-Zubiaurre I, Hellevik T. Transformed Immunosuppressive Networks of the Irradiated Tumor Stroma. *Front Immunol* (2018) 9:1679. doi: 10.3389/fimmu.2018.01679
9. Kalluri R, Zeisberg M. Fibroblasts in Cancer. *Nat Rev Cancer* (2006) 6(5):392–401. doi: 10.1038/nrc1877
10. Erez N, Truitt M, Olson P, Arron ST, Hanahan D. Cancer-Associated Fibroblasts are Activated in Incipient Neoplasia to Orchestrate Tumor-

Promoting Inflammation in an NF-kappaB-Dependent Manner. *Cancer Cell* (2010) 17(2):135–47. doi: 10.1016/j.ccr.2009.12.041
11. Kalluri R. The Biology and Function of Fibroblasts in Cancer. *Nat Rev Cancer* (2016) 16(9):582–98. doi: 10.1038/nrc.2016.73
12. Liu L, Zhang Z, Zhou L, Hu L, Yin C, Qing D, et al. Cancer Associated Fibroblasts-Derived Exosomes Contribute to Radioresistance Through Promoting Colorectal Cancer Stem Cells Phenotype. *Exp Cell Res* (2020) 391(2):111956. doi: 10.1016/j.yexcr.2020.111956
13. Ji X, Ji J, Shan F, Zhang Y, Chen Y, Lu X. Cancer-Associated Fibroblasts From NSCLC Promote the Radioresistance in Lung Cancer Cell Lines. *Int J Clin Exp Med* (2015) 8(5):7002–8.
14. Grinde MT, Vik J, Camilio KA, Martinez-Zubiaurre I, Hellevik T. Ionizing Radiation Abrogates the Pro-Tumorigenic Capacity of Cancer-Associated Fibroblasts Co-Implanted in Xenografts. *Sci Rep* (2017) 7:46714. doi: 10.1038/srep46714
15. Silzle T, Randolph GJ, Kreutz M, Kunz-Schughart LA. The Fibroblast: Sentinel Cell and Local Immune Modulator in Tumor Tissue. *Int J Cancer* (2004) 108 (2):173–80. doi: 10.1002/ijc.11542
16. Harper J, Sainson RC. Regulation of the Anti-Tumour Immune Response by Cancer-Associated Fibroblasts. *Semin Cancer Biol* (2014) 25:69–77. doi: 10.1016/j.semcancer.2013.12.005
17. Monteran L, Erez N. The Dark Side of Fibroblasts: Cancer-Associated Fibroblasts as Mediators of Immunosuppression in the Tumor Microenvironment. *Front Immunol* (2019) 10:1835. doi: 10.3389/fimmu.2019.01835
18. Wculek SK, Cueto FJ, Mujal AM, Melero I, Krummel MF, Sancho D. Dendritic Cells in Cancer Immunology and Immunotherapy. *Nat Rev Immunol* (2020) 20(1):7–24. doi: 10.1038/s41577-019-0210-z
19. Chen DS, Mellman I. Oncology Meets Immunology: The Cancer-Immunity Cycle. *Immunity* (2013) 39(1):1–10. doi: 10.1016/j.immuni.2013.07.012
20. Mellman I, Steinman RM. Dendritic Cells: Specialized and Regulated Antigen Processing Machines. *Cell* (2001) 106(3):255–8. doi: 10.1016/s0092-8674(01)00449-4
21. Mellman I. Dendritic Cells: Master Regulators of the Immune Response. *Cancer Immunol Res* (2013) 1(3):145–9. doi: 10.1158/2326-6066.CIR-13-0102
22. Galluzzi L, Zitvogel L, Kroemer G. Immunological Mechanisms Underneath the Efficacy of Cancer Therapy. *Cancer Immunol Res* (2016) 4(11):895–902. doi: 10.1158/2326-6066.CIR-16-0197
23. Adkins I, Fucikova J, Garg AD, Agostinis P, Spisek R. Physical Modalities Inducing Immunogenic Tumor Cell Death for Cancer Immunotherapy. *Oncoimmunology* (2014) 3(12):e968434. doi: 10.4161/21624011.2014.968434
24. Krysko DV, Garg AD, Kaczmarek A, Krysko O, Agostinis P, Vandenabeele P. Immunogenic Cell Death and DAMPs in Cancer Therapy. *Nat Rev Cancer* (2012) 12(12):860–75. doi: 10.1038/nrc3380
25. Delamarre L, Mellman I. Harnessing Dendritic Cells for Immunotherapy. *Semin Immunol* (2011) 23(1):2–11. doi: 10.1016/j.smim.2011.02.001
26. Hsu YL, Hung JY, Chiang SY, Jian SF, Wu CY, Lin YS, et al. Lung Cancer-Derived Galectin-1 Contributes to Cancer Associated Fibroblast-Mediated Cancer Progression and Immune Suppression Through TDO2/kynurenine Axis. *Oncotarget* (2016) 7(19):27584–98. doi: 10.18632/oncotarget.8488
27. Cheng JT, Deng YN, Yi HM, Wang GY, Fu BS, Chen WJ, et al. Hepatic Carcinoma-Associated Fibroblasts Induce IDO-producing Regulatory Dendritic Cells Through IL-6-mediated STAT3 Activation. *Oncogenesis* (2016) 5:e198. doi: 10.1038/oncsis.2016.7
28. De Monte L, Reni M, Tassi E, Clavenna D, Papa I, Recalde H, et al. Intratumor T Helper Type 2 Cell Infiltrate Correlates With Cancer-Associated Fibroblast Thymic Stromal Lymphopoietin Production and Reduced Survival in Pancreatic Cancer. *J Exp Med* (2011) 208(3):469–78. doi: 10.1084/jem.20101876
29. Hellevik T, Pettersen I, Berg V, Winberg JO, Moe BT, Bartnes K, et al. Cancer-Associated Fibroblasts From Human NSCLC Survive Ablative Doses of Radiation But Their Invasive Capacity is Reduced. *Radiat Oncol* (2012) 7:59. doi: 10.1186/1748-717X-7-59
30. Gorchs L, Hellevik T, Bruun JA, Camilio KA, Al-Saad S, Stuge TB, et al. Cancer-Associated Fibroblasts From Lung Tumors Maintain Their Immunosuppressive Abilities After High-Dose Irradiation. *Front Oncol* (2015) 5:87. doi: 10.3389/fonc.2015.00087
31. Hellevik T, Pettersen I, Berg V, Bruun J, Bartnes K, Busund LT, et al. Changes in the Secretory Profile of NSCLC-Associated Fibroblasts After Ablative Radiotherapy: Potential Impact on Angiogenesis and Tumor Growth. *Transl Oncol* (2013) 6(1):66–74. doi: 10.1593/tlo.12349
32. Berzaghi R, Ahktar MA, Islam A, Pedersen BD, Hellevik T, Martinez-Zubiaurre I. Fibroblast-Mediated Immunoregulation of Macrophage Function Is Maintained After Irradiation. *Cancers (Basel)* (2019) 11(5). doi: 10.3390/cancers11050689
33. Patente TA, Pinho MP, Oliveira AA, Evangelista GCM, Bergami-Santos PC, Barbuto JAM. Human Dendritic Cells: Their Heterogeneity and Clinical Application Potential in Cancer Immunotherapy. *Front Immunol* (2018) 9:3176. doi: 10.3389/fimmu.2018.03176
34. Ramos RN, Chin LS, Dos Santos AP, Bergami-Santos PC, Laginha F, Barbuto JA. Monocyte-Derived Dendritic Cells From Breast Cancer Patients are Biased to Induce CD4+CD25+Foxp3+ Regulatory T Cells. *J Leukoc Biol* (2012) 92 (3):673–82. doi: 10.1189/jlb.0112048
35. Toniolo PA, Liu S, Yeh JE, Ye DQ, Barbuto JA, Frank DA. Deregulation of SOCS5 Suppresses Dendritic Cell Function in Chronic Lymphocytic Leukemia. *Oncotarget* (2016) 7(29):46301–14. doi: 10.18632/oncotarget.10093
36. Worbs T, Hammerschmidt SI, Forster R. Dendritic Cell Migration in Health and Disease. *Nat Rev Immunol* (2017) 17(1):30–48. doi: 10.1038/nri.2016.116
37. Forster R, Davalos-Misslitz AC, Rot A. CCR7 and its Ligands: Balancing Immunity and Tolerance. *Nat Rev Immunol* (2008) 8(5):362–71. doi: 10.1038/nri2297
38. Houser BL, Tilburgs T, Hill J, Nicotra ML, Strominger JL. Two Unique Human Decidual Macrophage Populations. *J Immunol* (2011) 186(4):2633–42. doi: 10.4049/jimmunol.1003153
39. Chomarat P, Banchereau J, Davoust J, Palucka AK. IL-6 Switches the Differentiation of Monocytes From Dendritic Cells to Macrophages. *Nat Immunol* (2000) 1(6):510–4. doi: 10.1038/82763
40. Spary LK, Salimu J, Webber JP, Clayton A, Mason MD, Tabi Z. Tumor Stroma-Derived Factors Skew Monocyte to Dendritic Cell Differentiation Toward a Suppressive CD14(+) PD-L1(+) Phenotype in Prostate Cancer. *Oncoimmunology* (2014) 3(9):e955331. doi: 10.4161/21624011.2014.955331
41. Kalinski P, Hilkens CM, Snijders A, Snijdewint FG, Kapsenberg ML. Dendritic Cells, Obtained From Peripheral Blood Precursors in the Presence of PGE2, Promote Th2 Responses. *Adv Exp Med Biol* (1997) 417:363–7. doi: 10.1007/978-1-4757-9966-8_59
42. Relloso M, Puig-Kroger A, Pello OM, Rodriguez-Fernandez JL, de la Rosa G, Longo N, et al. DC-SIGN (CD209) Expression is IL-4 Dependent and is Negatively Regulated by IFN, TGF-Beta, and Anti-Inflammatory Agents. *J Immunol* (2002) 168(6):2634–43. doi: 10.4049/jimmunol.168.6.2634
43. Engering A, Geijtenbeek TB, van Vliet SJ, Wijers M, van Liempt E, Demaurex N, et al. The Dendritic Cell-Specific Adhesion Receptor DC-SIGN Internalizes Antigen for Presentation to T Cells. *J Immunol* (2002) 168(5):2118–26. doi: 10.4049/jimmunol.168.5.2118
44. Pustylnikov S, Sagar D, Jain P, Khan ZK. Targeting the C-type Lectins-Mediated Host-Pathogen Interactions With Dextran. *J Pharm Pharm Sci* (2014) 17(3):371–92. doi: 10.18433/j3n590
45. Liu Z, Roche PA. Macropinocytosis in Phagocytes: Regulation of MHC class-II-restricted Antigen Presentation in Dendritic Cells. *Front Physiol* (2015) 6:1. doi: 10.3389/fphys.2015.00001
46. Freynet O, Marchal-Somme J, Jean-Louis F, Mailleux A, Crestani B, Soler P, et al. Human Lung Fibroblasts may Modulate Dendritic Cell Phenotype and Function: Results From a Pilot In Vitro Study. *Respir Res* (2016) 17:36. doi: 10.1186/s12931-016-0345-4
47. Seguier S, Tartour E, Guerin C, Couty L, Lemitre M, Lallement L, et al. Inhibition of the Differentiation of Monocyte-Derived Dendritic Cells by Human Gingival Fibroblasts. *PloS One* (2013) 8(8):e70937. doi: 10.1371/journal.pone.0070937
48. Schirmer C, Klein C, von Bergen M, Simon JC, Saalbach A. Human Fibroblasts Support the Expansion of IL-17-Producing T Cells Via Up-Regulation of IL-23 Production by Dendritic Cells. *Blood* (2010) 116 (10):1715–25. doi: 10.1182/blood-2010-01-263509
49. Dewan MZ, Galloway AE, Kawashima N, Dewyngaert JK, Babb JS, Formenti SC, et al. Fractionated But Not Single-Dose Radiotherapy Induces an Immune-Mediated Abscopal Effect When Combined With anti-CTLA-4 Antibody. *Clin Cancer Res* (2009) 15(17):5379–88. doi: 10.1158/1078-0432.CCR-09-0265
50. Vanpouille-Box C, Alard A, Aryankalayil MJ, Sarfraz Y, Diamond JM, Schneider RJ, et al. DNA Exonuclease Trex1 Regulates Radiotherapy-

Induced Tumour Immunogenicity. *Nat Commun* (2017) 8:15618. doi: 10.1038/ncomms15618
51. Hayden MS, Ghosh S. NF-KappaB in Immunobiology. *Cell Res* (2011) 21 (2):223–44. doi: 10.1038/cr.2011.13
52. Dissanayake D, Hall H, Berg-Brown N, Elford AR, Hamilton SR, Murakami K, et al. Nuclear factor-kappaB1 Controls the Functional Maturation of Dendritic Cells and Prevents the Activation of Autoreactive T Cells. *Nat Med* (2011) 17(12):1663–7. doi: 10.1038/nm.2556
53. Hayden MS, West AP, Ghosh S. NF-KappaB and the Immune Response. *Oncogene* (2006) 25(51):6758–80. doi: 10.1038/sj.onc.1209943
54. Pordanjani SM, Hosseinimehr SJ. The Role of NF-kB Inhibitors in Cell Response to Radiation. *Curr Med Chem* (2016) 23(34):3951–63. doi: 10.2174/0929867323666160824162718
55. Liu T, Zhang L, Joo D, Sun SC. NF-KappaB Signaling in Inflammation. *Signal Transduct Target Ther* (2017) 2:17023. doi: 10.1038/sigtrans.2017.23
56. Melillo JA, Song L, Bhagat G, Blazquez AB, Plumlee CR, Lee C, et al. Dendritic Cell (DC)-Specific Targeting Reveals Stat3 as a Negative Regulator of DC Function. *J Immunol* (2010) 184(5):2638–45. doi: 10.4049/jimmunol.0902960
57. Owen KL, Brockwell NK, Parker BS. JAK-STAT Signaling: A Double-Edged Sword of Immune Regulation and Cancer Progression. *Cancers (Basel)* (2019) 11(12):2002. doi: 10.3390/cancers11122002
58. Li R, Fang F, Jiang M, Wang C, Ma J, Kang W, et al. STAT3 and NF-kappaB are Simultaneously Suppressed in Dendritic Cells in Lung Cancer. *Sci Rep* (2017) 7:45395. doi: 10.1038/srep45395

Conflict of Interest: The authors declare that the research was conducted in the absence of any commercial or financial relationships that could be construed as a potential conflict of interest.

frontiers in Immunology

ORIGINAL RESEARCH
published: 23 July 2021
doi: 10.3389/fimmu.2021.665002

Analysis of Interleukin-1 Signaling Alterations of Colon Adenocarcinoma Identified Implications for Immunotherapy

Xiaogang Zhou[1†], Yu Liu[2†], Jing Xiang[3†], Yuntao Wang[4†], Qiqian Wang[2†], Jianling Xia[2], Yunfei Chen[5*] and Yifeng Bai[2*]*

[1] Department of Gastrointestinal Surgery, Sichuan Provincial People's Hospital, University of Electronic Science and Technology of China, Chengdu, China, [2] Department of Oncology, Sichuan Provincial People's Hospital, University of Electronic Science and Technology of China, Chengdu, China, [3] Department of Outpatient, Sichuan Provincial People's Hospital, University of Electronic Science and Technology of China, Chengdu, China, [4] Department of Oncology, The Second Clinical Medical College, The Fifth People's Hospital affiliated to Chengdu University of Traditional Chinese Medicine, Chengdu, China, [5] The Third Department of Hepatobiliary Surgery and Organ Transplant Center, Sichuan Provincial People's Hospital, University of Electronic Science and Technology of China, Chengdu, China

OPEN ACCESS

Edited by:
Alessandro Poggi,
San Martino Hospital (IRCCS), Italy

Reviewed by:
Zong Sheng Guo,
University of Pittsburgh, United States
Peng Luo,
The University of Hong Kong, Hong Kong, SAR China

***Correspondence:**
Jianling Xia
545471440@qq.com
Yunfei Chen
cyfalan@163.com
Yifeng Bai
baiyifeng@med.uestc.edu.cn

[†]These authors have contributed equally to this work and share first authorship

Specialty section:
This article was submitted to Cancer Immunity and Immunotherapy, a section of the journal Frontiers in Immunology

Received: *06 February 2021*
Accepted: *06 July 2021*
Published: *23 July 2021*

Citation:
Zhou X, Liu Y, Xiang J, Wang Y, Wang Q, Xia J, Chen Y and Bai Y (2021) Analysis of Interleukin-1 Signaling Alterations of Colon Adenocarcinoma Identified Implications for Immunotherapy. Front. Immunol. 12:665002. doi: 10.3389/fimmu.2021.665002

Immune checkpoint inhibitors (ICIs) have made breakthrough progress in the treatment of various malignant tumors. However, only some patients receiving ICIs obtain long-lasting clinical effects, and some patients still do not achieve remission. Improving the treatment benefits of this part of the population has become a concern of clinicians. IL-1 signaling plays an important role in the tumor microenvironment (TME). However, the relationship between the IL-1 signaling mutation status and the prognosis of colon adenocarcinoma (COAD) patients receiving ICIs has not been reported. We downloaded the data of a COAD cohort receiving ICIs, including prognostic data and mutation data. Additionally, we downloaded the data of a COAD cohort from The Cancer Genome Atlas (TCGA) database, including clinical data, expression data and mutation data. Gene set enrichment analysis (GSEA) was used to assess differences in the activity of some key physiological pathways between the IL-1 signaling mutated-type (IL-1-MT) and IL-1 signaling wild-type (IL-1-WT) groups. The CIBERSORT algorithm was used to evaluate the contents of immune cells in the TME of COAD patients. The multivariate Cox regression model results suggested that IL-1-MT can be used as an independent predictor of a better prognosis in COAD patients receiving ICIs (P = 0.03, HR = 0.269, 95% CI: 0.082-0.883). Additionally, IL-1-MT COAD patients had significantly longer overall survival (OS) (log-rank P = 0.015). CIBERSORT analysis showed that the IL-1-MT group had high infiltration levels of activated dendritic cells (DCs), M1 macrophages, neutrophils, activated natural killer (NK) cells, activated CD4+ memory T cells and CD8+ T cells. Similarly, the IL-1-MT group had significantly upregulated immunogenicity, including in terms of the tumor mutation burden (TMB), neoantigen load (NAL) and number of mutations in DNA damage repair (DDR) signaling. GSEA showed that the IL-1-MT group was highly enriched in the immune response and proinflammatory mediators.

Additionally, the expression levels of immune-related genes, immune checkpoint molecules and immune-related signatures were significantly higher in the IL-1-MT group than in the IL-1-WT group. IL-1-MT may be an independent predictor of a good prognosis in COAD patients receiving ICIs, with significantly longer OS in IL-1-MT COAD patients. Additionally, IL-1-MT was associated with significantly increased immunogenicity, activated immune cell and inflammatory mediator levels and immune response-related scores.

Keywords: immune checkpoint inhibitors, colon adenocarcinoma, tumor microenvironment, IL-1, prognosis

INTRODUCTION

Immune checkpoint inhibitors (ICIs) have made breakthrough progress in the treatment of various malignant tumors (1–3). Recent studies have shown that colorectal cancer (CRC) patients who benefit from ICIs are mainly those with high mutation burden and mismatch repair deficiency (dMMR), and this population accounts for only approximately 5% of metastatic CRC (4). Therefore, only some patients receiving ICIs obtain long-lasting clinical effects (5, 6), and some patients still do not achieve remission. Improving the treatment benefits of this part of the population has become a concern of clinicians.

Various potential biomarkers have been found in colon adenocarcinoma (COAD) patients receiving immunotherapy, such as microsatellite instability (MSI), programmed cell death-ligand 1 (PD-L1) expression, tumor mutation burden (TMB) and BRAF and KRAS gene mutation status (6). However, the effects of the above biomarkers are still limited. For example, the dMMR/microsatellite instability high (MSI-H) COAD population is considered to derive the most benefits from ICI treatment, but the effective rate is only 30%-40% (7), and this subset only accounts for a small part of the COAD population. The heterogeneity of PD-L1 expression in time and space is related to differences in detection methods. Additionally, some patients with a low TMB can also respond to immunotherapy, and patients with a high TMB may not show good immunotherapy efficacy (8). Therefore, finding new markers to predict the efficacy of ICIs in COAD patients has become an important challenge.

There are certain correlations and influences between specific mutations or pathway mutations and ICI efficacy markers (9, 10). Mutations in DNA repair pathways are associated with better clinical benefits for patients with multiple tumors after receiving immunotherapy (10). Additionally, SERPINB3 or SERPINB4 mutations are associated with good prognosis in melanoma patients treated with cytotoxic T lymphocyte-associated protein-4 (CTLA-4) blockade (11). TET mutations are associated with higher objective response rates (ORRs), favorable clinical benefits and prolonged progression-free survival (PFS) and overall survival (OS) in pan-cancer cohorts treated with ICIs (PD-(L)1 and/or CTLA-4) (12). The role of interleukins in the antitumor immune response has received increasing attention (13, 14). Previous evidence has confirmed that interleukin-1 (IL-1) promotes the expression of cyclooxygenase-2 in COAD and can also increase the level of cyclooxygenase-2 in COAD cells (15, 16). Cyclooxygenase-2 is involved in the occurrence, development, tumor angiogenesis and metastasis of COAD. Moreover, IL-1 can increase the secretion of matrix metalloproteinases and vascular endothelial growth factor (VEGF) and promote the adhesion of endothelial cells, thus promoting the occurrence and progression of COAD (17). It has been reported that IL-1 family proteins, such as IL-1α, IL-1β and IL-18, may play distinct roles in immune responses during infections and inflammatory diseases (18). IL-1R transduces signals through myeloid differentiation factor 88 (MyD88), which triggers a series of events, leading to the expression of inflammatory genes and the recruitment of immune cells (19, 20). Additionally, studies have indicated that the secretion of IL-1 and other cytokines by monocytes, macrophages, cancer cells and fibroblasts contributes to the formation of tumor-related immunosuppression, which may also explain why IL-1 leads to the development of COAD (21).

However, in COAD, the impact of IL-1 pathway mutations on the clinical prognosis of immunotherapy remains unclear. Hence, in this study, we explored the association between the mutated IL-1 signaling status and the prognosis of COAD patients receiving ICIs and sought to illustrate the potential mechanism between the mutated IL-1 signaling status and the prognosis of patients treated with immunotherapy from the perspective of the immune microenvironment.

METHODS

Clinical Sample and Group Definition

To explore the impact of IL-1 signaling mutated-type (IL-1-MT) on the prognosis of COAD patients treated with immunotherapy, we downloaded the mutation and clinical data of an ICI-treated COAD cohort (22). The immunotherapy regimen for this cohort was PD-(L)1 or combination with CTLA-4 inhibitors. Additionally, we used the "TCGAbiolinks" R package (23) and downloaded the COAD expression data, mutation data and clinical data from TCGA (https://portal.gdc.cancer.gov/). Nonsynonymous mutation data were used to quantify the status of each patient's mutations in IL-1 signaling. If a patient had no mutations in IL-1 signaling, their status was defined as IL-1 signaling wild-type (IL-1-WT); otherwise, their status was defined as IL-1-MT.

Data Preprocessing

According to the definition of the TMB in published literature (24), we evaluated the TMB in the TCGA-COAD cohort. Additionally, the neoantigen load (NAL), immune-related genes and immune-related signatures/scores were collected from published studies (25, 26). We downloaded eight gene sets of DNA damage repair (DDR) signaling from the Molecular Signatures Database (MSigDB) and merged them into one DDR gene set (27). Next, we used these nine gene sets to analyze the number of mutations in each patient's DDR-related pathways. The CIBERSORT algorithm (28) was used to evaluate the proportions of 22 immune cells (https://cibersort.stanford.edu/index.php). Additionally, the ClusterProfiler R package (29) and pathways from the Gene Ontology (GO), Kyoto Encyclopedia of Genes and Genomes (KEGG) and REACTOME databases were used in gene set enrichment analysis (GSEA).

Statistical Analysis

In the ICI-treated COAD cohort, univariate and multivariate Cox regression models and Kaplan-Meier (KM) curves were used to analyze the influence of the IL-1 pathway mutation status and clinical characteristics on the survival of COAD patients. The Mann-Whitney U test was used to compare differences in continuous variables between the two groups (IL-1-MT and IL-1-WT). Fisher's exact test was used to compare differences in the categorical variables between the two groups (IL-1-MT and IL-1-WT). Log-rank P was used to reflect significant differences. $P < 0.05$ was considered significantly different, and all analyses in this study were completed using R software (version 3.6.3).

RESULTS

IL-1-MT Can Be Used as an Independent Predictor of Better Prognosis in COAD Patients Receiving ICIs

To explore the effect of the mutated IL-1 signaling status on the prognosis of COAD patients receiving ICIs, we downloaded the data of a cohort of COAD patients treated with ICIs from the CBioPortal webpage (https://www.cbioportal.org/). The IL-1 signaling gene set from MSigDB was collected, and the number of gene mutations in the IL-1 signaling pathway in each patient was calculated. Then, the univariate Cox regression model was used for subsequent analysis. We found that age and sample type were not significantly associated with the immunotherapy prognosis ($P > 0.05$), while IL-1-MT COAD patients treated with immunotherapy were associated with better prognosis ($P = 0.024$, hazard ratio (HR) = 0.255, 95% confidence interval (CI): 0.078-0.834; **Figure 1A**). The multivariate Cox regression model was used to analyze whether IL-1-MT could be used as an independent predictor of the prognosis of COAD patients. The results showed that only IL-1-MT could be used as an independent predictor of good prognosis in COAD patients receiving ICIs ($P = 0.03$, HR = 0.269, 95% CI: 0.082-0.883; **Figure 1A**). Next, the KM curve also showed that COAD patients who had mutations in IL-1 signaling had significantly prolonged OS compared to COAD patients who did not have mutations in IL-1 signaling (**Figure 1B**, log-rank $P = 0.015$). Moreover, we compared the differential expression of genes related IL-1 signaling pathway between IL1-MT and IL1-WT groups. We found that IL1-MT COAD patients had significantly higher expression levels of markers related to the IL-1 signaling pathway compared with IL1-WT COAD patients (**Figure 1C**).

The Relationships Between IL-1-MT and Mutation Characteristics and Clinical Characteristics

To analyze the relationship between IL-1-MT and the mutation characteristics of COAD patients, we analyzed nonsynonymous mutations in the ICI-treated COAD cohort and TCGA-COAD cohort. In the ICI-treated COAD cohort (**Figure 2A**), the genes with the top 20 mutation frequencies were APC, KRAS, TP53, PIK3CA, KMT2D, ARID1A, PTPRS, RNF43, KMT2C, TCF7L2, ZFHX3, FAT1, NCOR1, SMARCA4, NF1, PTCH1, SMAD4, ARID1B, BRCA2 and CREBBP. Most of these genes are tumor suppressor genes (TSGs), followed by oncogenes and unknown genes. Except for APC, KMT2D, ARID1A and RNF43, most of the mutation types were nonsense and frameshift mutations, and most of the remaining gene mutation types were missense mutations. Additionally, some genes had significantly increased mutation frequencies in the IL-1-MT group compared with the IL-1-WT group, such as KMT2D (60% *vs.* 25%), RNF43 (47% *vs.* 16%), KMT2D (47% *vs.* 15%), ZFHX3 (40% *vs.* 15%) and FAT1 (40% *vs.* 14%) (**Figure 2A**). In the TCGA-COAD cohort, the genes with the top 20 nonsynonymous somatic mutations were APC, TP53, TTN, KRAS, MUC16, SYNE1, PIK3CA, FAT4, RYR2, OBSCN, ZFHX4, DNAH5, PCLO, CSMD3, LRP1B, ABCA13, DNAH11, FAT3, USH2A and CSMD1. Because the detection method used for the TCGA-COAD cohort was whole-exome sequencing (WES), more somatic mutation data were available for this cohort. We found that the mutation frequencies of the top 20 genes in the IL-1-MT group were significantly higher than those in the IL-1-WT group (all $P < 0.05$; **Figure 2B**). Among these genes, only KRAS and PIK3CA are oncogenes. The mutation sites of IL-1 family genes that recruit MyD88, IRAK4 and TRAF6 were visualized in **Figure S1**. Next, we compared the differences in clinical characteristics between the IL-1-MT and IL-1-WT groups. In the ICI-treated COAD cohort, the IL-1-MT group contained older patients (**Figure 3A**; $P < 0.05$). However, in terms of the MSI score, sex ratio and origin of samples, we did not find significant differences between the two groups (**Figures 3B–D**; all $P > 0.05$). In the TCGA-COAD cohort, there were no significant differences between the IL-1-MT group and the IL-1-WT group in age or sex ratio (**Figures 3E, F**). Additionally, the IL-MT group had a higher proportion of early clinical patients (**Figure 3G**).

Immune Microenvironment Under Different IL-1 Signaling Mutation Statuses

The immune microenvironment is one of the key factors that affects whether patients receive ICIs, and it is based on the perspectives of tumor-infiltrating lymphocytes (TILs), immune-

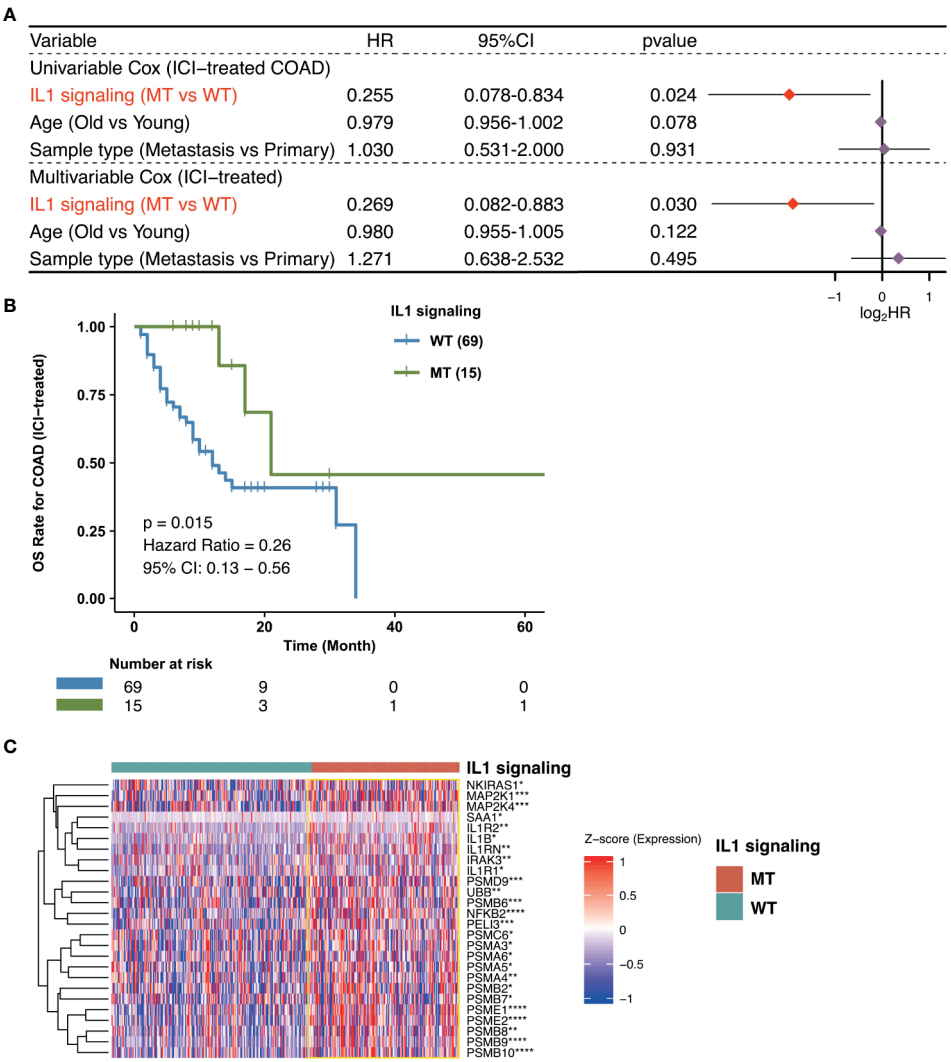

FIGURE 1 | Predictive values of clinical characteristics and the IL-1 signaling mutation status on ICI outcomes. **(A)** Forest plot of the results of the univariate Cox and multivariable Cox regression models. In the univariate Cox regression analysis, the factors with a p value below 0.05 were IL-1 signaling MT. Multivariate Cox regression analysis showed that the IL-1 signaling mutation status was an independent predictor of ICI therapy in COAD patients. The main part of the forest plot presents the risk ratio (HR) and 95% confidence interval (95% CI), where red dots indicate P < 0.05. The HR indicates predictors of favorable (HR < 1) or poor (HR > 1) OS. **(B)** Kaplan-Meier survival curves for the OS of 84 COAD patients in the ICI-treated cohort. We performed KM survival analysis on different subgroups of patients (IL-1 signaling mutation status). **(C)** Heatmap for the expression of markers related to IL1 signaling. (*P < 0.05; **P < 0.01; ***P < 0.001; ****P < 0.0001; Mann-Whitney U test).

related signatures, immune checkpoint molecules and immune-related genes. First, the CIBERSORT algorithm evaluated the proportions of 22 immune cells based on the expression data of COAD patients. **Figure 4A** shows the differences in the ratios of 22 immune cells between the IL-1-WT group and IL-1-MT group. We found that functionally active TILs were significantly enriched in the tumor microenvironment (TME) in patients with IL-1-MT COAD, such as activated dendritic cells (DCs), M1 macrophages, neutrophils, activated natural killer (NK) cells, activated CD4+ memory T cells and CD8+ T cells. In addition to the proportion of immune cell infiltration, immune-related signature analysis showed that IL-1-MT COAD patients had a higher score/activity related to the immune response (**Figures 4B**), such as BCR Shannon, homologous recombination defects, IFN-gamma response, immune score, leukocyte fraction, lymphocyte infiltration signature score, macrophage regulation, Th1 cells and Th2 cells. Similarly, the expression of immune checkpoint molecules, such as CD274 (PD-L1), HAVCR2, LAG3, IDO1, CTLA4, TIGIT, PDCD1 and PDCD1LG2, in the IL-1-MT group was significantly higher than that in the IL-1-WT group (**Figure 4C**). Immune-related genes, such as proinflammatory factors (IFNG, TNFSF10, TNFSF9, TNFSF4, TNFSF14, TNFRSF9, TNFRSF8, TNFRSF4, TNFRSF18 and TNFRSF14), chemokines (CXCL9, CXCL10 and CX3CL1), cytotoxic function

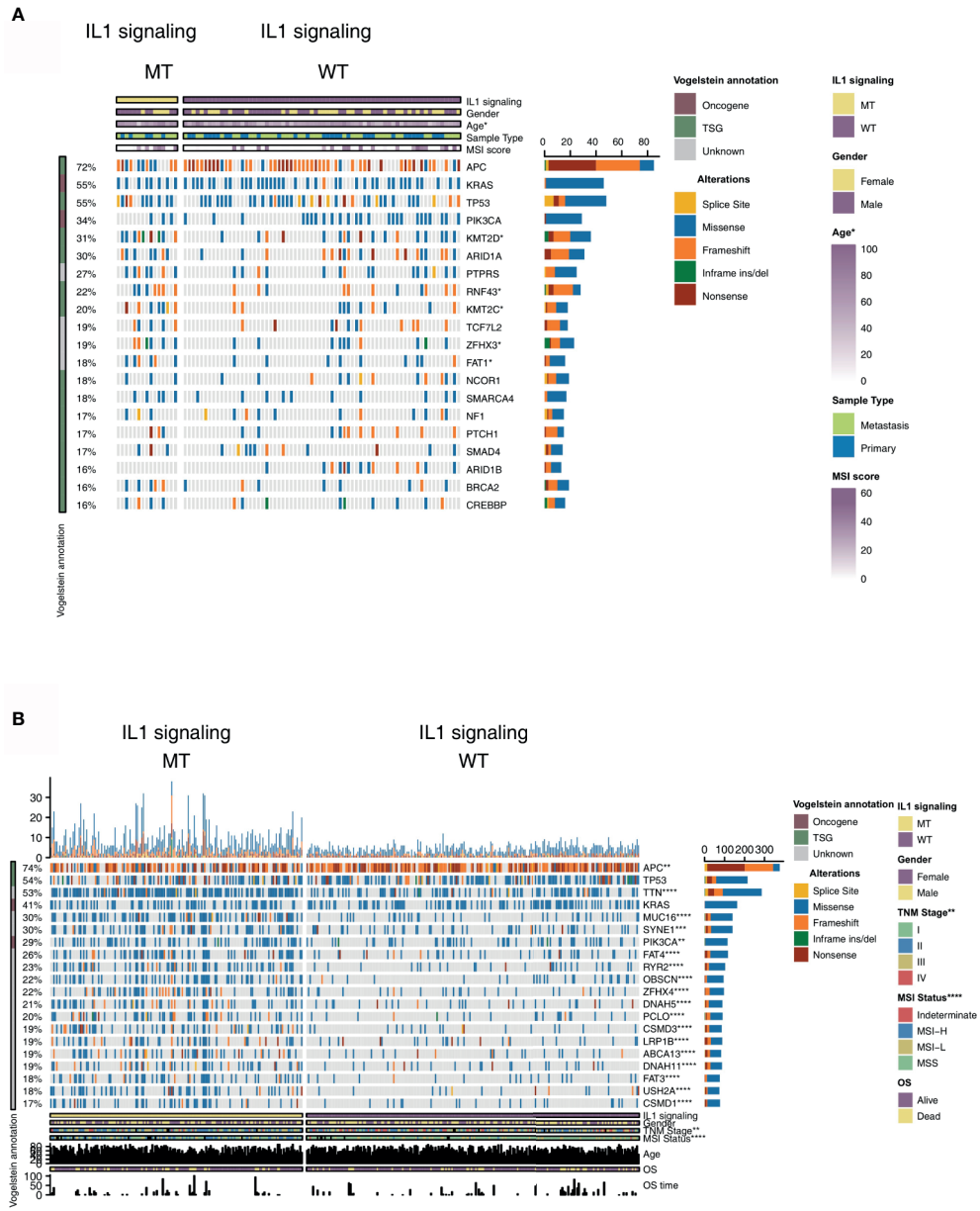

FIGURE 2 | Genomic profiles of COAD patients in the ICI-treated **(A)** and TCGA-COAD **(B)** cohorts. The top 20 genes with the highest mutation frequencies and the corresponding clinical information are shown in the figure. The top five genes with the highest mutation frequencies in the ICI-treated cohort were APC (72%), KRAS (55%), TP53 (55%), PIK3CA (34%) and KMT2D (31%). The top five genes with the highest mutation frequencies in the TCGA-COAD cohort were APC (74%), TP53 (54%), TTN (53%), KRAS (41%) and MUC16 (30%). For the mutation type, yellow indicates splice site mutations, blue indicates missense mutations, orange indicates frameshift mutations, green indicates inframe indel mutations and brown indicates nonsense mutations. The IL-1 signaling mutation status, sex, age, sample type and MSI score are shown as patient annotations (the upper/lower bar plot). The left bar plot marks the mutation rate of each gene. (*P < 0.05, **P < 0.01, ***P < 0.001 and ****P < 0.0001; Fisher's exact test).

markers (PRF1, GZ and CD8A) and antigen processing and presentation markers (TAP1, MICB, MICA, HLA-DRB5, HLA-DRB1, HLA-DRA, HLA-DQB2, HLA-DQB1, HLA-DQA1, HLA-DQA2, HLA-DPB1, HLA- DPA1, HLA-C, HLA-B and B2M), were also enriched in the IL-1-MT group (**Figure 4D**). Additionally, we found that the expression of IL-1 family genes with proinflammatory activity was significantly higher in the IL-1-MT group than the IL-1-WT group (**Figure S2**, **3**). The GSEA results showed the activity of IL1 related pathways significantly higher in the IL1-MT group compared to the IL1-WT group (**Figure 5**). Also, the activities of chemokines and other signaling pathways, such as CXCR chemokine receptor binding, positive regulation of interleukin-2 biosynthetic process, interferon-gamma biosynthetic process, cellular response to interferon-

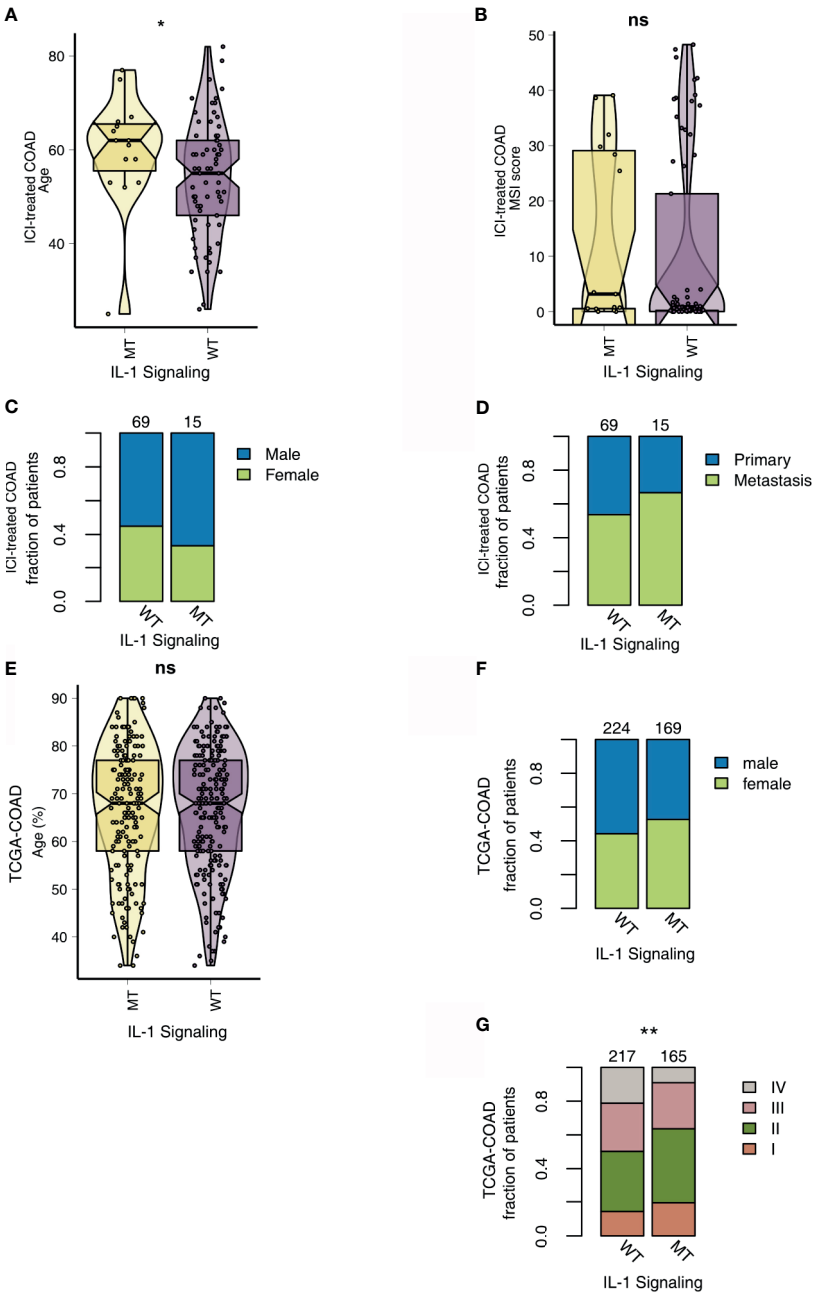

FIGURE 3 | Comparison of clinical characteristics between IL-1-MT and IL-1-WT tumors. **(A)** Comparison of age between IL-1-MT and IL-1-WT tumors in the ICI-treated COAD cohort. **(B)** Comparison of the MSI score between IL-1-MT and IL-1-WT tumors in the ICI-treated COAD cohort. **(C)** Comparison of the sex proportions between IL-1-MT and IL-1-WT tumors in the ICI-treated COAD cohort. **(D)** Comparison of the sample type proportions between IL-1-MT and IL-1-WT tumors in the ICI-treated COAD cohort. **(E)** Comparison of age between IL-1-MT and IL-1-WT tumors in the TCGA-COAD cohort. **(F)** Comparison of the sex proportions between IL-1-MT and IL-1-WT tumors in the TCGA-COAD cohort. **(G)** Correlation analysis of the clinical stage proportions between IL-1-MT and IL-1-WT tumors in the TCGA-COAD cohort. (*P < 0.05; **P < 0.01; ns, not significant).

beta, negative regulation of interleukin-10 production and interleukin-8 biosynthetic process, were significantly activated in the IL-1-MT group (**Figure 5**). Additionally, the enrichment scores of some signaling pathways involved in the immune response were significantly higher in the IL-1-MT group than in the IL-1-WT group, such as MHC class II protein complex, IgG binding, positive regulation of T-helper 1 type immune response, CD4-positive, alpha-beta T cell lineage commitment, regulation of T cell chemotaxis, positive regulation of natural killer cell-mediated cytotoxicity, T-helper 2 cell differentiation, leukocyte activation involved in inflammatory response and MHC protein complex. In contrast, some signaling pathway activities related to

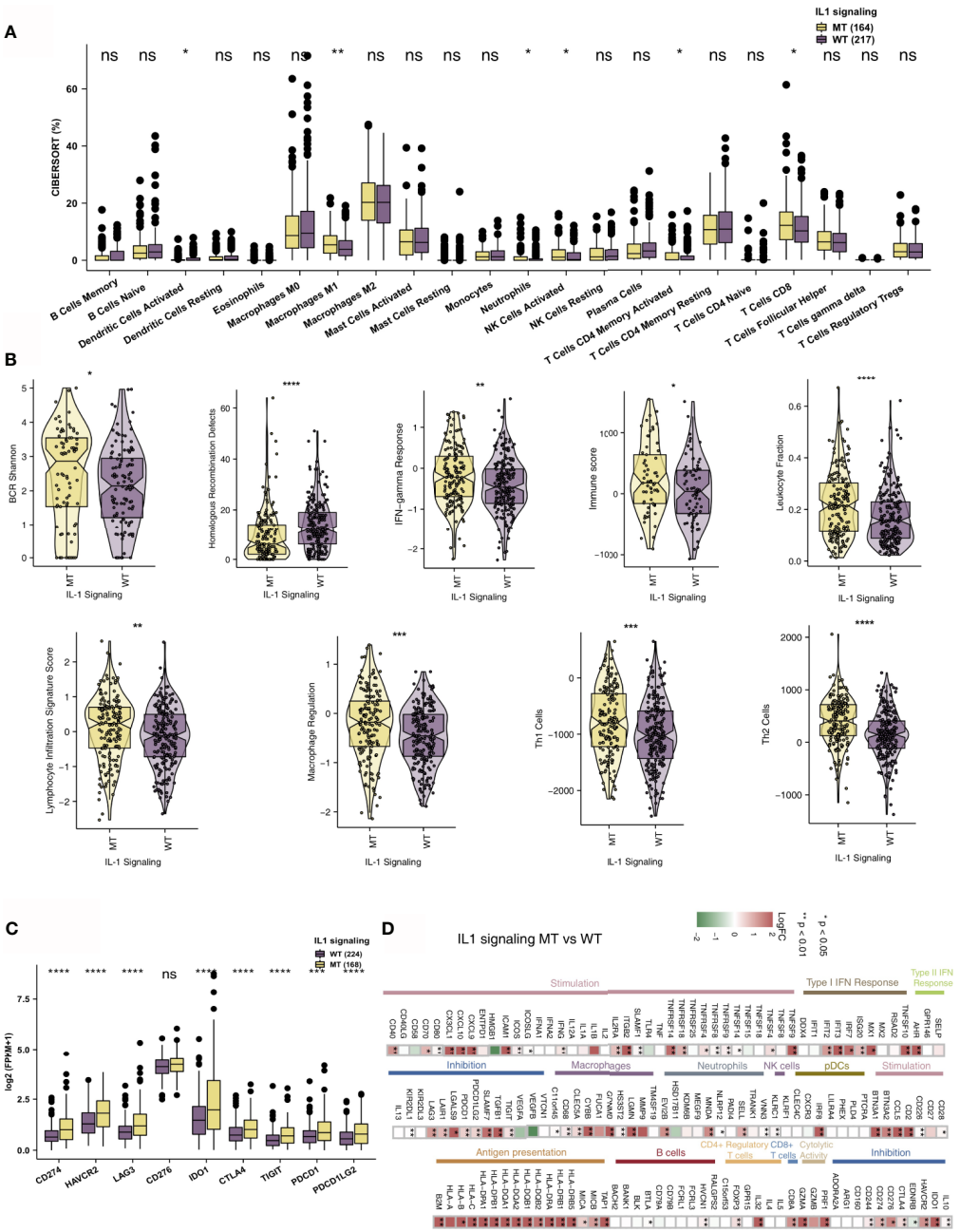

FIGURE 4 | IL-1-MT COAD is associated with an inflammatory TME. **(A)** Comparison of the fractions of 22 immune cells between IL-1-MT and IL-1-WT tumors in the TCGA-COAD cohort. **(B)** Comparison of the immune-related signatures between IL-1-MT and IL-1-WT tumors in the TCGA-COAD cohort. **(C)** Comparison of the expression levels of immune checkpoint molecules between IL-1-MT and IL-1-WT tumors in the TCGA-COAD cohort. **(D)** Heatmap depicting the mean differences in immune-related gene mRNA expression between IL-1-MT and IL-1-WT tumors across different cancer types. The x-axis of the heatmap indicates different cancer types, and the y-axis indicates gene names. Each square represents the fold change or difference of each indicated immune-related gene between IL-1-MT and IL-1-WT tumors in each cancer type. Red indicates upregulation, while blue indicates downregulation (*P < 0.05; **P < 0.01; ***P < 0.001; ****P < 0.0001; ns, not significant; Mann-Whitney U test).

immune depletion, such as PD-L1 expression and the PD-1 checkpoint pathway in cancer, Wnt signaling pathway, bile acid metabolic process and bile acid biosynthetic process, were significantly activated in the IL-1-WT group (**Figure 5**).

Differences in Immunogenicity Under Different IL-1 Signaling Mutation Status

The level of immunogenicity is one of the important factors that affects patients' acceptance of ICIs. Therefore, we started from

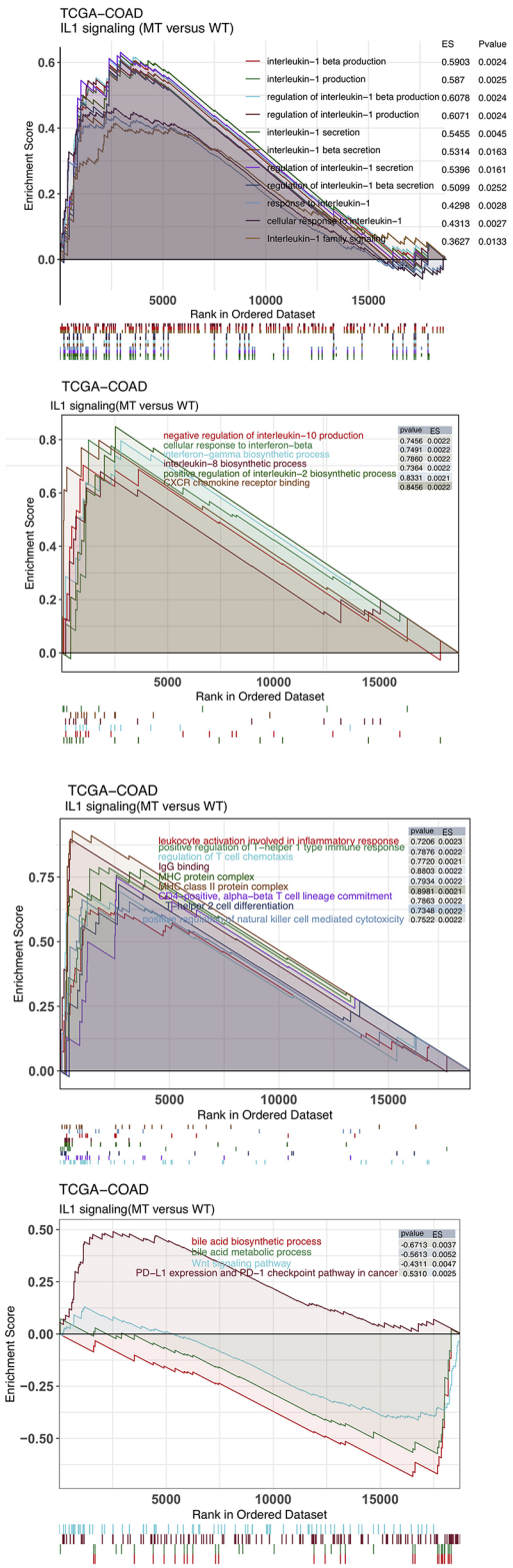

FIGURE 5 | The results of gene set enrichment analysis. The color of the curve corresponds to the font color of the pathway. GSEA of hallmark gene sets downloaded from the Molecular Signatures Database (MSigDB). Each run was performed with 1000 permutations. Enrichment results with significant differences ($P < 0.05$) between IL-1-MT and IL-1-WT tumors are shown.

the perspectives of the TMB, NAL, the MANTIS score and DDR pathway mutations. The DDR pathway gene set from MSigDB was used to count the DDR pathway mutations of each patient. In the ICI-treated COAD cohort, IL-1-MT COAD patients had a significantly increased number of DDR pathway mutations. Additionally, patients with IL-1-MT COAD had more mutations in the homologous recombination (HR), double-strand break (DSB) and Fanconi anemia (FA) pathways (**Figure 6A**). Similarly, in the TCGA-COAD cohort, IL-1-MT COAD patients had significantly increased gene mutations in all DDR-related pathways (**Figure 6B**; all $P < 0.05$). Additionally, in both the ICI-treated COAD cohort and TCGA-COAD cohort, the IL-1-MT group had a higher TMB than the IL-1-WT group (**Figures 6C, D**; all $P < 0.05$). In the TCGA-COAD cohort, the IL-1-MT group had a significantly increased NAL compared with the IL-1-WT group (**Figure 6E**, $P < 0.05$). The MANTIS score is used as a marker to measure the MSI status. The MSI phenotypes of samples with higher MANTIS scores are closer to MSI-H. **Figure 6F** shows that the MANTIS score in the IL-1-MT group was significantly higher than that in the IL-1-WT group ($P < 0.05$).

DISCUSSION

In this study, we used the prognostic and mutation data of COAD patients treated with ICIs and explored the influence of the IL-1 signaling mutation status on the prognosis of patients treated with immunotherapy. The results of univariate and multivariate Cox regression model analyses showed that IL-1-MT can be used as an independent predictor of good prognosis for COAD patients receiving ICIs. Additionally, compared with IL-1-WT COAD patients, IL-1-MT COAD patients had significantly improved OS. Two-way regulation can occur between tumor cells and immune cells in the TME. Tumor cells recruit and regulate the behavior of immune cells by secreting growth factors and cytokines, and the interaction between tumor cells and immune cells can also extend to the body. The balanced state of the cell mobilizes the resources inside and outside the cell, creates a TME suitable for its own growth and affects the response of tumor cells to immunotherapy (6, 30). We found that the TME of IL-1-MT COAD patients has a high infiltration level of activated immune cells. Additionally, the IL-1-MT group had significantly increased expression levels of immune checkpoint molecules, proinflammatory-related genes, antigen presentation-related genes, chemokine-related genes and cytotoxicity-related genes. IL-1-MT COAD patients had enhanced immunogenicity, which mainly manifested as an increased TMB and NAL and an increased number of DDR pathway mutations.

The activated immune cells enriched in the immune microenvironment in the IL-1-MT group may be a potential mechanism for improved prognosis after ICI treatment. Studies have shown that the presence of highly infiltrated TILs in tumors, especially CD4+ T cells and CD8+ T cells, is related to the good clinical prognosis of patients, which is manifested by longer PFS and OS (6, 7, 31, 32). Additionally, M1-type macrophages exert antitumor immunity, which is related to a better prognosis of immunotherapy (33). The expression of chemokines, such as CXCL9 and CXCL10, was significantly increased in the IL-1-MT group. These inflammatory mediators recruit CD8+ T cells, DCs and NK cells into tumor tissues to further exert an antitumor immune response (34). For example, CD8+ T cells can secrete cytotoxic mediators (such as perforin, granzyme and TNF) (34), CD4+ T cells secrete IL-6 and IFN-gamma further activates other immune cells (35). Moreover, we found that the IL-1-MT group had higher BCR Shannon index values, signature of HR defects, IFN-gamma responses, immune scores, leukocyte fractions, lymphocyte infiltration, signature scores, macrophage regulation, Th1 cells and Th2 cells. Studies have shown that IFN-gamma can further regulate the expression of MHC-I molecules on the surface of tumor cells by activating STAT1. The GSEA results also suggested that the chemokine signaling pathway and NK cells mediate cytotoxicity, and the activity of the MHC signaling pathway in the IL-1-MT group was significantly higher than that in the IL-WT group. Additionally, the expression levels of genes related to antigen processing and presentation and cytotoxicity were significantly higher in the IL-1-MT group than in the IL-1-WT group. The above results all suggest that an inflammatory immune environment forms in the tumors of IL-1-MT COAD patients, which may be a potential mechanism for these patients to have favorable clinical benefits after receiving ICIs.

The higher immunogenicity of the immune microenvironment in the IL-1-MT group may lead to a better prognosis after receiving ICIs. Studies have shown that higher immunogenicity can promote TIL levels in the TME (36–38). The TMB is a more reliable biomarker for predicting the efficacy of ICIs. A higher TMB is associated with better prognosis of immunotherapy (22, 39), and studies have shown that the NAL may be more accurate than the TMB in predicting the efficacy and prognosis of immunotherapy (11, 40). In addition to the TMB and NAL, the DDR pathway plays an important role in maintaining the stability of the body's DNA (9, 10, 41). The increase in genomic instability is the result of mutations in the DDR pathway and further increases the TMB and NAL, ultimately leading to an increase in the infiltration of TILs in the TME (6). Studies have shown that the treatment of advanced metastatic bladder cancer patients with mutations in the DDR pathway with ICIs has significantly improved clinical benefits (10). Additionally, another pan-cancer study showed that patients with co-mutations in the DDR pathway have significantly longer survival times than those without co-mutations in the DDR pathway (9). Our results also suggest that the IL-1-MT group has a significantly increased number of mutations in the TMB, NAL, and DDR pathways. This increased immunogenicity may be the biological basis of why IL-1-MT COAD patients receiving ICIs have a better clinical prognosis. However, there are still some limitations. First, targeted sequencing (MSK-IMPACT) was used in the ICI-treated COAD cohort to detect somatic mutations, and targeted sequencing provides fewer gene mutations than WES; second, the ICI-treated cohort lacked transcriptomics, copy number variation (CNV), proteomics data and data related to the tumor evolution; therefore, the association between IL1-MT signaling and the

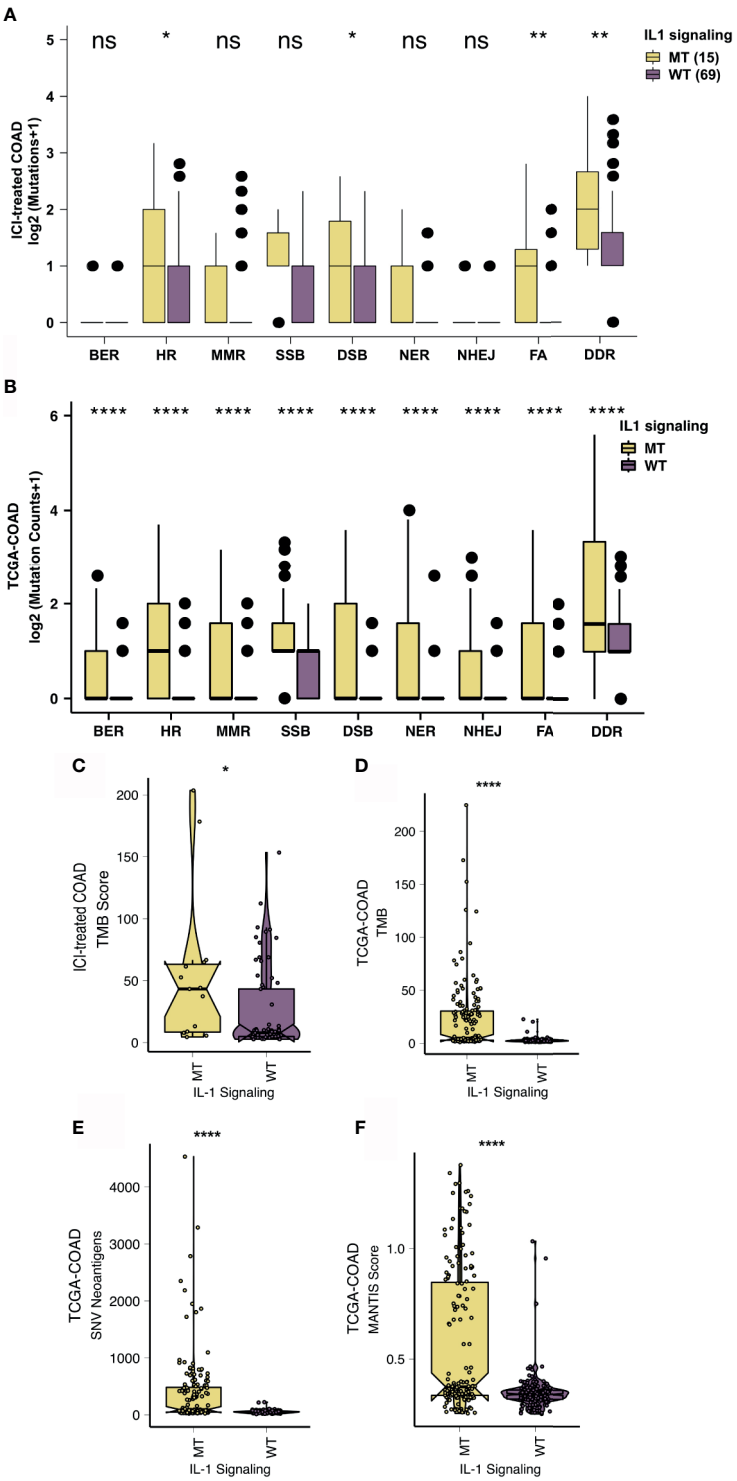

FIGURE 6 | IL-1-MT COAD is associated with enhanced tumor immunogenicity. Comparison of the mutation counts of nine DNA damage-related signaling pathways between IL-1-MT and IL-1-WT tumors in the ICI-treated COAD **(A)** and TCGA-COAD **(B)** cohorts. Comparison of the TMB between IL-1-MT and IL-1-WT tumors in the ICI-treated COAD **(C)** and TCGA-COAD **(D)** cohorts. Comparison of the NAL between IL-1-MT and IL-1-WT tumors in the TCGA-COAD cohort **(E)**. Comparison of the MANTIS score between IL-1-MT and IL-1-WT tumors in the TCGA-COAD cohort **(F)**. (*P < 0.05; **P < 0.01; ****P < 0.0001; ns, not significant; Mann-Whitney U test).

prognosis of COAD patients treated with ICIs could not be further explored. Thus, we can only use the TCGA-COAD to explore the association between the IL1-MT and prognosis of COAD patients treated with ICIs based on multi-omics analysis; third, in future research, molecular and animal experiments are needed to further verify our results. Therefore, more studies involving larger samples and diverse ethnic groups are still needed for subsequent analysis and verification.

CONCLUSIONS

In this study, IL-1-MT was found to be an independent predictor of good prognosis for COAD patients receiving ICIs. IL-MT COAD patients had a significantly prolonged OS. Additionally, IL-1-MT was associated with significantly increased immunogenicity, numbers of activated immune cells, inflammatory factors and immune response-related scores.

DATA AVAILABILITY STATEMENT

The original contributions presented in the study are included in the article/**Supplementary Material**. Further inquiries can be directed to the corresponding authors.

AUTHOR CONTRIBUTIONS

Conceptualization, QW, JLX, and YB. Formal analysis, XZ, YL, JX, CY, and YW. Visualization, XZ, YL, JX, and YW. Writing–original draft, XZ, YL, JX, and YW. Writing–review & editing, QW, JLX, YB, XZ, YL, JX, CY, and YW. All authors contributed to the article and approved the submitted version.

FUNDING

This work was supported by grants from the Key research and development project of science and technology department of Sichuan province (2021YFS0128).

ACKNOWLEDGMENTS

Special thanks to the English language polishing contributions from TopScience Editing.

SUPPLEMENTARY MATERIAL

The Supplementary Material for this article can be found online at: https://www.frontiersin.org/articles/10.3389/fimmu.2021.665002/full#supplementary-material

Supplementary Figure 1 | Lollipop plot shows the distribution of MYD88, IRAK4 and TRAF6 mutations in the TCGA-COAD cohort.

Supplementary Figure 2 | The heatmap showed the difference of IL-1 signaling related genes between the IL-1-MT and IL-1-WT group.

Supplementary Figure 3 | The comparison of the difference of the expression some genes with pro-inflammatory activity (such as IL1RN, IL1R2, IL1B, IL1R1, IL1RAP, IL1A) between the IL-1-MT and IL-1-WT group.

REFERENCES

1. Goodman A, Patel SP, Kurzrock R. PD-1-PD-L1 Immune-Checkpoint Blockade in B-Cell Lymphomas. *Nat Rev Clin Oncol* (2017) 14:203–20. doi: 10.1038/nrclinonc.2016.168
2. Hamid O, Robert C, Daud A, Hodi FS, Hwu W-J, Kefford R, et al. Safety and Tumor Responses With Lambrolizumab (Anti-PD-1) in Melanoma. *N Engl J Med* (2013) 369:134–44. doi: 10.1056/NEJMoa1305133
3. Brahmer JR, Tykodi SS, Chow LQM, Hwu W-J, Topalian SL, Hwu P, et al. Safety and Activity of Anti-PD-L1 Antibody in Patients With Advanced Cancer. *N Engl J Med* (2012) 366:2455–65. doi: 10.1056/NEJMoa1200694
4. Jung G, Benítez-Ribas D, Sánchez A, Balaguer F. Current Treatments of Metastatic Colorectal Cancer With Immune Checkpoint Inhibitors-2020 Update. *J Clin Med* (2020) 9(11):3520. doi: 10.3390/jcm9113520
5. Wolchok JD, Kluger H, Callahan MK, Postow MA, Rizvi NA, Lesokhin AM, et al. Nivolumab Plus Ipilimumab in Advanced Melanoma. *N Engl J Med* (2013) 369:122–33. doi: 10.1056/NEJMoa1302369
6. Lin A, Zhang J, Luo P. Crosstalk Between the MSI Status and Tumor Microenvironment in Colorectal Cancer. *Front Immunol* (2020) 11:2039. doi: 10.3389/fimmu.2020.02039
7. Le DT, Durham JN, Smith KN, Wang H, Bartlett BR, Aulakh LK, et al. Mismatch Repair Deficiency Predicts Response of Solid Tumors to PD-1 Blockade. *Science* (2017) 357:409–13. doi: 10.1126/science.aan6733
8. Chowell D, Morris LGT, Grigg CM, Weber JK, Samstein RM, Makarov V, et al. Patient HLA Class I Genotype Influences Cancer Response to Checkpoint Blockade Immunotherapy. *Science* (2018) 359:582–7. doi: 10.1126/science.aao4572
9. Wang Z, Zhao J, Wang G, Zhang F, Zhang Z, Zhang F, et al. Comutations in DNA Damage Response Pathways Serve as Potential Biomarkers for Immune Checkpoint Blockade. *Cancer Res* (2018) 78:6486–96. doi: 10.1158/0008-5472.CAN-18-1814
10. Teo MY, Seier K, Ostrovnaya I, Regazzi AM, Kania BE, Moran MM, et al. Alterations in DNA Damage Response and Repair Genes as Potential Marker of Clinical Benefit From PD-1/PD-L1 Blockade in Advanced Urothelial Cancers. *J Clin Oncol Off J Am Soc Clin Oncol* (2018) 36:1685–94. doi: 10.1200/JCO.2017.75.7740
11. Riaz N, Havel JJ, Kendall SM, Makarov V, Walsh LA, Desrichard A, et al. Recurrent SERPINB3 and SERPINB4 Mutations in Patients Who Respond to Anti-CTLA4 Immunotherapy. *Nat Genet* (2016) 48:1327–9. doi: 10.1038/ng.3677
12. Wu H-X, Chen Y-X, Wang Z-X, Zhao Q, He M-M, Wang Y-N, et al. Alteration in TET1 as Potential Biomarker for Immune Checkpoint Blockade in Multiple Cancers. *J Immunother Cancer* (2019) 7:264. doi: 10.1186/s40425-019-0737-3
13. Davis MR, Zhu Z, Hansen DM, Bai Q, Fang Y. The Role of IL-21 in Immunity and Cancer. *Cancer Lett* (2015) 358:107–14. doi: 10.1016/j.canlet.2014.12.047
14. Schwartz C, O'Grady K, Lavelle EC, Fallon PG. Interleukin 33: An Innate Alarm for Adaptive Responses Beyond Th2 Immunity-Emerging Roles in Obesity, Intestinal Inflammation, and Cancer. *Eur J Immunol* (2016) 46:1091–100. doi: 10.1002/eji.201545780
15. Duque J, Díaz-Muñoz MD, Fresno M, Iñiguez MA. Up-Regulation of Cyclooxygenase-2 by Interleukin-1beta in Colon Carcinoma Cells. *Cell Signal* (2006) 18:1262–9. doi: 10.1016/j.cellsig.2005.10.009
16. Maihöfner C, Charalambous MP, Bhambra U, Lightfoot T, Geisslinger G, Gooderham NJ. Expression of Cyclooxygenase-2 Parallels Expression of

Interleukin-1beta, Interleukin-6 and NF-KappaB in Human Colorectal Cancer. *Carcinogenesis* (2003) 24:665–71. doi: 10.1093/carcin/bgg006
17. Dinarello CA. Biologic Basis for Interleukin-1 in Disease. *Blood* (1996) 87:2095–147. doi: 10.1182/blood.V87.6.2095.bloodjournal8762095
18. Guo B, Fu S, Zhang J, Liu B, Li Z. Targeting Inflammasome/IL-1 Pathways for Cancer Immunotherapy. *Sci Rep* (2016) 6:36107. doi: 10.1038/srep36107
19. Takeda K, Akira S. TLR Signaling Pathways. *Semin Immunol* (2004) 16:3–9. doi: 10.1016/j.smim.2003.10.003
20. Kawai T, Akira S. Toll-Like Receptors and Their Crosstalk With Other Innate Receptors in Infection and Immunity. *Immunity* (2011) 34:637–50. doi: 10.1016/j.immuni.2011.05.006
21. Apte RN, Voronov E. Is Interleukin-1 a Good or Bad "Guy" in Tumor Immunobiology and Immunotherapy? *Immunol Rev* (2008) 222:222–41. doi: 10.1111/j.1600-065X.2008.00615.x
22. Samstein RM, Lee C-H, Shoushtari AN, Hellmann MD, Shen R, Janjigian YY, et al. Tumor Mutational Load Predicts Survival After Immunotherapy Across Multiple Cancer Types. *Nat Genet* (2019) 51:202–6. doi: 10.1038/s41588-018-0312-8
23. Colaprico A, Silva TC, Olsen C, Garofano L, Cava C, Garolini D, et al. TCGAbiolinks: An R/Bioconductor Package for Integrative Analysis of TCGA Data. *Nucleic Acids Res* (2016) 44:e71. doi: 10.1093/nar/gkv1507
24. Chalmers ZR, Connelly CF, Fabrizio D, Gay L, Ali SM, Ennis R, et al. Analysis of 100,000 Human Cancer Genomes Reveals the Landscape of Tumor Mutational Burden. *Genome Med* (2017) 9:34. doi: 10.1186/s13073-017-0424-2
25. Thorsson V, Gibbs DL, Brown SD, Wolf D, Bortone DS, Ou Yang T-H, et al. The Immune Landscape of Cancer. *Immunity* (2018) 48:812–30.e14. doi: 10.1016/j.immuni.2018.03.023
26. Bonneville R, Krook MA, Kautto EA, Miya J, Wing MR, Chen H-Z, et al. Landscape of Microsatellite Instability Across 39 Cancer Types. *JCO Precis Oncol* (2017) 2017:1. doi: 10.1200/PO.17.00073 PO.17.00073.
27. Liberzon A, Subramanian A, Pinchback R, Thorvaldsdóttir H, Tamayo P, Mesirov JP. Molecular Signatures Database (MSigDB) 3.0. *Bioinformatics* (2011) 27:1739–40. doi: 10.1093/bioinformatics/btr260
28. Chen B, Khodadoust MS, Liu CL, Newman AM, Alizadeh AA. Profiling Tumor Infiltrating Immune Cells With CIBERSORT. *Methods Mol Biol* (2018) 1711:243–59. doi: 10.1007/978-1-4939-7493-1_12
29. Yu G, Wang L-G, Han Y, He Q-Y. Clusterprofiler: An R Package for Comparing Biological Themes Among Gene Clusters. *OMICS* (2012) 16:284–7. doi: 10.1089/omi.2011.0118
30. Lin A, Wei T, Meng H, Luo P, Zhang J. Role of the Dynamic Tumor Microenvironment in Controversies Regarding Immune Checkpoint Inhibitors for the Treatment of non-Small Cell Lung Cancer (NSCLC) With EGFR Mutations. *Mol Cancer* (2019) 18:139. doi: 10.1186/s12943-019-1062-7
31. Lin A, Zhang H, Hu X, Chen X, Wu G, Luo P, et al. Age, Sex, and Specific Gene Mutations Affect the Effects of Immune Checkpoint Inhibitors in Colorectal Cancer. *Pharmacol Res* (2020) 159:105028. doi: 10.1016/j.phrs.2020.105028
32. Zhang J, Zhou N, Lin A, Luo P, Chen X, Deng H, et al. ZFHX3 Mutation as a Protective Biomarker for Immune Checkpoint Blockade in Non-Small Cell Lung Cancer. *Cancer Immunol Immunother* (2021) 70(1):137–51. doi: 10.1007/s00262-020-02668-8
33. Sami E, Paul BT, Koziol JA, ElShamy WM. The Immunosuppressive Microenvironment in BRCA1-IRIS-Overexpressing TNBC Tumors Is Induced by Bidirectional Interaction With Tumor-Associated Macrophages. *Cancer Res* (2020) 80:1102–17. doi: 10.1158/0008-5472.CAN-19-2374
34. Lu L, Pan K, Zheng H-X, Li J-J, Qiu H-J, Zhao J-J, et al. IL-17A Promotes Immune Cell Recruitment in Human Esophageal Cancers and the Infiltrating Dendritic Cells Represent a Positive Prognostic Marker for Patient Survival. *J Immunother* (2013) 36:451–8. doi: 10.1097/CJI.0b013e3182a802cf
35. Altorki NK, Markowitz GJ, Gao D, Port JL, Saxena A, Stiles B, et al. The Lung Microenvironment: An Important Regulator of Tumour Growth and Metastasis. *Nat Rev Cancer* (2019) 19:9–31. doi: 10.1038/s41568-018-0081-9
36. Tougeron D, Fauquembergue E, Rouquette A, Le Pessot F, Sesboüé R, Laurent M, et al. Tumor-Infiltrating Lymphocytes in Colorectal Cancers With Microsatellite Instability Are Correlated With the Number and Spectrum of Frameshift Mutations. *Mod Pathol Off J United States Can Acad Pathol Inc* (2009) 22:1186–95. doi: 10.1038/modpathol.2009.80
37. Snyder A, Makarov V, Merghoub T, Yuan J, Zaretsky JM, Desrichard A, et al. Genetic Basis for Clinical Response to CTLA-4 Blockade in Melanoma. *N Engl J Med* (2014) 371:2189–99. doi: 10.1056/NEJMoa1406498
38. Sahin IH, Akce M, Alese O, Shaib W, Lesinski GB, El-Rayes B, et al. Immune Checkpoint Inhibitors for the Treatment of MSI-H/MMR-D Colorectal Cancer and a Perspective on Resistance Mechanisms. *Br J Cancer* (2019) 121:809–18. doi: 10.1038/s41416-019-0599-y
39. Rizvi H, Sanchez-Vega F, La K, Chatila W, Jonsson P, Halpenny D, et al. Molecular Determinants of Response to Anti-Programmed Cell Death (PD)-1 and Anti-Programmed Death-Ligand 1 (PD-L1) Blockade in Patients With Non-Small-Cell Lung Cancer Profiled With Targeted Next-Generation Sequencing. *J Clin Oncol Off J Am Soc Clin Oncol* (2018) 36:633–41. doi: 10.1200/JCO.2017.75.3384
40. Hellmann MD, Nathanson T, Rizvi H, Creelan BC, Sanchez-Vega F, Ahuja A, et al. Genomic Features of Response to Combination Immunotherapy in Patients With Advanced Non-Small-Cell Lung Cancer. *Cancer Cell* (2018) 33:843–852.e4. doi: 10.1016/j.ccell.2018.03.018
41. Luo P, Lin A, Li K, Wei T, Zhang J. DDR Pathway Alteration, Tumor Mutation Burden, and Cisplatin Sensitivity in Small Cell Lung Cancer: Difference Detected by Whole Exome and Targeted Gene Sequencing. *J Thorac Oncol Off Publ Int Assoc Study Lung Cancer* (2019) 14:e276–9. doi: 10.1016/j.jtho.2019.08.2509

Conflict of Interest: The authors declare that the research was conducted in the absence of any commercial or financial relationships that could be construed as a potential conflict of interest.

frontiers in Immunology

REVIEW
published: 19 October 2021
doi: 10.3389/fimmu.2021.749190

The Role of Plasmacytoid Dendritic Cells in Cancers

Binhui Zhou[1,2*], *Toby Lawrence*[3,4] *and Yinming Liang*[1,2,3*]

[1] Laboratory of Mouse Genetics, Institute of Psychiatry and Neuroscience, Xinxiang Medical University, Henan, China, [2] Laboratory of Genetic Regulators in the Immune System, Henan Collaborative Innovation Center of Molecular Diagnosis and Laboratory Medicine, Xinxiang Medical University, Henan, China, [3] Henan Key Laboratory of Immunology and Targeted Therapy, School of Laboratory Medicine, Xinxiang Medical University, Henan, China, [4] Centre for Inflammation Biology and Cancer Immunology, King's College London, London, United Kingdom

Plasmacytoid dendritic cells (pDCs) are a special subtype of dendritic cells with the morphology of plasma cells. pDCs produce massive amounts of type I interferon (IFN-I), which was originally found to play an extremely pivotal role in antiviral immunity. Interestingly, accumulated evidence indicates that pDCs can also play an important role in tumorigenesis. In the human body, most of the IFN-α is secreted by activated pDCs mediated by toll-like receptor (TLR) stimulation. In many types of cancer, tumors are infiltrated by a large number of pDCs, however, these pDCs exhibit no response to TLR stimulation, and reduced or absent IFN-α production. In addition, tumor-infiltrating pDCs promote recruitment of regulatory T cells (Tregs) into the tumor microenvironment, leading to immunosuppression and promoting tumor growth. In this review, we discuss recent insights into the development of pDCs and their roles in a variety of malignancies, with special emphasis on the basic mechanisms.

Keywords: plasmacytoid dendritic cells, malignancy, regulatory T cells, type I interferon, immunosuppression

OPEN ACCESS

Edited by:
Catherine Sautes-Fridman, INSERM U1138 Centre de Recherche des Cordeliers (CRC), France

Reviewed by:
Tiziana Schioppa, University of Brescia, Italy
Joanna Bandola-Simon, National Institutes of Health (NIH), United States

***Correspondence:**
Yinming Liang
yinming.liang@gris.org.cn
Binhui Zhou
zhoubinhui@126.com

Specialty section:
This article was submitted to Cancer Immunity and Immunotherapy, a section of the journal Frontiers in Immunology

Received: *29 July 2021*
Accepted: *05 October 2021*
Published: *19 October 2021*

Citation:
Zhou B, Lawrence T and Liang Y (2021) The Role of Plasmacytoid Dendritic Cells in Cancers. Front. Immunol. 12:749190. doi: 10.3389/fimmu.2021.749190

INTRODUCTION

Plasmacytoid dendritic cells (pDCs) are a unique subgroup of dendritic cells (DCs) with plasma cell morphology and have been extensively studied in recent years. The main function of pDCs is the production of IFN-I following recognition of viruses or nucleic acids through TLR7 and TLR9 (1, 2). Therefore, pDCs play a pivotal role in antiviral immunity. Previous studies have shown that DCs are critical in mounting effective immune responses to cancer (3–6). However, pDCs have received less attention in tumor immunity than other DC subgroups. In fact, similar to cDCs, pDCs link the innate and adaptive immune responses by regulating the biological function of lymphocytes, myeloid DCs and NK cells through producing two kinds of pro-inflammatory cytokines including tumor necrosis factor (TNF)-α and interleukin (IL)-6 (1, 7), and play an important role in cancer immunity.

pDCs are continuously produced from hematopoietic stem cells in the bone marrow (BM) and emerge as mature cells into the periphery (8). Under steady state conditions, the pDC precursor cells in the bone marrow enters the blood circulation, and then enters the secondary lymphatic tissue through the lymphatic circulation. In addition, a small amount of pDCs are also observed in the peripheral tissues such as liver, lung and gut, while they are believed to be absent in the skin (9). Interestingly, previous publications reported that pDCs infiltrate various types of solid tumors,

including head and neck, liver, breast, colorectal, ovary, stomach, lung and skin cancers (10–17). Depending on the microenvironment and the type of stimulus, pDCs are capable of exerting either immunogenic or tolerogenic functions (18–20). In this review, we summarize current knowledge about the role of pDCs in different malignancies.

PDCS DEVELOPMENT AND IDENTIFICATION

The development of pDCs depends on multiple factors including Flt3 ligand (Flt3L) (21), transcription factor Spi-B (22, 23), and the basic helix-loop-helix protein E2-2 (24, 25). Among them, Flt3L together with Flt3 activate transcription factor E2-2 in a STAT3-dependent manner to control the expression level of transcription factors necessary for the development and function of pDC (18, 26). Spi-B regulates human plasmacytoid dendritic cell survival through direct induction of the antiapoptotic gene BCL2-A1 (27), and plays a key role in pDC differentiation, whereas BCL11A activation is shown to direct CDP commitment to pDC lineage and regulate the transcriptional level of E2-2, Id2, Id3 and Mtg16 through a positive feedback loop (18, 22, 28). In addition, transcription factor E2-2 also plays an essential and specific regulator in pDC development (29, 30). By using single-cell sequencing, Ginhoux's team showed that pDCs developed from a $Ly6D^{high}CD2^{high}$ lymphoid progenitor cell in the bone marrow and differentiated independently of the myeloid cDC lineage (31).

Concerning their identification, human pDCs express CD4, blood-derived dendritic cell antigen 2 (BDCA2, also termed CD303), CD123 (IL-3R), HLA-DR, ILT3 and ILT7 on the surface, and Toll-like receptor (TLR)7 and TLR9 within endosomal compartments (7, 30, 32), but lack most of the lineage surface markers for T, B, natural killer (NK) cells and monocytes (33, 34). And in mice, pDCs not only express B220 (CD45R), CD11c and Ly6C (35), but also express a variety of factors that modulate the function of pDCs, such as Siglec-H, Bst-2, Pdc-Trem and Ly49Q (1, 36).

ROLE OF PDCS IN CANCERS

PDCS and Melanoma

Functional studies of pDCs in cancer have mostly focused on mouse models of melanoma. Despite the fact cutaneous melanoma is a highly immunogenic solid tumor, the occurrence and development of melanoma is related to its ability to escape immunosurveillance (7). Previous studies have shown that circulating pDC levels were decreased in blood of melanoma patients (37), however, pDCs were increased in primary tumors and tumor-draining lymph nodes, and pDC infiltration was associated with poor prognosis and early relapse (38, 39). In addition, melanoma cells were shown to recruit pDCs into the tumor microenvironment *via* stromal-derived factor-1 (SDF-1, also named CXCL12) (40). Moreover, IL-3 up-regulates the expression of chemokine receptor 6 (CCR6) in pDCs, as another mechanism for pDCs recruitment into the tumor microenvironment in melanoma, through CCR6/CCL20 (chemokine ligand 20) activation (41) (**Figure 1A**). Aspord et al. showed that pDCs in melanoma triggered IL-5-/IL-13-producing CD4 type 2 T helper (Th2) cells and IL-10-producing Tregs through the expression of OX40L and ICOSL, the secretion of Th2 cytokines leading to melanoma progression (39). Moreover, the expression level of MxA (a IFN-α inducible protein) in primary cutaneous melanomas was drastically inhibited in the majority of the cases (42) and the poor IFN-α production by pDCs has been associated with melanoma growth (40, 42, 43). Interestingly, Aspord and co-workers additionally demonstrated that the development of melanoma was strongly inhibited by imiquimod treatment (a TLR7 agonist) using an innovative melanoma-bearing humanized mouse model (44). They found pDCs in tumor site were mobilized and their cytotoxic functions were increased, in addition, the expression levels of type I IFN (IFN-α) response genes were up-regulated, thereby inhibiting melanoma growth (44). Another study suggested that CpG B-type oligodeoxynucleotide (ODN) PF-3512676 activates pDCs in the sentinel lymph nodes of melanoma patients through the TLR pathway, prompting pDCs to release IFN-α, thereby enhances antitumor immunity (45). Furthermore, *in vitro* experiments have shown that the expression of cytotoxic molecule TRAIL was induced on pDCs by virus, imiquimod or IFN-α stimulation, and can be used to effectively lyse melanoma cells (7, 46, 47) (**Table 1**).

Numerous studies have shown that the infiltration of a large number of pDCs is related to immunosuppression in the tumor microenvironment (12, 63–66) (**Figure 1B**). Evidence suggested that the interaction between LAG-3 and MHC-II induced TLR-independent activation of pDCs with enhanced IL-6 and limited IFN-α secretion, induced the production of CCL2 in monocytes, and generated Tregs from allogenic $CD4^+$ $CD25^-$ T cells, which ultimately leads to immunosuppression in tumors (67, 68). On the other hand, ILT7L was reported to down-regulate the expression level of IFN-α through its interaction with ILT7 receptors, and IDO (indoleamine 2,3-dioxygenase) released by pDCs strongly promotes the activation of Tregs, which leads to anergy, eventually helping tumor cells escape immune surveillance (69, 70). In addition, *in vitro* experiments showed that activated pDCs up-regulate the expression levels of MHC class I and class II molecules and CD95 on melanoma cells (71), and researchers speculate that tumor cells are more easily recognized by CTL *in vivo* (72). However, even if pDCs were activated in tumors, only weak and cytoplasmic expression of CD95 was detected on melanoma cells, suggesting that the progressive loss of CD95 in tumor cells as a possible mechanism of tumor escape (71). Melanoma cells have also acquired mechanisms to subvert the immune-stimulatory functions of pDCs, such as secrete immunosuppressive cytokines, including IL-10, TGF-β and PGE2, to suppress the expression level of TLR7/9 and IRF7, resulting in pDCs producing only a small amount of I-IFN (43, 73). Moreover, Wnt5a was strongly expressed in melanoma cells which

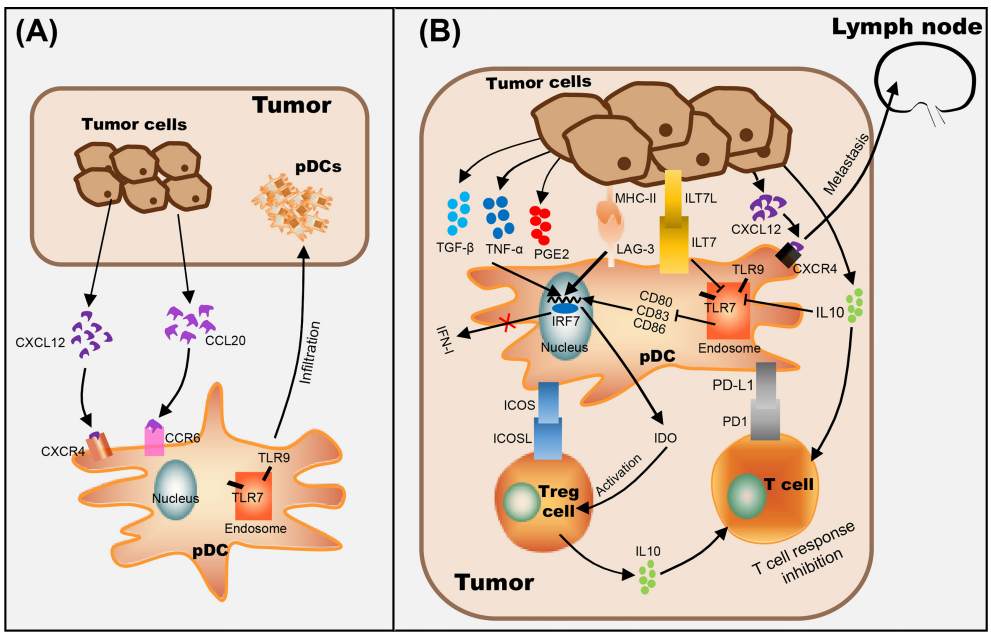

FIGURE 1 | The role of pDCs in tumor progression. **(A)** pDC recognizes CCL20 secreted by tumor cells through CCR6 on the cell membrane and makes it migrate to the tumor site. **(B)** Mechanisms of tumor-infiltrated pDC on immunosuppression include recruitment of immature pDCs lacking the expression of costimulatory molecules (through CCR6/CCL20 pathway), suppression of type I IFN secretion by pDCs (by ILT7L-ILT7 interaction or immunosuppressive cytokines secreted by tumor cells, such as IL-10), alternate pDC activation (through the interaction between LAG-3$^+$ pDC and MHC II$^+$ tumor cells), and/or promote pDC tolerance by activating Tregs (through ICOSL/ICOS interaction and IDO production) and enhancing the expression level of anti-inflammatory cytokine IL-10. In addition, the up-regulation of CXCR4 on the surface of pDC and the promotion of CXCL12 secretion by tumor cells are positively correlated with lymph node metastasis of tumor cells.

TABLE 1 | Therapeutic approaches for various cancers through pDCs.

Type of cancers	Role of pDCs	Therapeutic approach	References
Melanoma	Limit IFN-α secretion, recruit Tregs and enhance immunosuppression.	TLR9-agonist	(45, 48, 49)
		TLR7-agonist	(46, 50)
		TLR-4 ligand	(51)
		Pim-3-targeting bifunctional shRNA	(52)
		IFN-α therapy	(53)
		IFN-α therapy + checkpoint inhibitor	(54)
		pDC-based vaccination	(55–57)
Lung cancer	Induce immunosuppression and promote the proliferation of lung cancer cells.	TLR4-agonist	(58)
Gastric cancer	Promote the differentiation of naive CD4$^+$ T cells into Tregs and facilitate tumor immune escape.	TLR3 agonist	(59)
Breast cancer	Contribute to the immune escape of breast cancer cells and promote tumor growth.	–	–
Liver cancer	Promote Tregs to produce IL-10, thereby inhibit T cell responses and assist immunosuppression and tumor progression.	–	–
Squamous cell carcinoma	Limit IFN-α secretion and promote tumor progression.	CD317 antibody	(60)
Leukemia	Recruit Tregs into CMML.	CD123-targeted therapy	(61)
Ovarian cancer	Limit IFN-α secretion recruit Tregs and enhance immunosuppression	Prophylactic vaccines	(62)

suppressed the activation and IFN-α production of pDCs stimulated by CpG oligodeoxynucleotide, thus weakening the anti-tumor effects of CpG (73).

In recent years, different approaches have emerged for the treatment of melanoma that affect pDC functions. For example, ponophosphoryl lipid A (MPLA), a toll-like receptor 4 ligand, exhibits the capability to enhance anti-PD-L1 antibody-mediated anti-cancer immunity by activating pDC to produce IFN-α (51). Furthermore, the ssRNA-Pim-3-shRNA dual-function therapy established by Liu's group not only enhanced the activation and

IFN-α secretion of pDCs, promoted the apoptosis and inhibited the proliferation of melanoma cells, but also enhanced the activation of $CD8^+$ T cells and NK cells and simultaneously reduced the proportion of Tregs and myeloid-derived suppressor cells (MDSCs), and ultimately reversed the tumor immunosuppressive microenvironment (52). Targeted delivery of IFN-α into the tumor site enhance the local immune response and the benefit of the checkpoint inhibition (53). Interestingly, the combination of intratumoral injection of IFN-α and anti-PD-1 immunotherapy (Clinicaltrials.gov research identifier: NCT02339324) suppressed PD-L1-mediated escape (43, 54). In addition, subcutaneous injection of TLR9-activating oligodeoxynucleotide PF-3512676 enhanced activation of pDCs and cytotoxicity of NK cells (48). Hofmann et al. also injected PF-3512676 in cutaneous or subcutaneous melanoma metastasis of 5 patients with melanoma in a phase I study, and observed local tumor regression (49). Furthermore, the combined topical use of imiquimod and monobenzone caused local regression of cutaneous metastases in 52% of 21 melanoma patients (stage III-IV) in a phase II study (50). On the other hand, by activating autologous pDCs and simultaneously loading with melanoma-associated peptides, and then injecting them into the lymph nodes, induced a systemic IFN-I response and activated NK cells (55). Other studies support the development of a pDC-based vaccine (HLA-A*0201$^+$ pDCs) to produce tumor-specific T cells for adoptive cellular immunotherapy in melanoma patients (56, 57) (**Table 1**).

PDCS and Lung Cancer

Lung cancer has a very high morbidity and mortality rate in the smoking population (74). According to the morphology of cancer cells, lung cancer can be divided into four subtypes, including small cell carcinoma, adenocarcinoma, squamous cell carcinoma, and large cell carcinoma (75). Like other types of cancer, lung cancer is also accompanied by a drastic accumulation of pDCs (63, 76). Previous research has shown that pDCs are robustly increased in the peripheral blood of non-small cell lung carcinoma (NSCLC), and the degree of pDC accumulation is related to the clinical grade of disease (76). Another study also observed that tumor-infiltrating pDCs (TIpDCs) were significantly increased in lung tumor masses compared to healthy tissues, these pDCs expressed higher levels of CD33 and PD-L1, associated with reduced cytotoxic activity towards tumor cells and in fact promoting their proliferation (63). Moreover, TIpDCs produced higher levels of IL-1α, which promotes angiogenesis and enhances the invasiveness of cancer cells, thereby promoting the progression of lung cancer (63). On the other hand, Perrot et al. reported that the expression levels of the activation markers CD80, CD83, CD86, or CD208/DC-LAMP on pDCs infiltrating NSCLC, were completely suppressed and only partial upregulation of CD86 was detected after TLR7 activation. In addition, even after TLR9 stimulation, only very weak T cell proliferation and IFN-α secretion was induced by TIpDCs. Therefore, the abnormal differentiation of TIpDCs seems to be an additional factor contributing to tumor immune escape (77).

It is worth noting that in previous studies, CpG-oligodeoxynucleotides can stimulate the activation of pDCs and induce anti-tumor immunity in a mouse model of melanoma (73). However, in the lung cancer microenvironment, the anti-tumor effect of CpG-oligodeoxynucleotides is ineffective, and the accumulation of pDCs promotes the tumor infiltration of Tregs and immature myeloid dendritic cells (mDCs), thereby inducing immunosuppression and promoting the proliferation of lung cancer cells (16). These studies show that the activity of pDCs is regulated by the tumor microenvironment, and the role of pDCs is multifaceted in different types of tumors.

Interestingly, numerous studies have reported the anti-tumor effects of LPS (78–82). In a mouse model of melanoma-induced metastatic lung cancer, Rega et al. showed that the administration of low-dose LPS caused immunosuppression, which was associated with the infiltration of pDCs, Tregs, MDSCs and $CD8^+$ Tregs, while the growth inhibition of lung tumor caused by large dose of LPS was associated with the massive infiltration of pDCs, as well as Th1 and Th17 polarization (58).

PDCS and Gastric Cancer

Gastric cancer (GC) is one of the five most common cancers worldwide as well as the third biggest cause of cancer-related mortality (83). Previous studies have shown that pDCs play a crucial role in GC (66). Although the population of pDCs in the peripheral blood of GC patients is significantly elevated, the plasma concentration of IFN-α was significantly decreased (66, 84). On this basis, circulating pDCs showed a positive correlation with advanced stages and lymph node metastasis in gastric cancer (84). In addition, the accumulation of pDCs in peripheral blood and tumor tissues predicted poor clinical outcome in GC patients (85).

Previous studies have shown that gastric microbiota dysbiosis and immune system dysfunction are critical factors for the occurrence and development of GC (15, 86–88). In different microhabitats, it was observed that BDCA2$^+$ pDCs and Foxp3$^+$ Tregs were significantly increased in tumoral and peritumoral tissues, and there was a positive correlation between them (15). Moreover, pDCs can effectively promote the differentiation of naive $CD4^+$ T cells into Tregs, thereby facilitating tumor immune escape (89). Interestingly, TLR agonist stimulation caused metabolic reprogramming in DCs, which was critical for immune activation (59). Basit et al. demonstrated that TLR-stimulation of pDCs significantly increases the expression level of genes that regulate oxidative phosphorylation and glutamine metabolism, thereby promoting pDC activation, leading to higher production of IFN-α and inducing T cell responses (90).

PDCS and Breast Cancer

Breast cancer (BC) is the most frequent malignancy and the second biggest cause of cancer- associated mortality in women worldwide (91, 92), and approximately 70-80% of patients with early stage and non-metastatic disease can be cured (93). The most aggressive type of breast cancer is triple-negative breast cancer (TNBC), which does not express of HER2/neu, estrogen

receptor and progesterone receptor (91). In a large majority of cases, immunity against breast cancer does not exhibit a protective effect, which indicates that breast cancer cells escape immunosurveillance (91). In addition, previous research has shown that the breast tumor microenvironment makes immune cells dysfunctional and is conducive to immunosuppression, thereby preventing the establishment of anti-tumor immunity (94). Published studies have shown that pDCs infiltrate breast tumors, but are impaired by TGF-β and TNF-α to produce IFN-α (95), and associated with poor clinical prognosis (64, 96), indicating that pDCs might contribute to the immune escape of breast tumors and ultimately promote their growth (96). Another study showed that the production of GM-CSF and pDCs infiltration was significantly increased in breast cancer, and pDCs activated by GM-CSF promoted the differentiation of $CD4^+$ T cells into Tregs, leading to immunosuppression (64, 97, 98). In addition, pDCs-derived TNF-α in breast tumors triggered activation of the NF-κB signaling pathway in cancer cells, which in turn upregulated the expression level of CXCR4 and led to increased metastasis to lymph nodes, which ultimately promoted cancer progression (99, 100).

PDCS and Liver Cancer

Liver cancer is the fifth most common malignancy in men and the ninth most commonly occurring cancer in women, which can be divided into primary liver cancer and secondary or metastatic liver cancer according to its cause, and has a poor prognosis. The therapeutic effect of chemotherapy in liver cancer is very limited, and it can only prolong the survival of patients by 2.3 to 2.8 months on average (101). The immune regulation in the liver tumor microenvironment may contribute to the immune escape of tumor cells, thereby greatly reducing the efficacy of immunotherapy (102). Previous studies have shown that pDCs also heavily infiltrate liver cancer tissues, which promotes vascular invasion and lymph node metastasis, resulting in a shorter overall survival and a higher recurrence rate for patients (103). Like melanoma (39), pDCs exposed to liver tumor-derived factors increased the expression levels of ICOSL to promote Tregs to produce increased IL-10, thereby strongly inhibiting T cell responses and ultimately assisting immunosuppression and tumor progression (12). Furthermore, the increase of intratumoral pDCs was associated with increased infiltration of Tregs, therefore, the evaluation of intratumoral pDCs represents an excellent predictor of the prognosis of liver cancer patients (103).

PDCS and Squamous Cell Carcinoma

Squamous cell carcinoma (SSC) is a tumor of the upper aerodigestive tract with high fatality rate and poor prognosis (104, 105). In primary oral squamous cell carcinoma (OSCC), tumor cells produce high levels of CXCL12 (106), which promotes the infiltration of pDCs expressing the corresponding receptor CXCR4, which has also been observed in head and neck SSC (107). However, there is evidence that tumor-induced down-regulation of TLR9 in pDCs was observed within the tumor environment (108), and simultaneously various cytokines in the tumor microenvironment such as VEGF, TGF-β and IL-10 inhibit the maturation and activation of TIpDCs (109), resulting in a significant decrease in the expression of IFN-α, indicating TIpDCs dysfunction (108, 110). In addition, the increase in the number of TIpDCs is associated with lymph node metastasis and overall survival (110). Another study showed that the use of CD317 antibody to deplete pDCs in the tumor microenvironment significantly promoted the recovery of T cell function, and inhibited the tumor infiltration of Tregs and monocyte-derived suppressor cells, thereby breaking the immunosuppressive state (60). This further supports that the high infiltration of pDCs in tumors promotes the progression of SSC.

The subtyping of pDCs is also of great significance in SSC. BDCA2 is a specific marker of human pDCs, but high BDCA2 is expressed by immature pDCs, while pDCs expressing CD123 have higher maturity and ability to secrete cytokines (60, 111). In head and neck SSC, the Poropatich group identified a subgroup pDCs expressing high levels of OX40 in the tumor microenvironment, which is conducive to anti-tumor immunity by increasing the expression levels of local IL-12 and IFN-α and enhancing the interaction between cDC and $CD8^+$ T cell *via* OX40/OX40L-signaling axis (112). Additionally, $CD56^+$ pDCs express higher levels of perforin and granzyme b, which confers strong cytotoxic activity, but the proportion of such cells is significantly decreased in head and neck SSC (113). Similar studies have shown that pDCs can be divided into two subgroups through the expression level of CD2, where $CD2^{high}$ pDCs secrete higher levels of IL12p40 and express higher levels of costimulatory molecule CD80, and exhibit higher efficiency in triggering T cell proliferation (114). It can be seen that up-regulating CD56 or CD2 of pDCs will have a positive effect on anti-tumor immunity in SSC. Therefore, whether the combination of chemoradiation and intratumor injection of activated pDCs could also improve clinical outcome in patients is worthy of further study.

PDCS and Leukemia

Leukemia is the common name for several malignant disorders, which are manifested by a robust increase in the number of leucocytes in the blood and/or the bone marrow (115). Previous studies have found that infiltrating $CD123^+$ pDCs have been observed in the hematopoietic tissues of a fraction of chronic myelomonocytic leukemia (CMML) patients, and the excess of pDCs is associated with the accumulation of Tregs and the increased risk of acute leukemia transformation (33). However, in chronic myeloid leukemia (CML), pDCs are derived from precursors that express a low level of *BCR-ABL*, and develop normally and usually express the co-stimulatory antigen CD86. In addition, CML-pDCs also retain their ability to mature and produce IFN-α, thereby regulating anti-leukemic immunity in CML (116). On the other hand, due to different clinical and pathological manifestations, pDC neoplasms can be divided into two types including mature pDC proliferation associated with myeloid neoplasms and blastic pDC neoplasm (BPDCN) (117), and BPDCN is an aggressive hematopoietic clonal neoplasm that prone to leukemia transformation and poor prognosis (118). And in acute myeloid leukemia (AML), Zalmai et al. identified a

group of pDC-AML with completely different phenotype from BPDCN, with high expression of CD34 and CD303, low expression of CD123 and cTCL1, and no expression of CD56 (119). Molecular analysis indicated that these pDCs were inactive and neoplastic, and exhibited frequent RUNX1 mutations (119). Moreover, studies showed that clinical use of tagraxofusp (SL-401) completely inhibited protein synthesis leading to cell death of pDCs, which had a positive effect on inhibiting acute transformation in leukemia (61, 118).

PDCS and Ovarian Cancer

Ovarian cancer (OC) is the most aggressive gynecological cancer in women (11). High infiltration of pDCs is significantly associated with early relapse in ovarian cancer (11, 65, 120). At the same time, TApDCs not only exhibit less production of IFN-α, mainly mediated through tumor-derived TNF-α and TGF-β (120), but also induce tumor infiltration of $ICOS^+$ $Foxp3^+$ Tregs and drive immunosuppression *via* ICOS/ICOSL stimulation (65). Additionally, both TApDCs and $ICOS^+$ $Foxp3^+$ Tregs predict disease progression in epithelial ovarian cancer patients (65). On the other hand, published reports indicate that pDCs control the homeostasis of $CD4^+$ $Foxp3^+$ Tregs and Th17 cells *in vivo* by expressing sialic acid-binding Ig-like lectin (Siglec)-H (121). And pDCs in tumor ascites induced $IL\text{-}10^+$ $CCR7^+$ $CD45RO^+$ $CD8^+$ Tregs which was independent of $CD4^+$ $CD25^+$ T cells, and inhibit tumor-associated antigen-specific T cell effector functions through IL-10 (122). Moreover, the results of Zou et al. showed that high expression of CXCL12 was observed in malignant human ovarian epithelial tumor cells, and CXCL12 induced adhesion, transmigration and chemotaxis of pDCs, and inhibited tumor macrophage IL-10-induced pDC apoptosis through CXCR4, resulting in poorly proliferating T cells (13). Interestingly, the Figdor group tested the immunomodulatory capacity of prophylactic live-attenuated and inactivated viral vaccines on pDCs, and found that prophylactic vaccines significantly induce the activation and maturation of pDCs, the expression of MHC class I and class II, and the production of IFN-α, that transform pDCs from an immunosuppressed state to an immune activated state (62). The above studies provide new ideas for the remission and treatment of ovarian cancer, by targeting ICOS/ICOSL to inhibit the accumulation of $ICOS^+$ $Foxp3^+$ Tregs in ovarian cancer, thereby eliminating immunosuppression. In addition, it can also play a positive role in restoring the function of pDCs by regulating the expression of Siglec-H. Using viruses as vaccine vectors to activate pDCs is also a new regulatory idea, but it should be noted that even live-attenuated viral, the impact of the virus itself must be considered.

CONCLUSIONS

pDCs are an promising target for cancer immunotherapy; however, accumulating evidence indicates that the complex interaction of pDCs with tumor cells and their microenvironment appears to contribute to immunologic tolerance (7). In many types of cancers, tumor cells secrete the chemokine CXCL12 to induce the infiltration of a large number of immature pDCs, and the cytokines of VEGF, TNF-α, TGF-β and IL-10 secreted in tumor microenvironment inhibit the maturation and activation of pDCs, then make it unable to produce IFN-α. Additionally, pDCs recruit a large number of Tregs to the tumor site, leading to immunosuppression and promoting tumor growth. Therefore, it can provide ideas for clinical treatment of cancer in two aspects. On one hand, the injection of drugs to induce the activation of pDCs in tumors or the combination of chemoradiation and intratumor injection of activated pDCs may reverse the tumor microenvironment, thereby inhibiting tumor growth and improving patient survival rate (51, 105). On the other hand, we can eliminate the immunosuppressive effect in the tumor microenvironment by reducing the proportion of Tregs or inhibiting its function in the tumors. Published study demonstrated that daclizumab, a humanized anti-CD25 antibody, can block the IL-2 signaling pathway by binding to CD25, which in turn leads to the death of Tregs (123). In addition, some chemotherapeutic drugs can also reduce the number of Tregs by inhibiting Tregs gene synthesis and reducing cell expansion. Zhang et al. showed that the chemotherapeutic agent gemcitabine significantly reduced immunosuppression in the tumor microenvironment, accompanied by a decrease in Tregs and MDSCs, thereby inhibiting tumor growth (124). Furthermore, CTLA-4 is expressed on the surface of Tregs and transmits inhibitory signals in the immune response. Therefore, using monoclonal antibody to block the expression of CTLA-4, can reduce the inhibitory activity of Tregs, and achieve tumor suppression effects (125). However, more efforts are needed to develop more effective pDCs activators or Tregs inhibitors, which will help in the treatment of various malignancies clinically.

AUTHOR CONTRIBUTIONS

All authors listed have made direct and substantial contribution to this work, and approved the final manuscript.

FUNDING

This work was supported by grant from National Natural Science Foundation of China (Grant No. 32000491), and also sponsored by projects from Henan Province to YL (No. 21IRTSTHN030 and GZS2021002).

ACKNOWLEDGMENTS

We would like to thank Wushan Li for preparing **Figure 1** and Zhilong Liu and Yang Liu for assistance in preparation of the manuscript.

REFERENCES

1. Swiecki M, Colonna M. The Multifaceted Biology of Plasmacytoid Dendritic Cells. *Nat Rev Immunol* (2015) 15(8):471–85. doi: 10.1038/nri3865
2. Nestle FO, Conrad C, Tun-Kyi A, Homey B, Gombert M, Boyman O, et al. Plasmacytoid Predendritic Cells Initiate Psoriasis Through Interferon-Alpha Production. *J Exp Med* (2005) 202(1):135–43. doi: 10.1084/jem.20050500
3. Ferris ST, Durai V, Wu R, Theisen DJ, Ward JP, Bern MD, et al. Cdc1 Prime and Are Licensed by CD4 T Cells to Induce Anti-Tumour Immunity. *Nature* (2020) 584(7822):624–9. doi: 10.1038/s41586-020-2611-3
4. Zhivaki D, Borriello F, Chow OA, Doran B, Fleming I, Theisen DJ, et al. Inflammasomes Within Hyperactive Murine Dendritic Cells Stimulate Long-Lived T Cell-Mediated Anti-Tumor Immunity. *Cell Rep* (2020) 33 (7):108381. doi: 10.1016/j.celrep.2020.108381
5. de Winde CM, Munday C, Acton SE. Molecular Mechanisms of Dendritic Cell Migration in Immunity and Cancer. *Med Microbiol Immunol* (2020) 209(4):515–29. doi: 10.1007/s00430-020-00680-4
6. Wang Y, Xiang Y, Xin VW, Wang XW, Peng XC, Liu XQ, et al. Dendritic Cell Biology and Its Role in Tumor Immunotherapy. *J Hematol Oncol* (2020) 13(1):107. doi: 10.1186/s13045-020-00939-6
7. Saadeh D, Kurban M, Abbas O. Plasmacytoid Dendritic Cell Role in Cutaneous Malignancies. *J Dermatol Sci* (2016) 83(1):3–9. doi: 10.1016/j.jdermsci.2016.05.008
8. Reizis B. Plasmacytoid Dendritic Cells: Development, Regulation, and Function. *Immunity* (2019) 50(1):37–50. doi: 10.1016/j.immuni.2018.12.027
9. Kohli K, Janssen A, Forster R. Plasmacytoid Dendritic Cells Induce Tolerance Predominantly by Cargoing Antigen to Lymph Nodes. *Eur J Immunol* (2016) 46(11):2659–68. doi: 10.1002/eji.201646359
10. Sakakura K, Chikamatsu K, Takahashi K, Whiteside TL, Furuya N. Maturation of Circulating Dendritic Cells and Imbalance of T-Cell Subsets in Patients With Squamous Cell Carcinoma of the Head and Neck. *Cancer Immunol Immunother* (2006) 55(2):151–9. doi: 10.1007/s00262-005-0697-y
11. Labidi-Galy SI, Treilleux I, Goddard-Leon S, Combes JD, Blay JY, Ray-Coquard I, et al. Plasmacytoid Dendritic Cells Infiltrating Ovarian Cancer Are Associated With Poor Prognosis. *Oncoimmunology* (2012) 1(3):380–2. doi: 10.4161/onci.18801
12. Pedroza-Gonzalez A, Zhou G, Vargas-Mendez E, Boor PP, Mancham S, Verhoef C, et al. Tumor-Infiltrating Plasmacytoid Dendritic Cells Promote Immunosuppression by Tr1 Cells in Human Liver Tumors. *Oncoimmunology* (2015) 4(6):e1008355. doi: 10.1080/2162402X.2015.1008355
13. Zou W, Machelon V, Coulomb-L'Hermin A, Borvak J, Nome F, Isaeva T, et al. Stromal-Derived Factor-1 in Human Tumors Recruits and Alters the Function of Plasmacytoid Precursor Dendritic Cells. *Nat Med* (2001) 7 (12):1339–46. doi: 10.1038/nm1201-1339
14. Bellik L, Gerlini G, Parenti A, Ledda F, Pimpinelli N, Neri B, et al. Role of Conventional Treatments on Circulating and Monocyte-Derived Dendritic Cells in Colorectal Cancer. *Clin Immunol* (2006) 121(1):74–80. doi: 10.1016/j.clim.2006.06.011
15. Ling Z, Shao L, Liu X, Cheng Y, Yan C, Mei Y, et al. Regulatory T Cells and Plasmacytoid Dendritic Cells Within the Tumor Microenvironment in Gastric Cancer Are Correlated With Gastric Microbiota Dysbiosis: A Preliminary Study. *Front Immunol* (2019) 10:533. doi: 10.3389/fimmu.2019.00533
16. Sorrentino R, Morello S, Luciano A, Crother TR, Maiolino P, Bonavita E, et al. Plasmacytoid Dendritic Cells Alter the Antitumor Activity of CpG-Oligodeoxynucleotides in a Mouse Model of Lung Carcinoma. *J Immunol* (2010) 185(8):4641–50. doi: 10.4049/jimmunol.1000881
17. Vescovi R, Monti M, Moratto D, Paolini L, Consoli F, Benerini L, et al. Collapse of the Plasmacytoid Dendritic Cell Compartment in Advanced Cutaneous Melanomas by Components of the Tumor Cell Secretome. *Cancer Immunol Res* (2019) 7(1):12–28. doi: 10.1158/2326-6066.CIR-18-0141
18. Mitchell D, Chintala S, Dey M. Plasmacytoid Dendritic Cell in Immunity and Cancer. *J Neuroimmunol* (2018) 322:63–73. doi: 10.1016/j.jneuroim.2018.06.012
19. Villadangos JA, Young L. Antigen-Presentation Properties of Plasmacytoid Dendritic Cells. *Immunity* (2008) 29(3):352–61. doi: 10.1016/j.immuni.2008.09.002
20. Kerkmann M, Rothenfusser S, Hornung V, Towarowski A, Wagner M, Sarris A, et al. Activation With CpG-A and CpG-B Oligonucleotides Reveals Two Distinct Regulatory Pathways of Type I IFN Synthesis in Human Plasmacytoid Dendritic Cells. *J Immunol* (2003) 170(9):4465–74. doi: 10.4049/jimmunol.170.9.4465
21. Blom B, Ho S, Antonenko S, Liu YJ. Generation of Interferon Alpha-Producing Predendritic Cell (Pre-DC)2 From Human CD34(+) Hematopoietic Stem Cells. *J Exp Med* (2000) 192(12):1785–96. doi: 10.1084/jem.192.12.1785
22. Schotte R, Nagasawa M, Weijer K, Spits H, Blom B. The ETS Transcription Factor Spi-B Is Required for Human Plasmacytoid Dendritic Cell Development. *J Exp Med* (2004) 200(11):1503–9. doi: 10.1084/jem.20041231
23. Sasaki I, Hoshino K, Sugiyama T, Yamazaki C, Yano T, Iizuka A, et al. Spi-B Is Critical for Plasmacytoid Dendritic Cell Function and Development. *Blood* (2012) 120(24):4733–43. doi: 10.1182/blood-2012-06-436527
24. Nagasawa M, Schmidlin H, Hazekamp MG, Schotte R, Blom B. Development of Human Plasmacytoid Dendritic Cells Depends on the Combined Action of the Basic Helix-Loop-Helix Factor E2-2 and the Ets Factor Spi-B. *Eur J Immunol* (2008) 38(9):2389–400. doi: 10.1002/eji.200838470
25. Shortman K, Sathe P, Vremec D, Naik S, O'Keeffe M. Plasmacytoid Dendritic Cell Development. *Adv Immunol* (2013) 120:105–26. doi: 10.1016/B978-0-12-417028-5.00004-1
26. Laouar Y, Welte T, Fu X, Flavell R. STAT3 Is Required for Flt3L-Dependent Dendritic Cell Differentiation. *Immunity* (2003) 19:903–12. doi: 10.1016/s1074-7613(03)00332-7
27. Karrich JJ, Balzarolo M, Schmidlin H, Libouban M, Nagasawa M, Gentek R, et al. The Transcription Factor Spi-B Regulates Human Plasmacytoid Dendritic Cell Survival Through Direct Induction of the Antiapoptotic Gene BCL2-A1. *Blood* (2012) 119(22):5191–200. doi: 10.1182/blood-2011-07-370239
28. Ippolito GC, Dekker JD, Wang YH, Lee BK, Shaffer AL3rd, Lin J, et al. Dendritic Cell Fate Is Determined by BCL11A. *P Natl Acad Sci USA* (2014) 111(11):E998–1006. doi: 10.1073/pnas.1319228111
29. Cisse B, Caton ML, Lehner M, Maeda T, Scheu S, Locksley R, et al. Transcription Factor E2-2 Is an Essential and Specific Regulator of Plasmacytoid Dendritic Cell Development. *Cell* (2008) 135(1):37–48. doi: 10.1016/j.cell.2008.09.016
30. Cao W. Molecular Characterization of Human Plasmacytoid Dendritic Cells. *J Clin Immunol* (2009) 29(3):257–64. doi: 10.1007/s10875-009-9284-x
31. Dress RJ, Dutertre CA, Giladi A, Schlitzer A, Low I, Shadan NB, et al. Plasmacytoid Dendritic Cells Develop From Ly6D(+) Lymphoid Progenitors Distinct From the Myeloid Lineage. *Nat Immunol* (2019) 20(7):852–64. doi: 10.1038/s41590-019-0420-3
32. Saadeh D, Kurban M, Abbas O. Update on the Role of Plasmacytoid Dendritic Cells in Inflammatory/Autoimmune Skin Diseases. *Exp Dermatol* (2016) 25(6):415–21. doi: 10.1111/exd.12957
33. Lucas N, Duchmann M, Rameau P, Noel F, Michea P, Saada V, et al. Biology and Prognostic Impact of Clonal Plasmacytoid Dendritic Cells in Chronic Myelomonocytic Leukemia. *Leukemia* (2019) 33(10):2466–80. doi: 10.1038/s41375-019-0447-3
34. Vermi W, Soncini M, Melocchi L, Sozzani S, Facchetti F. Plasmacytoid Dendritic Cells and Cancer. *J Leukoc Biol* (2011) 90(4):681–90. doi: 10.1189/jlb.0411190
35. Nakano H, Yanagita M, Gunn MD. CD11c(+)B220(+)Gr-1(+) Cells in Mouse Lymph Nodes and Spleen Display Characteristics of Plasmacytoid Dendritic Cells. *J Exp Med* (2001) 194(8):1171–8. doi: 10.1084/jem.194.8.1171
36. Reizis B, Bunin A, Ghosh HS, Lewis KL, Sisirak V. Plasmacytoid Dendritic Cells: Recent Progress and Open Questions. *Annu Rev Immunol* (2011) 29:163–83. doi: 10.1146/annurev-immunol-031210-101345
37. Chevolet I, Speeckaert R, Schreuer M, Neyns B, Krysko O, Bachert C, et al. Clinical Significance of Plasmacytoid Dendritic Cells and Myeloid-Derived Suppressor Cells in Melanoma. *J Transl Med* (2015) 13:9. doi: 10.1186/s12967-014-0376-x
38. Jensen TO, Schmidt H, Moller HJ, Donskov F, Hoyer M, Sjoegren P, et al. Intratumoral Neutrophils and Plasmacytoid Dendritic Cells Indicate Poor Prognosis and Are Associated With Pstat3 Expression in AJCC Stage I/II Melanoma. *Cancer* (2012) 118(9):2476–85. doi: 10.1002/cncr.26511

39. Aspord C, Leccia MT, Charles J, Plumas J. Plasmacytoid Dendritic Cells Support Melanoma Progression by Promoting Th2 and Regulatory Immunity Through OX40L and ICOSL. *Cancer Immunol Res* (2013) 1 (6):402–15. doi: 10.1158/2326-6066.CIR-13-0114-T
40. Gerlini G, Urso C, Mariotti G, Di Gennaro P, Palli D, Brandani P, et al. Plasmacytoid Dendritic Cells Represent a Major Dendritic Cell Subset in Sentinel Lymph Nodes of Melanoma Patients and Accumulate in Metastatic Nodes. *Clin Immunol* (2007) 125(2):184–93. doi: 10.1016/j.clim.2007.07.018
41. Charles J, Di Domizio J, Salameire D, Bendriss-Vermare N, Aspord C, Muhammad R, et al. Characterization of Circulating Dendritic Cells in Melanoma: Role of CCR6 in Plasmacytoid Dendritic Cell Recruitment to the Tumor. *J Invest Dermatol* (2010) 130(6):1646–56. doi: 10.1038/jid.2010.24
42. Vermi W, Bonecchi R, Facchetti F, Bianchi D, Sozzani S, Festa S, et al. Recruitment of Immature Plasmacytoid Dendritic Cells (Plasmacytoid Monocytes) and Myeloid Dendritic Cells in Primary Cutaneous Melanomas. *J Pathol* (2003) 200(2):255–68. doi: 10.1002/path.1344
43. Monti M, Consoli F, Vescovi R, Bugatti M, Vermi W. Human Plasmacytoid Dendritic Cells and Cutaneous Melanoma. *Cells* (2020) 9(2):417. doi: 10.3390/cells9020417
44. Aspord C, Tramcourt L, Leloup C, Molens JP, Leccia MT, Charles J, et al. Imiquimod Inhibits Melanoma Development by Promoting pDC Cytotoxic Functions and Impeding Tumor Vascularization. *J Invest Dermatol* (2014) 134(10):2551–61. doi: 10.1038/jid.2014.194
45. Molenkamp BG, van Leeuwen PA, Meijer S, Sluijter BJ, Wijnands PG, Baars A, et al. Intradermal CpG-B Activates Both Plasmacytoid and Myeloid Dendritic Cells in the Sentinel Lymph Node of Melanoma Patients. *Clin Cancer Res* (2007) 13(10):2961–9. doi: 10.1158/1078-0432.CCR-07-0050
46. Kalb ML, Glaser A, Stary G, Koszik F, Stingl G. TRAIL(+) Human Plasmacytoid Dendritic Cells Kill Tumor Cells *In Vitro*: Mechanisms of Imiquimod- and IFN-Alpha-Mediated Antitumor Reactivity. *J Immunol* (2012) 188(4):1583–91. doi: 10.4049/jimmunol.1102437
47. Chaperot L, Blum A, Manches O, Lui G, Angel J, Molens JP, et al. Virus or TLR Agonists Induce TRAIL-Mediated Cytotoxic Activity of Plasmacytoid Dendritic Cells. *J Immunol* (2006) 176(1):248–55. doi: 10.4049/jimmunol.176.1.248
48. Pashenkov M, Goess G, Wagner C, Hormann M, Jandl T, Moser A, et al. Phase II Trial of a Toll-Like Receptor 9-Activating Oligonucleotide in Patients With Metastatic Melanoma. *J Clin Oncol* (2006) 24(36):5716–24. doi: 10.1200/JCO.2006.07.9129
49. Hofmann MA, Kors C, Audring H, Walden P, Sterry W, Trefzer U. Phase 1 Evaluation of Intralesionally Injected TLR9-Agonist PF-3512676 in Patients With Basal Cell Carcinoma or Metastatic Melanoma. *J Immunother* (2008) 31(5):520–7. doi: 10.1097/CJI.0b013e318174a4df
50. Teulings HE, Tjin EPM, Willemsen KJ, van der Kleij S, Ter Meulen S, Kemp EH, et al. Anti-Melanoma Immunity and Local Regression of Cutaneous Metastases in Melanoma Patients Treated With Monobenzone and Imiquimod; A Phase 2 a Trial. *Oncoimmunology* (2018) 7(4):e1419113. doi: 10.1080/2162402X.2017.1419113
51. Zhang W, Lim SM, Hwang J, Ramalingam S, Kim M, Jin JO. Monophosphoryl Lipid A-Induced Activation of Plasmacytoid Dendritic Cells Enhances the Anti-Cancer Effects of Anti-PD-L1 Antibodies. *Cancer Immunol Immunother* (2021) 70(3):689–700. doi: 10.1007/s00262-020-02715-4
52. Liu J, Hu Y, Guo Q, Yu X, Shao L, Zhang C. Enhanced Anti-Melanoma Efficacy of a Pim-3-Targeting Bifunctional Small Hairpin RNA *via* Single-Stranded RNA-Mediated Activation of Plasmacytoid Dendritic Cells. *Front Immunol* (2019) 10:2721. doi: 10.3389/fimmu.2019.02721
53. Zitvogel L, Galluzzi L, Kepp O, Smyth MJ, Kroemer G. Type I Interferons in Anticancer Immunity. *Nat Rev Immunol* (2015) 15(7):405–14. doi: 10.1038/nri3845
54. Atkins MB, Hodi FS, Thompson JA, McDermott DF, Hwu WJ, Lawrence DP, et al. Pembrolizumab Plus Pegylated Interferon Alfa-2b or Ipilimumab for Advanced Melanoma or Renal Cell Carcinoma: Dose-Finding Results From the Phase Ib KEYNOTE-029 Study. *Clin Cancer Res* (2018) 24 (8):1805–15. doi: 10.1158/1078-0432.CCR-17-3436
55. Tel J, Aarntzen EH, Baba T, Schreibelt G, Schulte BM, Benitez-Ribas D, et al. Natural Human Plasmacytoid Dendritic Cells Induce Antigen-Specific T-Cell Responses in Melanoma Patients. *Cancer Res* (2013) 73(3):1063–75. doi: 10.1158/0008-5472.CAN-12-2583
56. Aspord C, Leccia MT, Salameire D, Laurin D, Chaperot L, Charles J, et al. HLA-A(*)0201(+) Plasmacytoid Dendritic Cells Provide a Cell-Based Immunotherapy for Melanoma Patients. *J Invest Dermatol* (2012) 132 (10):2395–406. doi: 10.1038/jid.2012.152
57. Aspord C, Charles J, Leccia MT, Laurin D, Richard MJ, Chaperot L, et al. A Novel Cancer Vaccine Strategy Based on HLA-A*0201 Matched Allogeneic Plasmacytoid Dendritic Cells. *PloS One* (2010) 5(5):e10458. doi: 10.1371/journal.pone.0010458
58. Rega A, Terlizzi M, Luciano A, Forte G, Crother TR, Arra C, et al. Plasmacytoid Dendritic Cells Play a Key Role in Tumor Progression in Lipopolysaccharide-Stimulated Lung Tumor-Bearing Mice. *J Immunol* (2013) 190(5):2391–402. doi: 10.4049/jimmunol.1202086
59. Joffre O, Nolte MA, Spörri R, Reis e Sousa C. Inflammatory Signals in Dendritic Cell Activation and the Induction of Adaptive Immunity. *Immunol Rev* (2009) 227(1):234–47. doi: 10.1111/j.1600-065X.2008.00718.x
60. Yang LL, Mao L, Wu H, Chen L, Deng WW, Xiao Y, et al. pDC Depletion Induced by CD317 Blockade Drives the Antitumor Immune Response in Head and Neck Squamous Cell Carcinoma. *Oral Oncol* (2019) 96:131–9. doi: 10.1016/j.oraloncology.2019.07.019
61. Pemmaraju N, Lane AA, Sweet KL, Stein AS, Vasu S, Blum W, et al. Tagraxofusp in Blastic Plasmacytoid Dendritic-Cell Neoplasm. *N Engl J Med* (2019) 380(17):1628–37. doi: 10.1056/NEJMoa1815105
62. de Vries IJ, Tel J, Benitez-Ribas D, Torensma R, Figdor CG. Prophylactic Vaccines Mimic Synthetic CpG Oligonucleotides in Their Ability to Modulate Immune Responses. *Mol Immunol* (2011) 48(6-7):810–7. doi: 10.1016/j.molimm.2010.12.022
63. Sorrentino R, Terlizzi M, Di Crescenzo VG, Popolo A, Pecoraro M, Perillo G, et al. Human Lung Cancer-Derived Immunosuppressive Plasmacytoid Dendritic Cells Release IL-1alpha in an AIM2 Inflammasome-Dependent Manner. *Am J Pathol* (2015) 185(11):3115–24. doi: 10.1016/j.ajpath.2015.07.009
64. Sisirak V, Faget J, Gobert M, Goutagny N, Vey N, Treilleux I, et al. Impaired IFN-Alpha Production by Plasmacytoid Dendritic Cells Favors Regulatory T-Cell Expansion That may Contribute to Breast Cancer Progression. *Cancer Res* (2012) 72(20):5188–97. doi: 10.1158/0008-5472.CAN-11-3468
65. Conrad C, Gregorio J, Wang YH, Ito T, Meller S, Hanabuchi S, et al. Plasmacytoid Dendritic Cells Promote Immunosuppression in Ovarian Cancer *via* ICOS Costimulation of Foxp3(+) T-Regulatory Cells. *Cancer Res* (2012) 72(20):5240–9. doi: 10.1158/0008-5472.CAN-12-2271
66. Huang XM, Liu XS, Lin XK, Yu H, Sun JY, Liu XK, et al. Role of Plasmacytoid Dendritic Cells and Inducible Costimulator-Positive Regulatory T Cells in the Immunosuppression Microenvironment of Gastric Cancer. *Cancer Sci* (2014) 105(2):150–8. doi: 10.1111/cas.12327
67. Camisaschi C, De Filippo A, Beretta V, Vergani B, Villa A, Vergani E, et al. Alternative Activation of Human Plasmacytoid DCs *In Vitro* and in Melanoma Lesions: Involvement of LAG-3. *J Invest Dermatol* (2014) 134 (7):1893–902. doi: 10.1038/jid.2014.29
68. Castelli C, Triebel F, Rivoltini L, Camisaschi C. Lymphocyte Activation Gene-3 (LAG-3, CD223) in Plasmacytoid Dendritic Cells (pDCs): A Molecular Target for the Restoration of Active Antitumor Immunity. *Oncoimmunology* (2014) 3(11):e967146. doi: 10.4161/21624011.2014.967146
69. Gerlini G, Di Gennaro P, Mariotti G, Urso C, Chiarugi A, Pimpinelli N, et al. Indoleamine 2,3-Dioxygenase+ Cells Correspond to the BDCA2+ Plasmacytoid Dendritic Cells in Human Melanoma Sentinel Nodes. *J Invest Dermatol* (2010) 130(3):898–901. doi: 10.1038/jid.2009.307
70. Lombardi VC, Khaiboullina SF, Rizvanov AA. Plasmacytoid Dendritic Cells, a Role in Neoplastic Prevention and Progression. *Eur J Clin Invest* (2015) 45:1–8. doi: 10.1111/eci.12363
71. Salio M, Cella M, Vermi W, Facchetti F, Palmowski M, Smith C, et al. Plasmacytoid Dendritic Cells Prime IFN-Gamma-Secreting Melanoma Specific CD8 Lymphocytes and Are Found in Primary Melanoma Lesions. *Eur J Immunol* (2003) 33(4):1052–62. doi: 10.1002/eji.200323676
72. Kayagaki N, Yamaguchi N, Nakayama M, Eto H, Okumura K, Yagita H. Type I Interferons (IFNs) Regulate Tumor Necrosis Factor-Related Apoptosis-Inducing Ligand (TRAIL) Expression on Human T Cells A Novel Mechanism for the Antitumor Effects of Type I IFNs. *J Exp Med* (1999) 189(9):1451–60. doi: 10.1084/jem.189.9.1451

73. Hack K, Reilly L, Proby C, Fleming C, Leigh I, Foerster J. Wnt5a Inhibits the CpG Oligodeoxynucleotide-Triggered Activation of Human Plasmacytoid Dendritic Cells. *Clin Exp Dermatol* (2012) 37(5):557–61. doi: 10.1111/j.1365-2230.2012.04362.x
74. Romaszko A, Doboszyńska A. Multiple Primary Lung Cancer: A Literature Review. *Adv Clin Exp Med* (2018) 27(5):725–30. doi: 10.17219/acem/68631
75. Collins LG, Haines C, Perkel R, Enck RE. Lung Cancer: Diagnosis and Management. *Am Fam Physician* (2007) 75(1):56–63.
76. Shi W, Li X, Porter JL, Ostrodi DH, Yang B, Li J, et al. Level of Plasmacytoid Dendritic Cells Is Increased in Non-Small Cell Lung Carcinoma. *Tumour Biol* (2014) 35(3):2247–52. doi: 10.1007/s13277-013-1297-7
77. Perrot I, Blanchard D, Freymond N, Isaac S, Guibert B, Pacheco Y, et al. Dendritic Cells Infiltrating Human Non-Small Cell Lung Cancer Are Blocked at Immature Stage. *J Immunol* (2007) 178(5):2763–9. doi: 10.4049/jimmunol.178.5.2763
78. Drapier JC, Petit JF. Development of Antitumor Activity in LPS-Stimulated Mouse Granuloma Macrophages. *Inflammation* (1986) 10(2):195–204. doi: 10.1007/BF00916001
79. Nelson MH, Bowers JS, Bailey SR, Diven MA, Fugle CW, Kaiser AD, et al. Toll-Like Receptor Agonist Therapy can Profoundly Augment the Antitumor Activity of Adoptively Transferred CD8(+) T Cells Without Host Preconditioning. *J Immunother Cancer* (2016) 4:6. doi: 10.1186/s40425-016-0110-8
80. Li H, Lu X, Lu M, Liu H. Isolation, Purification and Antitumor Activity of Lipopolysaccharide From Cow Placenta. *Int J Biol Macromol* (2008) 43 (3):232–7. doi: 10.1016/j.ijbiomac.2008.05.005
81. Bandekar JR, Nerkar DP. Antitumor Activity of Lipopolysaccharide and Radio-Detoxified Lipopolysaccharide of Vibrio Parahaemolyticus. *Microbiol Immunol* (1987) 31(7):675–81. doi: 10.1111/j.1348-0421.1987.tb03128.x
82. Moriya N, Miwa H, Orita K. Antitumor Effect of Bacterial Lipopolysaccharide (LPS) Alone and in Combination With Lentinan on MH-134 Tumors in C3H/He Mice. *Acta Med Okayama* (1984) 38(1):49–55. doi: 10.18926/AMO/30363
83. Bagheri V, Abbaszadegan MR, Memar B, Motie MR, Asadi M, Mahmoudian RA, et al. Induction of T Cell-Mediated Immune Response by Dendritic Cells Pulsed With mRNA of Sphere-Forming Cells Isolated From Patients With Gastric Cancer. *Life Sci* (2019) 219:136–43. doi: 10.1016/j.lfs.2019.01.016
84. Liu W, Zhao J, Li Q, Wang Q, Zhou Y, Tong Z. Gastric Cancer Patients Have Elevated Plasmacytoid and CD1c(+) Dendritic Cells in the Peripheral Blood. *Oncol Lett* (2018) 15(4):5087–92. doi: 10.3892/ol.2018.7990
85. Liu X, Yu H, Yan C, Mei Y, Lin C, Hong Y, et al. Plasmacytoid Dendritic Cells and ICOS(+) Regulatory T Cells Predict Poor Prognosis in Gastric Cancer: A Pilot Study. *J Cancer* (2019) 10(26):6711–5. doi: 10.7150/jca.34826
86. Hooper LV, Littman DR, Macpherson AJ. Interactions Between the Microbiota and the Immune System. *Science* (2012) 336(6086):1268–73. doi: 10.1126/science.1223490
87. Brestoff JR, Artis D. Commensal Bacteria at the Interface of Host Metabolism and the Immune System. *Nat Immunol* (2013) 14(7):676–84. doi: 10.1038/ni.2640
88. Belkaid Y, Hand TW. Role of the Microbiota in Immunity and Inflammation. *Cell* (2014) 157(1):121–41. doi: 10.1016/j.cell.2014.03.011
89. Ito T, Yang M, Wang YH, Lande R, Gregorio J, Perng OA, et al. Plasmacytoid Dendritic Cells Prime IL-10-Producing T Regulatory Cells by Inducible Costimulator Ligand. *J Exp Med* (2007) 204(1):105–15. doi: 10.1084/jem.20061660
90. Basit F, Mathan T, Sancho D, de Vries IJM. Human Dendritic Cell Subsets Undergo Distinct Metabolic Reprogramming for Immune Response. *Front Immunol* (2018) 9:2489. doi: 10.3389/fimmu.2018.02489
91. Sisirak V, Faget J, Vey N, Blay JY, Menetrier-Caux C, Caux C, et al. Plasmacytoid Dendritic Cells Deficient in IFNalpha Production Promote the Amplification of FOXP3(+) Regulatory T Cells and Are Associated With Poor Prognosis in Breast Cancer Patients. *Oncoimmunology* (2013) 2(1): e22338. doi: 10.4161/onci.22338
92. Fahad Ullah M. Breast Cancer: Current Perspectives on the Disease Status. *Adv Exp Med Biol* (2019) 1152:51–64. doi: 10.1007/978-3-030-20301-6_4
93. Harbeck N, Penault-Llorca F, Cortes J, Gnant M, Houssami N, Poortmans P, et al. Breast Cancer. *Nat Rev Dis Primers* (2019) 5(1):66. doi: 10.1038/s41572-019-0111-2
94. Hurwitz AA, Watkins SK. Immune Suppression in the Tumor Microenvironment: A Role for Dendritic Cell-Mediated Tolerization of T Cells. *Cancer Immunol Immunother* (2012) 61(2):289–93. doi: 10.1007/s00262-011-1181-5
95. Sisirak V, Vey N, Goutagny N, Renaudineau S, Malfroy M, Thys S, et al. Breast Cancer-Derived Transforming Growth Factor-Beta and Tumor Necrosis Factor-Alpha Compromise Interferon-Alpha Production by Tumor-Associated Plasmacytoid Dendritic Cells. *Int J Cancer* (2013) 133 (3):771–8. doi: 10.1002/ijc.28072
96. Treilleux I. Dendritic Cell Infiltration and Prognosis of Early Stage Breast Cancer. *Clin Cancer Res* (2004) 10(22):7466–74. doi: 10.1158/1078-0432.CCR-04-0684
97. Ghirelli C, Reyal F, Jeanmougin M, Zollinger R, Sirven P, Michea P, et al. Breast Cancer Cell-Derived GM-CSF Licenses Regulatory Th2 Induction by Plasmacytoid Predendritic Cells in Aggressive Disease Subtypes. *Cancer Res* (2015) 75(14):2775–87. doi: 10.1158/0008-5472.CAN-14-2386
98. Faget J, Bendriss-Vermare N, Gobert M, Durand I, Olive D, Biota C, et al. ICOS-Ligand Expression on Plasmacytoid Dendritic Cells Supports Breast Cancer Progression by Promoting the Accumulation of Immunosuppressive CD4+ T Cells. *Cancer Res* (2012) 72(23):6130–41. doi: 10.1158/0008-5472.CAN-12-2409
99. Helbig G, Christopherson KW 2nd, Bhat-Nakshatri P, Kumar S, Kishimoto H, Miller KD, et al. NF-KappaB Promotes Breast Cancer Cell Migration and Metastasis by Inducing the Expression of the Chemokine Receptor CXCR4. *J Biol Chem* (2003) 278(24):21631–8. doi: 10.1074/jbc.M300609200
100. Gadalla R, Hassan H, Ibrahim SA, Abdullah MS, Gaballah A, Greve B, et al. Tumor Microenvironmental Plasmacytoid Dendritic Cells Contribute to Breast Cancer Lymph Node Metastasis *via* CXCR4/SDF-1 Axis. *Breast Cancer Res Treat* (2019) 174(3):679–91. doi: 10.1007/s10549-019-05129-8
101. Llovet JM, Ricci S, Mazzaferro V, Hilgard P, Gane E, Blanc J-F, et al. Sorafenib in Advanced Hepatocellular Carcinoma. *N Engl J Med* (2008) 359 (4):378–90. doi: 10.1056/NEJMoa0708857
102. Pardee AD, Butterfield LH. Immunotherapy of Hepatocellular Carcinoma: Unique Challenges and Clinical Opportunities. *Oncoimmunology* (2012) 1 (1):48–55. doi: 10.4161/onci.1.1.18344
103. Zhou ZJ, Xin HY, Li J, Hu ZQ, Luo CB, Zhou SL. Intratumoral Plasmacytoid Dendritic Cells as a Poor Prognostic Factor for Hepatocellular Carcinoma Following Curative Resection. *Cancer Immunol Immunother* (2019) 68 (8):1223–33. doi: 10.1007/s00262-019-02355-3
104. Kallini JR, Hamed N, Khachemoune A. Squamous Cell Carcinoma of the Skin Epidemiology, Classification, Management, and Novel Trends. *Int J Dermatol* (2015) 54(2):130–40. doi: 10.1111/ijd.12553
105. Moyer JS, Li J, Wei S, Teitz-Tennenbaum S, Chang AE. Intratumoral Dendritic Cells and Chemoradiation for the Treatment of Murine Squamous Cell Carcinoma. *J Immunother* (2008) 31(9):885–95. doi: 10.1097/CJI.0b013e3181880f1e
106. Oliveira-Neto HH, Silva ET, Leles CR, Mendonca EF, Alencar Rde C, Silva TA, et al. Involvement of CXCL12 and CXCR4 in Lymph Node Metastases and Development of Oral Squamous Cell Carcinomas. *Tumour Biol* (2008) 29(4):262–71. doi: 10.1159/000152944
107. Thiel A, Pries R, Jeske S, Trenkle T, Wollenberg B. Effect of Head and Neck Cancer Supernatant and CpG-Oligonucleotides on Migration and IFN-Alpha Production of Plasmacytoid Dendritic Cells. *Anticancer Res* (2009) 29(8):3019–25.
108. Hartmann E, Wollenberg B, Rothenfusser S, Wagner M, Wellisch D, Mack B, et al. Identification and Functional Analysis of Tumor-Infiltrating Plasmacytoid Dendritic Cells in Head and Neck Cancer. *Cancer Res* (2003) 63(19):6478–87.
109. Demoulin S, Herfs M, Delvenne P, Hubert P. Tumor Microenvironment Converts Plasmacytoid Dendritic Cells Into Immunosuppressive/Tolerogenic Cells: Insight Into the Molecular Mechanisms. *J Leukoc Biol* (2013) 93(3):343–52. doi: 10.1189/jlb.0812397
110. Han N, Zhang Z, Liu S, Ow A, Ruan M, Yang W, et al. Increased Tumor-Infiltrating Plasmacytoid Dendritic Cells Predicts Poor Prognosis in Oral Squamous Cell Carcinoma. *Arch Oral Biol* (2017) 78:129–34. doi: 10.1016/j.archoralbio.2017.02.012
111. Fraga GR, Chow P. Plasmacytoid Dendritic Cells in Keratoacanthoma and Squamous Cell Carcinoma: A Blinded Study of CD123 as a Diagnostic Marker. *J Cutan Pathol* (2020) 47(1):17–21. doi: 10.1111/cup.13573

112. Poropatich K, Dominguez D, Chan WC, Andrade J, Zha Y, Wray B, et al. OX40+ Plasmacytoid Dendritic Cells in the Tumor Microenvironment Promote Antitumor Immunity. *J Clin Invest* (2020) 130(7):3528–42. doi: 10.1172/JCI131992
113. Thiel A, Kesselring R, Pries R, Wittkopf N, Puzik A, Wollenberg B. Plasmacytoid Dendritic Cell Subpopulations in Head and Neck Squamous Cell Carcinoma. *Oncol Rep* (2011) 26(3):615–20. doi: 10.3892/or.2011.1350
114. Matsui T, Connolly JE, Michnevitz M, Chaussabel D, Yu CI, Glaser C, et al. CD2 Distinguishes Two Subsets of Human Plasmacytoid Dendritic Cells With Distinct Phenotype and Functions. *J Immunol* (2009) 182(11):6815–23. doi: 10.4049/jimmunol.0802008
115. Juliusson G, Hough R. Leukemia. *Prog Tumor Res* (2016) 43:87–100. doi: 10.1159/000447076
116. Inselmann S, Wang Y, Saussele S, Fritz L, Schütz C, Huber M, et al. Development, Function, and Clinical Significance of Plasmacytoid Dendritic Cells in Chronic Myeloid Leukemia. *Cancer Res* (2018) 78 (21):6223–34. doi: 10.1158/0008-5472.Can-18-1477
117. Facchetti F, Cigognetti M, Fisogni S, Rossi G, Lonardi S, Vermi W. Neoplasms Derived From Plasmacytoid Dendritic Cells. *Mod Pathol* (2016) 29(2):98–111. doi: 10.1038/modpathol.2015.145
118. Venugopal S, Zhou S, El Jamal SM, Lane AA, Mascarenhas J. Blastic Plasmacytoid Dendritic Cell Neoplasm-Current Insights. *Clin Lymphoma Myeloma Leuk* (2019) 19(9):545–54. doi: 10.1016/j.clml.2019.06.002
119. Zalmai L, Viailly PJ, Biichle S, Cheok M, Soret L, Angelot-Delettre F, et al. Plasmacytoid Dendritic Cells Proliferation Associated With Acute Myeloid Leukemia: Phenotype Profile and Mutation Landscape. *Haematologica* (2020). doi: 10.3324/haematol.2020.253740
120. Labidi-Galy SI, Sisirak V, Meeus P, Gobert M, Treilleux I, Bajard A, et al. Quantitative and Functional Alterations of Plasmacytoid Dendritic Cells Contribute to Immune Tolerance in Ovarian Cancer. *Cancer Res* (2011) 71 (16):5423–34. doi: 10.1158/0008-5472.CAN-11-0367
121. Takagi H, Fukaya T, Eizumi K, Sato Y, Sato K, Shibazaki A, et al. Plasmacytoid Dendritic Cells Are Crucial for the Initiation of Inflammation and T Cell Immunity *In Vivo*. *Immunity* (2011) 35(6):958–71. doi: 10.1016/j.immuni.2011.10.014
122. Wei S, Kryczek I, Zou LH, Daniel B, Cheng P, Mottram P, et al. Plasmacytoid Dendritic Cells Induce CD8+ Regulatory T Cells in Human Ovarian Carcinoma. *Cancer Res* (2005) 65(12):5020–6. doi: 10.1158/0008-5472.CAN-04-4043
123. Morita R, Hirohashi Y, Sato N. Depletion of Tregs *In Vivo*: A Promising Approach to Enhance Antitumor Immunity Without Autoimmunity. . *Immunother* (2012) 4(11):1103–5. doi: 10.2217/imt.12.116
124. Zhang Y, Bush X, Yan B, Chen JA. Gemcitabine Nanoparticles Promote Antitumor Immunity Against Melanoma. *Biomaterials* (2019) 189:48–59. doi: 10.1016/j.biomaterials.2018.10.022
125. Selby MJ, Engelhardt JJ, Quigley M, Henning KA, Chen T, Srinivasan M, et al. Anti-CTLA-4 Antibodies of IgG2a Isotype Enhance Antitumor Activity Through Reduction of Intratumoral Regulatory T Cells. *Cancer Immunol Res* (2013) 1(1):32–42. doi: 10.1158/2326-6066.CIR-13-0013

Conflict of Interest: The authors declare that the research was conducted in the absence of any commercial or financial relationships that could be construed as a potential conflict of interest.

frontiers | Frontiers in Immunology

REVIEW
published: 10 May 2022
doi: 10.3389/fimmu.2022.887189

Advances in Human Dendritic Cell-Based Immunotherapy Against Gastrointestinal Cancer

*Ling Ni**

Institute for Immunology and School of Medicine, Tsinghua University, Beijing, China

OPEN ACCESS

Edited by:
Manel Juan,
Hospital Clínic de Barcelona, Spain

Reviewed by:
Daniel Benitez-Ribas,
Hospital Clínic de Barcelona, Spain
Yunbin Ye,
Fujian Cancer Hospital, China

***Correspondence:**
Ling Ni
lingni@tsinghua.edu.cn

Specialty section:
This article was submitted to Cancer Immunity and Immunotherapy, a section of the journal Frontiers in Immunology

Received: *01 March 2022*
Accepted: *08 April 2022*
Published: *10 May 2022*

Citation:
Ni L (2022) Advances in Human Dendritic Cell-Based Immunotherapy Against Gastrointestinal Cancer. Front. Immunol. 13:887189. doi: 10.3389/fimmu.2022.887189

Dendritic cells (DCs), the strongest antigen-presenting cells, are a focus for orchestrating the immune system in the fight against cancer. Basic scientific investigations elucidating the cellular biology of the DCs have resulted in new strategies in this fight, including cancer vaccinology, combination therapy, and adoptive cellular therapy. Although immunotherapy is currently becoming an unprecedented bench-to-bedside success, the overall response rate to the current immunotherapy in patients with gastrointestinal (GI) cancers is pretty low. Here, we have carried out a literature search of the studies of DCs in the treatment of GI cancer patients. We provide the advances in DC-based immunotherapy and highlight the clinical trials that indicate the therapeutic efficacies and toxicities related with each vaccine. Moreover, we also offer the yet-to-be-addressed questions about DC-based immunotherapy. This study focuses predominantly on the data derived from human studies to help understand the involvement of DCs in patients with GI cancers.

Keywords: dendritic cells, gastrointestinal cancers, vaccines, immunotherapy, patients

INTRODUCTION

In the past decade, the immunotherapy that enhances anti-tumor immunity has revolutionized cancer treatment, leading to potent and durable immune responses in subsets of patients across various tumor types. Immune checkpoint inhibitors (ICIs) that target the T-cell inhibitory checkpoint proteins CTLA-4, PD-1, or the PD-1 ligand PD-L1 have been approved for the treatment of a variety of cancers, including melanoma, non-small-cell lung cancer, head–neck cancer, bladder cancer, renal cell cancer, hepatocellular carcinoma (HCC), and several other tumor types.

Despite the huge success these inhibitors have made, only a small subset of cancer patients benefits from ICI therapy. Adoptive chimeric antigen receptor (CAR)-T-cell transfer has also been approved for the treatment of hematological cancers, showing less effectivity against solid tumors.

Gastrointestinal (GI) malignancies are one of the deadliest cancers worldwide. GI malignancies include cancers arising in the oral cavity, esophagus, stomach, liver, pancreas, intestines, rectum, and anus. The GI cancers have a poor prognosis, which mainly depends on tumor stage when diagnosed. Current treatment strategies consist of surgery, chemotherapy, radiotherapy, and targeted therapies. A benefit has been demonstrated in ICI therapy, particularly in esophageal cancer (EC), gastric cancer (GC), and microsatellite instability-high (MSI-H) colorectal cancer (CRC), while pancreatic cancer (PC) and HCC show little response to immune modulation.

Dendritic cells (DCs) play a critical role in the generation of anti-tumor immune responses, mainly acting as the strongest antigen-presenting cells to prime naïve T cells and educating them into cytotoxic T lymphocytes (CTLs). DCs induce an immune response to pathogens and tumors while simultaneously maintaining tolerance to self. DC functional defects have been associated to the progression of various human cancers. Effective cancer vaccines have been a challenge since they target tumor antigens, some of which are self-antigens and thus induce self-tolerance. Here, we performed an extensive literature search of the studies of DC-based immunotherapy against GI cancer patients and provided the advances in DC-based immunotherapy in order to help better understand the status of DC-based immunotherapy.

ADVANCES IN DENDRITIC CELL-BASED IMMUNOTHERAPY IN ESOPHAGEAL CANCER

EC is a malignancy derived from esophagus, which is the most common digestive tract cancer in China. Despite progresses in various treatment strategies for EC, its 5-year survival rate is approximately 14%–22% with a poor prognosis. Among the various therapeutic strategies, attention has switched to immunotherapy, especially DC-based immunotherapy.

Dendritic Cells in Esophageal Cancer

For EC patients, there was an increase in the density of $S100^+$ DCs in both the tumor stroma and cancer epithelium (1). $CD1a^+$ immature DCs (iDCs) were predominantly present in the tumor bed, while DC-$Lamp^+$ mature DCs were observed to be exclusive in the tumor stroma. Notably, the density of mature DCs in the tumor mass was greatly reduced compared to that of $CD1a^+$ iDCs. The findings indicated that EC tissue comprised a high density of iDCs in the tumor bed and a low density of mature DCs in the tumor stroma (1). Nishimura et al. also evaluated 80 EC patients who underwent surgery without preoperative treatment and found that DC-$Lamp^+$ DCs are predominantly located in the peritumor (2). Tumor-infiltrating $CD8^+$ T cells ($CD8^+$ TILs) were found to be related with a favorable prognosis, and the density of DC-$Lamp^+$ DCs was associated with the density of $CD8^+$ TILs (2). Although the above advance has been made, the subsets of those intratumoral DCs in EC should be assessed.

Advances in Dendritic Cell-Based Esophageal Cancer Vaccines

DC-based vaccines are considered an alternative therapeutic approach to treat EC. For EC vaccines, the sources of tumor-associated antigens (TAAs) consisted of the tumor cell lysate, 18E7, and melanoma-associated antigen 3 (MAGE-A3). Gholamin et al. used monocyte-derived DCs to generate EC vaccine (3). In their study, the DCs (culture of monocytes with GM-CSF and IL-4) were transfected with total tumor RNA or normal RNA. Then, T cells were co-cultured with tumor RNA-transfected DCs and normal RNA- transfected DCs, respectively. Only DCs loaded with tumor RNA resulted in the induction of T-cell cytotoxicity and IFN-γ production. These findings offer important preliminary information to develop a total tumor RNA-loaded DC vaccine for EC treatment (3). Wu et al. also generated a DC-based vaccine by HPV18E7 gene-pulsing cord blood $CD34^+$ stem cell-derived DC, since human papillomavirus (HPV)-associated EC remains a malignancy with high incidence worldwide (4). They found that HPV18E7 gene transfection did not alter the morphology and phenotypes of mature DCs, while HPV18E7-DCs expressed moderate 18E7 protein. Importantly, the specific T cytotoxicity was significantly higher than that in controls, indicating the possibility of a DC-based vaccine therapy in HPV-associated EC. MAGE-A3 is a tumor-associated antigen target for the generation of anti-tumor DC vaccines against EC. Calreticulin (CALR) is a ligand for nascent major histocompatibility (MHC) class I and supports the induction of DC maturation. Adenovirus (Ad)-transduced DCs that overexpressed MAGE-A3 and CALR demonstrated mature phenotypes (5). Furthermore, the DCs also produced a higher amount of IL-12 and a lower level of IL-10. CALR/MAGE-A3-pulsing DCs activated $CD8^+$ CTLs, which killed MAGE-A3-positive EC cells. These data indicated the potential of CALR/MAGE-A3-pulsing DCs to induce MAGE-A3-specific anti-tumor immune responses in EC (5). However, the identification of novel tumor-associated/specific antigens to develop DC-based EC vaccines is imperative.

Advances in Dendritic Cell-Based Therapy in Esophageal Cancer

Interestingly, the combination therapy of pemetrexed and monocyte-derived DCs (GM-CSF plus IL-4) in the treatment of EC patients who previously failed first-line and second-line treatment regimens could lead to a partial response in a clinical study (6). The patients did not show grade 4 toxicity. The combination therapy of pemetrexed with DCs as a third-line treatment was effective as well as well tolerated in advanced EC patients (6). Immunotherapy using cytokine-induced killer (CIK)

cells or a combination of DCs and CIK cells (DC-CIK cells) showed promising clinical outcomes for treating EC. Of note, several groups systematically evaluated the safety and efficacy of CIK/DC-CIK treatment as an adjuvant therapy in the treatment of EC. These meta-analyses indicated that the combination of CIK/DC-CIK immunotherapy with chemotherapy was safe, prolonged the survival time, enhanced immune responses, and improved the treatment efficacy for EC (7, 8).

ADVANCES IN DENDRITIC CELL-BASED IMMUNOTHERAPY IN GASTRIC CANCER

GC remains the fifth most common cancer and the third deadliest cancer worldwide. Chemotherapy, surgery, and radiotherapy are treatment regimens for GC. However, its 5-year survival rate is 20%–30%. Recently, more and more attention is paid to DC-based immunotherapy.

Dendritic Cells in Gastric Cancer

The infiltration of $CD83^+$ DCs (mature DCs) into the tumors are related with GC development. By the analysis of 55 patients with GC, cytoplasmic TGF-β1 expression was observed in tumor cells from 76.4% of cases, and low $CD83^+$ DCs in the tumor border was found in 100% of tumors with TGF-β1 expression (9). TGF-β1 expression was associated with low $CD83^+$ DCs in 100% of the cases. The density of $CD1a^+$ and $CD83^+$ intratumoral DCs was negatively associated with lymph node metastases. Patients with a low density of tumor-infiltrating $CD83^+$ DCs had shorter survival rates, Therefore, tumor-infiltrating DCs might be important in initiating the primary anti-tumor immune response. In patients with resectable GC, the density of intratumoral DCs and TGF-β1 expression could be a useful predictor of prognosis (9). Kashimura et al. found a decrease in the number of $CD83^+$ DCs and an increase in the density of $Foxp3^+$ regulatory T cells (Tregs) in the primary tumor and metastatic lymph nodes (10). Patients with a low number of mature DCs and a high number of Tregs in primary lesions showed a poor prognosis. The number of $CD83^+$ mature DCs in negative lymph nodes was an independent predictor of prognosis in patients with metastatic lymph nodes (10).

Both plasmacytoid DCs (pDCs) and Tregs are immuno suppressive cells in the tumor microenvironment (TME) of GC. By the analysis of a cohort of 64 GC patients without preoperative chemotherapy, $BDCA2^+$ pDCs and $Foxp3^+$ Tregs were increased in tumors and peritumors compared to normal ones, and $BDCA2^+$ pDCs were positively associated with $Foxp3^+$ Tregs (11). Gastric microbiota dysbiosis might be involved for GC occurrence and progression. The composition, diversity, and function of gastric mucosal microbiota had more significant changes in tumors than those in normal and peritumoral tissues. Several non-abundant genera such as *Selenomonas* and *Stenotrophomonas* were positively associated with pDCs and Tregs, respectively, whereas *Gaiella* and *Comamonas* were inversely associated with pDCs and Tregs, respectively. Gastric mucosal microbiota might regulate the frequency of pDCs and Tregs, which might provide insights into establishing new approaches targeting gastric microbiota (11). Liu et al. also found that both $ICOS^+$ $Foxp3^+$ Treg cells and pDCs in peripheral blood and tumor tissues could predict poor clinical outcome in GC patients (12). Tregs and $ICOS^+$ Tregs are located mainly in tumor tissue, whereas pDCs are present in peritumoral tissue (13). Huang et al. also confirmed that pDCs were positively associated with $ICOS^+$ Tregs in peripheral blood and peritumoral tissue from GC patients (13). All these implied that pDCs might get involved in recruiting $ICOS^+$ Tregs *via* the ICOS-L/ICOS pathway and both contributed to the immunosuppression in the GC TME.

In the peripheral blood, patients with GC were identified to have a substantially higher percentage of peripheral pDCs and $CD1c^+$ myeloid DCs (mDC2) (14). Moreover, there was a trend of elevated circulating pDCs toward advanced stages and lymph node metastasis, while there were no differences in blood mDC2s among the various groups, suggesting that blood pDCs were a prognostic factor in GC patients and emphasizing the pivotal role of pDCs in the progression of GC (14). The phenotype and function of mDCs in the tumor mass from GC patients warrant further investigation.

Advances in Dendritic Cell-Based Gastric Cancer Vaccines

Cancer stem cells (CSCs) and GC cell lines were used for antigen targets for DC-based vaccines. CSCs are a small subset of cancer cells in solid tumors, which participate in tumor initiation, progression, recurrence, metastasis, and resistance to current treatments. Bagheri et al. generated DCs by culturing monocytes with GM-CSF plus IL-4 (GM/IL-4 DCs) while maturing them by the cytokine mixture (TNF-α, IL-1β, IL-6, and PEG2). Matured DCs pulsed with CSC mRNA induced Ifng gene expression in T cells (15). The cytotoxic activity of primed T cells with CSC antigens was significantly enhanced compared to control groups. Thus, the DCs loaded with CSC mRNA that elicited tumor-specific T-cell immune responses might be a potential DC-based vaccine for GC patients (15).

The cell lysate antigen of SGC-7901 cells is another option for DC-based GC vaccines. The secondary lymphoid tissue chemokine (SLC) is a chemokine in the T-cell zones of the spleen and lymph nodes as well as in endothelial venules. Human GM/IL-4 DCs were transduced with Ad-bearing SLC (Ad-SLC) and the recombinant Ad bearing the beta-galactosidase gene, respectively (16). Then, the DCs were loaded with the cell lysate antigens of SGC-7901 cells and co-cultured with autologous T cells. Transduction with Ad-SLC led to DC maturation and enhanced the chemotaxis function of DCs. Moreover, Ad-SLC transduction also led to upregulated RANTES expression and a similar level of IL-10 and IL-12p70 in DCs. The co-culture of autologous T cells with SGC-7901 cell lysate-loaded SLC^+ DCs led to a significantly promotion in the proliferation of autologous T cells and a strong cytotoxicity against SGC-7901 cells. Collectively, Ad-SLC enhanced DC maturation and, in turn, increased T-cell chemotaxis and elicited a specific GC-specific immune response. Thus, recombinant Ad-SLC-transduced DCs might be exploited as an adjuvant to induce an effective anti-GC cellular immunity (16).

Advances in Dendritic Cell-Based Therapy in Gastric Cancer

Cord blood-derived DCs and CIK (CB-DC-CIK) were clinically exploited for the treatment of GC (17). Patients with advanced GC were treated with CB-DC-CIK plus chemotherapy. No serious adverse effects were observed in patients with GC after the application of CB-DC-CIK. The combination therapy led to a significant increase in the overall disease-free survival (DFS) rate in comparison to chemotherapy alone. Furthermore, the percentage of $CD4^+$ T cells, NK cells, and NKT cells and the levels of IFN-γ, TNF-α, and IL-2 were significantly increased in the experimental group. Thus, the combination therapy of CB-DC-CIK and chemotherapy was safe and effective for the treatment of patients with advanced GC (17).

ADVANCES IN DENDRITIC CELL-BASED IMMUNOTHERAPY IN HEPATOCELLULAR CARCINOMA

HCC is one of the most common cancers worldwide with limited therapeutic strategies due to HCC-induced immunosuppression. The 5-year survival rate is less than 20%. Recently, a growing body of studies supported that the function of DCs in HCC was impaired.

Dendritic Cells in Hepatocellular Carcinoma

Huang et al. performed the weighted gene co-expression network analysis of DCs in HCC patients in public datasets (18). They observed that a high level of DC infiltration was correlated with poor prognosis. By the analysis of a TCGA cohort, more than 50% of the DC-related genes were markedly differentially expressed between HCC and normal samples. There were 17 differentially expressed genes (DEGs) significantly related with overall survival (OS) (18), implying that intratumoral DC might get involved in HCC progression.

Human $CD14^+$ $CTLA\text{-}4^+$ regulatory DCs ($CD14^+$ DCs) were identified, which accounted for approximately 13% of peripheral blood mononuclear cells (PBMCs) (19). $CD14^+$ DCs significantly suppressed the T-cell response *in vitro via* indoleamine-2,3-dioxygenase (IDO) and IL-10, which also expressed high levels of CTLA-4 and PD-1. CTLA-4 was essential for IL-10 and IDO production. These data indicated one underlying mechanism by which $CD14^+$ DCs elicited systemic immunosuppression in HCC, participating in HCC progression. This might also offer a previously unrecognized target of HCC immunotherapy (19). PD-1 expressed on DCs has a regulatory role in the anti-tumor immune response. Lim et al. observed PD-1 expression on all DC subsets ($CD1c^+$ mDC2, $CD141^+$ mDC1, and pDCs) in the peripheral blood of HCC patients (20). However, PD-1 was weakly expressed in mDC1 but not mDC2 and pDCs in the steady state. This finding provided a new insight into the mechanisms for PD-1-targeted cancer immunotherapies.

The number of tumor-infiltrating Tr1 cells ($CD4^+$ $FoxP3^-$ $IL\text{-}13^-$ $IL\text{-}10^+$) was associated with tumor-infiltrating pDCs, which enhanced Tr1-produced IL-10 *via* ICOS-L when exposed to tumor-derived factors. The Tr1 cells were characterized in the tumors from individuals with HCC or liver metastases from CRC, which expressed CD49b and the lymphocyte activation gene 3 (LAG-3). Moreover, Tr1 had a strong suppressive activity of T-cell responses in an IL-10-dependent way (21). These findings suggested a role of pDC-expressing ICOS-L in enhancing intratumoral Tr1-mediated immunosuppression in human HCC (21).

Some factors in the TME could modify the function of tumor-infiltrating DCs, such as the liver X receptor (LXR), IL-37 and alpha-fetoprotein (AFP). Sterol metabolism is linked to innate and adaptive immunity *via* LXR signaling. Human tumors express LXR ligands that reduced CCR7 expression on mature DCs and, in turn, their migration to lymphoid organs. $CD83^+CCR7^-$ DCs within the human HCC tumor could be detected (22). Thus, these findings indicated a new mechanism of tumor immune escape involving the products of cholesterol metabolism (22). Targeting this pathway could restore anti-tumor immunity in individuals with HCC. In GC, SLC could activate DCs by upregulating CCR7 and CD83 expression. The function of SLC should be addressed in the context of HCC. IL-37 is a tumor suppressor in various cancers. The amount of IL-37 was positively correlated with $CD1a^+$ iDC infiltration in HCC specimens (23). The survival rates of patients with both a high amount of IL-37 and a high number of iDCs were significantly enhanced compared with those of patients with low levels of IL-37 and iDCs. HCC cells that overexpressed IL-37 recruited more DCs through secreting specific chemokines. Moreover, IL-37 indirectly upregulated the expressions of MHC class II molecules, CD86 and CD40, on DCs and, in turn, increased T-cell-mediated anti-tumor immunity by inducing DCs to producing cytokines. Thus, DCs were responsible for IL-37-induced anti-tumor immunity in HCC, which might help develop novel cancer immunotherapeutic approaches (23). AFP is an oncofetal antigen and considered as the most common serum biomarker. HCC patients with high amounts of serum AFP showed a lower ratio of myeloid/plasmacytoid DCs in comparison to patients with low serum AFP as well as healthy donors (24). Although the isoforms of cord blood-derived normal AFP (nAFP) and HCC tumor-derived AFP (tAFP) only vary at one carbohydrate group, low amounts of tAFP, but not nAFP, markedly suppressed monocyte-derived DC differentiation. Importantly, tAFP-educated DCs expressed reduced levels of DC maturation markers and maintained a monocyte-like morphology and therefore failed to elicit potent T-cell proliferative responses. Collectively, novel immunotherapeutic strategies that target tAFP might be crucial to improve immune responses and clinical outcomes (24).

Advances in Dendritic Cell-Based Hepatocellular Carcinoma Vaccines

AFP is a promising tumor-associated antigen target for the generation of DC-based vaccines. An AFP-derived peptide-

loaded DC vaccine could promote an AFP-specific anti-tumor immune response in patients with HCC, and the clinical trial results showed these vaccine-induced $CD8^+$ T-cell responses (25). In addition, AFP-derived peptide-pulsed DCs enhanced NK cell activation and decreased the frequency of Treg cells in vaccinated HCC patients. Various antigen-loading approaches are related with the efficacy of DC-based vaccines. The recombinant adeno-associated virus (rAAV) is one safe virus vector in gene therapy, since the wild-type virus does not cause human disease. The study by Zhou et al. supported the superiority of the rAAV-AFP-engineered DC vaccine over the cancer cell lysate-loaded DC vaccine (26). Both rAAV-AFP-loaded and cancer cell lysate-loaded DCs led to DC maturation. However, rAAV-AFP-loaded DCs induced T-cell responses more potent than cancer cell lysate-pulsed DCs. Thus, the DCs loaded with rAAV-AFP were more effective than the DCs loaded with the tumor cell lysate, which might be exploited for the development of DC-based vaccines in AFP^-positive HCC (26).

Heat shock protein 70 (HSP70) is highly expressed in HCC, being one of HCC-associated antigens. A clinical phase I/II trial investigated the safety and efficacy of HSP70 mRNA-pulsing DC vaccine that was as a postoperative adjuvant therapy after tumor resection. There were no side events specific to the mRNA-pulsing DC vaccine. Similar DFS between the DC and control groups was observed. However, the OS of the DC group was significantly prolonged compared to that of the control group. Collectively, HSP70 mRNA-pulsing DC vaccines were safe as an adjuvant therapy (27).

Exosome is a subtype of membrane vesicle released from the cells or directly from the plasma membrane. DC-derived exosomes (DEXs) become a new class of vaccines for cancer immunotherapy and thus provide a cell-free vaccine for HCC immunotherapy. Li et al. found that GM/IL-4 DCs were loaded with recombinant rAAV/AFP and high-purity DEXs were generated. DEXs were found to be effective at inducing antigen-specific CTLs, demonstrating anti-tumor immunity against HCC (28). Moreover, DEX-sensitized DC precursors were likely to be more effective at triggering an MHC class I-restricted CTL response, allowing DCs to make full use of the minor antigen peptides and, in turn, maximally promoting specific immune responses against HCC. Thus, DEXs might replace mature DCs to act as cancer vaccines (28).

The tumor cell line lysate provides whole tumor antigens for the generation of HCC vaccines. Thirty HCC patients were divided into 2 groups in a clinical study. Group 1 (15 patients) received intradermal vaccination with mature DCs loaded with a liver tumor cell line lysate, while group 2 received supportive treatment (29). The patients in group 1 showed enhanced $CD8^+$ T-cell responses and improved OS. Thus, DC vaccination in advanced HCC patients was safe and well tolerated (29). However, the efficacy of this approach is not most satisfactory. Identifying new HCC-associated/specific antigens is quite urgent for developing DC-based HCC vaccines.

Another clinical trial investigated the safety and efficacy of the combination therapy of an autologous tumor lysate-loaded DC vaccine with *ex vivo* activated T-cell transfer (ATVAC) in a postoperative adjuvant therapy (30). Ninety-four patients with invasive HCC were enrolled, and 42 had the ATVAC after surgery. Compared with surgery alone, surgery plus ATVAC significantly enhanced the recurrence-free survival (RFS) and OS. There were no adverse events of grade 3 or more. Thus, the combination therapy of postoperative DC vaccine with T-cell adoptive transfer might be an effective and feasible treatment for preventing recurrence in HCC patients (30).

Although PD-1 blockade therapy got many successes and opportunities in various cancers, anti-PD-1 monoclonal antibodies still confronted several challenges. Shi et al. generated a nanobody (Nb) against PD-1 (PD-1 Nb20) to solve these challenges (31). The combination treatment of PD-1 Nb20 with the tumor-specific DC/tumor-fusion cell (FC) vaccine was observed to effectively improve the *in vitro* cytotoxicity of $CD8^+$ T cells to kill HCC HepG2 cells. In addition, the combination therapy was approved to be potent in a mouse tumor model. Collectively, these findings indicated that the combination therapy of PD-1 Nb20 with DC/tumor-FC vaccines greatly improved CTL capacity, offering a promising strategy for tumor patients who were not sensitive to anti-PD-1 therapy (31).

Advances in Dendritic Cell-Based Therapy in Hepatocellular Carcinoma

DC-CIK immunotherapy is also found to be safe and effective in the treatment of HCC patients. In a clinical cohort of 67 HCC patients treated with DC-CIKs (32), 29 patients displayed stable disease (SD) with none showing complete remission and five undergoing partial remission. DC-CIK cells had a great effect on the growth cycle of HepG 2 cells, mainly upregulating the gene expression of BAX (a pro-apoptotic protein) and downregulating the activity of proliferating cell nuclear antigen (PCNA, marker of the cell proliferation status). Thus, the co-culture of DCs and CIK cells inhibited the proliferation and migration of HCC cells by the regulation of PCNA and BAX. This strategy might be an effective method to treat advanced HCC (32). Yang et al. also found that DC-CIKs significantly enhanced the apoptosis ratio by increasing caspase-3 protein expression and reducing PCNA expression against liver cancer stem cells (LCSCs) (33). Su et al. showed that the combination of DC-CIK immunotherapy and transcatheter arterial chemoembolization (TACE) or TACE plus local ablation therapy improved 1- and 2-year OS and provides a better quality of life for patients with HCC clinically (34).

OK-432, a streptococcus-derived tumor suppressor, can activate DCs and, in turn, improve anti-tumor activity. In a clinical study, GM/IL-4 DCs were launched and stimulated with OK-432 (35). Two groups of HCC patients were treated with transcatheter hepatic arterial embolization (TAE) alone and TAE plus OK-432-matured DC transfer, respectively. OK-432 induced DC maturation, which expressed high levels of a homing receptor, preserved phagocytic capacity and markedly improved cytokine production as well as tumoricidal activity. The infusion of OK-432-matured DCs to HCC patients was safe

and feasible. In addition, the combination therapy of TAE with OK-432-activated DCs prolonged the RFS of patients compared with the TAE alone group. Thus, these findings indicated that the combination therapy of a DC-based immunotherapeutic approach with locoregional treatments benefited HCC patients (35).

The efficacy of the combination therapy of DC-CIKs pretreated with pembrolizumab (anti-PD-1) against HCC was also clinically investigated (36). The PD-1 blockade further improved the anti-tumoral effects of DC-CIKs, leading to a survival benefit. The blockade of PD-1 promoted the infiltration of immune cells into tumors. DC-CIKs and anti-PD-1 were more effective than DC-CIKs alone (36). Thus, blocking the PD-1/PD-L1 signaling pathway in DC-CIK cells prior to infusion is a promising treatment strategy against HCC.

ADVANCES IN DENDRITIC CELL-BASED IMMUNOTHERAPY IN PANCREATIC CANCER

PC is a challenging disease with a high mortality rate that might be associated with defective immune function. It has been reported that the function of DCs is impaired in PC patients. More and more evidence supported that blood mDCs and pDCs in PC showed decreased numbers and impaired functionality.

Dendritic Cells in Pancreatic Cancer

Pancreatic ductal adenocarcinoma (PDAC), the most common PC, is recognized to be a very aggressive tumor type with very high mortality. PDAC had decreased levels of blood mDCs and pDCs and an enhanced apoptosis of these DCs (37). Enhanced levels of PGE2 and CXCL8 were observed in subjects with PDAC and chronic pancreatitis. After tumor resection, the amounts of these inflammatory factors were partially recovered in PDAC, while the percentages of DCs were impaired in most of these patients approximately 12 weeks after tumor resection. These findings proved that solid PC, including PDAC, systemically altered blood DCs. The impaired DCs might not be tumor specific since chronic pancreatitis could also lead to similar results (37). Moreover, PDAC patients with long survival had significantly increased frequency of blood DCs in comparison to patients with short survival. Thus, inflammation contributed to the impairment of the blood mDCs and pDCs, while the preservation of the blood DCs might control the disease in PDAC patients (37). Furthermore, the blood DCs showed a partial maturation phenotype with a significantly increased expression of CD40, CD83, B7-H3, PD-L1, CCR6, and CCR7 and a decreased expression of DCIR and ICOSL in PDAC patients, which were partially induced by PGE2 (38). The alternations led to an impaired function of DCs. However, chronic pancreatitis also led to a similar partial mature phenotype of DCs as in PDAC. Thus, it was the systemic inflammation that contributed to semi-mature DCs in PDAC patients *via* PGE2. Diminishing the inflammation to preserve functional blood DCs could help control the disease and improve survival (38). A similar finding was observed in the other cohort of patients with PC, in which the frequency of the circulating mDCs in the patients was significantly reduced compared to that in healthy donors. There was no obvious difference in the blood mDCs between the patients with distant organ metastasis and locally advanced PC. The patients with more blood mDCs survived longer than patients with less (39, 40).

The transition of chronic pancreatic fibroinflammatory disease to tumorigenesis is a paradigm linking inflammation to carcinogenesis. The lipopolysaccharide (LPS) treatment facilitated pancreatic tumorigenesis (41). Blocking the MyD88-independent TRIF pathway resulted in protection, while blocking the MyD88-dependent pathway unexpectedly exacerbated pancreatic inflammation and tumor progression (41). Of note, DCs mediated MyD88 suppression, which induced a pancreatic antigen-restricted Th2 cell response and promoted the transition from pancreatitis to neoplasia, indicating that DCs played a critical role in pancreatic carcinogenesis and neoplastic transformation through promoting the DC-Th2 axis (41).

Tumor-derived exosomes (TDXs) can transfer miRNAs to recipient cells in the TME, promoting tumor invasion and metastasis. In context of PC, TDX miRNAs inhibited the mRNA expression of DCs and induced immune tolerance (42). Mechanistically, the miR-212-3p from PC-secreted exosomes downregulated regulatory factor X-associated protein (RFXAP) and, in turn, decreased MHC class II expression. In addition, one clinical study showed that miR-212-3p was inversely correlated with RFXAP in PC tissue. However, the functions and mechanisms of RFXAP in tumors warrant future investigation (42). miRNA-146a can also modulate DCs. The culture of human $CD14^+$ monocyte-derived DCs by a highly metastatic human PC cell line BxPC-3 culture media (BxCM) resulted in decreased DC differentiation and antigen- presentation function (43). BxCM-treated DCs upregulated miRNA-146a, the inhibition of which partially rescued the BxCM-induced impairments in DC differentiation and function (43).

In PDAC, Treg cells extensively interacted with tumor-associated mDCs and reduced the expression of costimulatory molecules that was required for the activation of $CD8^+$ T cells (44). Resultantly, $CD8^+$ TILs showed impaired effector function when Treg cell ablation was combined with DC depletion. These findings indicated that Treg TILs could promote immune tolerance by inhibiting intratumoral DC maturation (44). Trefoil factor 2 (TFF2) from PC cells, a chemokine/cytokine, may attract iDCs and affect the initial stage of DC maturation, thereby contributing to the induction of immune tolerance against PC (45). As a PC-derived factor, regenerating islet-derived protein 3A (Reg3A) could inhibit the differentiation and maturation of tumor-infiltrating DCs *via* the Reg3A-JAK2/STAT3 signaling pathway (46). HSP70 contributed to cell survival and tumor progression. HSP70 inhibition in DCs may emerge as a novel therapeutic strategy against pancreatic cancer (47).

Advances in Dendritic Cell-Based Pancreatic Cancer Vaccines

Various PC cell lines (Panc-1, KP-1NL, QGP-1, and KP-3L) were used to load DCs to generate DC-based vaccines against PC (48). The cytotoxicity against tumor cells induced by GM/IL-4 DCs fused with QGP-1 (DC/QGP-1) was very low, while DCs loaded with another PC cell line elicited a high cytotoxicity of PBMCs. DC/QGP-1 upregulated Treg expansion in comparison with DC/KP-3L (48). Moreover, the co-culture of DC/QGP-1 with PBMCs also resulted in an increase in the amount of IL-10 compared with that with DC/KP-3L. Thus, the cytotoxicity induced by DCs loaded with PC cell lines was variable among the cell lines. DC/QGP-1-mediated reduced cytotoxicity might be associated with IL-10 production and Treg expansion (48).

Various antigen-pulsing approaches have been investigated (49). Both tumor RNA and tumor fusion hybrid cells provide whole tumor antigens for the generation of DC-based vaccines. Chen et al. compared the anti-tumor immunity elicited by DC-tumor hybrids (patient-derived PC cells and DCs were fused) and DC-tumor RNA (autologous DCs were transfected with primary PC cell-derived total RNA) (49). They found that both RNA transfection and hybrid techniques could elicit tumor-specific CTL responses. However, DCs loaded with total tumor RNA led to an increase in the frequency of activated CTLs and $CD4^+$ T cells compared to DC-tumor hybrids. Moreover, DCs pulsed with tumor RNA induced stronger autologous tumor cell lysis. Thus, DC-tumor RNA was superior to DC-tumor hybrids in stimulating PC-specific CTL responses (49). Pancreatic CSCs participated in the malignant behaviors of PC, such as immune escape. Therefore, the development of immunotherapy-targeting pancreatic CSCs might contribute to PC treatment. Yin et al. cultured Panc-1 cells under sphere-forming conditions to enrich pancreatic CSCs (50), which expressed low levels of HLA-ABC and CD86. DCs loaded with Panc-1 CSC lysates elicited cytotoxicity against Panc-1 CSCs and parental Panc-1 cells. Thus, a CSCs-DC-based vaccine might be a promising approach for the treatment of PC (50).

Wilms' tumor 1 (WT1) has been used to generate a DC-based vaccine against PC. Three types of MHC class I and II-restricted WT1 epitopes have been identified. A clinical phase I trial investigated safety, clinical responses, and WT1-specific T-cell immune responses for DCs loaded with a mixture of three types of WT1 peptides (DC/WT1-I/II), in combination with chemotherapy (51). The combination therapy of DC/WT1-I/II and chemotherapy was well tolerated. In addition, the combination therapy of DC/WT1-I/II resulted in a significant increase in the percentage of WT1-specific IFN-γ-producing $CD4^+$ T cells. Among the PDAC patients vaccinated with DC/WT1-I/II, 4 of the 7 patients showed WT1 peptide-specific delayed-type hypersensitivity (DTH). Improved OS and PFS were detected in the WT1-specific DTH-positive patients in comparison with the negative-control patients. More importantly, all three PDAC patients with strong DTH had a median OS of 717 days. Thus, WT1-specific immune responses induced by the combination therapy of DC/WT1-I/II with chemotherapy might be related with disease stability in advanced PC (51). In addition, seven patients with PC who received the combination therapy of DC/WT1-I/II and chemotherapy showed significantly increased expressions of HLA-DR and CD83 on DCs (52). Therefore, the enhanced expressions of HLA-DR and CD83 might be prognostic markers of longer survival in patients with advanced PC who underwent chemoimmunotherapy (52).

Mesothelin (MSLN) is a potential candidate as a molecular target for PC immunotherapy. GM/IL-4 DCs were adenovirally transduced with the full-length MSLN gene (DC-AxCAMSLN) (53). Target cells were PC cell lines (PK1, CfPAC1, AsPC1) transduced with the MSLN gene. DC-AxCAMSLN stimulated MSLN-specific CTLs, which resultantly killed target cells. Both $CD8^+$ T cells and $CD4^+$ T cells sorted from these CTLs expressed significant levels of IFN-γ. In addition, the DC-AxCAMSLN also elicited a potent MSLN-specific cytotoxic activity against PC cell lines endogenously expressing MSLN (53). Therefore, the findings suggest the potential of developing DC-based vaccines using genetically modified DCs expressing MSLN.

Mucin 1, an epithelial cell glycoprotein, is aberrantly overexpressed in many cancers, including PC, providing an ideal TAA target for immunotherapy. GM/IL-4 DCs were generated and matured with TNF-α. Mature DCs could be transfected with amplified mucin 1 mRNA efficiently (54). The mucin 1-loaded DCs were robustly effective in stimulating mucin 1-specific CTL responses, which could only recognize and kill HLA-A2-restricted mucin 1-expressing PC and other target cells, providing a preclinical rationale for DC-based vaccines using mucin 1 as a target (54). The mucin 1 peptide epitope was identified. In a clinical phase I trial, TNF-α-stimulated GM/IL-4 DCs were pulsed with the mucin 1 peptide epitope (55). Mucin 1-positive patients with recurrent lesions or metastasis after surgery received DC vaccines intradermally for three or four vaccines. The patients did not show severe adverse events related with the vaccines or an autoimmunity symptom. Approximately 2 out of 7 patients expressed IFN-γ and granzyme B. The administration of mucin 1-peptide-pulsed DCs was well tolerated and able to induce a mucin 1-specific immune response in advanced PC patients. Further studies were needed to improve tumor rejection responses (55). Mucin 4 and survivin are another two TAA targets for DC-based vaccines. DCs co-transfected with two mRNAs encoding mucin 4 and survivin induced more potent CTL responses against PC target cells in comparison with the DCs transfected with a single mRNA (56). These findings provided a rationale for the clinical studies of DC vaccines encoding multiple TAA epitopes (56).

pBSDL-J28 is a glycoform of bile salt-dependent lipase (BSDL) in normal human pancreatic juices, which is not expressed in nontumoral pancreatic tissues and cells. Of note, pBSDL-J28 induced DC maturation and these DCs kept their full ability to internalize antigens, making this maturation atypical. In addition,

the allogeneic pBSDL-J28-treated DCs induced proliferative responses of lymphocytes. DCs loaded with the pBSDL-J28 C-terminal glycopolypeptide and stimulated with CD40L elicited T-cell proliferation (57). Therefore, pBSDL-J28 might be a promising TAA target for DC-based vaccine against PC.

Three distinct HLA-A2-restricted peptide epitopes were identified: human telomerase reverse transcriptase (hTERT, TERT572Y), survivin (SRV.A2), and carcinoembryonic antigen (CEA; Cap1-6D). Mehrotra et al. used these three peptide-loaded DCs in conjunction with TLR-3 agonist poly-ICLC to treat PC patients with metastatic or locally advanced unresectable PC in a clinical study (58). This treatment was well tolerated. An MHC class I tetramer analysis indicated a potent induction of antigen-specific T cells in three PC patients with SD. Thus, vaccination with peptide-pulsed DCs plus poly-ICLC was safe and elicited detectable tumor specific T-cell responses in patients with advanced PC (58).

Chemotherapy enhances the efficacy of DC-based vaccines for PC. Gemcitabine is a first-line chemotherapeutic drug for advanced PC. The medium of gemcitabine-treated PC cells stimulated DC maturation (59). The co-culture of gemcitabine-treated DCs with autologous T lymphocytes resulted in T-cell proliferative responses and the induction of specific anti-tumor CTLs. Enhanced DC maturation might be associated with the enhanced level of HSP70 by gemcitabine. Thus, gemcitabine changed the immunogenicity of tumor cells and enhanced the efficacy of DC-based vaccines for PC (59). In addition, gemcitabine inhibited the growth of PC cells by inducing apoptosis and upregulating Fas expression. Thus, gemcitabine sensitized PC cells to the CTL antitumor response, which was related with the upregulation of Fas on PC cells (60).

Advances in Dendritic Cell-Based Therapy in Pancreatic Cancer

DC-CIK immunotherapy has widely used in treating PC patients. Both chemotherapy drugs and miRNA-depleted TDXs could enhance the efficacy of DC-CIK immunotherapy. Zhang et al. conducted a meta-analysis of 14 clinical trials with 1,088 PC patients to compare DC-CIK immunotherapy plus chemotherapy (combined therapy) with chemotherapy alone (61). The combination therapy showed advantages over chemotherapy alone. The percentages of $CD3^+$ T cells, $CD4^+$ T cells, and $CD3^+CD56^+$ T cells as well as the cytokine levels of IFN-γ were significantly increased by the combined therapy. Moreover, the combination of DC-CIK immunotherapy and chemotherapy enhanced the PC patients' survival time, being an effective treatment strategy (61). TDXs might be potential candidates for tumor vaccines since they have numerous immune-regulating proteins. TDX-derived miRNAs, however, elicit immune tolerance. Que et al. depleted miRNA from PC-derived exosomes and retained 128 proteins, including several immune-activating proteins (62). Exosomes were depleted with miRNA-activated DC/CIKs and resultantly induced a higher cytotoxic capacity of CIKs than LPS and exosomes. Therefore, an miRNA-depleted exosome could be a promising agonist for stimulating DC/CIKs against PC (62).

The iDCs plus OK-432 in PC patients were administrated by preoperative endoscopic ultrasound-guided fine-needle injection (PEU-FNI) (63). The clinical trial included two groups, the DC group with iDC injection and non-DC group without iDC injection (non-DC group). The patients did not show severe toxicities in the DC group, except for one transient grade 3 fever. A similar incidence of postoperative complications was detected between the two groups (63). In the DC group, more $CD83^+$ cells presented in the regional lymph nodes and $Foxp3^+$ cells in the regional and distant lymph nodes. The two PC patients from the DC group with one being stage IV survived over 5 years without requiring adjuvant therapy (63). Thus, PEU-FNI was safe and feasible. Further investigation was warranted to confirm and enhance anti-tumor responses.

A direct injection of DCs without loading TAAs into tumors after chemotherapy-mediated apoptosis is more feasible. Zoledronate is the most potent and long-acting bisphosphonate, which is intended for clinical use. Hirooka et al. studied the safety, feasibility, and efficacy of one immunotherapy regimen including the combined intratumoral injection of zoledronate-treated DCs (Zol-DCs), gemcitabine, and T cells in locally advanced PC (64). Approximately 7 out of 15 patients underwent an SD, and the majority of the patients mounted long-term clinical responses. Additionally, the $CD8^+$/Treg ratio was significantly increased in SD patients after treatment. Before treatment, the patients with a neutrophil/lymphocyte ratio (NLR) lower than 5.0 underwent significantly longer survival. Thus, the combination therapy of Zol-DCs, systemic T cells, and gemcitabine might show a synergistically therapeutic effect on locally advanced PC. The combined immunotherapy might benefit patients with PC if precise biomarkers were used (64).

ADVANCES IN DENDRITIC CELL-BASED IMMUNOTHERAPY IN COLORECTAL CANCER

CRC remains the second most deadly cancer in Western countries. Chronic inflammation is a key component in the development and progression of CRC. Defects in DC recruitment, maturation, and cytokine release are a hallmark of the CRC strategy to escape immune surveillance.

Dendritic Cells in Colorectal Cancer

The analysis of a cohort of CRC patients revealed a high $CD1a^+$/$DC\text{-}LAMP^+$ tumor-infiltrating DC ratio, indicating that there were more iDCs than mature DCs in the CRC tumors (65). Moreover, there were decreased mature DCs in the front and main tumor mass (66), while increased mature DCs in both of these locations were correlated with the metastases in the nearby

lymph nodes. Of note, increased amounts of mature DCs in the tumor was correlated with the invasiveness of the tumor and especially with the metastasis to the surrounding lymph nodes (66). Gai et al. also showed that increased FOXP3$^+$ Tregs and decreased CD11c$^+$ mDC infiltration had a strong prognostic significance in CRC (67). Unlike FOXP3$^+$ Tregs, the frequency of CD123$^+$ pDCs was lower in most CRC tumor tissues (68).

In blood, the absolute number of pDCs in CRC patients with stage III–IV patients was significantly reduced compared with controls at the pre-operative time point, while the number of mDCs in CRC patients did not show an obvious difference in comparison to that in controls (69). Interestingly, the tolerogenic antigen CD85k was expressed highly on mDCs in CRC patients. CRC cells expressed anti-inflammatory cytokines such as IL-10 and TGF-β that could modulate the DC phenotype and supported tumor escape. Resultantly, tumor-infiltrating DCs displayed impaired antigen-presenting capacity and altered the expression pattern of immune costimulatory molecules (70). Thus, these alterations seemed to be correlated to cancer progression. This knowledge might contribute to the development of more efficacious immunotherapeutic approaches (69).

Advances in Dendritic Cell-Based Colorectal Cancer Vaccines

The tumor cell line lysate is also source of TAAs that are loaded on DCs. Chen et al. generated GM/IL4DCs, which were pulsed with lysates from Colo320, SW480, and SW620 CRC cell lines, respectively (71). SW480 lysates were the most effective in stimulating DC maturation and resultingly enhancing T-cell function among the three cell lines. Thus, SW480 lysates were the most efficient in promoting autogenous T-cell-mediated antitumor immune responses (71). The limited therapeutic effect was mainly due to the low immunogenicity of TAAs, so the α-gal epitope was synthesized on the SW620 to increase TAA immunogenicity (72). The α-gal epitope is absent in humans, but natural anti-gal antibody presents in human serum in a large number. DCs were then loaded with the α-gal-expressing SW620 lysate, which stimulated CTL response and increased the frequency of natural killer T cells and CD8$^+$ CTLs. Importantly, the CTLs had increased cytotoxicity against tumor cells. Thus, this novel strategy might be an effective treatment approach for CRC patients (72).

Anterior gradient-2 (AGR2) promotes tumor growth, cell migration, and cellular transformation. GM/IL-4DCs were transduced with a recombinant Ad bearing the AGR2 gene (AdAGR2/DCs), which expressed AGR2 protein without any significant changes in DC viability and cytokine secretion compared with unmodified DCs (73). AdAGR2 transduction promoted DC maturation. More importantly, AdAGR2/DCs induced potent AGR2-specific CTLs that could kill AGR2-expressing CRC cell lines. The data indicated that AGR2 might be a potentially promising antigen target for DC-based vaccines against CRC (73).

Several TAA epitopes are used in DC-based vaccines against CRC. Kulikova et al. described an approach to induce an anti-tumor immunity in mononuclear cell (MNC) cultures from CRC patients using DNA-transfected DCs encoding the TAA epitopes of CEA, mucin 4, and the epithelial cell adhesion molecule (74). DCs loaded with polyepitope promoted MNC anti-tumor activity, tumor cell apoptosis, and the frequency of perforin$^+$ lymphocytes. Moreover, DCs loaded with polyepitope induced a CTL response that was as efficient by tumor lysate-loaded DCs. Collectively, the findings indicated that polyepitope DNA-transfected DCs were efficient at inducing an antitumor immune response (74). Thus, the DNA construct was likely to be used in DC-based vaccines against CRC.

The optimization of antigen loading is one of the strategies for enhancing the efficacy of DC-based vaccines. CRC patients with liver metastases were vaccinated with either CEA-derived peptide-loaded or CEA mRNA-transfected DCs prior to the surgical resection of the metastases in one clinical trial (75). Approximately 8 out of 11 patients were detected with CEA peptide-specific T cells in the peptide group but none out of 5 patients in the RNA group. This finding indicated that CEA mRNA transfection was not superior to CEA-peptide loading in the generation of tumor-specific immune responses in CRC patients (75).

In a clinical phase I study, patients with advanced CRC received CEA-pulsed DCs mixed with tetanus toxoid and subsequent IL-2 treatment (76). Twelve patients were recruited. There were no severe adverse effects related with the treatment in patients who received the regular 4 DC vaccine injections. Two patients underwent SD, and 10 patients showed disease progression. Approximately 2 out of 9 patients showed an increase in the proliferation of CEA-specific T cells. The CEA-specific immune response was enhanced, and a small fraction of patients benefited from the treatment (76). Thus, these data indicated that it was safe and feasible to treat CRC patients using this strategy. This treatment protocol warranted further assessment in a large cohort of CRC patients.

The monoclonal antibodies against PD-L1/PD-1 have been exploited for the clinical treatment of various tumor types with a favorable therapeutic effect. Hu et al. showed that anti-PD-L1 treatment promoted DC maturation and enhanced the functionality of the mDC1 (77). In addition, anti-PD-L1 treatment might also enhance the number of CTLs with more potent anti-tumor capacity (77). Thus, the combination therapy of DC-based vaccines and anti-PD-L1 was likely to be an effective treatment regimen for CRC patients.

The activation of CD40/CD40L can improve DC-based vaccines against GI cancer, including CRC. Human DCs were loaded with tumor cell lysates followed by the transduction of Ad-carrying human CD40L (Ad-hCD40L) (78). Ad-hCD40L transduction induced a high expression of soluble CD40L and membrane-bound CD40L in/on DCs, which elicited a potent cellular CD40/CD40L interaction among DCs, resulting in the formation of cell aggregates. Thus, the endogenous expression of membrane-bound CD40L and the stimulation of CD40L/CD40 provoked a cellular interaction, which increased the DC function. Importantly, a Th1 cytokine/chemokine expression was induced, enabling the cytotoxicity of effector cells toward

the human bile duct and colorectal and pancreatic tumor cells (78). The findings indicate a promising approach for the DC-based immunotherapy of GI malignancies by activating the CD40/CD40L signaling.

Advances in Dendritic Cell-Based Therapy in Colorectal Cancer

Several meta-analyses of clinical trials with CRC patients all showed that the combination of CIK/DC-CIK immunotherapy and chemotherapy prolonged the survival time, enhanced immune responses, and alleviated chemotherapy-mediated side effects (79–82).

PERSPECTIVE

This paper summarized DC subsets in peripheral blood as well as in the tumor from GI cancer patients (**Table 1**). Overall, DC-based vaccines consist of two main approaches: *in vitro* generated DC vaccines and *in vivo* DC-targeting vaccines (**Figure 1**). DC-based vaccines in this review paper were all *in vitro*-generated DC ones. *In vivo* DC targeting is a vaccine approach to deliver antigens directly to DCs *in vivo* using chimeric targets composed of an anti-DC receptor antibody and antigen, which were first studied by Michael Nussenzweig and Ralph Steinman (83, 84). By the immunization of the antigen linked to the anti-DEC-205 antibody, strong, potent, and broader immune responses at low

TABLE 1 | Summary of DC subsets and TAAs in GI cancer.

Tumor types	Blood	Tumor mass	Sources of TAAs for DC vaccines	DC-based therapy
EC	/	$CD1a^+$ DCs↑ DC-$Lamp^+$ DCs↓	EC cell line, 18E7, MAGE-A3	DC vaccine, chemotherapy plus DC injection, DC-CIK
GC	mDC2↑ pDCs↑	$CD83^+$ DCs↓ pDCs↑	CSCs, GC cell line	DC vaccine, chemotherapy plus CB-DC-CIK
HCC	$CD14^+$ DCs↑ $PD\text{-}1^+$ mDCs↑ $PD\text{-}1^+$ pDCs↑	$CD83^+CCR7^-$ DCs↑ pDCs↑	HCC cell line, AFP, DC-derived exosomes, HSP70	DC vaccine, DC-CIK, DC-CIK plus TACE, OK-432-DCs plus TAE, DC-CIK plus anti-PD-1
PC	mDCs↓ pDCs↓	/	PC cell line, primary tumor cells, CSCs, WT1, MSLN, mucin 1, mucin 4, survivin, pBSDL-J28, hTERT, CEA	DC vaccine, DC-CIK, Zol-DCs, and gemcitabine and T cells
CRC	mDCs→ $CD85K^+$ mDCs↑ pDCs↓	$CD1a^+$/DC-$LAMP^+$↑ pDCs↓ mDCs↓	CRC cell lines, α-gal epitope-expressing CRC cell line, AGR2, CEA, mucin 4, epithelial cell adhesion molecule	DC vaccine, DC-CIK

EC, esophageal cancer; GC, gastric cancer; CRC, colorectal cancer; PC, pancreatic cancer; HCC, hepatocellular carcinoma; DC, dendritic cell; mDC, myeloid dendritic cell; pDC, plasmacytoid dendritic cell; AFP, alpha-fetoprotein; HSP70, heat shock protein 70; CSC, cancer stem cell; CIK, cytokine-induced killer cell; TACE, transcatheter arterial chemoembolization; TAE, hepatic arterial embolization; Zol-DC, zoledronate-pulsed DC; AGR2, anterior gradient-2; CEA, carcinoembryonic antigen. ↓decrease; ↑increase.

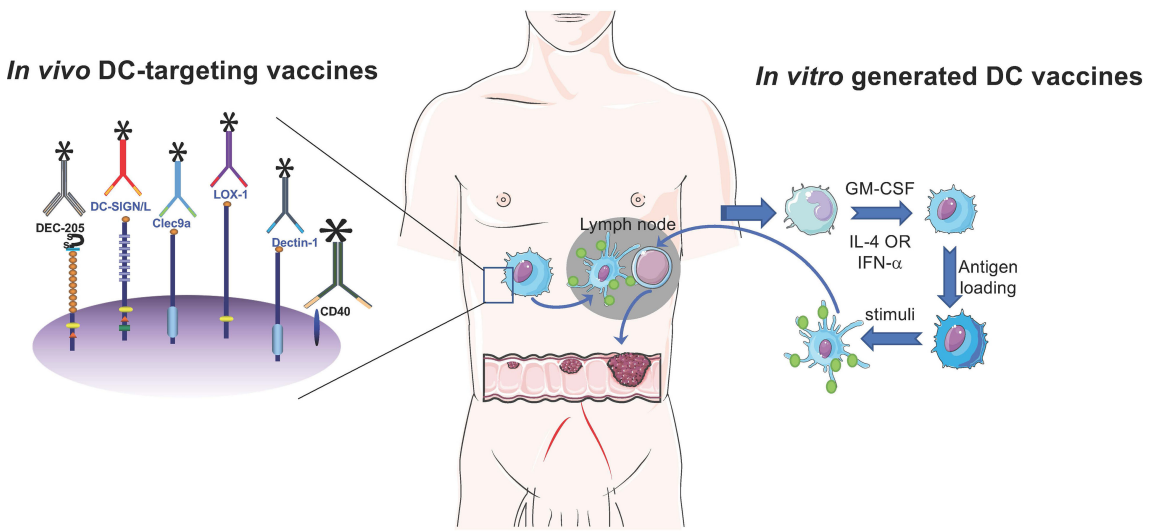

FIGURE 1 | Schematic overview of DC-based CRC vaccines. DC-based vaccines consist of two main approaches: *in vitro* generated DC vaccines and *in vivo* DC-targeting vaccines. *In vivo* DC targeting is a vaccine approach to deliver antigens directly to DCs *in vivo* using chimeric targets composed of an anti-DC receptor antibody and an antigen. *In vitro*-generated vaccines often used monocyte-derived DCs. Briefly, DCs are generated by culture of monocytes in the presence of GM-CSF and IL-4 (or IFN-α), which are then loaded with tumor-associated antigens (TAAs). After maturation, TAA-loaded DCs are injected into CRC patients.

antigen doses were induced in mice. However, in the context of GI cancer patients, DCs *in vivo* demonstrated a functional defect, including DC recruitment, maturation, and cytokine release, which might contribute to tumor growth and progression. Therefore, the use of *in vitro*-generated DC vaccines might be a better option. The clinical trials for the treatment of GI cancer are basically exploiting *in vitro*-generated DCs (**Table 2**).

The efficacious vaccines should consider several factors, such as DC subsets, tumor-associated antigen targets, antigen-loading methods, proper adjuvants, the selection of various injection routes, and so on. Appropriate adjuvants can dramatically improve the anti-tumoral efficacy of DC-based vaccines. DCIR-targeted vaccines and CD40L (adjuvant) activated DCs, which, in turn, primed $CD8^+$ T cells to secrete type 2 cytokines and IFN-γ (85). In contrast, $CD8^+$ T cells primed by DCs that were activated with the DCIR-targeted vaccines and TLR7/8 ligands produced higher levels of IFN-γ and granzyme B and perforin but no type 2 cytokines (85). TLR2 ligands are known to promote the induction of Treg cells, which are not likely to be used as adjuvants in the context of cancer (86). The TLR3 ligand induces type 1 IFN responses and promotes cross-presentation (87, 88), which is widely used in clinical trials.

Currently, the whole tumor cell lysates (primary or cell line) are often used for preparing DC-based vaccines in GI cancer, since they comprise whole tumor-associated antigens. The

TABLE 2 | Summary of clinical trials of DC-based therapy.

ClinicalTrials.gov Identifier	Status	Diseases	Interventions	Phase
NCT00005956	Completed	Breast cancer, GC, ovarian cancer	HER-2/neu intracellular domain protein plus autologous DCs	NA
NCT00019591	Completed	CRC	Ras peptide-pulsed DCs	1 and 2
NCT00027534	Unknown	Breast cancer, GI cancer, ovarian cancer	Autologous DCs infected with CEA-6D expressing fowlpox-tricom	1
NCT00103142	Completed	CRC	Autologous DCs	2
NCT00154713	Unknown	CRC	CEA-pulsed DCs	1 and 2
NCT00176761	Terminated	CRC	Tumor-pulsed DCs	2
NCT00228189	Completed	CRC	CEA-loaded DC vaccine	2
NCT00311272	Completed	CRC	DCs loaded with tumor antigens	2
NCT00558051	Completed	Metastatic CRC	Alpha-type-1 DC-based vaccines	1
NCT01413295	Completed	CRC	Autologous DCs pulsed with tumor antigens	2
NCT01637805	Unknown	Stage IV GC	CEA-loaded DC vaccine	1
NCT01671592	Completed	CRC	Alpha-type-1 DC vaccines	1
NCT01691625	Unknown	EC	Concurrent chemoradiotherapy plus DC-CIK immunotherapy	NA
NCT01783951	Completed	GC	DC-CIK	1 and 2
NCT01839539	Unknown	CRC	DC-CIK	2
NCT01885702	Active, not recruiting	CRC	Neoantigen-loaded DC	1 and 2
NCT02202928	Unknown	CRC	Autologous tumor lysate-pulsed DCs and CIK	2
NCT02215837	Unknown	GC	Autologous tumor lysate-pulsed DCs plus CIK	2
NCT02496273	Active, not recruiting	GC	CEA-loaded DC vaccine	1
NCT02503150	Unknown	Metastatic CRC	Autologous tumor lysate- pulsed human DC vaccine	3
NCT02504229	Unknown	GC	DC-CIK	2
NCT02602249	Unknown	GC	Mucin1-gene-DC-CTL or MUC1-peptide-DC-CTL	1
NCT02686944	Completed	GI	Allogeneic, proinflammatory DC suspension	1
NCT02693236	Unknown	EC	Mucin1 and survivin-loaded DC plus CIK	1 and 2
NCT02882659	Unknown	HCC, CRC	Autologous dendritic killer cell-based immunotherapy	1
NCT02919644	Recruiting	Stage IV CRC	Autologous DCs loaded with tumor homogenate	2
NCT03152565	Completed	CRC	Avelumab plus autologous DC vaccine	1
NCT03185429	Unknown	GI	Tumor-specific antigen-loaded DCs	NA
NCT03214939	Unknown	CRC	Autologous antigen-activated DCs	1
NCT03300843	Terminated	Melanoma, GI, breast cancer, ovarian cancer,	Peptide-loaded DC vaccine	2
NCT03410732	Unknown	GC	Activated autologous DCs	2
NCT03730948	Recruiting	CRC	mDC3 vaccine	1
NCT04567069	Recruiting	GC	Autologous DCs loaded with MG-7 antigen	1 and 2

EC, esophageal cancer; GI, gastrointestinal cancer; GC, gastric cancer; CRC, colorectal cancer; HCC, hepatocellular carcinoma; NA, not applicable; DC, dendritic cell; CEA, carcinoembryonic antigen; CIK, cytokine-induced killer cell.

identification of tumor-specific or associated neoantigens is also a key factor that can specifically enhance the efficacy of DC-based vaccines. For DC-based cancer immunotherapy in the future, a combination of existing treatment regimens will be the trend. DC-based vaccines can be combined with chemotherapy that kills tumor cells and release neoantigens. In addition, the combination of DC vaccines and immune checkpoint blockade (ICB) is another trend since the ICB therapy, such as PD-1/PD-L1 inhibitors, enhances the T-cell-mediated immune response. Although the clinical trials indicated that DC-based immunotherapy alone and in combination with chemotherapy was well tolerated and prolonged the survival time of GI cancer patients, the efficacies are still a big challenge.

AUTHOR CONTRIBUTIONS

The author confirms being the sole contributor of this work and has approved it for publication.

FUNDING

This work was supported by grants from National Key Research and Development Program of China (2021YFC2302403), Tsinghua University Spring Breeze Fund (2020Z99CFG008) and National Natural Science Foundation of China (NSFC) (31991173 and 31991170).

REFERENCES

1. Liu J, Lu G, Li Z, Tang F, Liu Y, Cui G. Distinct Compartmental Distribution of Mature and Immature Dendritic Cells in Esophageal Squamous Cell Carcinoma. *Pathol Res Pract* (2010) 206:602–6. doi: 10.1016/j.prp.2010.03.011
2. Nishimura J, Tanaka H, Yamakoshi Y, Hiramatsu S, Tamura T, Toyokawa T, et al. Impact of Tumor-Infiltrating LAMP-3 Dendritic Cells on the Prognosis of Esophageal Squamous Cell Carcinoma. *Esophagus* (2019) 16:333–44. doi: 10.1007/s10388-019-00669-w
3. Gholamin M, Moaven O, Farshchian M, Mahmoudi M, Sankian M, Memar B, et al. Induction of Cytotoxic T Lymphocytes Primed With Tumor RNA-Loaded Dendritic Cells in Esophageal Squamous Cell Carcinoma: Preliminary Step for DC Vaccine Design. *BMC Cancer* (2010) 10:261. doi: 10.1186/1471-2407-10-261
4. Wu L, Yang W, Chen LX, Chen SR, Zhang JK. *In Vitro* Antigen-Specific Cytotoxic T Cell Response Against Esophageal Carcinoma Cells Induced by HPV18E7-Transfected Dendritic Cells. *Histol Histopathol* (2010) 25:197–203. doi: 10.14670/HH-25.197
5. Liu X, Song N, Liu Y, Liu Y, Li J, Ding J, et al. Efficient Induction of Anti-Tumor Immune Response in Esophageal Squamous Cell Carcinoma *via* Dendritic Cells Expressing MAGE-A3 and CALR Antigens. *Cell Immunol* (2015) 295:77–82. doi: 10.1016/j.cellimm.2015.03.011
6. Zhang B, Li R, Chang CX, Han Y, Shi SB, Tian J. Pemetrexed Plus Dendritic Cells as Third-Line Therapy for Metastatic Esophageal Squamous Cell Carcinoma. *Onco Targets Ther* (2016) 9:3901–6. doi: 10.2147/OTT.S107319
7. Liu Y, Mu Y, Zhang A, Ren S, Wang W, Xie J, et al. Cytokine-Induced Killer Cells/Dendritic Cells and Cytokine-Induced Killer Cells Immunotherapy for the Treatment of Esophageal Cancer in China: A Meta-Analysis. *Onco Targets Ther* (2017) 10:1897–908. doi: 10.2147/OTT.S132507
8. Yuan X, Zhang AZ, Ren YL, Wang XL, Jiang CH, Yang L, et al. Et Al: Cytokine-Induced Killer Cells/Dendritic Cells and Cytokine-Induced Killer Cells Immunotherapy for the Treatment of Esophageal Cancer: A Meta-Analysis. *Med (Baltimore)* (2021) 100:e24519. doi: 10.1097/MD.0000000000024519
9. Ananiev J, Gulubova MV, Manolova IM. Prognostic Significance of CD83 Positive Tumor-Infiltrating Dendritic Cells and Expression of TGF-Beta 1 in Human Gastric Cancer. *Hepatogastroenterology* (2011) 58:1834–40. doi: 10.5754/hge10320
10. Kashimura S, Saze Z, Terashima M, Soeta N, Ohtani S, Osuka F, et al. CD83 (+) Dendritic Cells and Foxp3(+) Regulatory T Cells in Primary Lesions and Regional Lymph Nodes Are Inversely Correlated With Prognosis of Gastric Cancer. *Gastric Cancer* (2012) 15:144–53. doi: 10.1007/s10120-011-0090-9
11. Ling Z, Shao L, Liu X, Cheng Y, Yan C, Mei Y, et al. Regulatory T Cells and Plasmacytoid Dendritic Cells Within the Tumor Microenvironment in Gastric Cancer Are Correlated With Gastric Microbiota Dysbiosis: A Preliminary Study. *Front Immunol* (2019) 10:533. doi: 10.3389/fimmu.2019.00533
12. Liu X, Yu H, Yan C, Mei Y, Lin C, Hong Y, et al. Plasmacytoid Dendritic Cells and ICOS(+) Regulatory T Cells Predict Poor Prognosis in Gastric Cancer: A Pilot Study. *J Cancer* (2019) 10:6711–5. doi: 10.7150/jca.34826
13. Huang XM, Liu XS, Lin XK, Yu H, Sun JY, Liu XK, et al. Et Al: Role of Plasmacytoid Dendritic Cells and Inducible Costimulator-Positive Regulatory T Cells in the Immunosuppression Microenvironment of Gastric Cancer. *Cancer Sci* (2014) 105:150–8. doi: 10.1111/cas.12327
14. Liu W, Zhao J, Li Q, Wang Q, Zhou Y, Tong Z. Gastric Cancer Patients Have Elevated Plasmacytoid and CD1c(+) Dendritic Cells in the Peripheral Blood. *Oncol Lett* (2018) 15:5087–92. doi: 10.3892/ol.2018.7990
15. Bagheri V, Abbaszadegan MR, Memar B, Motie MR, Asadi M, Mahmoudian RA, et al. Induction of T Cell-Mediated Immune Response by Dendritic Cells Pulsed With mRNA of Sphere-Forming Cells Isolated From Patients With Gastric Cancer. *Life Sci* (2019) 219:136–43. doi: 10.1016/j.lfs.2019.01.016
16. Xue G, Cheng Y, Ran F, Li X, Huang T, Yang Y, et al. SLC Gene-Modified Dendritic Cells Mediate T Cell-Dependent Anti-Gastric Cancer Immune Responses *In Vitro*. *Oncol Rep* (2013) 29:595–604. doi: 10.3892/or.2012.2154
17. Mu Y, Wang WH, Xie JP, Zhang YX, Yang YP, Zhou CH. Efficacy and Safety of Cord Blood-Derived Dendritic Cells Plus Cytokine-Induced Killer Cells Combined With Chemotherapy in the Treatment of Patients With Advanced Gastric Cancer: A Randomized Phase II Study. *Onco Targets Ther* (2016) 9:4617–27. doi: 10.2147/OTT.S107745
18. Huang C, Jiang X, Huang Y, Zhao L, Li P, Liu F. Identifying Dendritic Cell-Related Genes Through a Co-Expression Network to Construct a 12-Gene Risk-Scoring Model for Predicting Hepatocellular Carcinoma Prognosis. *Front Mol Biosci* (2021) 8:636991. doi: 10.3389/fmolb.2021.636991
19. Han Y, Chen Z, Yang Y, Jiang Z, Gu Y, Liu Y, et al. Et Al: Human CD14+ CTLA-4+ Regulatory Dendritic Cells Suppress T-Cell Response by Cytotoxic T-Lymphocyte Antigen-4-Dependent IL-10 and Indoleamine-2,3-Dioxygenase Production in Hepatocellular Carcinoma. *Hepatology* (2014) 59:567–79. doi: 10.1002/hep.26694
20. Lim TS, Chew V, Sieow JL, Goh S, Yeong JP, Soon AL, et al. PD-1 Expression on Dendritic Cells Suppresses CD8(+) T Cell Function and Antitumor Immunity. *Oncoimmunology* (2016) 5:e1085146. doi: 10.1080/2162402X.2015.1085146
21. Pedroza-Gonzalez A, Zhou G, Vargas-Mendez E, Boor PP, Mancham S, Verhoef C, et al. Et Al: Tumor-Infiltrating Plasmacytoid Dendritic Cells Promote Immunosuppression by Tr1 Cells in Human Liver Tumors. *Oncoimmunology* (2015) 4:e1008355. doi: 10.1080/2162402X.2015.1008355
22. Villablanca EJ, Raccosta L, Zhou D, Fontana R, Maggioni D, Negro A, et al. Tumor-Mediated Liver X Receptor-Alpha Activation Inhibits CC Chemokine Receptor-7 Expression on Dendritic Cells and Dampens Antitumor Responses. *Nat Med* (2010) 16:98–105. doi: 10.1038/nm.2074
23. Liu Y, Zhao JJ, Zhou ZQ, Pan QZ, Zhu Q, Tang Y, et al. IL-37 Induces Anti-Tumor Immunity by Indirectly Promoting Dendritic Cell Recruitment and Activation in Hepatocellular Carcinoma. *Cancer Manag Res* (2019) 11:6691–702. doi: 10.2147/CMAR.S200627
24. Pardee AD, Shi J, Butterfield LH. Tumor-Derived Alpha-Fetoprotein Impairs the Differentiation and T Cell Stimulatory Activity of Human Dendritic Cells. *J Immunol* (2014) 193:5723–32. doi: 10.4049/jimmunol.1400725
25. Bray SM, Vujanovic L, Butterfield LH. Dendritic Cell-Based Vaccines Positively Impact Natural Killer and Regulatory T Cells in Hepatocellular Carcinoma Patients. *Clin Dev Immunol* (2011) 2011:249281. doi: 10.1155/2011/249281
26. Zhou J, Ma P, Li J, Song W. Comparative Analysis of Cytotoxic T Lymphocyte Response Induced by Dendritic Cells Pulsed With Recombinant Adeno-

Associated Virus Carrying Alpha-Fetoprotein Gene or Cancer Cell Lysate. *Mol Med Rep* (2015) 11:3174–80. doi: 10.3892/mmr.2014.3059
27. Matsui HM, Hazama S, Nakajima M, Xu M, Matsukuma S, Tokumitsu Y, et al. Novel Adjuvant Dendritic Cell Therapy With Transfection of Heat-Shock Protein 70 Messenger RNA for Patients With Hepatocellular Carcinoma: A Phase I/II Prospective Randomized Controlled Clinical Trial. *Cancer Immunol Immunother* (2021) 70:945–57. doi: 10.1007/s00262-020-02737-y
28. Li J, Huang S, Zhou Z, Lin W, Chen S, Chen M, et al. Exosomes Derived From rAAV/AFP-Transfected Dendritic Cells Elicit Specific T Cell-Mediated Immune Responses Against Hepatocellular Carcinoma. *Cancer Manag Res* (2018) 10:4945–57. doi: 10.2147/CMAR.S178326
29. El Ansary M, Mogawer S, Elhamid SA, Alwakil S, Aboelkasem F, Sabaawy HE, et al. Immunotherapy by Autologous Dendritic Cell Vaccine in Patients With Advanced HCC. *J Cancer Res Clin Oncol* (2013) 139:39–48. doi: 10.1007/s00432-012-1298-8
30. Shimizu K, Kotera Y, Aruga A, Takeshita N, Katagiri S, Ariizumi S, et al. Postoperative Dendritic Cell Vaccine Plus Activated T-Cell Transfer Improves the Survival of Patients With Invasive Hepatocellular Carcinoma. *Hum Vaccin Immunother* (2014) 10:970–6. doi: 10.4161/hv.27678
31. Shi W, Yang X, Xie S, Zhong D, Lin X, Ding Z, et al. A New PD-1-Specific Nanobody Enhances the Antitumor Activity of T-Cells in Synergy With Dendritic Cell Vaccine. *Cancer Lett* (2021) 522:184–97. doi: 10.1016/j.canlet.2021.09.028
32. Li QY, Shi Y, Huang DH, Yang T, Wang JH, Yan GH, et al. Cytokine-Induced Killer Cells Combined With Dendritic Cells Inhibited Liver Cancer Cells. *Int J Clin Exp Med* (2015) 8:5601–10.
33. Yang T, Zhang W, Wang L, Xiao C, Wang L, Gong Y, et al. Co-Culture of Dendritic Cells and Cytokine-Induced Killer Cells Effectively Suppresses Liver Cancer Stem Cell Growth by Inhibiting Pathways in the Immune System. *BMC Cancer* (2018) 18:984. doi: 10.1186/s12885-018-4871-y
34. Su Y, Yang Y, Ma Y, Zhang Y, Rao W, Yang G, et al. The Efficacy and Safety of Dendritic Cells Co-Cultured With Cytokine-Induced Killer Cell Therapy in Combination With TACE-Predominant Minimally-Invasive Treatment for Hepatocellular Carcinoma: A Meta-Analysis. *Clin Lab* (2016) 62:599–608. doi: 10.7754/Clin.Lab.2015.150804
35. Nakamoto Y, Mizukoshi E, Kitahara M, Arihara F, Sakai Y, Kakinoki K, et al. Prolonged Recurrence-Free Survival Following OK432-Stimulated Dendritic Cell Transfer Into Hepatocellular Carcinoma During Transarterial Embolization. *Clin Exp Immunol* (2011) 163:165–77. doi: 10.1111/j.1365-2249.2010.04246.x
36. Zhang W, Song Z, Xiao J, Liu X, Luo Y, Yang Z, et al. Blocking the PD-1/PD-L1 Axis in Dendritic Cell-Stimulated Cytokine-Induced Killer Cells With Pembrolizumab Enhances Their Therapeutic Effects Against Hepatocellular Carcinoma. *J Cancer* (2019) 10:2578–87. doi: 10.7150/jca.26961
37. Tjomsland V, Sandstrom P, Spangeus A, Messmer D, Emilsson J, Falkmer U, et al. Pancreatic Adenocarcinoma Exerts Systemic Effects on the Peripheral Blood Myeloid and Plasmacytoid Dendritic Cells: An Indicator of Disease Severity? *BMC Cancer* (2010) 10:87. doi: 10.1186/1471-2407-10-87
38. Tjomsland V, Spangeus A, Sandstrom P, Borch K, Messmer D, Larsson M. Semi Mature Blood Dendritic Cells Exist in Patients With Ductal Pancreatic Adenocarcinoma Owing to Inflammatory Factors Released From the Tumor. *PloS One* (2010) 5:e13441. doi: 10.1371/journal.pone.0013441
39. Hirooka S, Yanagimoto H, Satoi S, Yamamoto T, Toyokawa H, Yamaki S, et al. The Role of Circulating Dendritic Cells in Patients With Unresectable Pancreatic Cancer. *Anticancer Res* (2011) 31:3827–34.
40. Yamamoto T, Yanagimoto H, Satoi S, Toyokawa H, Yamao J, Kim S, et al. Circulating Myeloid Dendritic Cells as Prognostic Factors in Patients With Pancreatic Cancer Who Have Undergone Surgical Resection. *J Surg Res* (2012) 173:299–308. doi: 10.1016/j.jss.2010.09.027
41. Ochi A, Nguyen AH, Bedrosian AS, Mushlin HM, Zarbakhsh S, Barilla R, et al. MyD88 Inhibition Amplifies Dendritic Cell Capacity to Promote Pancreatic Carcinogenesis *via* Th2 Cells. *J Exp Med* (2012) 209:1671–87. doi: 10.1084/jem.20111706
42. Ding G, Zhou L, Qian Y, Fu M, Chen J, Chen J, et al. Pancreatic Cancer-Derived Exosomes Transfer miRNAs to Dendritic Cells and Inhibit RFXAP Expression *via* miR-212-3p. *Oncotarget* (2015) 6:29877–88. doi: 10.18632/oncotarget.4924
43. Du J, Wang J, Tan G, Cai Z, Zhang L, Tang B, et al. Aberrant Elevated microRNA-146a in Dendritic Cells (DC) Induced by Human Pancreatic Cancer Cell Line BxPC-3-Conditioned Medium Inhibits DC Maturation and Activation. *Med Oncol* (2012) 29:2814–23. doi: 10.1007/s12032-012-0175-2
44. Jang JE, Hajdu CH, Liot C, Miller G, Dustin ML, Bar-Sagi D. Crosstalk Between Regulatory T Cells and Tumor-Associated Dendritic Cells Negates Anti-Tumor Immunity in Pancreatic Cancer. *Cell Rep* (2017) 20:558–71. doi: 10.1016/j.celrep.2017.06.062
45. Sung GH, Chang H, Lee JY, Song SY, Kim HS. Pancreatic-Cancer-Cell-Derived Trefoil Factor 2 Impairs Maturation and Migration of Human Monocyte-Derived Dendritic CellsIn Vitro. *Anim Cells Syst (Seoul)* (2018) 22:368–81. doi: 10.1080/19768354.2018.1527721
46. Guo J, Liao M, Hu X, Wang J. Tumour-Derived Reg3A Educates Dendritic Cells to Promote Pancreatic Cancer Progression. *Mol Cells* (2021) 44:647–57. doi: 10.14348/molcells.2021.0145
47. Giri B, Sharma P, Jain T, Ferrantella A, Vaish U, Mehra S, et al. Hsp70 Modulates Immune Response in Pancreatic Cancer Through Dendritic Cells. *Oncoimmunology* (2021) 10:1976952. doi: 10.1080/2162402X.2021.1976952
48. Andoh Y, Makino N, Yamakawa M. Dendritic Cells Fused With Different Pancreatic Carcinoma Cells Induce Different T-Cell Responses. *Onco Targets Ther* (2013) 6:29–40. doi: 10.2147/OTT.S37916
49. Chen J, Guo XZ, Li HY, Wang D, Shao XD. Comparison of Cytotoxic T Lymphocyte Responses Against Pancreatic Cancer Induced by Dendritic Cells Transfected With Total Tumor RNA and Fusion Hybrided With Tumor Cell. *Exp Biol Med (Maywood)* (2015) 240:1310–8. doi: 10.1177/1535370215571884
50. Yin T, Shi P, Gou S, Shen Q, Wang C. Dendritic Cells Loaded With Pancreatic Cancer Stem Cells (CSCs) Lysates Induce Antitumor Immune Killing Effect *In Vitro*. *PloS One* (2014) 9:e114581. doi: 10.1371/journal.pone.0114581
51. Koido S, Homma S, Okamoto M, Takakura K, Mori M, Yoshizaki S, et al. Treatment With Chemotherapy and Dendritic Cells Pulsed With Multiple Wilms' Tumor 1 (WT1)-Specific MHC Class I/II-Restricted Epitopes for Pancreatic Cancer. *Clin Cancer Res* (2014) 20:4228–39. doi: 10.1158/1078-0432.CCR-14-0314
52. Takakura K, Koido S, Kan S, Yoshida K, Mori M, Hirano Y, et al. Prognostic Markers for Patient Outcome Following Vaccination With Multiple MHC Class I/II-Restricted WT1 Peptide-Pulsed Dendritic Cells Plus Chemotherapy for Pancreatic Cancer. *Anticancer Res* (2015) 35:555–62.
53. Miyazawa M, Iwahashi M, Ojima T, Katsuda M, Nakamura M, Nakamori M, et al. Dendritic Cells Adenovirally-Transduced With Full-Length Mesothelin cDNA Elicit Mesothelin-Specific Cytotoxicity Against Pancreatic Cancer Cell Lines *In Vitro*. *Cancer Lett* (2011) 305:32–9. doi: 10.1016/j.canlet.2011.02.013
54. Chen J, Li HY, Wang D, Zhao JJ, Guo XZ. Human Dendritic Cells Transfected With Amplified MUC1 mRNA Stimulate Cytotoxic T Lymphocyte Responses Against Pancreatic Cancer *In Vitro*. *J Gastroenterol Hepatol* (2011) 26:1509–18. doi: 10.1111/j.1440-1746.2011.06778.x
55. Rong Y, Qin X, Jin D, Lou W, Wu L, Wang D, et al. A Phase I Pilot Trial of MUC1-Peptide-Pulsed Dendritic Cells in the Treatment of Advanced Pancreatic Cancer. *Clin Exp Med* (2012) 12:173–80. doi: 10.1007/s10238-011-0159-0
56. Chen J, Guo XZ, Li HY, Liu X, Ren LN, Wang D, et al. Generation of CTL Responses Against Pancreatic Cancer *In Vitro* Using Dendritic Cells Co-Transfected With MUC4 and Survivin RNA. *Vaccine* (2013) 31:4585–90. doi: 10.1016/j.vaccine.2013.07.055
57. Franceschi C, Collignon A, Isnardon D, Benkoel L, Verine A, Silvy F, et al. A Novel Tumor-Associated Pancreatic Glycoprotein Is Internalized by Human Dendritic Cells and Induces Their Maturation. *J Immunol* (2011) 186:4067–77. doi: 10.4049/jimmunol.1000408
58. Mehrotra S, Britten CD, Chin S, Garrett-Mayer E, Cloud CA, Li M, et al. Vaccination With Poly(IC : LC) and Peptide-Pulsed Autologous Dendritic Cells in Patients With Pancreatic Cancer. *J Hematol Oncol* (2017) 10:82. doi: 10.1186/s13045-017-0459-2
59. Pei Q, Pan J, Zhu H, Ding X, Liu W, Lv Y, et al. Gemcitabine-Treated Pancreatic Cancer Cell Medium Induces the Specific CTL Antitumor Activity by Stimulating the Maturation of Dendritic Cells. *Int Immunopharmacol* (2014) 19:10–6. doi: 10.1016/j.intimp.2013.12.022
60. Pei Q, Pan J, Ding X, Wang J, Zou X, Lv Y. Gemcitabine Sensitizes Pancreatic Cancer Cells to the CTLs Antitumor Response Induced by BCG-Stimulated Dendritic Cells *via* a Fas-Dependent Pathway. *Pancreatology* (2015) 15:233–9. doi: 10.1016/j.pan.2015.04.001

61. Zhang Y, Zhang X, Zhang A, Li K, Qu K. Clinical Applications of Dendritic Cells-Cytokine-Induced Killer Cells Mediated Immunotherapy for Pancreatic Cancer: An Up-to-Date Meta-Analysis. *Onco Targets Ther* (2017) 10:4173–92. doi: 10.2147/OTT.S143382
62. Que RS, Lin C, Ding GP, Wu ZR, Cao LP. Increasing the Immune Activity of Exosomes: The Effect of miRNA-Depleted Exosome Proteins on Activating Dendritic Cell/Cytokine-Induced Killer Cells Against Pancreatic Cancer. *J Zhejiang Univ Sci B* (2016) 17:352–60. doi: 10.1631/jzus.B1500305
63. Endo H, Saito T, Kenjo A, Hoshino M, Terashima M, Sato T, et al. Phase I Trial of Preoperative Intratumoral Injection of Immature Dendritic Cells and OK-432 for Resectable Pancreatic Cancer Patients. *J Hepatobil Pancreat Sci* (2012) 19:465–75. doi: 10.1007/s00534-011-0457-7
64. Hirooka Y, Kawashima H, Ohno E, Ishikawa T, Kamigaki T, Goto S, et al. Comprehensive Immunotherapy Combined With Intratumoral Injection of Zoledronate-Pulsed Dendritic Cells, Intravenous Adoptive Activated T Lymphocyte and Gemcitabine in Unresectable Locally Advanced Pancreatic Carcinoma: A Phase I/II Trial. *Oncotarget* (2018) 9:2838–47. doi: 10.18632/oncotarget.22974
65. Kocian P, Sedivcova M, Drgac J, Cerna K, Hoch J, Kodet R, et al. Tumor-Infiltrating Lymphocytes and Dendritic Cells in Human Colorectal Cancer: Their Relationship to KRAS Mutational Status and Disease Recurrence. *Hum Immunol* (2011) 72:1022–8. doi: 10.1016/j.humimm.2011.07.312
66. Pryczynicz A, Cepowicz D, Zareba K, Gryko M, Holody-Zareba J, Kedra B, et al. Dysfunctions in the Mature Dendritic Cells Are Associated With the Presence of Metastases of Colorectal Cancer in the Surrounding Lymph Nodes. *Gastroenterol Res Pract* (2016) 2016:2405437. doi: 10.1155/2016/2405437
67. Gai XD, Li C, Song Y, Lei YM, Yang BX. *In Situ* Analysis of FOXP3(+) Regulatory T Cells and Myeloid Dendritic Cells in Human Colorectal Cancer Tissue and Tumor-Draining Lymph Node. *BioMed Rep* (2013) 1:207–12. doi: 10.3892/br.2012.35
68. Gai XD, Song Y, Li C, Lei YM, Yang B. Potential Role of Plasmacytoid Dendritic Cells for FOXP3+ Regulatory T Cell Development in Human Colorectal Cancer and Tumor Draining Lymph Node. *Pathol Res Pract* (2013) 209:774–8. doi: 10.1016/j.prp.2013.08.011
69. Orsini G, Legitimo A, Failli A, Ferrari P, Nicolini A, Spisni R, et al. Quantification of Blood Dendritic Cells in Colorectal Cancer Patients During the Course of Disease. *Pathol Oncol Res* (2014) 20:267–76. doi: 10.1007/s12253-013-9691-4
70. Chistiakov DA, Orekhov AN, Bobryshev YV. Dendritic Cells in Colorectal Cancer and a Potential for Their Use in Therapeutic Approaches. *Curr Pharm Des* (2016) 22:2431–8. doi: 10.2174/1381612822666160203141740
71. Chen L, Meng D, Zhao L, Liu R, Bai P, Wang L, et al. Selective Colorectal Cancer Cell Lysates Enhance the Immune Function of Mature Dendritic Cells *In Vitro*. *Mol Med Rep* (2015) 11:1877–84. doi: 10.3892/mmr.2014.2930
72. Xing X, Zou Z, He C, Hu Z, Liang K, Liang W, et al. Enhanced Antitumor Effect of Cytotoxic T Lymphocytes Induced by Dendritic Cells Pulsed With Colorectal Cancer Cell Lysate Expressing Alpha-Gal Epitopes. *Oncol Lett* (2019) 18:864–71. doi: 10.3892/ol.2019.10376
73. Lee HJ, Hong CY, Kim MH, Lee YK, Nguyen-Pham TN, Park BC, et al. *In Vitro* Induction of Anterior Gradient-2-Specific Cytotoxic T Lymphocytes by Dendritic Cells Transduced With Recombinant Adenoviruses as a Potential Therapy for Colorectal Cancer. *Exp Mol Med* (2012) 44:60–7. doi: 10.3858/emm.2012.44.1.006
74. Kulikova EV, Kurilin VV, Shevchenko JA, Obleukhova IA, Khrapov EA, Boyarskikh UA, et al. Dendritic Cells Transfected With a DNA Construct Encoding Tumour-Associated Antigen Epitopes Induce a Cytotoxic Immune Response Against Autologous Tumour Cells in a Culture of Mononuclear Cells From Colorectal Cancer Patients. *Scand J Immunol* (2015) 82:110–7. doi: 10.1111/sji.12311
75. Lesterhuis WJ, De Vries IJ, Schreibelt G, Schuurhuis DH, Aarntzen EH, De Boer A, et al. Immunogenicity of Dendritic Cells Pulsed With CEA Peptide or Transfected With CEA mRNA for Vaccination of Colorectal Cancer Patients. *Anticancer Res* (2010) 30:5091–7.
76. Liu KJ, Chao TY, Chang JY, Cheng AL, Ch'ang HJ, Kao WY, et al. A Phase I Clinical Study of Immunotherapy for Advanced Colorectal Cancers Using Carcinoembryonic Antigen-Pulsed Dendritic Cells Mixed With Tetanus Toxoid and Subsequent IL-2 Treatment. *J BioMed Sci* (2016) 23:64. doi: 10.1186/s12929-016-0279-7
77. Hu Z, Ma Y, Shang Z, Hu S, Liang K, Liang W, et al. Improving Immunotherapy for Colorectal Cancer Using Dendritic Cells Combined With Anti-Programmed Death-Ligand *In Vitro*. *Oncol Lett* (2018) 15:5345–51. doi: 10.3892/ol.2018.7978
78. Sadeghlar F, Vogt A, Mohr RU, Mahn R, van Beekum K, Kornek M, et al. Induction of Cytotoxic Effector Cells Towards Cholangiocellular, Pancreatic, and Colorectal Tumor Cells by Activation of the Immune Checkpoint CD40/CD40L on Dendritic Cells. *Cancer Immunol Immunother* (2021) 70:1451–64. doi: 10.1007/s00262-020-02746-x
79. Liu Y, Zheng Z, Zhang Q, Zhou X, Feng Y, Yan A. FOLFOX Regimen Plus Dendritic Cells-Cytokine-Induced Killer Cells Immunotherapy for the Treatment of Colorectal Cancer: A Meta-Analysis. *Onco Targets Ther* (2017) 10:2621–33. doi: 10.2147/OTT.S138011
80. Zhang L, Mu Y, Zhang A, Xie J, Chen S, Xu F, et al. Cytokine-Induced Killer Cells/Dendritic Cells-Cytokine Induced Killer Cells Immunotherapy Combined With Chemotherapy for Treatment of Colorectal Cancer in China: A Meta-Analysis of 29 Trials Involving 2,610 Patients. *Oncotarget* (2017) 8:45164–77. doi: 10.18632/oncotarget.16665
81. Zhou X, Mo X, Qiu J, Zhao J, Wang S, Zhou C, et al. Chemotherapy Combined With Dendritic Cell Vaccine and Cytokine-Induced Killer Cells in the Treatment of Colorectal Carcinoma: A Meta-Analysis. *Cancer Manag Res* (2018) 10:5363–72. doi: 10.2147/CMAR.S173201
82. Lin T, Song C, Chuo DY, Zhang H, Zhao J. Clinical Effects of Autologous Dendritic Cells Combined With Cytokine-Induced Killer Cells Followed by Chemotherapy in Treating Patients With Advanced Colorectal Cancer: A Prospective Study. *Tumour Biol* (2016) 37:4367–72. doi: 10.1007/s13277-015-3957-2
83. Bonifaz L, Bonnyay D, Mahnke K, Rivera M, Nussenzweig MC, Steinman RM. Efficient Targeting of Protein Antigen to the Dendritic Cell Receptor DEC-205 in the Steady State Leads to Antigen Presentation on Major Histocompatibility Complex Class I Products and Peripheral CD8+ T Cell Tolerance. *J Exp Med* (2002) 196:1627–38. doi: 10.1084/jem.20021598
84. Bonifaz LC, Bonnyay DP, Charalambous A, Darguste DI, Fujii S, Soares H, et al. *In Vivo* Targeting of Antigens to Maturing Dendritic Cells *via* the DEC-205 Receptor Improves T Cell Vaccination. *J Exp Med* (2004) 199:815–24. doi: 10.1084/jem.20032220
85. Klechevsky E, Flamar AL, Cao Y, Blanck JP, Liu M, O'Bar A, et al. Cross-Priming CD8+ T Cells by Targeting Antigens to Human Dendritic Cells Through DCIR. *Blood* (2010) 116:1685–97. doi: 10.1182/blood-2010-01-264960
86. Manicassamy S, Ravindran R, Deng J, Oluoch H, Denning TL, Kasturi SP, et al. Toll-Like Receptor 2-Dependent Induction of Vitamin A-Metabolizing Enzymes in Dendritic Cells Promotes T Regulatory Responses and Inhibits Autoimmunity. *Nat Med* (2009) 15:401–9. doi: 10.1038/nm.1925
87. Jongbloed SL, Kassianos AJ, McDonald KJ, Clark GJ, Ju X, Angel CE, et al. Human CD141+ (BDCA-3)+ Dendritic Cells (DCs) Represent a Unique Myeloid DC Subset That Cross-Presents Necrotic Cell Antigens. *J Exp Med* (2010) 207:1247–60. doi: 10.1084/jem.20092140
88. Meixlsperger S, Leung CS, Ramer PC, Pack M, Vanoaica LD, Breton G, et al. CD141+ Dendritic Cells Produce Prominent Amounts of IFN-Alpha After dsRNA Recognition and can be Targeted *via* DEC-205 in Humanized Mice. *Blood* (2013) 121:5034–44. doi: 10.1182/blood-2012-12-473413

Conflict of Interest: The author declares that the research was conducted in the absence of any commercial or financial relationships that could be construed as a potential conflict of interest.

GLOSSARY

ICI	immune checkpoint inhibitor
GI	gastrointestinal
EC	esophageal cancer
GC	gastric cancer
CRC	colorectal cancer
PC	pancreatic cancer
HCC	hepatocellular carcinoma
DC	dendritic cell
CTL	cytotoxic T lymphocyte
iDC	immature dendritic cell
$CD8^+$ TILs	tumor-infiltrating $CD8^+$ T cells
TAA	tumor-associated antigen
MAGE-A3	melanoma-associated antigen 3
HPV	human papillomavirus
CALR	calreticulin
MHC	major histocompatibility
Ad	adenovirus
CIK	cytokine-induced killer cells
Tregs	regulatory T cells
pDC	plasmacytoid dendritic cell
TME	tumor microenvironment
mDC2	$CD1c^+$ myeloid dendritic cell
CSC	cancer stem cell
SLC	secondary lymphoid tissue chemokine
CB-DC-CIK	cord blood-derived dendritic cell and cytokine-induced killer cell
DEG	differentially expressed gene
OS	overall survival
PBMC	peripheral blood mononuclear cell
IDO	indoleamine-2,3-dioxygenase
mDC1	$CD141^+$ mDC
LAG-3	lymphocyte activation gene 3
LXR	liver X receptor
AFP	alpha-fetoprotein
nAFP	normal AFP
tAFP	tumor-derived AFP
LMM	low molecular mass
rAAV	recombinant adeno-associated virus
DEXs	DC-derived exosomes
HSP70	heat shock protein 70
DFS	disease-free survival
ATVAC	autologous tumor lysate-pulsed DC vaccine plus *ex vivo* activated T-cell transfer
Nb	nanobody
FC	tumor-specific DC/tumor-fusion cell
PCNA	proliferating cell nuclear antigen
LCSC	liver cancer stem cell
TACE	transcatheter arterial chemoembolization
TAE	hepatic arterial embolization
PDAC	pancreatic ductal adenocarcinoma
LPS	lipopolysaccharide
BxCM	BxPC-3-culture medium
TDX	tumor-derived exosome
RFXAP	regulatory factor X-associated protein
TFF2	trefoil factor 2
Reg3A	regenerating islet-derived protein 3a
WT1	Wilms' tumor 1
MSLN	mesothelin
FAPP	fetoacinar pancreatic protein
hTERT	human telomerase reverse transcriptase
CEA	carcinoembryonic antigen
PEU-FNI	preoperative endoscopic ultrasound-guided fine-needle injection

(Continued)

Continued

Zol-DCs	zoledronate-pulsed DCs
SD	stable disease
NLR	neutrophil/lymphocyte ratio
AGR2	anterior gradient-2
MNC	mononuclear cell
Ad-hCD40L	Ad-encoding human CD40L

frontiers | Frontiers in Immunology

TYPE Original Research
PUBLISHED 01 August 2022
DOI 10.3389/fimmu.2022.931316

OPEN ACCESS

EDITED BY
Jingtao Chen,
The First Hospital of Jilin University, China

REVIEWED BY
Salman M. Toor,
Hamad bin Khalifa University, Qatar
Rolf Kiessling,
Karolinska Institutet (KI), Sweden

*CORRESPONDENCE
Behzad Baradaran
baradaranb@tbzmed.ac.ir
Nicola Silvestris
n.silvestris@oncologico.bari.it

†These authors share last authorship

SPECIALTY SECTION
This article was submitted to Cancer Immunity and Immunotherapy, a section of the journal Frontiers in Immunology

RECEIVED 28 April 2022
ACCEPTED 11 July 2022
PUBLISHED 01 August 2022

CITATION
Ghorbaninezhad F, Masoumi J, Bakhshivand M, Baghbanzadeh A, Mokhtarzadeh A, Kazemi T, Aghebati-Maleki L, Shotorbani SS, Jafarlou M, Brunetti O, Santarpia M, Baradaran B and Silvestris N (2022) CTLA-4 silencing in dendritic cells loaded with colorectal cancer cell lysate improves autologous T cell responses *in vitro*. *Front. Immunol.* 13:931316. doi: 10.3389/fimmu.2022.931316

CTLA-4 silencing in dendritic cells loaded with colorectal cancer cell lysate improves autologous T cell responses *in vitro*

Farid Ghorbaninezhad[1,2,3], Javad Masoumi[1], Mohammad Bakhshivand[1,2], Amir Baghbanzadeh[1], Ahad Mokhtarzadeh[1,4], Tohid Kazemi[1,2], Leili Aghebati-Maleki[1], Siamak Sandoghchian Shotorbani[1,2], Mahdi Jafarlou[1], Oronzo Brunetti[5], Mariacarmela Santarpia[6], Behzad Baradaran[1,2*†] and Nicola Silvestris[6*†]

[1]Immunology Research Center, Tabriz University of Medical Sciences, Tabriz, Iran, [2]Department of Immunology, Faculty of Medicine, Tabriz University of Medical Sciences, Tabriz, Iran, [3]Student Research Committee, Tabriz University of Medical Sciences, Tabriz, Iran, [4]Pharmaceutical Analysis Research Center, Tabriz University of Medical Sciences, Tabriz, Iran, [5]Medical Oncology Unit, Istituto di Ricovero e Cura a Carattere Scientifico (IRCCS) Istituto Tumori "Giovanni Paolo II" of Bari, Bari, Italy, [6]Medical Oncology Unit, Department of Human Pathology "G. Barresi", University of Messina, Messina, Italy

Dendritic cell (DC)-based immunotherapy has increased interest among anti-cancer immunotherapies. Nevertheless, the immunosuppressive mechanisms in the tumor milieu, e.g., inhibitory immune checkpoint molecules, have been implicated in diminishing the efficacy of DC-mediated anti-tumoral immune responses. Therefore, the main challenge is to overcome inhibitory immune checkpoint molecules and provoke efficient T-cell responses to antigens specifically expressed by cancerous cells. Among the inhibitory immune checkpoints, cytotoxic T-lymphocyte-associated protein 4 (CTLA-4) expression on DCs diminishes their maturation and antigen presentation capability. Accordingly, we hypothesized that the expression of CTLA-4 on DCs inhibits the T cell-mediated anti-tumoral responses generated following the presentation of tumor antigens by DCs to T lymphocytes. In this study, we loaded colorectal cancer (CRC) cell lysate on DCs and inhibited the expression of CTLA-4 by small interfering RNA (siRNA) in them to investigate the DCs' functional and phenotypical features, and T-cell mediated responses following DC/T cell co-culture. Our results demonstrated that blockade of CTLA-4 could promote stimulatory properties of DCs. In addition, CTLA-4 silenced CRC cell lysate-loaded DCs compared to the DCs without CTLA-4 silencing resulted in augmented T cell proliferation and cytokine production, i.e., IFN-γ and IL-4. Taken together, our findings suggest CTLA-4 silenced CRC cell lysate-loaded

DCs as a promising therapeutic approach however further studies are needed before this strategy can be used in clinical practice.

KEYWORDS

dendritic cell, T lymphocyte, colorectal cancer, tumor cell lysate, CTLA-4, cancer immunotherapy

Introduction

Immunotherapy is a new alternative option for cancer treatment that has been developed due to advances in understanding various cancers pathogenesis (1). Unlike conventional therapies, immunotherapy manipulates and utilizes the patient's own immune cells to fight cancer (2). Nowadays, cancer immunotherapies focus on specializing immune responses against tumors by involving dendritic cells (DCs) and stimulating anti-tumoral T-cell responses (3, 4). DCs are the immune system's specialized antigen-presenting cells (APCs), important for linking the gap between innate and adaptive immunity, including the stimulation of anti-tumoral T cells (5, 6). The tumor-associated antigens (TAAs) which are processed and presented by DCs can activate anti-tumoral specific T cell responses (7). Various studies have indicated that DCs pulsed with a tumor cell lysate could provoke tumor antigen-specific T cell responses (8, 9). The induction of T cell-mediated anti-tumoral immunity through DCs reduces tumor volume and increases immunological memory to prevent cancer recurrence (3, 4).

As a result of DCs' capability to initiate cellular immunity, they are promising candidates for cancer immunotherapy (10). Efficient DC-based cancer immunotherapy depends on the capacity of DCs to present TAAs to T cells, while its ineffectiveness is mostly related to the inhibitory immune checkpoint molecules, which make DCs incompetent (11). Among the inhibitory immune checkpoints expressed by DCs is cytotoxic T-lymphocyte-associated protein-4 (CTLA-4) (12). CTLA-4, which comprises three domains (ligand-binding region, transmembrane region, and cytoplasmic region) and a leading peptide, is an inhibitory molecule that can be expressed on various immune cells and modulate their function (13). It's expression on DCs reduces their maturation and antigen presentation capacity (14). Furthermore, it has been reported that CTLA-4 stimulates the expression of inhibitory molecules, e.g., IL-10 and indoleamine 2,3-dioxygenase 1 (IDO1) in DCs (15).

Colorectal cancer (CRC) is the third most frequent cancer globally, accounting for approximately 935,000 deaths per year, and has been ranked as the second major cause of cancer deaths in 2020 (16). Chemotherapy, surgery, and radiotherapy are among the conventional treatments for this malignancy (17, 18). These conventional therapies may be related to adverse side effects, i.e., chemotherapy resistance, systemic toxicity, and cancer recurrence (2, 19). Most patients with CRC are constituted with Proficient Mismatch Repair (pMMR) and microsatellite stable (MSS) subtypes which have shown resistance to various therapies. The main reason for this is supposed to be antigen presentation weakness, diminished tumor-specific antigen expression, activation of immunosuppressive pathways, immune checkpoint signaling pathways, and presence of immune regulatory cells (20). Currently, various clinical trials in phases I/II or also III have been evaluating CTLA-4 targeted antibodies, including Ipilimumab and Tremelimumab, in different CRC subtypes, some of which have reported promising primary results. Phase II study of Ipilimumab and Nivolumab in combination with radiotherapy in MSS metastatic CRC has revealed that a combination of immune checkpoint inhibitors with radiation could significantly increase the disease control rate (21). First-line Nivolumab along with low-dose Ipilimumab, has demonstrated strong and durable clinical benefit and was well tolerated in Microsatellite Instability-High/Mismatch Repair-Deficient (MSI-H/dMMR) metastatic CRC patients in phase II study (22). Even though the Phase II study of the Tremelimumab in patients with refractory metastatic CRC had not demonstrated clinically meaningful effects (23), other studies have shown the improvement in its combination with other immune checkpoint inhibitors. In a randomized phase II study on refractory MSS CRC patients, the combination of Durvalumab and Tremelimumab has prolonged median overall survival by 2.5 months compared with patients who had received the best supportive care (24). The results of Phase II single-arm study of Durvalumab and Tremelimumab with concurrent radiotherapy showed an increase in circulating $CD8^+$ T lymphocyte activation, differentiation, and proliferation in patients with pMMR metastatic CRC (25). It is worth to state that in 2018, the Food and Drug Administration (based on clinical trial NCT02060188) had approved ipilimumab for use in combination with nivolumab for the treatment of patients 12 years of age and older with MSI-H/dMMR metastatic CRC that had not responded to chemotherapy regimens fluoropyrimidine, oxaliplatin, and irinotecan.

Considering above mentioned issues, it seems that suppressing CTLA-4 expression on DCs along with loading these cells with a tumor cell lysate increases anti-tumoral specific T cell responses more efficiently, suggesting that this could be a possible and applicable cancer immunotherapy strategy. In this study, we demonstrated that CTLA-4 silencing in CRC cell lysate-loaded DCs enhances their stimulation and leads to boosted autologous T cells' activation and cytokine production. Overall, these findings illustrate that CTLA-4-silenced tumor lysate-loaded DCs are a very attractive option for upgrading the effectiveness of DC vaccines in cancer immunotherapies.

Materials and methods

Materials

Complete media (CM) including RPMI 1640 (Gibco, USA, NY) that contains 10% Fetal Bovine Serum (FBS) (Gibco, USA, NY), Streptomycin 100 µg/mL, Penicillin 100 IU/mL (Gibco, USA, NY), 2 mmol/L of L-glutamine (Gibco, USA, NY). 2-mercaptoethanol (2ME) was ordered from Gibco (USA, NY). Recombinant human granulocyte macrophage colony stimulating factor (rh GM-CSF) was purchased from Sigma Chemical Co (Munich, Germany) and recombinant human interleukin-4 (rh IL-4) from eBioscience (CA, USA). Lipopolysaccharide (LPS) was ordered from Sigma Chemical Co (Munich, Germany). Carboxyfluorescein succinimidyl ester (CFSE) cell labeling kit was obtained from BioLegend (San Diego, United States). Human pan T cell isolation Kit was purchased from MiltenyiBiotec, Germany. Antibodies used to phenotype the cells were anti-HLA-DR-APC and anti-CD86-PerCP-cy5.5 from BioLegend (San Diego, United States), anti-CD40-CF-blue, anti-CD11c-FITC, and anti-CD14-FITC from Immunostep (Salamanca, Spain). Ficoll was obtained from Sigma Chemical Co (Munich, Germany). Bradford protein assay kit was purchased from Bio-Rad, (Hercules, CA).

Tumor cell lysate preparation

Human CRC cell lines, including HT-29, HCT-116, and SW-480 cells, were purchased from the National Cell Bank of Iran (Pasteur Institute, Tehran, Iran). These cell lines were grown in CM and maintained at 37°C under humidification and 5% CO2. When the confluency of cultured cells reached 70-80%, they were detached using Trypsin, washed twice in serum-free media, and resuspended in sterile Phosphate Buffered Saline solution (PBS) at a concentration of 1×10^7 cells/mL. Six rapid freeze-thaw cycles in liquid nitrogen and 37°C water bath were used to generate tumor cell lysates from cell suspensions. The produced lysate was then sonicated for 15 seconds to maximize the release of tumor antigens from lysed malignant cells. To remove cellular debris, the tumor cell lysates were centrifuged at 1500 rpm for 15 minutes at 4°C. The collected supernatant was passed through a 0.2-µm filter. The protein content in the lysates was determined using the Bradford assay. All lysates were maintained at -80°C until they were utilized.

Peripheral mononuclear cells (PBMCs) isolation and DC generation

Fresh peripheral blood (PB) from three healthy individuals was collected in sterile falcons containing heparin, and PBMCs were isolated from these samples by fractionation over Ficoll gradients. The plastic adherence method was used to isolate monocytes from PBMCs. For this purpose, PBMCs were cultured at a concentration of 5×10^6 per mL of serum-free RPMI-1640 medium in 6-well plates. Following 2 hours of incubation at 37°C, the non-adherent cells were washed off, and the adherent cells were cultured within the CM supplemented with 50 µM 2ME, 40 ng/mL, and 20 ng/mL of rh GM-CSF and rh IL-4, respectively. On days 2 and 4, the cultures were fed by removing half of the medium and replacing it with fresh CM containing rh GM-CSF and rh IL-4. After collecting immature DCs (iDCs) on day 6, 80 ng/mL of mixed human CRC cell lines lysate was added to the culture medium. After 5 hours of incubation at 37°C, 100 ng/mL of LPS was added to the culture medium. Tumor cell lysate-loaded mature DCs (mDCs) were generated after 24 hours of incubation at 37°C.

Morphological and phenotypical characterization of DCs

The morphology of monocytes and DCs were observed, and photos were taken using an inverted light microscope (Optika, XDS-3, Italy). To analyze the phenotype of iDCs, mDCs, and CTLA-4-silenced mDCs, these cells were stained with specific surface markers including HLA-DR (anti-HLA-DR-APC), CD40 (anti-CD40-CF-blue), CD86 (anti-CD86- PerCP-cy5.5), and CD11c (anti-CD11c-FITC). The MACSQuant cytometer (Miltenyi Biotec, Auburn, CA, USA) was used to evaluate the cells, and the obtained data were analyzed using FlowJo software v10.5.3.

siRNA preparation and transfection into DCs

CTLA-4-siRNA and transfection reagent were ordered from Santa Cruz Biotechnology (Santa Cruz, Canada). The sequence of ordered CTLA-4-siRNA is shown in Table 1. To obtain the

optimum pulse voltage for CTLA-4-siRNA transfection, mDCs were harvested and subsequently transfected with different pulse voltages (160, 180, and 200 V) using Gene Pulser Xcell (Bio-Rad, USA). The transfection efficiency of siRNA in different pulse voltages was evaluated with FITC-labeled control siRNA (Santa Cruz Biotechnology, Santa Cruz, Canada). After obtaining a 160 V as the optimum pulse voltage for siRNA transfection, mDCs were transfected with different concentrations of CTLA-4-siRNA (40, 60, and 80 ρmol). Immediately after electroporation, mDCs were transferred into a 6-well plate containing CM. The relative expression of CTLA-4 was evaluated after 48 and 72 hours of incubation using quantitative real-time PCR (qRT-PCR). The optimum dose of siRNA and pulse voltage were determined for further experiments based on the provided results.

Autologous $CD3^+$ T cells isolation and CFSE labeling

The separation of autologous $CD3^+$ T cells from PBMCs of the same individuals used for DC generation was performed by magnetic activated cell sorting (MACS) using a human Pan T Cell Isolation Kit according to the manufacturer's instructions. Briefly, following isolating the PBMCs, the cell suspension was centrifuged for 10 minutes at 300 g. The supernatant was removed, and then 40 µl MACS buffer and 10 µL of pan T cell biotin Ab cocktail were added per 1×10^7 total cells. After incubating for 5 min at 2–8°C, 30 µL of MACS buffer and 20 uL of Pan T Cell Microbead cocktail were added per 1×10^7 total cells. Following a 10-minute incubation at 2–8°C, cells were washed with 1–2 mL of MACS buffer and resuspended in 500 uL of MACS buffer. After placing the MACS column in the MACS separator's magnetic field, the cell suspension was added to this column. Negatively selected $CD3^+$ T cells were unlabeled cells that had passed through the column. CFSE labeling of isolated $CD3^+$ T cells was performed according to the protocol provided by the manufacturer. In brief, purified T cells were resuspended in PBS and incubated with CFSE at a concentration of 5 µM for 5 minutes at room temperature in the dark. The reaction was quenched by adding RPMI-1640 medium containing 20% FBS. After the final washing step, the cells were resuspended in pre-warmed cell culture media.

$CD3^+$ T-cells' proliferation assay

To assess mDCs and CTLA-4-silenced-mDCs for their ability to stimulate the proliferation of autologous T cells, DC-T cell co-culture was performed. mDCs and CTLA-4-silenced-mDCs as stimulator and CFSE-labeled autologous $CD3^+$ T cells as responder cells were co-cultured in the ratios of 1:5 and1:10 in V bottom 96-well plate. T cells activated by phytohemagglutinin (PHA) (5%) (Sigma Chemical Co., Munich, Germany) were served as a positive control, whereas co-cultured iDCs with T-cells were considered as an unstimulated group. After 4 days of incubation at dark conditions, flow cytometry was used to analyze the proliferation of the CFSE-labeled T cells. Unlabeled $CD3^+$ T cells were used as unstained.

Cytokine assay

To evaluate the capability of mDCs and CTLA-4-silenced-mDCs to promote cytokine production in autologous T cells,

Table 1. List of primer sequences and siRNA.

Gene		Sequences
CTLA-4 siRNA	Sense	GUAUCUGAGUUGACUUGACAGAACA
	Antisense	UGUCUGUCAAGUCAACUCAGAUACCA
CTLA-4	F	TCAGTCCTTGGATAGTGAGGTTC
	R	TCAGTCCTTGGATAGTGAGGTTC
TNF-α	F	TTCTCCTTCCTGATCGTGGCA
	R	TAGAGAGAGGTCCCTGGGGAA
IL-10	F	AGGAAGAGAAACCAGGGAGC
	R	GAATCCCTCCGAGACACTGG
T-bet	F	TCTCCTCTCCTACCCAACCAG
	R	CATGCTGACTGCTCGAAACTCA
FOXP3	F	CAGCCAGTCTATGCAAACC
	R	GTCTTGTGTCAGTTTGAGGGTC
GATA3	F	GCATCCAGACCAGAAACCGAA
	R	TCGCGTTTAGGCTTCATGATACT
18S	F	CTACGTCCCTGCCCTTTGTACA
	R	ACACTTCACCGGACCATTCAA

freshly isolated $CD3^+$ T cells were cultured with mDCs and CTLA-4-silenced-mDCs in the ratios of 1:5 in 24-well plate. The supernatants of the co-cultures were obtained 48 hours after stimulation with DCs, and the quantities of IFN-γ, IL-4, and TGF-β were measured using commercial ELISA kits (R&D Systems, Minnneapolis, MN, USA). As well, IL-12 and IL-10 levels were evaluated in supernatants of the mDCs and CTLA-4-silenced-mDCs cultures using ELISA kits (R&D Systems, Minnneapolis, MN, USA).

RNA isolation and qRT-PCR

Total cellular RNA was extracted using the TRIzol reagent (Roche Diagnostics, Mannheim, Germany) according to the manufacturer's guidelines. The concentration of RNA was then measured by a spectrophotometer. The RNA was maintained at -80°C, and the Complementary DNA (cDNA) was synthesized using a BioFACT 2step 2X RT-PCR Pre-Mix (Taq), and the Applied Biosystems StepOnePlusTM Real-Time PCR System (Life Technologies, Carlsbad, CA, USA) was used to assess the expression of all genes in this manuscript. To normalize the expression of target mRNAs, the 18s gene was employed as an internal control. The sequences of primers are provided in Table 1. All reactions were carried out in triplicate, and the relative mRNA expression was calculated using the $2^{-\Delta\Delta Ct}$ method.

Statistical analysis

All the raw data were analyzed with GraphPad Prism v8.0.2 (GraphPad Software, San Diego, California USA). Student's t-test and One-way ANOVA test were used to compare data between two and more than two groups, respectively. Each parameter was measured in triplicate, and data of each group were expressed as mean ± SD with the significance cut-off of p-value ≤ 0.05 (ns: not significant; *: P≤ 0.05; **: P≤ 0.01; ***: P≤ 0.001; and ****: P≤ 0.0001).

Results

siRNA transfection in mDCs significantly decreased the gene expression of CTLA-4

To achieve the optimum voltage for transfection, mDCs were transfected with different pulse voltages (160, 180, and 200 V). There was no significant difference in transfection rate between selected voltages, and it is shown to be near 90% in all of them. Therefore, the least voltage (160V) was selected in order to reduce stress in cells during pulsing (Figure 1A). Furthermore, after the transfection of CTLA-4-siRNA in different concentrations into mDCs, to assess siRNA effectiveness in gene silencing, the qRT-PCR was used. Compared with untransfected mDCs, which is considered as a control group, 60 pmol of CTLA-4 siRNA compared to 40 and 80 pmol more significantly reduced CTLA-4 mRNA expression in transfected cells at both 48 and 72 h incubation time (Figure 1B, P≤ 0.0001). As a result, the following experiments were conducted using a 60 pmol as the optimal dose of CTLA-4-siRNA and 160 V as the optimal transfection voltage.

CTLA-4 silencing significantly increased maturation and activation of DCs

Microscopic analysis revealed morphological changes during *in vitro* culture of adherent monocytes and differentiated DCs (Figure 2A). Using the surface expression of markers related to DC maturation and antigen presentation, phenotypic evaluation of iDCs, mDCs, and CTLA-4-silenced mDCs was performed as detailed in the "Materials and methods" section. Flow cytometry analysis showed that all three of these cells had typical expressions of CD11c, HLA-DR, CD86, and CD40 (Figure 2B). We further analyzed the differences in the surface expression of these markers between these three groups of DCs based on median fluorescence intensity (MFI). Conversion of iDCs to mDCs increased the surface expression of CD11c (P≤ 0.05), HLA-DR (P≤ 0.0001), CD86 (P≤ 0.01), and CD40 (P≤ 0.0001) markers (Figure 2C). CTLA-4 suppression in mDCs, significantly elevated the expression of CD11c (P≤ 0.01), CD86 (P≤ 0.01), and CD40 (P≤ 0.0001) compared with mDCs, whereas increased HLA-DR expression was not significantly different (Figure 2C). Furthermore, activated DCs are known to produce inflammatory cytokines. Accordingly, to further characterize the impact of CTLA-4 silencing in the activation of mDCs, the concentration of IL-12 and IL-10 in the cell culture supernatants and the expression of TNF-α and IL-10 mRNAs were evaluated by ELISA and qRT-PCR, respectively. According to the findings, CTLA-4 silencing resulted in enhanced TNF-α (Figure 3A, P≤ 0.01) and decreased IL-10 (Figure 3A, P≤ 0.0001) expression in mDCs. Also, compared with mDCs, IL-12 levels in the cell culture supernatants were increased after CTLA-4 inhibition (Figure 3B, P≤ 0.05). Interestingly, IL-10 was higher in the supernatants of CTLA-4-silenced mDCs compared with mDCs, but the difference was not significant (Figure 3B).

Deletion of CTLA-4 in DCs improved T-cell responses

To determine the impact of CTLA-4 suppression in mDCs, on the T cell anti-tumor activity, proliferation, and cytokine secretion of $CD3^+$ T cells were assessed in the following experiments. Co-culture assay was done with mDCs and

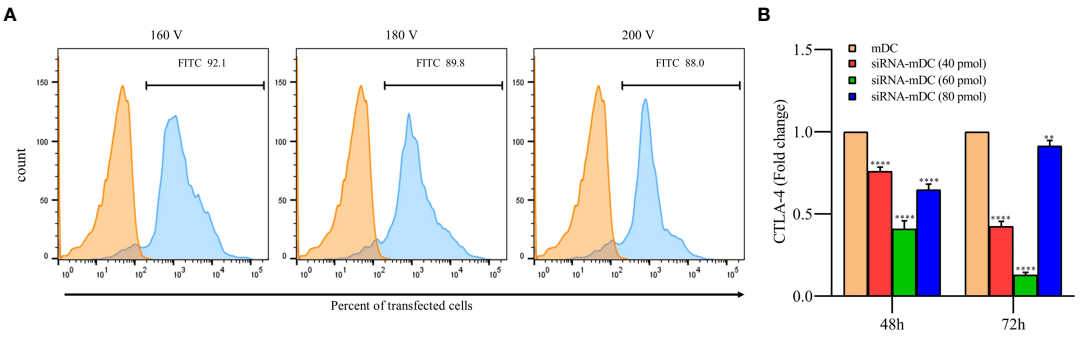

FIGURE 1
siRNA transfection outstandingly silenced CTLA-4 gene in mDCs. **(A)** Percentages of transfected mDCs obtained for the different pulse voltages. More than 92% of the mDCs were transfected with FITC-labeled control siRNA at 160 V. The viability of all transfected and un-transfected DCs, determined by the Trypan blue exclusion test, was above 90 percent. **(B)** CTLA-4 mRNA expression was suppressed in mDCs after 72 hours of transfection with 60 pmol of CTLA-4 siRNA compared with untransfected mDCs; (**P≤ 0.01 and ****P≤ 0.0001). CTLA-4, Cytotoxic T-lymphocyte-associated protein-4; mDCs, Tumor cell lysate-loaded mature dendritic cells; siRNA-mDCs, CTLA-4-silenced mDCs.

CTLA-4-silenced-mDCs as stimulator and CFSE-labeled autologous $CD3^+$ T cells as a responder in 1:5 and 1:10 ratios to assess proliferation as previously described in the "Materials and methods" section. The results indicated that compared to 1:10, the ratio of 1:5 resulted in increased T cell proliferation in all groups (P≤ 0.05) (Figures 4A, B). Furthermore, in both 1:10 and 1:5 ratios, CTLA-4-silenced mDCs showed a higher capacity to stimulate $CD3^+$ T cell proliferation than mDCs (P≤ 0.05 and P≤ 0.01, respectively) (Figures 4A, B). In addition, the anti-tumor activity of T cells was assessed by measuring IFN-γ, IL-4, and TGF-β levels in the supernatant of T cell/DC co-cultures. Co-cultures of autologous T cells and CTLA-4-silenced-mDCs resulted in considerably higher IFN-γ (Figure 5A, P≤ 0.05) and IL-4 (Figure 5A, P≤ 0.01) levels than T cell/mDCs co-culture, which is Coordinated with the increased proliferation of $CD3^+$ T cells. TGF-β levels were diminished in the supernatants of T cell/CTLA-4-silenced mDCs co-culture compared with T cell/mDCs co-culture, but the difference was not significant (Figure 5A). The findings are consonant with enhanced GATA3 and T-bet mRNA expression in T cells purified from the T cell/CTLA-4-

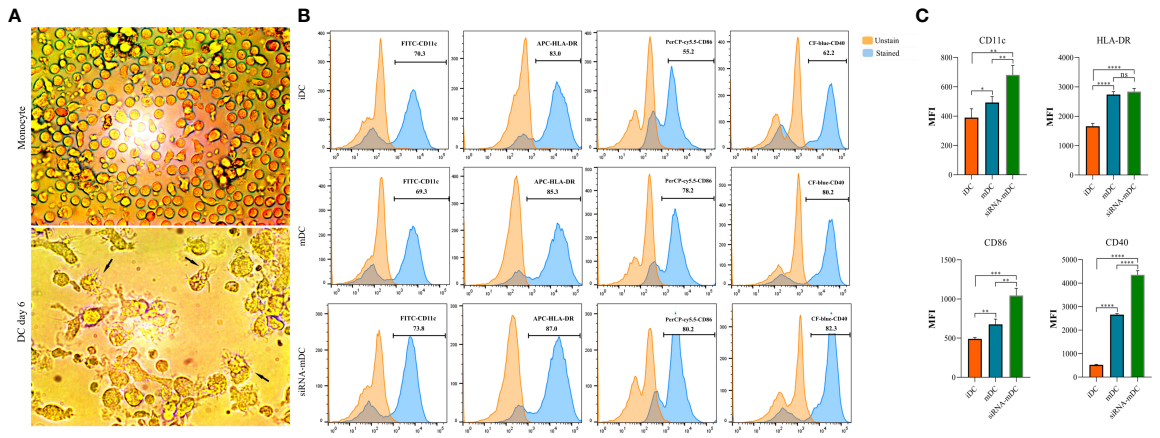

FIGURE 2
Morphological and phenotypical characterization of DCs. **(A)** Morphological changes during *in vitro* culture of adherent monocytes and differentiated DCs. Arrows indicate DCs with typical morphology having sharp dendrites. **(B)** Phenotypic characterization of iDCs, mDCs, and CTLA-4-silenced mDCs quantified by flow cytometry for the expression of surface markers, including CD11c, HLA-DR, CD86, and CD40. Results are expressed as the percentage of stained cells for these markers (figures **(A, B)** provided as representative of all samples). **(C)** The expression levels of CD11c, HLA-DR, CD86, and CD40 between iDCs, mDCs, and CTLA-4-silenced mDCs are represented as MFI. (ns, not significant, *P≤ 0.05, **P≤ 0.01, ***P≤ 0.001, and ****P≤ 0.0001). DCs, dendritic cells; CTLA-4, Cytotoxic T-lymphocyte-associated protein-4; iDCs, Immature dendritic cells; mDCs, Tumor cell lysate-loaded mature dendritic cells; siRNA-mDCs, CTLA-4-silenced mDCs; HLA-DR, Human leukocyte antigen-DR isotype; MFI, Median fluorescence intensity.

10.3389/fimmu.2022.931316

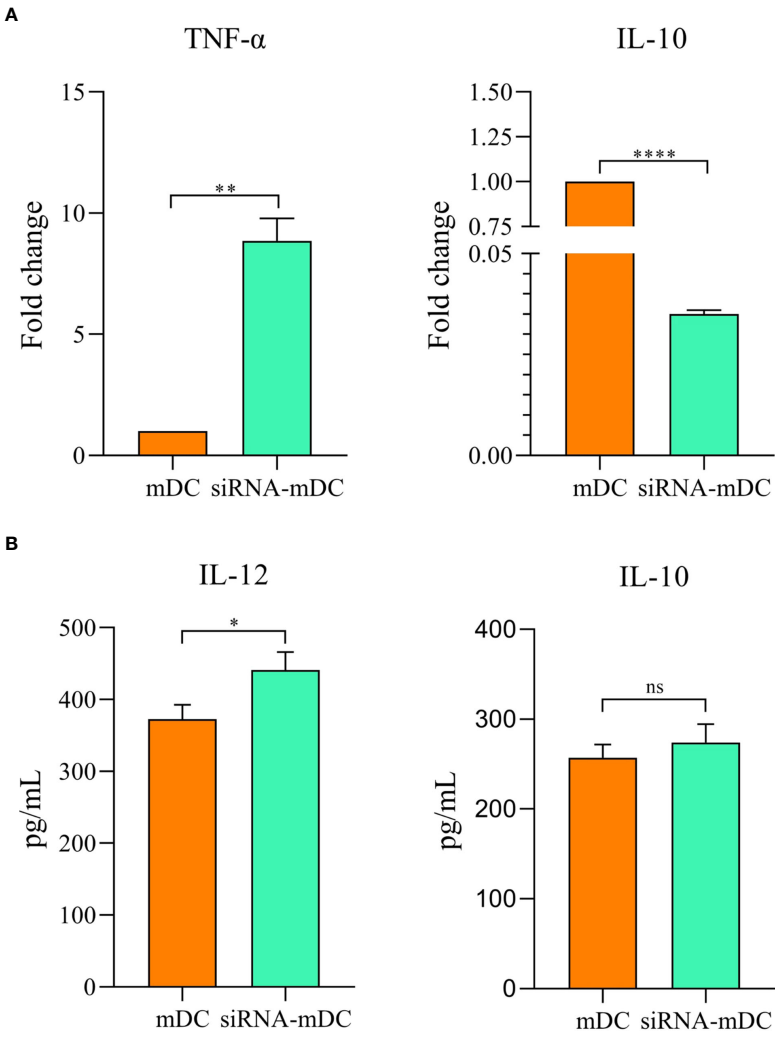

FIGURE 3
Cytokine expression and secretion profile in mDCs and CTLA-4-silenced-mDCs. The expression levels of TNF-α and IL-10 **(A)** were assessed by qRT-PCR. IL-12 and IL-10 **(B)** quantities in the cell culture supernatants was evaluated by ELISA; (ns, not significant, *P≤ 0.05, **P≤ 0.01, and ****P≤ 0.001). CTLA-4, Cytotoxic T-lymphocyte-associated protein-4; mDCs, Tumor cell lysate-loaded mature dendritic cells; siRNA-mDCs, CTLA-4-silenced mDCs; qRT-PCR, Quantitative Real-time polymerase chain reaction; ELISA, Enzyme-linked immunosorbent assay.

silenced-mDCs co-culture compared with T cell/mDCs co-culture (Figure 5B). Interestingly, FOXP3 mRNA was found to be considerably higher in T cells purified from the T cell/CTLA-4-silenced-mDCs co-culture than in T cell/mDCs co-culture (Figure 5B).

Discussion

There is considerable interest in utilizing DCs to stimulate antigen-specific anti-tumoral $CD4^+$ and $CD8^+$ T cell responses in cancer immunotherapy. In this regard, synthetic peptides or proteins obtained from TAAs, i.e., MUC1, Her-2/neu, tyrosinase, CEA, and Melan-A/MART, can be loaded into DCs to stimulate antigen-specific T cells. Vaccinating against a single antigen has limitations since it's unclear whether the defined antigens can trigger an effective anti-cancer immunity (9). Tumor cell lysates are a reliable source of tumor antigens, particularly for malignancies without tumor-specific antigens, which can be presented to T cells by DCs *via* the MHC class I and class II molecules (26). As a result, lysate-pulsed DCs are more potent to trigger T cell activation. Nevertheless, several immunosuppressive mechanisms utilized by cancerous cells in their milieu cause abnormalities in the function of DCs, which contribute to tumor cell escape from the immune system and diminish the efficacy of DC-based immunotherapy. Inhibitory immune checkpoint molecules are regarded as key participants in the TME's immune-modulatory scenario (27). Among these

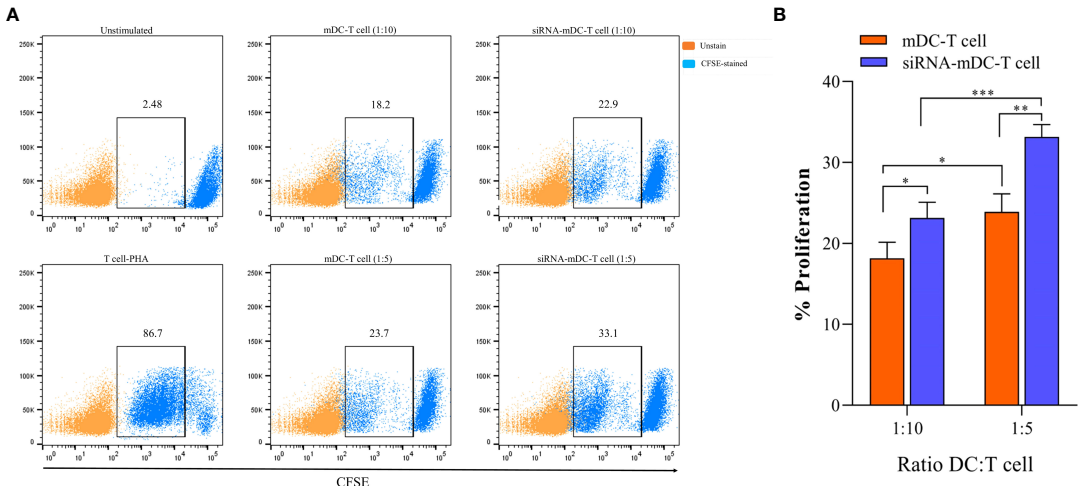

FIGURE 4
CTLA-4-silenced-mDCs significantly increase CD3+ T cells' proliferation. **(A)** The percentage of CFSE-labeled autologous $CD3^+$ T cells provoked by mDCs and CTLA-4-silenced-mDCs at a 1:5 and 1:10 DC/T cell ratio were determined by FACS *via* calculating the CFSE loss. **(B)** Enhanced mDC's capacity in T cell proliferation following CTLA-4 knockdown; (*P≤ 0.05, **P≤ 0.01, and ***P≤ 0.001). CTLA-4, Cytotoxic T-lymphocyte-associated protein-4; mDCs, Tumor cell lysate-loaded mature dendritic cells; siRNA-mDCs, CTLA-4-silenced mDCs; FACS, Fluorescent activated cell sorting.

molecules, the importance of CTLA-4 in the inhibition of anti-tumor T cell responses has been subjected to the argument for over a decade. CTLA-4 is a T cell activation inhibitory receptor that binds to the B7 ligand family, CD80 and CD86, on the surface of APCs with a high affinity and disrupts CD28-mediated signaling to T cell (28). When CTLA-4 is inhibited, CD28 binds to CD80/CD86, enhancing $CD4^+$ and $CD8^+$ T cell-mediated immunity (29). According to various studies, CTLA-4 is expressed in non-T cells like DCs and has immunomodulatory effects on them (12, 14). CTLA-4 expression in DCs decreases their maturation by reducing CD83 expression. Furthermore, CTLA-4-expressing DCs have a reduced ability to present antigens to T cells (14). IL-10 upregulates following CTLA-4 engagement on DCs, while IL-8 and IL-12 production diminishes (12).

Several investigators have attempted to pulse DCs with tumor cell lysates (30, 31) or suppress inhibitory immune checkpoints, e.g., PD-L1/PD-L2 (32, 33) in DCs to increase the efficacy of DC-based cell therapy outcomes. However, none of them evaluated the effect of tumor antigen loading on DCs as well as CTLA-4 inhibition in them concomitantly. Since CTLA-4 is expressed on DCs and has a significant effect on diminishing their function, we aimed to inhibit the expression of CTLA-4 in CRC cell lysate-pulsed-DCs *via* transfection of siRNA to enhance the efficacy of DC-based cancer immunotherapy. We used CTLA-4 siRNA duplexes, which have longevity, stability, and remarkable specificity, to suppress CTLA-4 expression on CRC cell lysate-loaded monocyte-derived DCs.

Our results showed that in comparison to untransfected mDCs, CTLA-4 mRNA expression in transfected mDCs was significantly inhibited after 72 hours of transfection with 60 pmol of CTLA-4 siRNA at 160 V (Figure 1B). After determining the optimal dose and pulse voltage required for siRNA transfection into mDCs, we investigated the stimulatory impact of CTLA-4 suppression in mDCs on their antigen-presenting features by evaluation of surface molecule expression patterns and cytokine secretion characteristics. Hence, despite the non-significant increase in HLA-DR expression, our results indicated that inhibition of CTLA-4 in mDCs significantly amplified the expression of CD11c, CD40, and CD86 (Figure 2C), implying the potential of CTLA-4-silenced mDCs to stimulate T lymphocytes. Another important signal for T cell activation is cytokines released by DCs. Activated DCs produce inflammatory cytokines, i.e., TNF-α and IL-12, while the production of IL-10 is the hallmark of tolerogenic DCs (34). According to our results, following CTLA-4 knockdown in mDCs, the expression of TNF-α and IL-10 (Figure 3A) was increased and decreased, respectively. In addition, after CTLA-4 suppression in mDCs, the quantities of IL-12 in the cell culture supernatants were significantly amplified. In contrast, the increase in the quantities of IL-10 in the supernatants of CTLA-4-silenced mDCs was not significant (Figure 3B).

Since antigen-loaded DCs can stimulate T cell-mediated immunity, we further investigated the stimulatory capacity of our CTLA-4-silenced mDCs in antigen-specific T-cell responses.

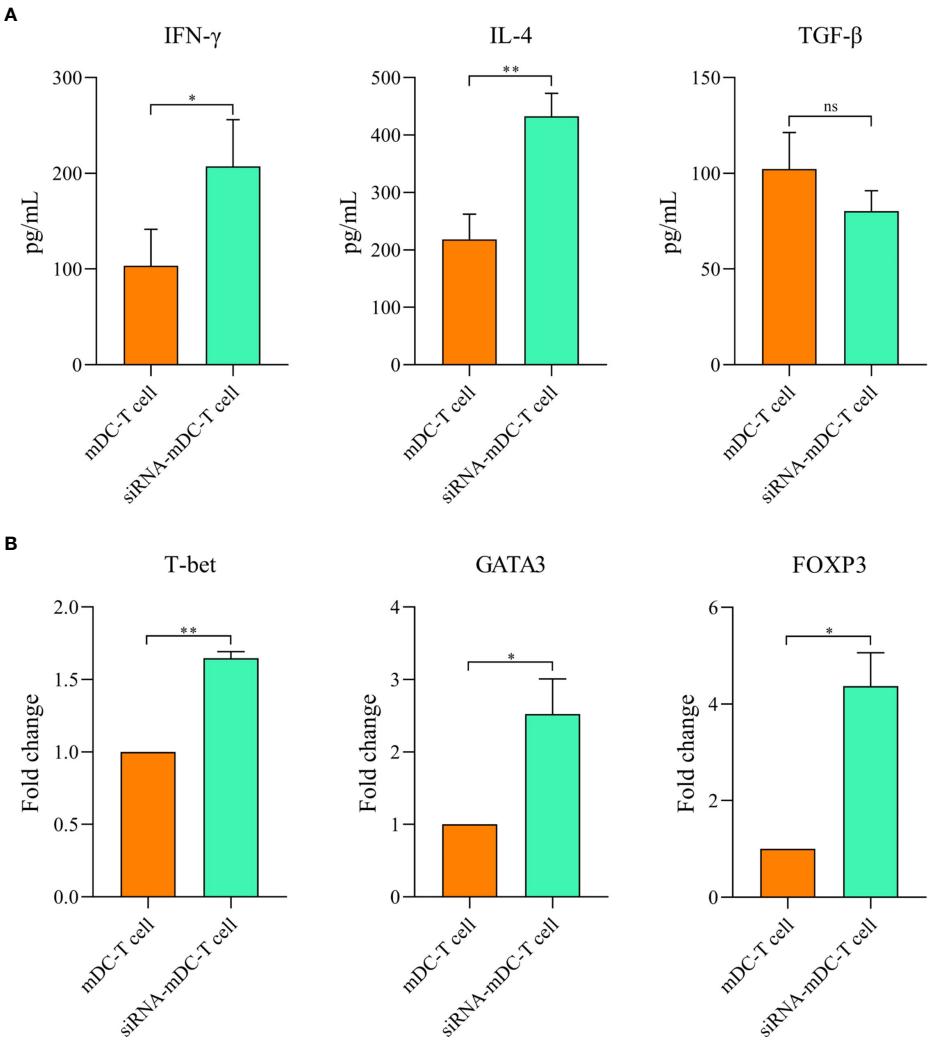

FIGURE 5
Silencing of CTLA-4 in mDCs strengthened T cell-mediated effector functions. Cytokine production by T cells following co-culture with mDCs and CTLA-4-silenced-mDCs. **(A)** The DC/T cell co-culture supernatants were evaluated for IFN-γ, IL-4, and TGF-β secretion by $CD3^+$ T cells by ELISA. **(B)** Expression analysis of T cell-associated transcription factors, i.e., GATA3, T-bet, and FOXP3 by $CD3^+$ T cells following co-culture with mDCs and CTLA-4-silenced-mDCs were determined *via* qRT-PCR; (ns, not significant, *P≤ 0.05, and **P≤ 0.01). CTLA-4, Cytotoxic T-lymphocyte-associated protein-4; DC, dendritic cell; mDCs, Tumor cell lysate-loaded mature dendritic cells; siRNA-mDCs, CTLA-4-silenced mDCs; ELISA, Enzyme-linked immunosorbent assay; GATA3, GATA binding protein 3; T-bet, T-box protein expressed in T cells; FOXP3, Forkhead box P3; qRT-PCR, Quantitative reverse transcription polymerase chain reaction.

Based on our results, CRC cell lysate loading in DCs along with CTLA-4 inhibition significantly increased $CD3^+$ T cell proliferation in autologous co-culture assay compared with DCs where only loaded with CRC cell lysate (Figure 4B). The effect of CTLA-4 inhibition in DCs on cytokine secretion profile by T cells was also determined. The results showed that suppression of CTLA-4 considerably increased the production of IFN-γ, a marker associated with T helper type 1, and IL-4 (Figure 5A), a marker associated with T helper type 2. However, the decrease in the TGF-β (marker of regulatory T cell) levels following T cell/CTLA-4-silenced mDCs co-culture was not significant (Figure 5A). Next, we evaluated the expression of transcription factors related to the T cell responses. Enhanced GATA3 (T helper 2 marker) and T-bet (T helper 1 marker) mRNA expression in $CD3^+$ T cells co-cultured with CTLA-4-silenced-mDCs was observed (Figure 5B). Surprisingly, the expression of FOXP3 mRNA, a transcription factor related to regulatory T cells, was increased in T cell/CTLA-4-silenced-mDCs co-culture (Figure 5B).

As previously stated, various investigators have attempted to separately load tumor cell lysates on DCs or silence inhibitory immune checkpoints, such as PD-L1/PD-L2, in order to develop

effective DC-based cell therapy. Aerts et al. have demonstrated that following the use of tumor lysate–loaded DCs, the tumor-specific T-cell response was established by the production of IFN-γ in the mesothelioma-murine model, which was consistent with our findings (35). In accordance with our results, it was reported that T cells release higher quantities of IFN-γ and show a higher rate of proliferation when they are stimulated by apoptotic tumor cell-loaded DCs (8). In another study, it has been indicated that human gastric tumor lysates loaded DCs can boost the proliferation of $CD3^+$ T cells (36). In accordance with our results, Schnurr et al. have reported the increased IL-12 secretion by panc-1 tumor cell lysates loaded DCs (37). In addition, in a breast tumor-bearing human-SCID model, suppression of PD-L1 boosted DC maturation, proliferation, and IL-12 secretion, as well as T-cell-mediated responses (38). Roeven and colleagues have reported that suppression of PD-L1/PD-L2 in human monocyte-derived DCs significantly boosted *ex vivo* antigen-specific T-cell responses (39). Furthermore, Van den Bergh et al. have indicated that PD-L1/2-silenced DCs exhibited an increased capacity to enhance T-cell proliferation and TNF-α production than normal DCs, which was consistent with our findings (32). Oh and colleagues have shown that PD-L1 elimination in DCs improves anti-tumor $CD8^+$ T-cell responses (40). Some studies have reported that in the high stimulatory conditions like exposure to mature autologous DCs or stimulation with CD3, $CD4^+$ T cells acquire regulatory properties including the FOXP3 expression, while producing effector cytokines like IFN-γ, IL-2, IL-4 and IL-10 (41–44). This

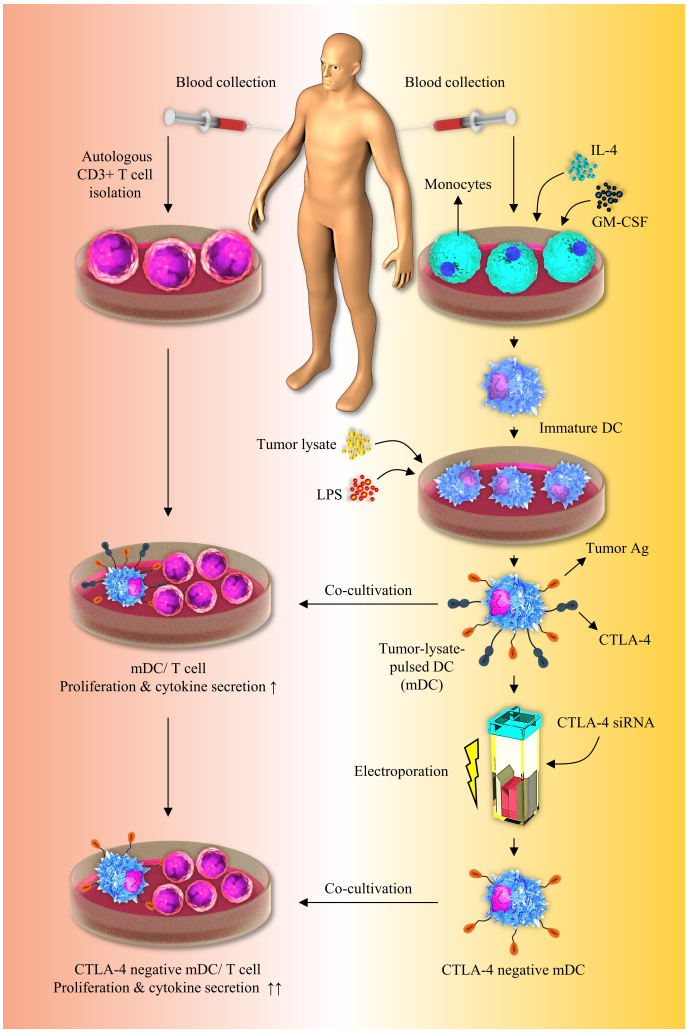

FIGURE 6
Inhibition of CTLA-4 molecules augments T-cell responses to tumor-lysate-pulsed-DCs. Silencing of CTLA-4 gene in DCs *via* using siRNA improves their stimulatory properties. Co-culture of tumor-lysate-pulsed CTLA-4-scilenced DCs with $CD3^+$ T cells improves T-cell mediated responses. CTLA-4, Cytotoxic T-lymphocyte-associated protein-4; DC, dendritic cell; siRNA, small interfering RNA.

may be the reason laying behind the FOXP3 high expression in T cell/CTLA-4-silenced-mDCs co-cultures. Although in previous studies, DCs were separately loaded with tumor lysates or suppressed for inhibitory immune checkpoints like PD-L1/PD-L2, however, there is no study regarding the concomitant silencing of CTLA-4 and tumor cell lysate loading on DCs in order to boost the effectiveness of DC-based immunotherapy. Our result showed that CTLA-4 knockdown in CRC cell lysate-loaded DCs enhances autologous T cell activation and cytokine secretion, implying a promising therapeutic option for future preclinical and clinical investigations (Figure 6).

Conclusion

Despite DCs having been loaded with tumor lysates or inhibited for inhibitory immune checkpoints in previous studies, there has been no investigation on the simultaneous silencing of CTLA-4 and tumor cell lysate loading on DCs. This study has implied that CTLA-4 knockdown in CRC cell lysate-loaded DCs remarkably improves their maturation and stimulatory activity. Furthermore, these modified DCs can robustly enhance the activation and cytokine secretion of co-cultured T-cells more than DCs where only pulsed with tumor lysate. As a result of these findings, it is suggested that this anti-cancer therapeutic strategy be investigated further in preclinical investigations in order to confirm this concept.

Data availability statement

The raw data supporting the conclusions of this article will be made available by the authors, without undue reservation.

Ethics statement

The studies involving human participants were reviewed and approved by ethical code: IR.TBZMED.REC.1399.938. The patients/participants provided their written informed consent to participate in this study. Written informed consent was obtained from the individual(s) for the publication of any potentially identifiable images or data included in this article.

Author contributions

FG is the first author of the manuscript, performed the majority of experiments, and wrote the initial version of the manuscript; JM contributed to cellular assays, data analysis, and revised the manuscript; MB contributed to data analysis and manuscript preparation; AB contributed to molecular assays; OB, AM, TK, LA-M, SS, and MS commented on the manuscript and provided critical feedback; BB and NS are the corresponding authors of the manuscript, supervised the project, and also contributed to the revising of the main text of the manuscript. All authors contributed to the article and approved the submitted version.

Funding

This study was supported by the Immunology Research Center, Tabriz University of Medical Sciences, Tabriz, Iran (Grant numbers: 66133 & 60603).

Conflict of interest

The authors declare that the research was conducted in the absence of any commercial or financial relationships that could be construed as a potential conflict of interest.

Publisher's note

All claims expressed in this article are solely those of the authors and do not necessarily represent those of their affiliated organizations, or those of the publisher, the editors and the reviewers. Any product that may be evaluated in this article, or claim that may be made by its manufacturer, is not guaranteed or endorsed by the publisher.

References

1. Carter BW, Bhosale PR, Yang WT. Immunotherapy and the role of imaging. *Cancer* (2018) 124:2906–22. doi: 10.1002/cncr.31349

2. Johdi NA, Sukor NF. Colorectal cancer immunotherapy: Options and strategies. *Front Immunol* (2020) 11:1624. doi: 10.3389/fimmu.2020.01624

3. Palucka K, Banchereau J. Cancer immunotherapy *via* dendritic cells. *Nat Rev Cancer* (2012) 12:265–77. doi: 10.1038/nrc3258

4. Anguille S, Smits EL, Lion E, Van Tendeloo VF, Berneman ZN. Clinical use of dendritic cells for cancer therapy. *Lancet Oncol* (2014) 15:e257–267. doi: 10.1016/S1470-2045(13)70585-0

5. Gardner A, De Mingo Pulido Á., Ruffell B. Dendritic cells and their role? A3B2 show [#,32] ?> in immunotherapy. *Front Immunol* (2020) 11:924. doi: 10.3389/fimmu.2020.00924

6. Shadbad MA, Hajiasgharzadeh K, Derakhshani A, Silvestris N, Baghbanzadeh A, Racanelli V, et al. From melanoma development to RNA-modified dendritic cell vaccines: Highlighting the lessons from the past. *Front Immunol* (2021) 12. doi: 10.3389/fimmu.2021.623639

7. Rosalia RA, Cruz LJ, Van Duikeren S, Tromp AT, Silva AL, Jiskoot W, et al. CD40-targeted dendritic cell delivery of PLGA-nanoparticle vaccines induce potent

anti-tumor responses. *Biomaterials* (2015) 40:88–97. doi: 10.1016/j.biomaterials.2014.10.053

8. Delirezh N, Moazzeni SM, Shokri F, Shokrgozar MA, Atri M, Kokhaei P. Autologous dendritic cells loaded with apoptotic tumor cells induce T cell-mediated immune responses against breast cancer *in vitro*. *Cell Immunol* (2009) 257:23–31. doi: 10.1016/j.cellimm.2009.02.002

9. Wu YG, Wu GZ, Wang L, Zhang YY, Li Z, Li DC. Tumor cell lysate-pulsed dendritic cells induce a T cell response against colon cancer *in vitro* and *in vivo*. *Med Oncol* (2010) 27:736–42. doi: 10.1007/s12032-009-9277-x

10. Gallois A, Bhardwaj N. Dendritic cell-targeted approaches to modulate immune dysfunction in the tumor microenvironment. *Front Immunol* (2013) 4:436. doi: 10.3389/fimmu.2013.00436

11. Veglia F, Gabrilovich DI. Dendritic cells in cancer: the role revisited. *Curr Opin Immunol* (2017) 45:43–51. doi: 10.1016/j.coi.2017.01.002

12. Laurent S, Carrega P, Saverino D, Piccioli P, Camoriano M, Morabito A, et al. CTLA-4 is expressed by human monocyte-derived dendritic cells and regulates their functions. *Hum Immunol* (2010) 71:934–41. doi: 10.1016/j.humimm.2010.07.007

13. Baumeister SH, Freeman GJ, Dranoff G, Sharpe AH. Coinhibitory pathways in immunotherapy for cancer. *Annu Rev Immunol* (2016) 34:539–73. doi: 10.1146/annurev-immunol-032414-112049

14. Wang XB, Fan ZZ, Anton D, Vollenhoven AV, Ni ZH, Chen XF, et al. CTLA4 is expressed on mature dendritic cells derived from human monocytes and influences their maturation and antigen presentation. *BMC Immunol* (2011) 12:21. doi: 10.1186/1471-2172-12-21

15. Han Y, Chen Z, Yang Y, Jiang Z, Gu Y, Liu Y, et al. Human CD14+ CTLA-4 + regulatory dendritic cells suppress T-cell response by cytotoxic T-lymphocyte antigen-4-dependent IL-10 and indoleamine-2,3-dioxygenase production in hepatocellular carcinoma. *Hepatology* (2014) 59:567–79. doi: 10.1002/hep.26694

16. Sung H, Ferlay J, Siegel RL, Laversanne M, Soerjomataram I, Jemal A, et al. Global cancer statistics 2020: GLOBOCAN estimates of incidence and mortality worldwide for 36 cancers in 185 countries. *CA Cancer J Clin* (2021) 71:209–49. doi: 10.3322/caac.21660

17. Derakhshani A, Hashemzadeh S, Asadzadeh Z, Shadbad MA, Rasibonab F, Safarpour H, et al. Cytotoxic T-lymphocyte antigen-4 in colorectal cancer: Another therapeutic side of capecitabine. *Cancers* (2021) 13:2414. doi: 10.3390/cancers13102414

18. Derakhshani A, Javadrashid D, Hemmat N, Dufour A, Solimando A, Duijf P, et al. Identification of common and distinct pathways in inflammatory bowel disease and colorectal cancer: A hypothesis based on weighted gene Co-expression network analysis. *Front Genet* (2022) 13. doi: 10.3389/fgene.2022.848646

19. Nomiri S, Hoshyar R, Chamani E, Rezaei Z, Salmani F, Larki P, et al. Prediction and validation of GUCA2B as the hub-gene in colorectal cancer based on co-expression network analysis: In-silico and *in-vivo* study. *Biomed. Pharmacotherapy* (2022) 147:112691. doi: 10.1016/j.biopha.2022.112691

20. Xie YH, Chen YX, Fang JY. Comprehensive review of targeted therapy for colorectal cancer. *Signal Transduct Target Ther* (2020) 5:22. doi: 10.1038/s41392-020-0116-z

21. Parikh AR, Szabolcs A, Allen JN, Clark JW, Wo JY, Raabe M, et al. Radiation therapy enhances immunotherapy response in microsatellite stable colorectal and pancreatic adenocarcinoma in a phase II trial. *Nat Cancer* (2021) 2:1124–35. doi: 10.1038/s43018-021-00269-7

22. Lenz HJ, Van Cutsem E, Luisa Limon M, Wong KYM, Hendlisz A, Aglietta M, et al. First-line nivolumab plus low-dose ipilimumab for microsatellite instability-High/Mismatch repair-deficient metastatic colorectal cancer: The phase II CheckMate 142 study. *J Clin Oncol* (2022) 40:161–70. doi: 10.1200/JCO.21.01015

23. Chung KY, Gore I, Fong L, Venook A, Beck SB, Dorazio P, et al. Phase II study of the anti-cytotoxic T-lymphocyte-associated antigen 4 monoclonal antibody, tremelimumab, in patients with refractory metastatic colorectal cancer. *J Clin Oncol* (2010) 28:3485–90. doi: 10.1200/JCO.2010.28.3994

24. Chen EX, Jonker DJ, Loree JM, Kennecke HF, Berry SR, Couture F, et al. Effect of combined immune checkpoint inhibition vs best supportive care alone in patients with advanced colorectal cancer: The Canadian cancer trials group CO.26 study. *JAMA Oncol* (2020) 6:831–8. doi: 10.1001/jamaoncol.2020.0910

25. Segal NH, Cercek A, Ku G, Wu AJ, Rimner A, Khalil DN, et al. Phase II single-arm study of durvalumab and tremelimumab with concurrent radiotherapy in patients with mismatch repair-proficient metastatic colorectal cancer. *Clin Cancer Res* (2021) 27:2200–8. doi: 10.1158/1078-0432.CCR-20-2474

26. Melief CJ, van der Burg SH. Immunotherapy of established (pre)malignant disease by synthetic long peptide vaccines. *Nat Rev Cancer* (2008) 8:351–60. doi: 10.1038/nrc2373

27. Zhu S, Yang N, Wu J, Wang X, Wang W, Liu YJ, et al. Tumor microenvironment-related dendritic cell deficiency: a target to enhance tumor immunotherapy. *Pharmacol Res* (2020) 159:104980. doi: 10.1016/j.phrs.2020.104980

28. Alemohammad H, Najafzadeh B, Asadzadeh Z, Baghbanzadeh A, Ghorbaninezhad F, Najafzadeh A, et al. The importance of immune checkpoints in immune monitoring: A future paradigm shift in the treatment of cancer. *BioMed Pharmacother* (2021) 146:112516. doi: 10.1016/j.biopha.2021.112516

29. Hargadon KM, Johnson CE, Williams CJ. Immune checkpoint blockade therapy for cancer: An overview of FDA-approved immune checkpoint inhibitors. *Int Immunopharmacol* (2018) 62:29–39. doi: 10.1016/j.intimp.2018.06.001

30. Hatfield P, Merrick AE, West E, O'donnell D, Selby P, Vile R, et al. Optimization of dendritic cell loading with tumor cell lysates for cancer immunotherapy. *J Immunother* (2008) 31:620–32. doi: 10.1097/CJI.0b013e31818213df

31. Fu C, Zhou N, Zhao Y, Duan J, Xu H, Wang Y. Dendritic cells loaded with CD44(+) CT-26 colon cell lysate evoke potent antitumor immune responses. *Oncol Lett* (2019) 18:5897–904. doi: 10.3892/ol.2019.10952

32. Van Den Bergh JMJ, Smits E, Berneman ZN, Hutten TJA, De Reu H, Van Tendeloo VFI, et al. Monocyte-derived dendritic cells with silenced PD-1 ligands and transpresenting interleukin-15 stimulate strong tumor-reactive T-cell expansion. *Cancer Immunol Res* (2017) 5:710–5. doi: 10.1158/2326-6066.CIR-16-0336

33. Peng Q, Qiu X, Zhang Z, Zhang S, Zhang Y, Liang Y, et al. PD-L1 on dendritic cells attenuates T cell activation and regulates response to immune checkpoint blockade. *Nat Commun* (2020) 11:4835. doi: 10.1038/s41467-020-18570-x

34. Nutt SL, Chopin M. Transcriptional networks driving dendritic cell differentiation and function. *Immunity* (2020) 52:942–56. doi: 10.1016/j.immuni.2020.05.005

35. Aerts J, De Goeje PL, Cornelissen R, Kaijen-Lambers MEH, Bezemer K, van der Leest CH, et al. Autologous dendritic cells pulsed with allogeneic tumor cell lysate in mesothelioma: From mouse to human. *Clin Cancer Res* (2018) 24:766–76. doi: 10.1158/1078-0432.CCR-17-2522

36. Kohnepoushi C, Nejati V, Delirezh N, Biparva P. Poly lactic-co-Glycolic acid nanoparticles containing human gastric tumor lysates as antigen delivery vehicles for dendritic cell-based antitumor immunotherapy. *Immunol Invest* (2019) 48:794–808. doi: 10.1080/08820139.2019.1610889

37. Schnurr M, Galambos P, Scholz C, Then F, Dauer M, Endres S, et al. Tumor cell lysate-pulsed human dendritic cells induce a T-cell response against pancreatic carcinoma cells: an *in vitro* model for the assessment of tumor vaccines. *Cancer Res* (2001) 61:6445–50.

38. Ge Y, Xi H, Ju S, Zhang X. Blockade of PD-1/PD-L1 immune checkpoint during DC vaccination induces potent protective immunity against breast cancer in hu-SCID mice. *Cancer Lett* (2013) 336:253–9. doi: 10.1016/j.canlet.2013.03.010

39. Roeven MW, Hobo W, van der Voort R, Fredrix H, Norde WJ, Teijgeler K, et al. Efficient nontoxic delivery of PD-L1 and PD-L2 siRNA into dendritic cell vaccines using the cationic lipid SAINT-18. *J Immunother* (2015) 38:145–54. doi: 10.1097/CJI.0000000000000071

40. Oh SA, Wu D-C, Cheung J, Navarro A, Xiong H, Cubas R, et al. PD-L1 expression by dendritic cells is a key regulator of T-cell immunity in cancer. *Nat Cancer* (2020) 1:681–91. doi: 10.1038/s43018-020-0075-x

41. Paul AG, Van Kooten PJ, Van Eden W, van der Zee R. Highly autoproliferative T cells specific for 60-kDa heat shock protein produce IL-4/IL-10 and IFN-gamma and are protective in adjuvant arthritis. *J Immunol* (2000) 165:7270–7. doi: 10.4049/jimmunol.165.12.7270

42. Kemper C, Chan AC, Green JM, Brett KA, Murphy KM, Atkinson JP. Activation of human CD4+ cells with CD3 and CD46 induces a T-regulatory cell 1 phenotype. *Nature* (2003) 421:388–92. doi: 10.1038/nature01315

43. Verhasselt V, Vosters O, Beuneu C, Nicaise C, Stordeur P, Goldman M. Induction of FOXP3-expressing regulatory CD4pos T cells by human mature autologous dendritic cells. *Eur J Immunol* (2004) 34:762–72. doi: 10.1002/eji.200324552

44. Cavatorta DJ, Erb HN, Felippe MJ. Activation-induced FoxP3 expression regulates cytokine production in conventional T cells stimulated with autologous dendritic cells. *Clin Vaccine Immunol* (2012) 19:1583–92. doi: 10.1128/CVI.00308-12

frontiers | Frontiers in Immunology

TYPE Mini Review
PUBLISHED 24 November 2022
DOI 10.3389/fimmu.2022.1007823

OPEN ACCESS

EDITED BY
Shyamasree Ghosh,
National Institute of Science Education and Research (NISER), India

REVIEWED BY
Sanjima Pal,
McGill University, Canada
Diane Bimczok,
Montana State University, United States

*CORRESPONDENCE
Mi Deng
mideng@bjmu.edu.cn

SPECIALTY SECTION
This article was submitted to Cancer Immunity and Immunotherapy, a section of the journal Frontiers in Immunology

RECEIVED 31 July 2022
ACCEPTED 25 October 2022
PUBLISHED 24 November 2022

CITATION
Wang Y, Yang T, Liang H and Deng M (2022) Cell atlas of the immune microenvironment in gastrointestinal cancers: Dendritic cells and beyond. *Front. Immunol.* 13:1007823. doi: 10.3389/fimmu.2022.1007823

Cell atlas of the immune microenvironment in gastrointestinal cancers: Dendritic cells and beyond

Yinuo Wang[1,2], Ting Yang[1,2], Huan Liang[2] and Mi Deng[1,2,3]*

[1]Peking University International Cancer Institute, Peking University Health Science Center, Peking University, Beijing, China, [2]School of Basic Medical Sciences, Peking University Health Science Center, Peking University, Beijing, China, [3]Peking University Cancer Hospital and Institute, Peking University Health Science Center, Peking University, Beijing, China

Gastrointestinal (GI) cancers occur in the alimentary tract and accessory organs. They exert a global burden with high morbidity and mortality. Inside the tumor microenvironment, dendritic cells (DCs) are the most efficient antigen-presenting cells and are necessary for adaptive immune responses such as T and B-cell maturation. However, the subsets of DCs revealed before were mostly based on flow cytometry and bulk sequencing. With the development of single-cell RNA sequencing (scRNA-seq), the tumor and microenvironment heterogeneity of GI cancer has been illustrated. In this review, we summarize the classification and development trajectory of dendritic cells at the single-cell level in GI cancer. Additionally, we focused on the interaction of DCs with T cells and their effect on the response to immunotherapy. Specifically, we focused on the newly identified tumor-infiltrating dendritic cells and discuss their potential function in antitumor immunity.

KEYWORDS

dendritic cells, T cells, gastrointestinal cancer, scRNA-seq, transcriptome

Introduction

Gastrointestinal carcinoma refers to malignancies that occur in the alimentary tract and accessory organs. It consists of six main types of cancer: oesophageal cancer (OC), gastric cancer (GC), liver cancer (LC), gallbladder and biliary tract cancer (BTC), pancreatic cancer (PC) and colorectal cancer (CRC) (1). There were 5.09 million new cases of GI cancer and 3.61 million related deaths, accounting for 26.4% of the worldwide cancer incidence and 36.3% of all cancer-related deaths, respectively (2). Additionally, these numbers are on the upward trend compared to the epidemiological data before (3).

At present, the main treatments for GI cancers include surgery, chemotherapy, radiotherapy and targeted therapy, and the rise of immunotherapy improves the ways against the tumors and has gradually become the first-line therapy in GI cancer. Apart from pancreatic cancer, most clinical trials of GI cancer combine the anti-PD-1 antibody with sequential chemotherapy or targeted therapy to create new therapeutic paradigms (Supplementary Table 1a). The overall response rate (ORR) ranged from 26.7%-76.7%. Unfortunately, in pancreatic cancer, immune checkpoint blockade (ICB) therapy fails (ORR is almost 0%) and does not prolong the survival time compared with chemotherapy (4–7). Although ICB combined with chemotherapy has a higher ORR than targeted therapy, approximately half of patients still cannot benefit from it due to nonresponse, drug resistance, recurrence or disease progression. The overall resistance to ICB therapy is 11%-71% across all tumor types (8). These data from clinical trials indicate that releasing only T-cell brakes cannot fully eliminate tumors. To elicit whole-body immune activation and long-lasting immune memory, novel therapy methods need to be developed.

Dendritic cells (DCs), as the most efficient antigen-presenting cells, bridge the innate and adaptive immune systems. In the tumor microenvironment, DCs represent a heterogeneous group. Single-cell RNA sequencing can identify new DC subpopulations. Additionally, new insights provided by the single-cell transcriptome and spatial transcriptome will likely reveal a plethora of new immunotherapeutic interventions targeting specific DC subsets or their products for the treatment of a variety of human disorders, including cancers. In this review, we focus on high-resolution data on dendritic cells in GI cancer.

Canonical development and traditional classification of DCs

Hematopoiesis gives rise to most immune cells. The classical three subtypes of DCs, monocyte-derived dendritic cells (Mo-DC), conventional dendritic cells (cDC) and plasmacytoid dendritic cells (pDC), all come from common dendritic progenitors (CDPs), common monocyte progenitors (cMoPs) (9) and IL-7R$^+$ lymphoid progenitor cells (10). In one way, cMoPs give rise to CD14$^+$ or CD16$^+$ monocytes. When circulating monocytes encounter antigens, they differentiate into Mo-DCs and migrate to tissues later (11). In another way, the CDPs come to pre-pDCs and pre-cDCs. cDCs have two subtypes, type 1 (cDC1) and type 2 (cDC2), marked by CLEC9A$^+$/CD141$^+$/XCR1$^+$ and CLEC10A$^+$/SIRPα^+/CD1c$^+$ expression, respectively. cDCs have superior antigen presentation capacity. cDC1s present antigens to CD8$^+$ T cells by MHC-I/TCR interactions, and cDC2s present antigens to CD4$^+$ T cells by MHC-II/TCR interactions. Additionally, cDC1s cross-presented tumor-associated antigen (TAA) or tumor-specific antigen (TSA) to generate antigen-specific cytotoxic T cells is crucial in antitumor immunity (12). Furthermore, pDCs have a rounded shape that resembles plasma cells. Marked by CD123 in human, pDCs function during viral infection. They produce type I interferon upon stimulation with toll-like receptor (TLR) 7/9 (13).

DCs are the most potent antigen-presenting cells (APCs). They have four main functions, phagocytosis, antigen presentation, costimulatory/inhibitory ability and cytokine secretion ability, to regulate immunity. As professional phagocytes, DCs have separate pathways to process endogenous and exogenous antigens (14–16). After antigen uptake, DCs matured. They upregulate costimulatory molecules, such as cluster of differentiation 80/86 (CD80/86) and inducible T-cell costimulatory ligand (ICOSL), to provide the second signal of T-cell activation and proliferation. In addition, they secrete proinflammatory cytokines, such as interleukin-12 (IL-12), to promote differentiation from Th0 to Th1 (17) and tumor necrosis factor-alpha (TNF-α) to induce tumor cell apoptosis (18). Recently, a subset of DCs, CD103$^+$DCs, have been considered to be crucial for trafficking to the lymph nodes and activating CD8$^+$ T cells (19). Additionally, anti-PD-L1 blockade requires CD103$^+$ DCs to promote but only have a partial response. Only when combined with FLT3L and poly I:C therapy can anti-PD-L1 blockade efficiently reduce tumors (20). Additionally, another study using an anti-PD-1 antibody and a multipeptide vaccine found that PD-1$^+$ DCs decreased and memory precursor CD8$^+$ T cells were upregulated (21). Altogether, these studies indicate the key subclusters of DCs in the response to immunotherapy and their regulation of memory CD8$^+$ T cells.

The updated taxonomy, ontogeny and new functions of DCs defined by scRNA-seq

With high-resolution sequencing technology at the single-cell level, novel clusters of DCs were discovered, and taxonomy was updated. First, cDC1 s and cDC2s come from the common dendritic cell progenitor (cDC progenitor), characterized by CD34^{int}CD100$^+$ (22). Moreover, a novel DC subcluster, AXL$^+$ DCs characterized by AXL and SIGLEC6, was first identified in the peripheral blood of humans (23). AXL$^+$DCs have a spectrum gene signature consisting of pDCs and cDCs, which indicates that they have the ability to give rise to both of them. Additionally, AXL$^+$DCs were also found in the cord blood, which reveals their origin (24). However, they are more similar to cDCs in the adult cord clood than pDCs in the peripheral blood transcriptionally. Furthermore, by inhibiting AXL receptor tyrosine kinase, Li et al. found that cDCs increase type I interferon secretion and enhance the proliferation of TCF1$^+$PD1$^+$CD8$^+$ T cells. This pathway sensitive the anti-PD1 blockade and restored the response (25).

Moreover, Rudensky et al. identified two functionally distinct cDC2 subclusters, T-bet$^+$cDC2s and T-bet-cDC2s, in mice (26).

T-bet$^+$cDC2s have an anti-inflammatory profile, while T-bet$^-$ cDC2s show pro-inflammatory characteristics, secreting more TNF-α and IL-6 than T-bet$^+$cDC2s. The researchers also validated that siglec-H$^+$ cells have the progenitor nature to give rise to these cDC2 subclusters within the spleen. And in human, CD1c^{lo}CLEC10A$^-$CLEC4A^{hi} cDC2s and CD1c$^+$CLEC10A$^+$CLEC4A^{lo} cDC2s are counterparts of T-bet$^+$cDC2s and T-bet$^-$cDC2s in mice. Moreover, T-bet$^+$cDC2s and CD1c^{lo}CLEC10A$^-$CLEC4A^{hi} cDC2s in the peripheral blood of mice and human respectively are absent consistently.

Recently, DCs were also found to maintain the exhaustion state in lymphoid or nonlymphoid tissue, which is vital during T-cell function (27, 28). Dähling et al. found that cDC1s prevent the overactivation of the precursors of exhausted T(Tpex) cells by providing a CCL21-dependent niche. They control their differentiation to exhausted T cells to balance the exhaustion state in the body (29). In addition, Schenkel et al. discovered that cDC1s helped tumor-specific CD8$^+$ T cells, TCF-1$^+$CD8$^+$ T cells, to proliferate and differentiate into a heterogeneous population and thus reduced tumor burden (30). These studies revealed new insights into the contribution of DCs to immunity.

Phenotypic alterations and novel tumor-infiltrating DCs identified by scRNA-seq

Although numerous potential stimulatory signals for DCs exist in the TME, many tumors also contain abundant amounts of immunosuppressive cytokines, such as IL-10 (31, 32). Orsini et al. found that colorectal cancer patients exhibited an impaired capacity to generate immature DCs from blood monocytes and lower expression levels of the costimulatory marker CD40 (33). Studies have found that the immunosuppressive chemokine CCL2 produced by tumor cells induces the autocrine secretion of lipocalin 2 (LCN2) and cooperatively generates immunoregulatory DCs (regDCs) with decreased HLA-DR expression and increased PD-L1 expression (34). In addition, the circulating pDCs recruited into the tumor microenvironment are characterized by decreased expression of costimulatory molecules and a reduced ability to produce type I interferons. Additionally, Li et al. found that pDCs played a potential role in recruiting Tregs, and both of them participate in the immunosuppressive microenvironment of GI cancer (35). Liu et al. also demonstrated that ICOS$^+$ Tregs and pDCs predict a poor prognosis of gastric cancer (36). However, Abolhalaj et al. found that the myeloid/plasmacytoid dendritic cell ratio (mDC/pDC) was elevated in tonsillar cancer (37). Therefore, the landscape of tumor-infiltrating DCs and their functions need to be clarified.

Single-cell RNA sequencing has promoted the precise understanding of the tumor microenvironment. In Supplementary Table 1b, we summarize some high-quality single-cell RNA-seq data of GI cancers based on human tumor sample sequencing. In general, the ratio of DCs and T cells ranges from 1:5~1:12 (38–41). The proportion of mDCs is higher than that of pDCs, but the study did not give an accurate number (38). Three groups of DCs, cDC1s (highly expressed CLEC9A/BATF3), cDC2s (highly expressed CD1C/CLEC10A), and plasmacytoid DCs (highly expressed LILRA4), were detected in tumor and adjacent tissues.

Furthermore, the subtypes of tumor-infiltrating DCs are conserved across GI cancers. Recently, a novel tumor-infiltrating DC that highly expresses CCL19/LAMP3/CCR7 was identified. LAMP3$^+$ cDCs were first identified by Zhang et al. (42) in hepatocarcinoma and is a kind of tumor-infiltrating DC that arises from cDC1 and cDC2. LAMP3$^+$ cDCs were found in 15 different cancer types, which demonstrates that they have a broad appearance in tumors (43). They have the ability to migrate to hepatic lymph nodes because of high CCR7 expression. Apart from nasopharyngeal cancer and pancreatic adenocarcinoma, LAMP3$^+$ cDCs preferentially come from cDC1s, which highly express IL12B and BTLA. Moreover, cDC2-derived LAMP3$^+$ cDCs showed high expression of CCL17. Although these two kinds of LAMP3$^+$ cDCs have distinct gene signatures, both of them have the capacity to induce Treg differentiation and recruitment. Additionally, the upregulated expression of PD-L1 and PD-L2 in LAMP3$^+$ cDCs was consistent. And LAMP3$^+$DCs were predicted to interact with PD-1 on Tregs, central memory T cells (CD4$^+$ T cells highly expressing IL7R and TCF7), and effector memory T cells (CD8$^+$ T cells highly expressing SELL GZMK) to regulate multiple kinds of T cells (42). Additionally, CCR7- and LAMP3-upregulated DCs were also detected in colorectal tumors (44). Altogether, these facts indicated that LAMP3$^+$ cDCs are newly identified regulatory-like dendritic cells in the TME.

Moreover, different from the previous theory mentioned above, scRNA-seq further predicts the ligand–receptor interaction between DCs and T cells (42). cDC1s (DC-CLEC9A) have the ability to present antigens to CD4$^+$T cells and cDC2 (DC-CD1c) are able to interact with CD8$^+$T cells. Moreover, Cheng et al. performed a pan-cancer scRNA-seq and found that the proportion of cDC2s was higher than that of cDC1s in tumors. Some research found that ascites from hepatocarcinoma patients were enriched with DCs expressing FCER1A (DC-FCER1A) (42).

Spatial distribution of dendritic cells in GI cancer

Apart from cell clustering at the single-cell level, the location of dendritic cells in the tumor is also crucial for their biological behavior. In oesophageal cancer, PD-L1$^+$ or PD-L1$^-$ DCs were nearest to PD-L1$^+$ or PD-L1$^-$ tumor cells, respectively (45). The closer distance between these two cells is correlated with better overall survival and progression-free survival. Moreover, in gastric cancer, DCs are sparse and scattered in the tumor (46). In hepatocarcinoma, cDCs were found to be significantly enriched in the normal regions instead of the tumor regions by spatial transcriptomics. Between the normal region and tumor region, there is a complete capsule that blocks the immune cells from

entering the tumor (47). Furthermore, pDCs highly marked with BDCA-2 are located in the tertiary lymphoid structure (TLS) and correlate with prolonged survival in colorectal cancer (48). These data indicate that anti-tumor cDCs are not enriched in the tumor and that pro-tumor pDCs may contribute to tumor progression in GI cancer.

Additionally, a kind of dendritic cell termed follicular dendritic cells (FDCs) specifically originate from stromal cells located in the primary lymphoid organs, secondary lymphoid organs and TLSs (49). FDCs mainly induce a humoral response, unlike the cDCs and pDCs mentioned before. They mainly secrete C-X-C motif chemokine ligand 13 (CXCL13) to recruit B cells to B-cell follicles and assist them in differentiating into plasma cells and memory cells. Unlike MHC-TCR antigen presentation in T-cell activation, FDCs present unprocessed antigen to B cells with immune complexes (50). FDCs, B cells, and T cells dominantly form the tertiary lymphoid structure, and TLSs are correlated with better overall survival and progression-free survival (51–53).

However, the spatial information of DCs is relatively limited. Many studies utilizing spatial transcriptomics have not paid much attention to dendritic cell distribution and its potential role in presenting antigens in tumors (54, 55). Therefore, it is necessary to identify the distribution of DCs in GI cancers since it is vital for antigen presentation behavior.

The difference between clinical samples and tumors from mouse models

The single-cell transcriptome and spatial transcriptome have revealed the DC atlas of human (Figure 1). However, the mouse model is the main preclinical model used to study dendritic cells and the immune system. To compare the difference in dendritic cells and T cells between human clinical samples and mouse tumors in GI cancer, we summarized the scRNA-seq data of mouse models in Supplementary Table 1b. Obviously, the subcluster differs between human and mice. Zhao et al. sequenced BALB/C, C57BL/6, SCID and SCID-HT29 liver cancer mouse models by scRNA-seq. They identified six DC subclusters, some of which were consistent with human data. Undeniably, the representative gene LILRA4, which is highly expressed in pDCs in humans, did not exist in mice. Additionally, the remarkable LAMP3 gene expression in human regDCs was dismissed in the mouse (56). A similar situation occurred in the CRC/GC mouse model, in which the classification of DC cells was too broad (57, 58). Additionally, DC gene expression in esophageal squamous cell carcinoma mouse models mostly does not match that in human tumors (59). Guilliams et al. (60) systematically compared murine and human liver cells at the single-cell level and found that the subclusters were mostly conserved. However, the gene expression of cDC1 s and cDC2s is quite distinct. Altogether, there is some discrepancy in the gene expression of the main immune clusters between mice and humans. The diversity of mouse cancer models is limited and cannot represent the heterogeneity of clinical samples.

To address the problem mentioned above, humanized model technology is appealing. The humanized mouse model (humice) refers to human CD34$^+$ cells/peripheral blood mononuclear cells (PBMCs) engrafted in severe combined immunodeficiency mice. Zhao et al. established the humice platform of liver cancer. Flow cytometry monitors at least twenty-one human immune subsets,

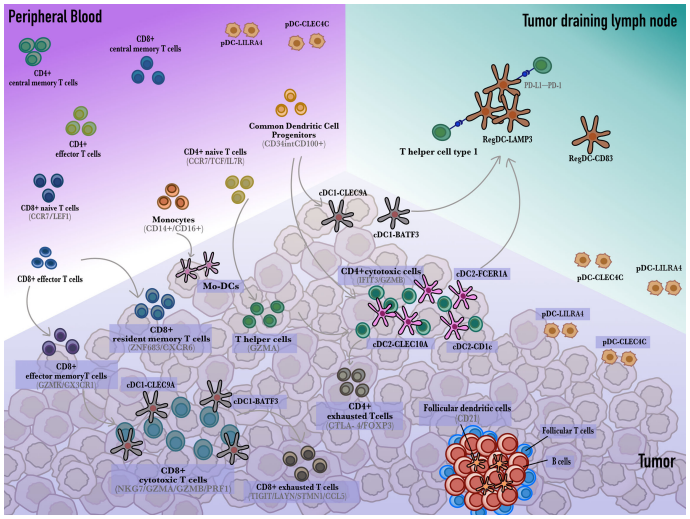

FIGURE 1
The developmental trajectory of dendritic cells and T cells. Monocytes circulate in the peripheral blood and differentiate into dendritic cells that sample and cargo tumor antigens. In the tumor draining lymph nodes, dendritic cells present antigens to CD4$^+$ or CD8$^+$ T cells to activate them into cytotoxic T cells. Additionally, cDCs also interact with resident CD8$^+$ T cells to develop into CD8$^+$ cytotoxic T cells. Besides, cDC1s and cDC2s give rise to regulatory LAMP3$^+$ DC which induce CD8$^+$ T cells exhaustion through the PD-L1-PD-1 axis.

including pDC and mDC, in peripheral blood and various cytokine secretion in sera for 8 weeks. Then, the patients' tumors were implanted subcutaneously in the humice. They found that the therapeutic effect of pembrolizumab was significantly better than that of ipilimumab. There were obvious toxic and side effects in humice when using ipilimumab, which is consistent with the clinical information (61). Therefore, the humice system provides a platform to detect the interaction between human immune cells and better imitates the cancer immunity of humans.

Therapeutic strategy of DC-based cancer treatment

DC-based immunotherapy mainly refers to DC-based cancer vaccines. DC vaccines are mostly based on Mo-DCs from patients, which are accessible and have a mature culture protocol. Monocytes can be induced to differentiate into DCs stimulated by IL-4 and GM-CSF and to mature by LPS (62–64), which is a convenient source to generate DC vaccines. Then, using tumor lysates or predicted personalized tumor antigens, mo-DCs are activated and transferred to the patients. There are ~80 phase I/II clinical trials to treat gastrointestinal cancer (Supplemental Table 2). DC vaccines are currently recommended to use a 'prime-boost' strategy. Traditional treatment modalities first induce immunogenic cell death (ICD), and subsequent DC vaccination can boost a stronger immune response (65). DC vaccines have successfully treated highly immunogenic cancer. Provenge is the first FDA-approved DC vaccine used to treat prostate cancer since 2010 (66). These attempts have elucidated the safety and response of DC vaccines elicited in patients. Generally, the strategy using DC vaccine is now recommended to combine chemotherapy or ICB therapy because the single ORR of DC vaccine did not exceed 15% (67).

Although some regimens do not target DCs directly, scRNA-seq detected changes in DCs contributing to a better response. In an MC38 CRC mouse model treated with anti-CD40 agonist therapy, $CCL22^+$ cDC1s along with $CCL5^+$ CD8 effector memory T cells were enriched, and an elevated cDC1 gene signature was correlated with longer overall survival (68). In another study, when undergoing anti-PD-1 or anti-CTLA-4 blockade therapy, CD8 effector memory T cells highly expressing GZMK and HSPA1A were also upregulated in patients, which the latter has not been annotated previously in liver cancer (69). However, scRNA-seq of patients or mouse models before and after treatment is limited, and more attention should be given to not only T cells.

Conclusion

Currently, scRNA-seq has identified novel subclusters and the precise function of DCs. In summary, conventional dendritic cells (cDC1 and cDC2) are the most efficient antigen presenting cells in the tumor draining lymph nodes and tumor microenvironment. The immunotherapy response is correlated with the interaction of cDCs and tumor-specific T cells. However, cDC1s and cDC2s can also differentiate into a subset of regulatory DCs ($LAMP3^+$ DCs) to hamper anti-tumor immunity. Therefore, the future strategy to develop novel DC vaccines is to elicit a $CD8^+$ T-cell response and prevent it from being changed by the immunosuppressive tumor microenvironment, thus eliminating the tumor burden.

Author contributions

YW collected literature data. YW, TY and HL conceived and wrote the manuscript. MD revised the manuscript. All authors contributed to the article and approved the submitted version.

Funding

This work was supported by the Imported Scholar Project and Startup from Peking University Health Science Center (BMU2021YJ063 to MD), the Biotechnology Innovation Plan from Beijing Sungen Biomedical Technology Co., Ltd (2022066 to MD), and the Excellent Young Scientists Fund Program (overseas) from National Natural Science Fund (2021HY-7 to MD). The funder Beijing Sungen Biomedical Technology Co., Ltd was not involved in the study design, collection, analysis, interpretation of data, the writing of this article or the decision to submit it for publication.

Conflict of interest

The authors declare that the research was conducted in the absence of any commercial or financial relationships that could be construed as a potential conflict of interest.

Publisher's note

Supplementary material

The Supplementary Material for this article can be found online at: https://www.frontiersin.org/articles/10.3389/fimmu.2022.1007823/full#supplementary-material

References

1. Abdul-Latif M, Townsend K, Dearman C, Shiu KK, Khan K. Immunotherapy in gastrointestinal cancer: The current scenario and future perspectives. *Cancer Treat Rev* (2020) 88:102030. doi: 10.1016/j.ctrv.2020.102030

2. Sung H, Ferlay J, Siegel RL, Laversanne M, Soerjomataram I, Jemal A, et al. Global cancer statistics 2020: GLOBOCAN estimates of incidence and mortality worldwide for 36 cancers in 185 countries. *CA Cancer J Clin* (2021) 71(3):209–49. doi: 10.3322/caac.21660

3. Arnold M, Abnet CC, Neale RE, Vignat J, Giovannucci EL, McGlynn KA, et al. Global burden of 5 major types of gastrointestinal cancer. *Gastroenterology.* (2020) 159(1):335–49.e15. doi: 10.1053/j.gastro.2020.02.068

4. Brahmer JR, Tykodi SS, Chow LQ, Hwu WJ, Topalian SL, Hwu P, et al. Safety and activity of anti-PD-L1 antibody in patients with advanced cancer. *New Engl J Med* (2012) 366(26):2455–65. doi: 10.1056/NEJMoa1200694

5. Weiss GJ, Waypa J, Blaydorn L, Coats J, McGahey K, Sangal A, et al. A phase ib study of pembrolizumab plus chemotherapy in patients with advanced cancer (PembroPlus). *Br J Cancer.* (2017) 117(1):33–40. doi: 10.1038/bjc.2017.145

6. Royal RE, Levy C, Turner K, Mathur A, Hughes M, Kammula US, et al. Phase 2 trial of single agent ipilimumab (anti-CTLA-4) for locally advanced or metastatic pancreatic adenocarcinoma. *J Immunother.* (2010) 33(8):828–33. doi: 10.1097/CJI.0b013e3181eec14c

7. O'Reilly EM, Oh D-Y, Dhani N, Renouf DJ, Lee MA, Sun W, et al. Durvalumab with or without tremelimumab for patients with metastatic pancreatic ductal adenocarcinoma: A phase 2 randomized clinical trial. *JAMA Oncol* (2019) 5(10):1431–8. doi: 10.1001/jamaoncol.2019.1588

8. Schoenfeld AJ, Hellmann MD. Acquired resistance to immune checkpoint inhibitors. *Cancer Cell* (2020) 37(4):443–55. doi: 10.1016/j.ccell.2020.03.017

9. Geissmann F, Manz MG, Jung S, Sieweke MH, Merad M, Ley K. Development of monocytes, macrophages, and dendritic cells. *Science.* (2010) 327(5966):656–61. doi: 10.1126/science.1178331

10. Rodrigues PF, Alberti-Servera L, Eremin A, Grajales-Reyes GE, Ivanek R, Tussiwand R. Distinct progenitor lineages contribute to the heterogeneity of plasmacytoid dendritic cells. *Nat Immunol* (2018) 19(7):711–22. doi: 10.1038/s41590-018-0136-9

11. Randolph GJ, Beaulieu S, Lebecque S, Steinman RM, Muller WA. Differentiation of monocytes into dendritic cells in a model of transendothelial trafficking. *Science.* (1998) 282(5388):480–3. doi: 10.1126/science.282.5388.480

12. Sánchez-Paulete AR, Teijeira A, Cueto FJ, Garasa S, Pérez-Gracia JL, Sánchez-Arráez A, et al. Antigen cross-presentation and T-cell cross-priming in cancer immunology and immunotherapy. *Ann Oncol* (2017) 28:xii44–55. doi: 10.1093/annonc/mdx237

13. Cella M, Jarrossay D, Facchetti F, Alebardi O, Nakajima H, Lanzavecchia A, et al. Plasmacytoid monocytes migrate to inflamed lymph nodes and produce large amounts of type I interferon. *Nat Med* (1999) 5(8):919–23. doi: 10.1038/11360

14. Hilligan KL, Ronchese F. Antigen presentation by dendritic cells and their instruction of CD4+ T helper cell responses. *Cell Mol Immunol* (2020) 17(6):587–99. doi: 10.1038/s41423-020-0465-0

15. ten Broeke T, Wubbolts R, Stoorvogel W. MHC class II antigen presentation by dendritic cells regulated through endosomal sorting. *Cold Spring Harbor Perspect Biol* (2013) 5(12):a016873–a. doi: 10.1101/cshperspect.a016873

16. Blum JS, Wearsch PA, Cresswell P. Pathways of antigen processing. *Annu Rev Immunol* (2013) 31:443–73. doi: 10.1146/annurev-immunol-032712-095910

17. Heufler C, Koch F, Stanzl U, Topar G, Wysocka M, Trinchieri G, et al. Interleukin-12 is produced by dendritic cells and mediates T helper 1 development as well as interferon-gamma production by T helper 1 cells. *Eur J Immunol* (1996) 26(3):659–68. doi: 10.1002/eji.1830260323

18. deLuca LS, Gommerman JL. Fine-tuning of dendritic cell biology by the TNF superfamily. *Nat Rev Immunol* (2012) 12(5):339–51. doi: 10.1038/nri3193

19. Roberts EW, Broz ML, Binnewies M, Headley MB, Nelson AE, Wolf DM, et al. Critical role for CD103(+)/CD141(+) dendritic cells bearing CCR7 for tumor antigen trafficking and priming of T cell immunity in melanoma. *Cancer Cell* (2016) 30(2):324–36. doi: 10.1016/j.ccell.2016.06.003

20. Salmon H, Idoyaga J, Rahman A, Leboeuf M, Remark R, Jordan S, et al. Expansion and activation of CD103(+) dendritic cell progenitors at the tumor site enhances tumor responses to therapeutic PD-L1 and BRAF inhibition. *Immunity.* (2016) 44(4):924–38. doi: 10.1016/j.immuni.2016.03.012

21. Karyampudi L, Lamichhane P, Scheid AD, Kalli KR, Shreeder B, Krempski JW, et al. Accumulation of memory precursor CD8 T cells in regressing tumors following combination therapy with vaccine and anti-PD-1 antibody. *Cancer Res* (2014) 74(11):2974–85. doi: 10.1158/0008-5472.CAN-13-2564

22. Villani A-C, Satija R, Reynolds G, Sarkizova S, Shekhar K, Fletcher J, et al. Single-cell RNA-seq reveals new types of human blood dendritic cells, monocytes, and progenitors. *Science* (2017) 356(6335):eaah4573. doi: 10.1126/science.aah4573

23. Alcántara-Hernández M, Leylek R, Wagar LE, Engleman EG, Keler T, Marinkovich MP, et al. High-dimensional phenotypic mapping of human dendritic cells reveals interindividual variation and tissue specialization. *Immunity.* (2017) 47(6):1037–50.e6. doi: 10.1016/j.immuni.2017.11.001

24. Jin X, Meng L, Yin Z, Yu H, Zhang L, Liang W, et al. Characterization of dendritic cell subtypes in human cord blood by single-cell sequencing. *Biophysics Rep* (2019) 5(4):199–208. doi: 10.1007/s41048-019-00096-5

25. Li H, Liu Z, Liu L, Zhang H, Han C, Girard L, et al. AXL targeting restores PD-1 blockade sensitivity of STK11/LKB1 mutant NSCLC through expansion of TCF1+ CD8 T cells. *Cell Rep Med* (2022) 3(3):100554. doi: 10.1016/j.xcrm.2022.100554

26. Brown CC, Gudjonson H, Pritykin Y, Deep D, Lavallée VP, Mendoza A, et al. Transcriptional basis of mouse and human dendritic cell heterogeneity. *Cell.* (2019) 179(4):846–63.e24. doi: 10.1016/j.cell.2019.09.035

27. Zammit DJ, Cauley LS, Pham QM, Lefrançois L. Dendritic cells maximize the memory CD8 T cell response to infection. *Immunity.* (2005) 22(5):561–70. doi: 10.1016/j.immuni.2005.03.005

28. Wakim LM, Waithman J, van Rooijen N, Heath WR, Carbone FR. Dendritic cell-induced memory T cell activation in nonlymphoid tissues. *Science.* (2008) 319(5860):198–202. doi: 10.1126/science.1151869

29. Dähling S, Mansilla AM, Knöpper K, Grafen A, Utzschneider DT, Ugur M, et al. Type 1 conventional dendritic cells maintain and guide the differentiation of precursors of exhausted T cells in distinct cellular niches. *Immunity.* (2022) 55(4):656–70.e8. doi: 10.1016/j.immuni.2022.03.006

30. Schenkel JM, Herbst RH, Canner D, Li A, Hillman M, Shanahan SL, et al. Conventional type I dendritic cells maintain a reservoir of proliferative tumor-antigen specific TCF-1(+) CD8(+) T cells in tumor-draining lymph nodes. *Immunity.* (2021) 54(10):2338–53.e6. doi: 10.1016/j.immuni.2021.08.026

31. DeVito NC, Plebanek MP, Theivanthiran B, Hanks BA. Role of tumor-mediated dendritic cell tolerization in immune evasion. *Front Immunol* (2019) 10:2876. doi: 10.3389/fimmu.2019.02876

32. Chrisikos TT, Zhou Y, Slone N, Babcock R, Watowich SS, Li HS. Molecular regulation of dendritic cell development and function in homeostasis, inflammation, and cancer. *Mol Immunol* (2019) 110:24–39. doi: 10.1016/j.molimm.2018.01.014

33. Orsini G, Legitimo A, Failli A, Ferrari P, Nicolini A, Spisni R, et al. Defective generation and maturation of dendritic cells from monocytes in colorectal cancer patients during the course of disease. *Int J Mol Sci* (2013) 14(11):22022–41. doi: 10.3390/ijms141122022

34. Kudo-Saito C, Shirako H, Ohike M, Tsukamoto N, Kawakami Y. CCL2 is critical for immunosuppression to promote cancer metastasis. *Clin Exp Metastasis.* (2013) 30(4):393–405. doi: 10.1007/s10585-012-9545-6

35. Li S, Wu J, Zhu S, Liu Y-J, Chen J. Disease-associated plasmacytoid dendritic cells. *Front Immunol* (2017) 8. doi: 10.3389/fimmu.2017.01268

36. Liu X, Yu H, Yan C, Mei Y, Lin C, Hong Y, et al. Plasmacytoid dendritic cells and ICOS(+) regulatory T cells predict poor prognosis in gastric cancer: A pilot study. *J Cancer.* (2019) 10(26):6711–5. doi: 10.7150/jca.34826

37. Abolhalaj M, Askmyr D, Sakellariou CA, Lundberg K, Greiff L, Lindstedt M. Profiling dendritic cell subsets in head and neck squamous cell tonsillar cancer and benign tonsils. *Sci Rep* (2018) 8(1):8030. doi: 10.1038/s41598-018-26193-y

38. Zheng Y, Chen Z, Han Y, Han L, Zou X, Zhou B, et al. Immune suppressive landscape in the human esophageal squamous cell carcinoma microenvironment. *Nat Commun* (2020) 11(1):6268. doi: 10.1038/s41467-020-20019-0

39. Kumar V, Ramnarayanan K, Sundar R, Padmanabhan N, Srivastava S, Koiwa M, et al. Single-cell atlas of lineage states, tumor microenvironment, and subtype-specific expression programs in gastric cancer. *Cancer Discovery* (2022) 12(3):670–91. doi: 10.1158/2159-8290.CD-21-0683

40. Zhang M, Yang H, Wan L, Wang Z, Wang H, Ge C, et al. Single-cell transcriptomic architecture and intercellular crosstalk of human intrahepatic cholangiocarcinoma. *J Hepatol* (2020) 73(5):1118–30. doi: 10.1016/j.jhep.2020.05.039

41. Zhang Y, Song J, Zhao Z, Yang M, Chen M, Liu C, et al. Single-cell transcriptome analysis reveals tumor immune microenvironment heterogenicity and granulocytes enrichment in colorectal cancer liver metastases. *Cancer Lett* (2020) 470:84–94. doi: 10.1016/j.canlet.2019.10.016

42. Zhang Q, He Y, Luo N, Patel SJ, Han Y, Gao R, et al. Landscape and dynamics of single immune cells in hepatocellular carcinoma. *Cell.* (2019) 179(4):829–45.e20. doi: 10.1016/j.cell.2019.10.003

43. Cheng S, Li Z, Gao R, Xing B, Gao Y, Yang Y, et al. A pan-cancer single-cell transcriptional atlas of tumor infiltrating myeloid cells. *Cell.* (2021) 184(3):792–809.e23. doi: 10.1016/j.cell.2021.01.010

44. Qian J, Olbrecht S, Boeckx B, Vos H, Laoui D, Etlioglu E, et al. A pan-cancer blueprint of the heterogeneous tumor microenvironment revealed by single-cell profiling. *Cell Res* (2020) 30(9):745–62. doi: 10.1038/s41422-020-0355-0

45. Ma X, Guo Z, Wei X, Zhao G, Han D , Zhang T, et al. Spatial distribution and predictive significance of dendritic cells and macrophages in esophageal cancer treated with combined chemoradiotherapy and PD-1 blockade. *Front Immunol* (2021) 12:786429. doi: 10.3389/fimmu.2021.786429

46. Du T, Gao H, Wu H, Li J, Li P, Gao J, et al. Comprehensive dissection of immune microenvironment in the progression of early gastric cancer at spatial and single-cell resolution. *bioRxiv* (2022). doi: 10.1101/2022.02.16.480776

47. Wu R, Guo W, Qiu X, Wang S, Sui C, Lian Q, et al. Comprehensive analysis of spatial architecture in primary liver cancer. *Sci Adv* (2021) 7(51):eabg3750. doi: 10.1126/sciadv.abg3750

48. Kießler M, Plesca I, Sommer U, Wehner R, Wilczkowski F, Müller L, et al. Tumor-infiltrating plasmacytoid dendritic cells are associated with survival in human colon cancer. *J Immunother Cancer* (2021) 9(3):e001813. doi: 10.1136/jitc-2020-001813

49. Kranich J, Krautler NJ. How follicular dendritic cells shape the b-cell antigenome. *Front Immunol* (2016) 7:225. doi: 10.3389/fimmu.2016.00225

50. Krautler NJ, Kana V, Kranich J, Tian Y, Perera D, Lemm D, et al. Follicular dendritic cells emerge from ubiquitous perivascular precursors. *Cell.* (2012) 150 (1):194–206. doi: 10.1016/j.cell.2012.05.032

51. Helmink BA, Reddy SM, Gao J, Zhang S, Basar R, Thakur R, et al. B cells and tertiary lymphoid structures promote immunotherapy response. *Nature.* (2020) 577(7791):549–55. doi: 10.1038/s41586-019-1922-8

52. Petitprez F, de Reyniès A, Keung EZ, Chen TW, Sun CM, Calderaro J, et al. B cells are associated with survival and immunotherapy response in sarcoma. *Nature.* (2020) 577(7791):556–60. doi: 10.1038/s41586-019-1906-8

53. Cabrita R, Lauss M, Sanna A, Donia M, Skaarup Larsen M, Mitra S, et al. Tertiary lymphoid structures improve immunotherapy and survival in melanoma. *Nature.* (2020) 577(7791):561–5. doi: 10.1038/s41586-019-1914-8

54. Väyrynen SA, Zhang J, Yuan C, Väyrynen JP, Dias Costa A, Williams H, et al. Composition, spatial characteristics, and prognostic significance of myeloid cell infiltration in pancreatic cancer. *Clin Cancer Res* (2021) 27(4):1069–81. doi: 10.1158/1078-0432.CCR-20-3141

55. Guo JA, Hoffman HI, Weekes CD, Zheng L, Ting DT, Hwang WL. Refining the molecular framework for pancreatic cancer with single-cell and spatial technologies. *Clin Cancer Res* (2021) 27(14):3825–33. doi: 10.1158/1078-0432.CCR-20-4712

56. Zhao Q, Molina-Portela MDP, Parveen A, Adler A, Adler C, Hock E, et al. Heterogeneity and chimerism of endothelial cells revealed by single-cell transcriptome in orthotopic liver tumors. *Angiogenesis.* (2020) 23(4):581–97. doi: 10.1007/s10456-020-09727-9

57. Nagaoka K, Shirai M, Taniguchi K, Hosoi A, Sun C, Kobayashi Y, et al. Deep immunophenotyping at the single-cell level identifies a combination of anti-IL-17 and checkpoint blockade as an effective treatment in a preclinical model of data-guided personalized immunotherapy. *J Immunother Cancer* (2020) 8(2):e001358. doi: 10.1136/jitc-2020-001358

58. Geller AE, Shrestha R, Woeste MR, Guo H, Hu X, Ding C, et al. The induction of peripheral trained immunity in the pancreas incites anti-tumor activity to control pancreatic cancer progression. *Nat Commun* (2022) 13(1):759. doi: 10.1038/s41467-022-28407-4

59. Yao J, Cui Q, Fan W, Ma Y, Chen Y, Liu T, et al. Single-cell transcriptomic analysis in a mouse model deciphers cell transition states in the multistep development of esophageal cancer. *Nat Commun* (2020) 11(1):3715. doi: 10.1038/s41467-020-17492-y

60. Guilliams M, Bonnardel J, Haest B, Vanderborght B, Wagner C, Remmerie A, et al. Spatial proteogenomics reveals distinct and evolutionarily conserved hepatic macrophage niches. *Cell.* (2022) 185(2):379–96.e38. doi: 10.1016/j.cell.2021.12.018

61. Zhao Y, Shuen TWH, Toh TB, Chan XY, Liu M, Tan SY, et al. Development of a new patient-derived xenograft humanised mouse model to study human-specific tumour microenvironment and immunotherapy. *Gut.* (2018) 67(10):1845–54. doi: 10.1136/gutjnl-2017-315201

62. Inaba K, Inaba M, Romani N, Aya H, Deguchi M, Ikehara S, et al. Generation of large numbers of dendritic cells from mouse bone marrow cultures supplemented with granulocyte/macrophage colony-stimulating factor. *J Exp Med* (1992) 176 (6):1693–702. doi: 10.1084/jem.176.6.1693

63. Lutz MB, Kukutsch N, Ogilvie AL, Rössner S, Koch F, Romani N, et al. An advanced culture method for generating large quantities of highly pure dendritic cells from mouse bone marrow. *J Immunol Methods* (1999) 223(1):77–92. doi: 10.1016/S0022-1759(98)00204-X

64. Son YI, Egawa S, Tatsumi T, Redlinger REJr., Kalinski P, Kanto T. A novel bulk-culture method for generating mature dendritic cells from mouse bone marrow cells. *J Immunol Methods* (2002) 262(1-2):145–57. doi: 10.1016/S0022-1759(02)00013-3

65. Harari A, Graciotti M, Bassani-Sternberg M, Kandalaft LE. Antitumour dendritic cell vaccination in a priming and boosting approach. *Nat Rev Drug Discovery* (2020) 19(9):635–52. doi: 10.1038/s41573-020-0074-8

66. Kantoff PW, Higano CS, Shore ND, Berger ER, Small EJ, Penson DF, et al. Sipuleucel-T immunotherapy for castration-resistant prostate cancer. *New Engl J Med* (2010) 363(5):411–22. doi: 10.1056/NEJMoa1001294

67. Garg AD, Coulie PG, Van den Eynde BJ, Agostinis P. Integrating next-generation dendritic cell vaccines into the current cancer immunotherapy landscape. *Trends Immunol* (2017) 38(8):577–93. doi: 10.1016/j.it.2017.05.006

68. Zhang L, Li Z, Skrzypczynska KM, Fang Q, Zhang W, O'Brien SA, et al. Single-cell analyses inform mechanisms of myeloid-targeted therapies in colon cancer. *Cell.* (2020) 181(2):442–59.e29. doi: 10.1016/j.cell.2020.03.048

69. Ma L, Wang L, Khatib SA, Chang C-W, Heinrich S, Dominguez DA, et al. Single-cell atlas of tumor cell evolution in response to therapy in hepatocellular carcinoma and intrahepatic cholangiocarcinoma. *J Hepatology.* (2021) 75(6):1397–408. doi: 10.1016/j.jhep.2021.06.028

frontiers | Frontiers in Immunology

TYPE Original Research
PUBLISHED 25 January 2023
DOI 10.3389/fimmu.2023.1105244

OPEN ACCESS

EDITED BY
Mi Deng,
Peking University, China

REVIEWED BY
Zhaohui Wang,
Duke University, United States
Ana Patricia Cardoso,
University of Porto, Portugal
Diane Bimczok,
Montana State University, United States

*CORRESPONDENCE
I. Jolanda M. de Vries
Jolanda.deVries@radboudumc.nl

†These authors share last authorship

SPECIALTY SECTION
This article was submitted to Cancer Immunity and Immunotherapy, a section of the journal Frontiers in Immunology

RECEIVED 22 November 2022
ACCEPTED 12 January 2023
PUBLISHED 25 January 2023

CITATION
Subtil B, Iyer KK, Poel D, Bakkerus L, Gorris MAJ, Escalona JC, Dries Kvd, Cambi A, Verheul HMW, de Vries IJM and Tauriello DVF (2023) Dendritic cell phenotype and function in a 3D co-culture model of patient-derived metastatic colorectal cancer organoids. *Front. Immunol.* 14:1105244. doi: 10.3389/fimmu.2023.1105244

Dendritic cell phenotype and function in a 3D co-culture model of patient-derived metastatic colorectal cancer organoids

Beatriz Subtil[1,2], Kirti K. Iyer[2,3], Dennis Poel[2,3], Lotte Bakkerus[3], Mark A. J. Gorris[1,4], Jorge Cuenca Escalona[1], Koen van den Dries[2], Alessandra Cambi[2], Henk M. W. Verheul[5], I. Jolanda M. de Vries[1*†] and Daniele V. F. Tauriello[2†]

[1]Department of Tumor Immunology, Radboud Institute for Molecular Life Sciences, Radboud University Medical Center, Nijmegen, Netherlands, [2]Department of Cell Biology, Radboud Institute for Molecular Life Sciences, Radboud University Medical Center, Nijmegen, Netherlands, [3]Department of Medical Oncology, Radboud Institute for Molecular Life Sciences, Radboud University Medical Center, Nijmegen, Netherlands, [4]Oncode Institute, Nijmegen, Netherlands, [5]Department of Medical Oncology, Erasmus Medical Center, Rotterdam, Netherlands

Colorectal cancer (CRC) remains one of the most aggressive and lethal cancers, with metastasis accounting for most deaths. As such, there is an unmet need for improved therapies for metastatic CRC (mCRC). Currently, the research focus is shifting towards the reciprocal interactions within the tumor microenvironment (TME), which prevent tumor clearance by the immune system. Dendritic cells (DCs) play a key role in the initiation and amplification of anti-tumor immune responses and in driving the clinical success of immunotherapies. Dissecting the interactions between DCs and CRC cells may open doors to identifying key mediators in tumor progression, and possible therapeutic targets. This requires representative, robust and versatile models and tools. Currently, there is a shortage of such *in vitro* systems to model the CRC TME and its tumor-immune cell interactions. Here we develop and establish a dynamic organotypic 3D co-culture system to recapitulate and untangle the interactions between DCs and patient-derived mCRC tumor organoids. To our knowledge, this is the first study investigating human DCs in co-culture with tumor organoids in a 3D, organotypic setting. This system reveals how mCRC organoids modulate and shape monocyte-derived DCs (MoDCs) behavior, phenotype, and function, within a collagen matrix, using techniques such as brightfield and fluorescence microscopy, flow cytometry, and fluorescence-activated cell sorting. Our 3D co-culture model shows high viability and extensive interaction between DCs and tumor organoids, and its structure resembles patient tissue sections. Furthermore, it is possible to retrieve DCs from the co-cultures and characterize their phenotypic and functional profile. In our study, the expression of activation markers in both mature and immature DCs and their ability to activate T cells were impacted by co-culture with tumor

10.3389/fimmu.2023.1105244

organoids. In the future, this direct co-culture platform can be adapted and exploited to study the CRC-DC interplay in more detail, enabling novel and broader insights into CRC-driven DC (dys)function.

KEYWORDS

human dendritic cells, dendritic cell dysfunction, immunosuppression, 3D co-culture, tumor microenvironment, metastatic colorectal cancer, patient-derived tumor organoids

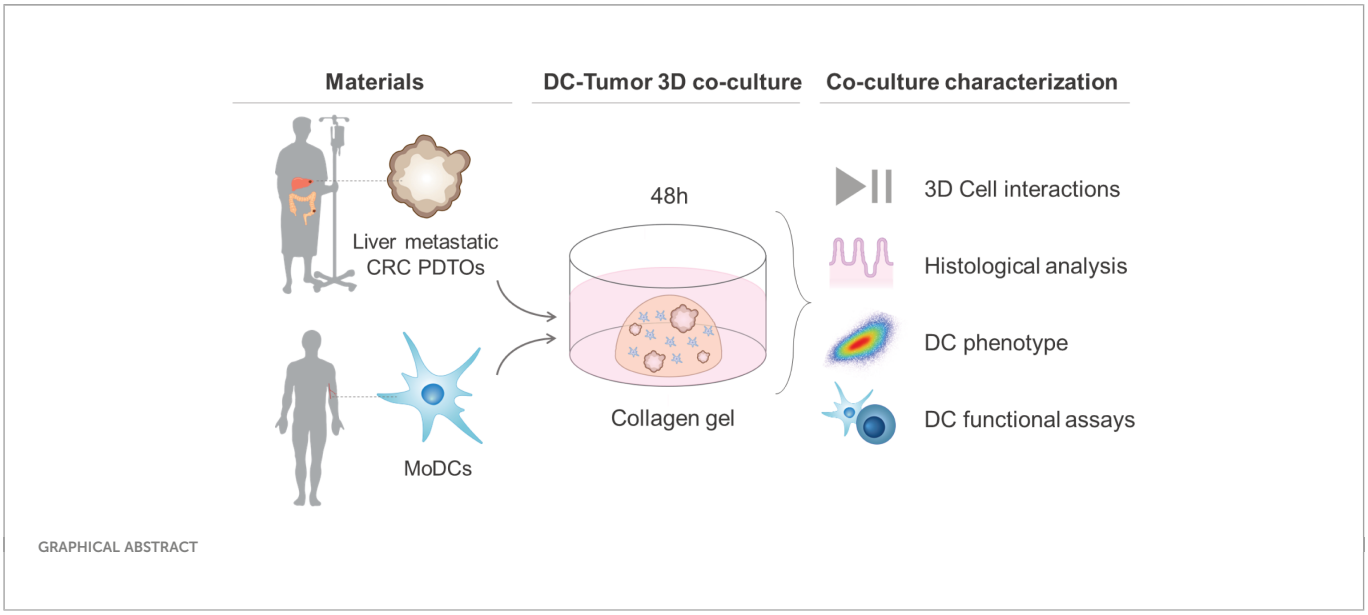

GRAPHICAL ABSTRACT

1 Introduction

Colorectal cancer (CRC) is one of the world's most prevalent cancers and the second leading cause of cancer-associated mortality. For patients diagnosed at an early stage, the 5-year survival rate is as high as 90%. The survival rate, however, drops to only around 15% for advanced and metastatic disease (1). During disease progression, approximately half of patients develop metastases, with the liver as the most frequent metastatic site (1, 2). Most CRC-related deaths are thus not caused by the primary tumor but by distant metastases, which are often resistant to treatment (surgery, chemo-, targeted- and immunotherapy) (3). Treatment unresponsiveness in metastatic disease has been linked to a strongly immunosuppressive tumor microenvironment (TME) (4–6). CRC has evolved a number of escape mechanisms to induce immune suppression including the exclusion and corruption of immune cells. This either occurs through direct cell-to-cell contact or paracrine signaling, for which the molecular mechanisms remain incompletely understood. It is therefore crucial to further our understanding of the complex interactions between tumors and immune cells in order to eventually develop and improve treatment strategies.

Dendritic cells (DCs) are the key orchestrators of anti-tumor immune responses and have been shown to be locally and systemically impaired in cancer patients, including CRC (7). Under physiological conditions, DCs constantly patrol and scan the environment for danger signals in an immature state. In the presence of tumor antigens and danger signals, DCs become activated, mature, and trigger anti-tumor immune responses (8). As such, they have the unique capacity to link the innate and adaptive immune system by (cross)-presenting antigens and priming T cells (9, 10). Importantly, this implies that effector T cell responses against cancer-specific antigens require functional and mature DCs (11, 12). In an immunosuppressive tumor setting, DCs become locked in or regress into an immature state, which compromises their ability to activate T cells leading to T cell anergy and Treg recruitment, and in this way foster tumor tolerance (13–16). In agreement, several studies implicate dysfunctional DCs in immune evasion, tumor growth, metastasis initiation, and treatment resistance in CRC, clearly indicating that DCs not only dictate the outcome of anti-tumor immunity but also of treatment response (17).

Despite the critical role of DCs in anti-tumor immunity and immunotherapy response in cancer, the CRC-specific mechanisms shaping and regulating DC phenotype and functionality are still largely unknown. Unveiling the crosstalk between CRC and DCs brings hope for identifying and modulating key mechanisms and pathways involved in tumor progression and spread. This presupposes unexplored opportunities for therapeutically reverting tumor-induced DC suppression and enhancing anti-tumor immunity (16, 18).

To gain insights into these CRC-DC interactions, it is crucial to have suitable and representative models and tools to study and unveil the underlying molecular mechanisms. Animal models of CRC,

despite mimicking several features of the human disease, cannot faithfully represent the complexity of the human TME. In addition, mouse and human DC subsets differ considerably, impairing subset-specific studies. There is a shortage of *in vitro* systems that faithfully model the primary and metastatic CRC TME and its tumor-stromal cell interactions. Moreover, existing *in vitro* 2D co-culture systems, albeit highly accessible and inexpensive, fail to recapitulate cell shape and polarization, as well as, tumor complexity, heterogeneity, and 3D spatial interactions within the TME (19). As such, there is a pressing need for clinically and physiologically relevant systems that enable the dissection of cellular interactions, and assessment of individual contributions to certain phenotypes within the CRC TME.

3D co-culture models using tumor spheroids or organoids aim to overcome the shortcomings of previous *in vitro* models and shorten the gap between the ability to manipulate the system and physiological relevance (20, 21). These appear to be promising tools to better recreate the complex interactions between tumor cells and other cells that compose the TME, including DCs. To date, spheroid-based TME models for different tumors have been developed to investigate DCs behavior and plasticity (22–24). However, spheroids fall short of representing glandular differentiation and polarization, as well as tumor heterogeneity, one of the key features of CRC. In contrast, patient-derived tumor organoids (PDTOs) are heterogenous self-organizing populations of tumor cells, resembling the architecture, and preserving morphological and mutational features of the tissue of origin (20, 21, 25–27). As such, PDTOs represent a relevant and appropriate *in vitro* platform for biological studies and testing personalized medicine. Furthermore, studies have shown that organoid co-culture systems can be successfully used to study and recapitulate interactions between cancer cells and immune cells (27–30). Recently, a co-culture model of MoDCs and healthy human gastric organoids in a controlled and complex microphysiological chip platform was developed (31). Yet, studying DC-CRC interactions using PDTOS in a 3D context is still an unexplored field with many opportunities.

Here, we describe the development of a representative and relevant 3D co-culture system between human DCs and patient-derived liver metastatic CRC organoids. In our co-culture system, monocyte-derived DCs (MoDCs) from healthy donors were used as a human DC model and cultured in a 3D collagen matrix in the presence or absence of PDTOs. MoDCs were added to the co-culture system in an immature (iDCs) or mature state (mDCs) as both can be found infiltrating the TME, and have different roles and behaviors (12). The two CRC liver metastasis PDTOs used in this study were selected based on their different morphology – cystic and compact/dense. Furthermore, we present an associated toolbox that includes live-cell microscopy, histological analysis, immunofluorescence, flow cytometry, and cell sorting to assess and characterize the tumor effect on the behavior, phenotype, and functionality of DCs.

2 Materials and methods

2.1 Human samples and patient material

Blood samples (buffy coats) from healthy donors were obtained *via* Sanquin Blood Bank (Sanquin Bloedvoorziening, Nijmegen, the Netherlands). Needle biopsies and resection material from liver metastasis of CRC patients and tumor tissue sections were obtained within the context of the ORCHESTRA trial (NCT01792934). All healthy donors and patients gave written informed consent.

2.2 Isolation of peripheral blood mononuclear cells

Peripheral blood mononuclear cells (PBMCs) were isolated from buffy coats by density gradient centrifugation at 500 x g at room temperature (RT) for 30 minutes using Lymphoprep medium (StemCell Technologies, 07861). The layer containing the PBMCs was isolated and extensively washed with PBS supplemented with 0.1% BSA and 2 mM EDTA. The residual red blood cells were removed using red blood cell ACK lysis buffer (Gibco, A1049201). Monocytes and pan T cells were isolated from the healthy donor PBMCs as described below.

2.3 Isolation and differentiation of (mature and immature) monocyte-derived dendritic cells

Monocytes were isolated from the PBMCs using CD14 Microbeads (Miltenyi Biotec, 130-050-201) according to the manufacturer's instructions. For differentiation of MoDCs, monocytes were cultured in X-VIVO 15 (Lonza, BE02-060F) supplemented with 2% human serum and with 450 U/ml GM-CSF (Miltenyi Biotec, 130-093-868) and 300 U/ml IL-4 (Miltenyi Biotec, 130-093-924) for differentiation for 5 days (cytokines and medium were refreshed at day 3). After differentiation, MoDCs were matured for 24h with 1000 U/ml IL-6 (Proteintech, HZ-1019), 1000 U/ml IL-1β (Peprotech, 200-01B), 500 U/ml TNF-α (Peprotech, 300-01A), and 10 μg/ml PGE2 (Prostin E2 Pfizer). On day 6, immature (iDCs) and mature (mDCs) MoDCs were harvested after 1h incubation at 4°C in cold PBS and with the help of a cell scraper.

2.4 Isolation of pan T cells

For the allogeneic T cell assays/mixed lymphocyte reaction assays, T cells were isolated from the PBL fraction of PBMCs using the Pan T cell isolation Kit *(*Miltenyi Biotec, 130-096-535*)* according to manufacturer instructions.

2.5 Establishment of patient-derived tumor organoids

The following procedure was used to establish patient-derived tumor organoids [Iyer, Poel, et al. (manuscript in preparation)]. Patient biopsies were collected in Advanced DMEM/F12 (Gibco, 12634010), supplemented with 1x GlutaMAX™-I (Gibco, 35050038), 10 mM HEPES Buffer solution (Gibco, 15630056), and Penicillin Streptomycin (10000 U/mL Penicillin, 10000 μg/mL Streptomycin) (hereafter referred to as +3 Advanced medium), and

10 µM Rho-kinase inhibitor. The collection medium was removed, and the biopsies were washed with cold HBSS (Lonza). Then, the biopsies were transferred to a petri dish for mechanical digestion, washed twice with +3 advanced medium, and transferred into a 15 ml tube. The tumor tissue was incubated in 20 mg/mL Collagenase-II (Sigma-Aldrich) and 10 µM Rho-kinase inhibitor for tissue dissociation, and placed in the water bath at 37°C for 30 minutes. After tissue digestion, 10% FBS (Gibco) was added to stop the collagenase digestion. The minced and digested tissues were passed through a pre-wetted 200µM filter (Pluriselect) into a 15 ml tube. The tissue was centrifuged for 5 minutes at 400 x *g* and 4°C. Lastly, the supernatant was removed, and the pellet was resuspended in Cultrex Ready Basement membrane extract (BME) (Bio-Techne, 3434-050-RTU).

2.6 Culture of patient-derived tumor organoids and single cell counting

Organoids were cultured in 25 µl domes of 70% (v/v) BME in +3 Advanced medium supplemented with 5% (v/v) R-spondin-CM (provided by courtesy of the Kuo lab, Stanford University), 5% (v/v) Noggin-CM (provided by courtesy of the Clevers lab, Hubrecht Institute), B27 Supplement without vit. A (Gibco, 12587010), 10mM Nicotinamide (Sigma, N0636), 0.2 mg/mL Normocin™ (*Invivo*Gen, ant-nr-1), 1.25 mM n-acetylcysteine, 10 nM Gastrin-I (human) (Bio-Techne, 3006/1), 50 ng/mL hrEGF (Peprotech, AF-100-15), 3 µM SB202190 (Seleck, S1077), and 2 µM Galunisertib (LY2157299) 26. Organoids were kept until passage 25. For passaging and co-cultures, PDTOs were collected by adding ice-cold medium to dissolve the BME. For the co-culture, a trypsinization step was included to count the number of PDTO single cells present in a certain volume. In this study two PDTOs were used and selected based on their different morphology: PDTO013 hereafter referred to as PDTO cystic and PDTO024 as PDTO dense. [Iyer, Poel, et al. (manuscript in preparation)].

2.7 Generation of co-cultures between PDTOs and DCs in a 3D collagen gel

Bovine Collagen type I (fibrillar), the most widely used and investigated extracellular matrix for 3D cell culture, was used as a scaffold for PDTOs and DCs co-cultures. The collagen mix consisted of 3.1 mg/ml Bovine PureCol I (Advanced Biomatrix, 5005) (final concentration of 1.7 mg/ml), 10x MEM (Gibco, 11430-030) (final concentration of 0.74x), 7.5% sodium bicarbonate (Gibco, 25080-060) (final concentration of 0.28%), and the cells in X-VIVO 2% human serum. The mixture was prepared as described elsewhere (32). To avoid fragmentation by mechanical disruption, the PDTOs were collected carefully in a volume corresponding to the desired amount of counted cells in another identical sample. PDTOs and/or DCs were embedded in the collagen mix in a ratio of 1:1 (50,000:50,000 cells per 25 µl dome). The collagen gel domes were solidified for 30-45 min at 37°C, inverted to ensure polymerization in 3D and prevent cell attachment to the bottom of the well. The gels were kept in culture for 48h in X-VIVO 15 + 2% human serum.

2.8 Cell labeling for live imaging and flow cytometry

The cell viability within the 3D collagen gels was assessed using the ReadyProbes® Cell Viability Imaging Kit (ThermoFisher, R37609): NucBlue™ Live reagent stains the nuclei of all the cells and NucGreen™ Dead reagent stains only the nuclei of cells with compromised plasma membranes. The viability was quantified in the conditions with mDCs and iDCs alone, by using three different images of each condition from two different experiments/donors. The percentage of viable cells was calculated based on the cells stained with NucBlue™ Live and NucGreen™ Dead (cells stained with NucBlue™ – live cells, NucBlue™ and NucGreen™ – dead cells). Ibidi µ-Plate 24 Well Black ID 14 mm (82426) were used for imaging. For live imaging, the microscope Zeiss Axio Observer with a 10x magnification was used. For the time series, images were taken every 30 seconds or 1 minute. Images and movies were processed using Image J (Fiji). For the flow cytometry-based phagocytosis/uptake assay, prior to the generation of the co-cultures, DCs were stained with a CFSE cell-labeling dye (C34554, Invitrogen) and PDOs with a FarRed cell-labeling dye (C34564, Invitrogen) according to manufactures' instructions.

2.9 Co-culture fixation, embedding, and slide preparation

Co-cultures were fixed in formalin for 1h to preserve the co-culture structure, cell morphology, and localization. The fixed co-cultures were placed in Tissue-Tek® Paraform® cassettes (Sakura, 7019) and embedded in paraffin. The formalin-fixed, paraffin-embedded (FFPE) co-cultures were sectioned at 5 µm thickness with a microtome (Microm) for stainings and mounted on SuperFrost microscope slides (VWR, 631-9483). For 3D immunofluorescence stainings, the co-cultures were fixed for 1h with 4% PFA.

2.10 Immunofluorescence in collagen gels and slides

The following protocol was performed for immunofluorescence stainings in paraffine sections: following deparaffinization and rehydration, the slides were boiled in Tris-EDTA buffer for antigen retrieval. After incubation with blocking solution, the primary antibodies were added: 1:300 anti-CD11c (Abcam, ab52632) and 1:100 anti-pan cytokeratin (PanCK) (Abcam, ab7753) and incubated overnight at 4°C in a humidified chamber. The following day, the slides were washed three times with PBS. Slides were incubated for 1h at room temperature in the dark with 2.5 µg/ml DAPI (Roche, 10236276001), and the secondary antibodies, donkey anti-rabbit 488 (Invitrogen, A21206) and donkey anti-mouse 647 (Invitrogen, A31571) both 1:200. Samples and slides were washed and mounted with Fluoromount Mounting Medium (Sigma-Aldrich, F4680).

A slightly different protocol was followed for immunofluorescence stainings in 3D collagen co-cultures. Cultures

were incubated with a blocking solution (20 mM Glycine, 2% BSA, and 0.3% Triton in Phosphate buffer) for 1h at RT. Primary antibodies were added as described above for the paraffin sections. After overnight incubation and PBS washes, 2.5 µg/ml DAPI and the secondary antibodies were added and incubated for 2h at RT. Following the washing steps, the cultures were mounted in a microscopy slide with Mowiol (Sigma-Aldrich, 81381).

Once dry, the slides were imaged with a Zeiss AI Sample Finder microscope or with a Zeiss confocal laser scanning microscope LSM880. Image processing and analysis were performed using Image J (FijiJ). To quantify DCs location in relation to the tumor border, images were processed and segmented into regions of interest. Two distance maps were applied (normal and inverted) generating positive and negative values for each DC location.

2.11 Multiplex immunohistochemistry of patient samples

Multiplex immunohistochemistry of patient FFPE samples was done in sequential staining cycles using the Opal 7-color Automation IHC Kit (Akoya Biosciences, NEL801001KT) on the BOND RX IHC & ISH Research Platform (Leica Biosystems), which was optimized and performed as described before (33, 34). The multiplex panel consisted of 1:200 anti-CD14 (Cell Marque, 114R-16) with Opal620, 1:200 anti-CD19 (Abcam, ab134114) with Opal690, 1:150 anti-BDCA2 (Dendritics, DDX0043) with Opal540, 1:100 anti-CD1c (Thermo Fisher Scientific, TA505411) with Opal520, 1:100 XCR1 (Cell Signaling Technologies, 44665S) with Opal570 and 1:1500 anti-pan cytokeratin (Abcam, ab86734) with Opal650. Slides were counterstained with DAPI for 5 minutes and enclosed in Fluoromount-G mounting medium (SouthernBiotech, 0100-01). Whole tissue slides were imaged using the microscope Vectra 3 Automated Quantitative Pathology Imaging System (Version 3.0.4, PerkinElmer Inc.). For comparison to the co-cultures with PDTOs, only DAPI, CD1c, and Pan cytokeratin are shown.

2.12 Hematoxylin and Eosin staining

Hematoxylin-Eosin (HE) histological stainings were performed according to standard protocols. Once dry, the slides were imaged with a slide scanner (3DHISCTECH Pannoramic 1000, Sysmex).

2.13 Co-culture dissociation/disaggregation

After 48h of co-culture, Collagenase I (Sigma-Aldrich, C0130) solution was added to the co-culture medium (20 U/ml) for collagen dissolution and co-culture disaggregation for 45 min at 37°C. The cells were collected and viability was assessed prior to centrifugation using trypan blue and BIO-RAD TC20™ Automated Cell Counter. The cells were washed and used for flow cytometry or sorting staining protocols. Samples containing PDTOs were filtered through a Corning® Cell Strainer (70 µm Nylon MESH) before the staining protocol. For the flow cytometry-based phagocytosis/uptake assay a trypsinization step was included to yield single cells before acquisition.

2.14 Flow cytometry

Phenotypic characterization of DCs surface markers was performed as followed: Firstly, Fc receptors were blocked using Fc blocking reagent (Miltenyi, 130-059-901) for 10 min at 4°C to avoid non-specific antibody binding. Secondly, cells were stained with fixable Viability Dye eFluor™ 506 (Invitrogen, 65-0866-14) for 20 min at 4°C. Thirdly, cells were stained with directly labeled primary antibodies - anti-CD86-PE (BD Biosciences, 555658) 1:15, BV421 anti-PD-L1-BV421 (BD Biosciences, 563738) 1:25, anti-HLA-DR-PerCP (BioLegend, 307628) 1:20 - for 25 min at 4°C. Lastly, cells were washed before acquisition. The acquisition was performed on a FACSVerse flow cytometer (BD Biosciences). The acquired data was analyzed with FlowJo Version 10. The values were plotted as mean fluorescence intensity (MFI), mean ± standard deviation (SD), normalized to the conditions with only DCs (iDCs or mDCs, correspondingly). Relevant gating strategies used are depicted in the Results section.

2.15 Fluorescent-activated cell sorting

To isolate a pure population of DCs, for functional readouts, fluorescent-activated cell sorting (FACS) was performed using the BD FACSMelody Cell Sorter. To sort out residual PDTOs after the filtration step, the sterile antibody anti-CD326 (EpCAM)-PE human (Invitrogen, 12-9326-42) at 1:30 dilution was used. Cells were sorted with >98% purity. Relevant gating strategies are depicted in the Results section. Sorted DCs were then plated in triplicates with T cells for a mixed lymphocyte reaction as described in the following section.

2.16 Mixed lymphocyte reaction

Allogeneic T cell assays (mixed lymphocyte reaction) were performed to evaluate the ability of DCs to induce T cell proliferation after being sorted from the co-cultures. To detect T cell proliferation Pan T cells were labeled with 5 µM of Cell Trace CFSE (Invitrogen, C34554). DCs and CFSE-labelled T cells were seeded in a round-bottom 96-well plate at a 1:10 ratio in triplicates and co-cultured for 6 days. In order to assess T cell proliferation, at day 6, T cells were collected and stained with anti-CD8-APC (BD Biosciences, 555369) at 1:50 for 25 min at 4°C. Samples were acquired and analyzed with FlowJo Version 10. The values were plotted as mean MFI of the average of technical replicates, normalized to the conditions with DCs only (iDCs or mDCs), mean ± SD. Relevant gating strategies used are depicted in the Results section.

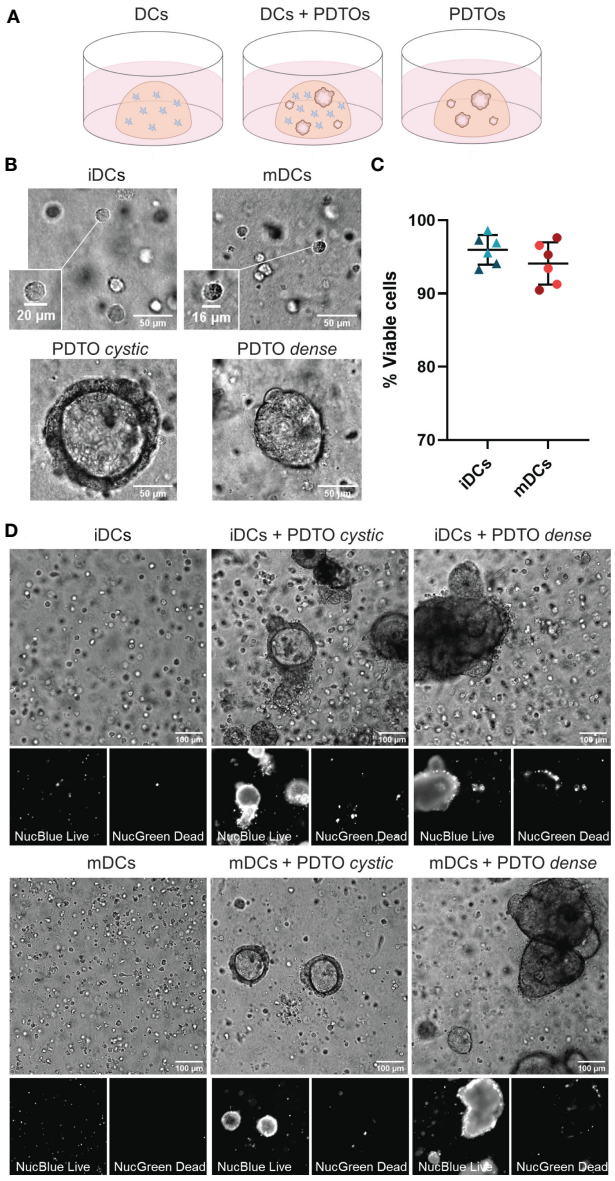

FIGURE 1
3D co-culture of PDTOs and DCs: Setup, morphology, and viability. **(A)** Schematic representation of the co-culture system and the three different conditions used in this study: DCs cultured alone, DCs and PDTOs co-cultured, and PDTOs cultured alone. **(B)** Closeup and morphology of iDCs and mDCs. The PDTOs are derived from CRC liver metastasis of two different patients, PDTO cystic as the name suggests presents a cystic morphology, whereas PDTO dense has a compact morphology. **(C)** Quantification of mDCs and iDCs viability when cultured alone in 3D in the collagen matrix after 48h, based on NucBlue™ Live and NucGreen™ Dead stainings, in two different experiments/donors. **(D)** The viability of mDCs, iDCs, and PDTOs was evaluated, after 48h of co-culture, during live imaging with NucBlue™ Live reagent (staining the nuclei of all cells) and NucGreen™ Dead reagent (staining only dead cells). The large majority of DCs seem to be viable alone, and in co-culture. iDCs - immature MoDCs, mDCs - mature MoDCs, PDTOs - patient-derived tumor organoids.

2.17 Statistical analysis

All statistical analyses were performed using GraphPad Prism V9 (GraphPad Software Inc, San Diego, CA). Unless otherwise indicated, results are presented as mean ± SD in scattered dot plots. Concerning MFI values, the statistical significance between different conditions was analyzed by a mixed-effects model followed by a Dunnett's *post-hoc* multiple comparisons test on the log2 transformed ratio values. When comparing DCs distribution in the tissue an unpaired t-test was used. The statistical significance was annotated as follows: *p < 0.05, **p < 0.01, ***p < 0.001, ****p < 0.0001.

3 Results

3.1 DCs remain viable in 3D during co-culture with CRC liver metastasis PDTOs

The main goal of this study was to set up a robust and dynamic 3D co-culture system between human DCs and CRC liver metastasis PDTOs that would allow investigation of how patient tumor cells shape DCs behavior, phenotype, and function. For this system, immature and mature DCs were cultured in a 3D fibrillar collagen drop in the presence or absence of PDTOs (Figure 1A). We observed that both DCs and organoids remained in the 3D collagen matrix and did not attach to the bottom. Within our co-culture system, it was also possible to visualize size differences between iDCs and mDCs, with the latter being slightly smaller, and between PDTO cystic and PDTO dense (Figure 1B and Supplementary Figure 1). During live cell imaging, NucBlue™ Live (staining all cells) and NucGreen™ Dead (staining dead cells) reagents were used to evaluate the viability of cells in the collagen matrix. After 48h the majority of DCs were alive both alone - mean viability of iDCs and mDCs cultured in the absence of PDTOs was 97 and 95%, respectively - and in co-culture with PDTOs (Figure 1C, D).

3.2 DCs interact with CRC liver metastasis PDTOs and engulf tumor-derived fragments in the 3D co-culture system

To confirm that the DCs were not only alive but also actively interacted with tumor cells, we recorded time series. As shown in Figure 2A (Supplementary Movie 1 and 2), during co-culture iDCs dynamically interacted with the tumor organoids by migrating towards and into the organoid, as well as, agglomerating near and engaging with the border. Next, we performed 3D immunofluorescence in fixed samples at 48h. CD11c and PanCK stainings allowed clear differentiation of DCs and tumor cells, respectively. Stainings also confirmed the presence of iDCs in close proximity to and gathered around and inside the tumor organoids (Figure 2B). Additionally, it is possible to observe iDCs surrounding and seemingly engulfing tumor cells or -derived fragments (Figures 2B, C). An additional assay, flow cytometry-based, was performed by labeling DCs and PDOs with fluorescent dyes, which provides further evidence for direct and functional interaction between iDCs and tumor cells, and engulfment/uptake of tumor cells within the co-culture (Supplementary Figure 2). In our system iDCs were found to be more frequently interacting with and taking up tumor cells than mDCs. Together, these results indicate that our co-culture system supports DC viability and function, and facilitates DC-tumor interactions, including the uptake of tumor cells or cell-derived fragments.

10.3389/fimmu.2023.1105244

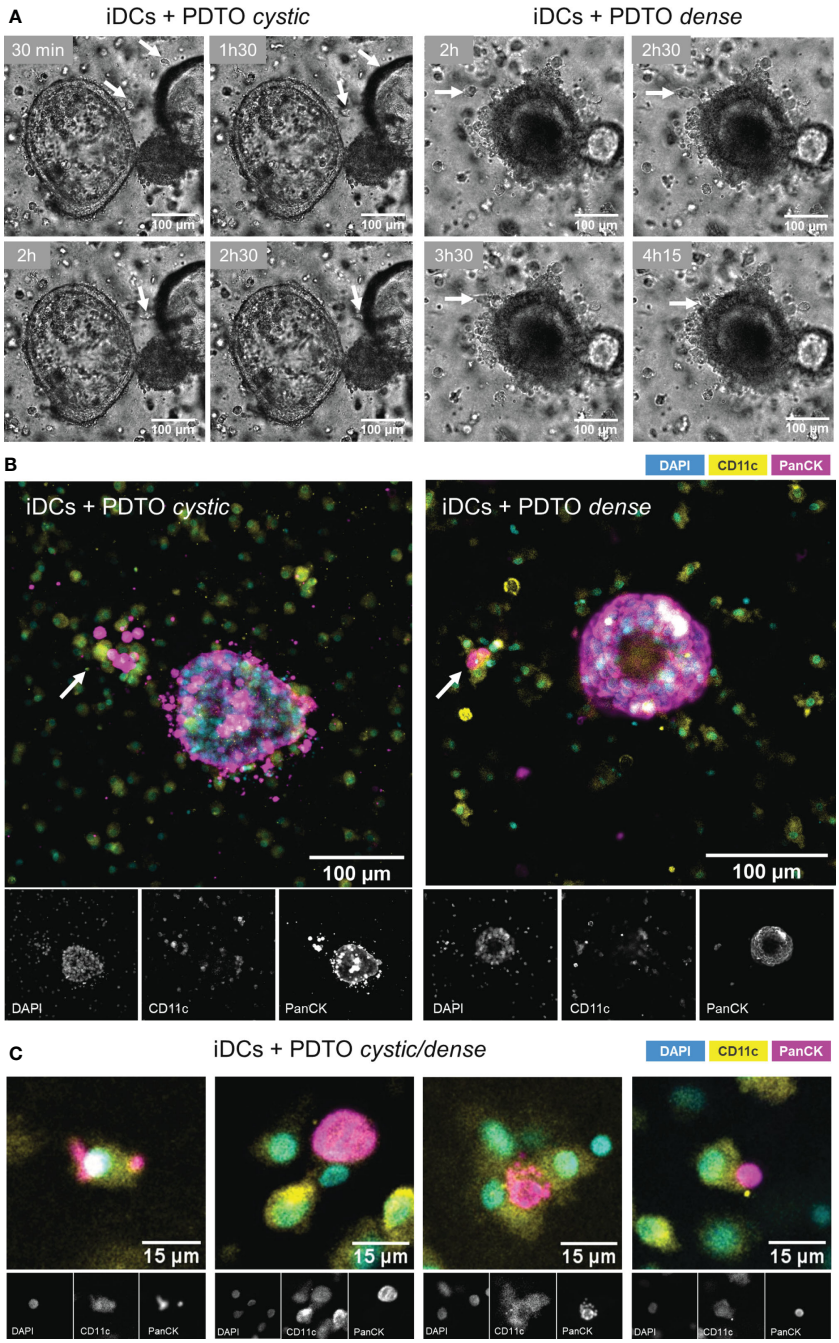

FIGURE 2
Visualization of DCs - PDTOs interactions within the co-culture. **(A)** Time series frames: iDCs establish direct contacts with co-cultured PDTOs by migrating towards and agglomerating near the tumor organoid borders (examples pinpointed by the arrows). **(B)** 3D immunofluorescence stainings with DAPI, CD11c, and PanCK, to distinguish DCs and tumor cells. **(C)** Examples of iDCs in close proximity to and surrounding/engulfing tumor-derived fragments. iDCs - immature MoDCs, mDCs - mature MoDCs, PDTOs - patient-derived tumor organoids.

3.3 DCs distribution in relation to PDTOs in the 3D co-culture system is maturation status-dependent and resembles patient tumor samples

To evaluate the co-culture structure and architecture we subjected our co-culture system to a standard H&E staining. We observed that DCs are distributed evenly throughout the matrix when alone in the collagen matrix (Supplementary Figure 3A, B). In the presence of the tumor organoids, iDCs can be found surrounding the tumor cells (Supplementary Figure 3C). Histological comparison of H&E staining in tissue sections obtained from two different patients with CRC liver metastasis and co-culture sections confirmed that the two organoid morphologies, PDTO cystic and PDTO dense, mimic two types of tumor lesions present in patients (Figure 3A and Supplementary Figure 3D).

We next looked in more detail at the distribution of DCs, relative to tumor organoids. Immunofluorescence of CD11c (MoDCs) and

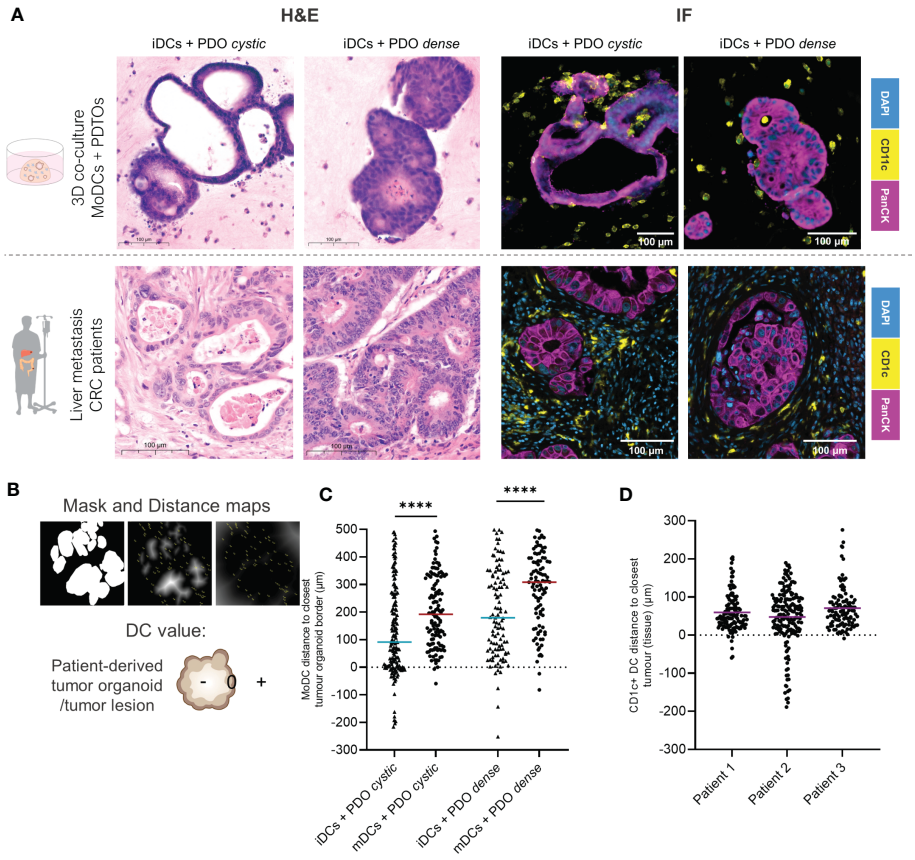

FIGURE 3
DCs distribution in relation to the tumor lesions within the co-culture in comparison to patient tumor samples by immunofluorescence. **(A)** Parallel between H&E and immunofluorescence stainings of DCs and organoids/tumors in fixed sections of the 3D co-culture and of CRC liver metastasis in patients. On the IF panel, representative examples of immunofluorescence stainings of CD11c and PanCK in the co-culture and of CD1c and PanCK in liver metastasis tumor sections. DCs are present agglomerating around, surrounding and infiltrating tumor organoids and tumor lesions in patients. Additional and larger images are included in Supplementary Figures 3 and 4. **(B)** Analysis of DCs distribution within the co-culture by image processing including segmentation and distance maps (normal and inverted). Each DC was assigned a positive, 0 or negative value depending on whether they were found outside, at the border, or inside the tumor, respectively. **(C)** The scatter dot plot shows differences in DC distribution around and inside the tumor organoids. Each dot represents one DC, line at the median. The p values were determined using an unpaired t-test. Statistical significance was annotated as follows: ****p < 0.0001 based on two sections from two independent experiments. **(D)** The scatter dot plot shows differences in DC distribution around and inside the tumor lesions, based on sections from 3 different patients. Each dot represents one DC, line at the median. The p values were determined using an unpaired t-test. Statistical significance was annotated as follows: ***p < 0.001, ****p < 0.0001 based on sections from 3 different patients. iDCs - immature MoDCs, mDCs - mature MoDCs, PDTOs - patient-derived tumor organoids.

PanCK (tumor cells) was performed in fixed sections of the co-cultures after 48h. Comparison to patient tissue sections, stained with CD1c—indicating DCs with a myeloid origin—and PanCK, suggested that our co-cultures achieve representative interactions between cancer cells and DCs, even in the absence of other stromal cells (Figure 3A). DCs, in particular iDCs, are found close to the tumor organoid border and inside, with a satellite-like disposition around tumor organoids and small clusters of tumor cells (Figure 3A and Supplementary Figures 4A, B). Therefore, we hypothesized that DCs distribution within the co-cultures may be influenced by their maturation status.

To assess DCs distribution in relation to tumor glands in both the co-culture and patient tissue sections, distance maps were applied generating positive or negative values for each DC location depending on their distance to the closest epithelial tumor gland (Figure 3B). The results show that iDCs are significantly in closer proximity to the tumor border and are more often found inside the tumor when compared to mDCs for both PDTOs. With this analysis, we demonstrate that DC distribution within the co-culture system differs depending on DC maturation status. Moreover, the results suggest that both iDCs and mDCs are found in closer proximity to PDTO cystic than to PDTO dense (Figure 3C). In the analyzed patient sections of CRC liver metastasis, we observed that CD1c+ DCs agglomerate close to tumors (<100 µm) surrounding and infiltrating lesions, as seen in our co-culture system (Figure 3D). The distribution and position of myeloid DCs (CD1c+ DCs) were found to be comparable to the distribution of iDCs within the co-culture in terms of range and mean distance to the tumors.

3.4 Phenotypic characterization of DCs after retrieval from the 3D co-culture

After investigating cell interactions and the structure of the co-culture, we next evaluated if it was possible to retrieve the DCs from the collagen scaffold and assess the tumor organoids' influence on

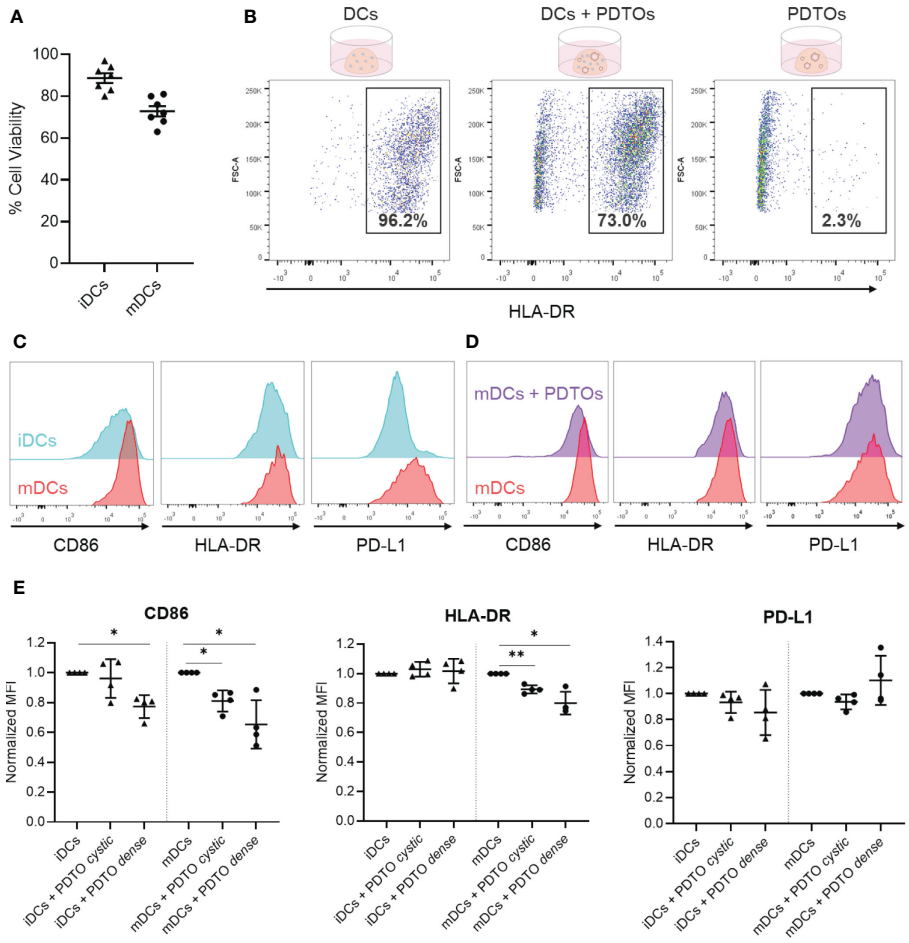

FIGURE 4
Recovery of DCs after co-culture with tumor PDTOs - viability, gating strategy, and phenotypic characterization to assess tumor-induced phenotypical changes. **(A)** DCs viability was assessed by trypan blue staining after collagenase treatment to disassemble the collagen scaffold (before centrifugation). **(B)** For flow cytometry analysis, cells were gated based on size, single cells, and live cells. Depicted is the HLA-DR-based gating strategy to distinguish PDTOs and DCs, using three conditions: DCs only, DCs and PDTOs co-culture, and PDTOs only. **(C)** Representative histogram plots to exemplify basal expression of CD86, HLA-DR, and PD-L1 markers in iDCs and mDCs. **(D)** Representative histogram plot of CD86, HLA-DR and PDL-1 to highlight the phenotypic shift of mDCs cultured in the presence of PDTOs. **(E)** Scattered dot plots showing normalized MFI values to iDCs and mDCs, respectively. Each dot/triangle represents a different donor, 4 donors were used in total. Data plotted as normalized values of raw MFI, mean with SD. The statistical significance between different conditions (mDCs/iDCs with and without PDTOs) was analyzed by a mixed-effects model followed by a Dunnett's *post-hoc* multiple comparisons test on the log2 transformed ratio values. The statistical significance was annotated as follows: *p < 0.05, **p < 0.01. (Raw data can be found in Supplementary Figure 5).

their phenotype. To retrieve the cells, the collagen matrix was disassembled with collagenase. For assessment of DCs viability after 48h culture and collagenase treatment, the samples containing only mDCs or iDCs were stained with trypan blue prior to any centrifugation step. Results show that the viability was moderate to high for all DCs, albeit slightly lower for mDCs as compared to iDCs (Figure 4A).

Successful recovery of cells from the collagen matrix allowed surface stainings to be performed for immunophenotyping with flow cytometry, using HLA-DR expression to identify DCs (Figure 4B). Subsequently, we analyzed the phenotypic profile of DCs after being in contact with CRC organoids. For that, we analyzed the expression of the CD86 co-stimulatory molecule, the HLA-DR antigen presentation machinery, and the co-inhibitory molecule PD-L1 – all required for successful antigen presentation and priming of T cells. Representative histogram plots of CD86, HLA-DR, and PD-L1 highlight the distinct basal expression of the selected maturation markers in mDCs versus iDCs, confirming their phenotypic differences (Figure 4C). It is also shown in Figure 4D, as an example, a whole-population tumor-induced reduction in CD86 and HLA-DR expression in mDCs after 48h of co-culture with PDTO dense. In Figure 4E (and Supplementary Figure 5) it is shown how the expression of the markers is altered in iDCs and mDCs upon co-culture with PDTOs.

Interestingly, the results show that there is a decreased expression of the co-stimulatory CD86 marker in both iDCs and mDCs in the presence of the PDTOs (Figure 4E), suggesting a tumor-induced immunosuppressive effect. For HLA-DR, its expression remained stable in iDCs, whereas a decrease is noted for mDCs. PD-L1 expression was also impacted, and differently, by the two different PDTOs, but no statistically significant differences were observed. In general, co-culture with tumor cells seems to have a stronger impact on the expression of the studied markers on mDCs. And, notably, our system allows us to detect phenotypic differences induced by

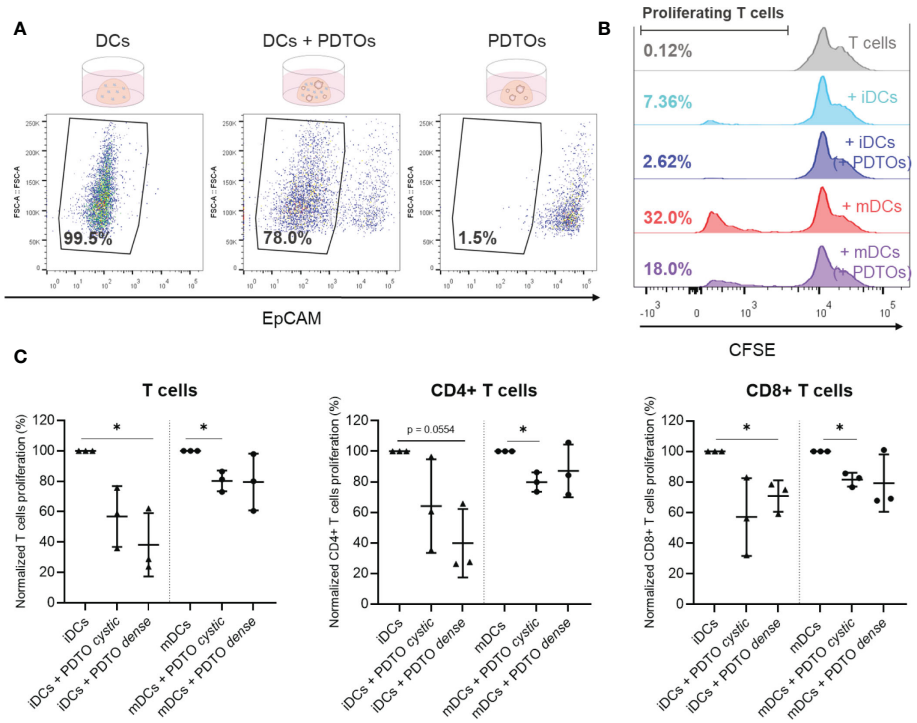

FIGURE 5
Sorting and functional characterization of DCs after co-culture with PDTOs – Allogeneic T cell assay. **(A)** Isolation of DCs, using EpCAM to sort out PDTOs. DCs gate defined based on EpCAM expression. **(B)** Representative CFSE histogram plots are shown. Numbers indicate the percentage of gated proliferating T cells. **(C)** Proliferation of allogeneic T cells after 6 days of co-culture with sorted DCs. Scattered dot plots show the percentage of proliferating T cells in each condition (average of technical replicates), normalized to proliferating T cells in the conditions with only iDCs and mDCs, respectively, mean with SD. The statistical significance between different conditions (mDCs/iDCs with and without PDTOs) was analyzed by a mixed-effects model followed by a Dunnett's *post-hoc* multiple comparisons test on the log2 transformed ratio values. The statistical significance was annotated as follows: *p < 0.05. (Raw data can be found in Supplementary Figure 6).

individual PDTOs; i.e., our PDTO dense seems to have a stronger suppressive effect on DCs than our PDTO cystic.

Together, these data demonstrate that after co-culture it is possible to retrieve DCs from the collagen matrix with high viability, which further allows phenotypic profiling and study of the impact of tumor organoids on DCs phenotype.

3.5 Functional analysis of DC activity following 3D co-culture

Finally, we explored the possibility of functionally characterizing DCs after co-culture with the tumor organoids using an allogenic T cell assay based on HLA-DR mismatch, which provides information about the DCs' ability to activate T cells and induce T cell proliferation. For this assay, a pure population of DCs is required after co-culturing. We therefore isolated DCs by FACS sorting out PDTOs with EpCAM labeling. Part of the used gating strategy is depicted in Figure 5A, demonstrating that EpCAM expression presents two clearly distinct populations (negative and positive). Representative histograms are presented in Figure 5B, where it is shown that iDCs have inherently a lower ability to activate T cell proliferation when compared to mDCs, as expected. Interestingly, we observed that DCs previously co-cultured with PDTOs were less capable of stimulating allogeneic T cells (both CD4+ and CD8+ T cells) proliferation when compared with iDCs and mDCs cultured alone (Figures 5B, C and Supplementary Figure 5).

Altogether, these results reveal that it is possible to perform functional readouts with DCs isolated from the 3D co-culture. Our results suggest that co-culture with PDTOs not only impacts DC phenotype but also their T cell activating abilities.

4 Discussion

Currently, there is a shortage of representative and dynamic *in vitro* models to study and dissect interactions between CRC and immune cells. In view of this gap, our main aim was to establish a 3D patient-derived co-culture model to mimic and investigate the interactions between DCs and metastatic CRC. Here, we present a co-culture of MoDCs and PDTOs in a 3D collagen matrix - amenable to live-cell microscopy, histological analysis, immunofluorescence, flow cytometry, and cell sorting - allowing comprehensive analysis and characterization of the impact of tumor cells on DCs phenotype and functions. As far as we know, this is the first study and model investigating human DCs in a tumor organoid 3D context.

4.1 Co-culture setup, cell viability and interactions, and structure

One of the main strengths of this study is the use of PDTOs as a tumor model. Firstly, several mechanisms are specific to humans and difficult to reproduce in animal models (35). Secondly, the 3D

architecture of the tumor organoids recapitulates and preserves both histological and mutational features of the original tumor, which is particularly relevant given the heterogeneity of CRC. Thirdly, PDTOs provide a high degree of translational information supporting their clinical relevance (36–38). Finally, previous studies show that patient-derived tumor organoid co-cultures with T cells recapitulate and preserve tumor-immune cell interactions and treatment response within the TME (27, 29).

Despite their physiological relevance, using only two organoids is a limitation of this study, which in the future can be surpassed by the use of additional organoid lines. MoDCs were chosen as a DC model, as these are the most used and accessible source of human DCs. Nevertheless, MoDCs are generated *ex vivo* from monocytes, as such, the use of primary DC subsets isolated directly from the blood would be desirable to further improve the physiological relevance of the system.

Another key point of the presented co-culture system is the 3D collagen matrix setup. The 3D environment allows spatiotemporal analysis and insights into tumor-DC dynamics. The collagen type and concentration were chosen based on previous work showing that it supports and allows DCs to migrate, locate and engage with each other and with other cells in co-culture (32, 39). Key challenges of 3D co-culture systems include the batch-to-batch variability of scaffold materials, costs, and the absence of important elements such as vascular flow or interaction with other organs (26, 40). Some of these challenges can be partially overcome in more complex microphysiological chip platforms as previously described (31). Nevertheless, we believe that the here proposed simple, feasible, and reproducible setup and toolbox is valuable to examine 1-1 immune cell-tumor interactions and mediators while maintaining tumor heterogeneity, spatiotemporal interactions, and physiological relevance.

In line with previous research, in our co-culture model, the collagen setup and concentration support cell viability and 3D disposition of both DCs and PDTOs. Moreover, it fosters DC functions, including migration and engulfing of tumor fragments, and facilitates DC-tumor interactions. As described in our study, DCs - in particular, iDCs likely due to their increased phagocytic ability in comparison with mDCs (41) - cluster around and inside the tumor organoids, sampling tumor material, and extensively interact with the organoids. This was the first milestone to be achieved, as the goal of this system was to be able to study and uncover DC-tumor interactions.

Next, we wanted to compare the structure and cell organization within our co-culture with patient tissue sections. Interestingly, we found the distribution of DCs within the co-culture system to be maturation status-dependent, and different for both PDTOs in the study, potentially showing the adaptability and specificity of the model. Remarkably, our relatively simple co-culture system, is comparable to mCRC patient sections, in terms of tumor lesion morphology, DC distribution, and distance range to tumor lesions for the samples analyzed. Of note, the patient tissue sections were not from the same patients from which the organoids were derived, further suggesting the representability of the system.

4.2 Tumor-induced DC phenotype and (dys) function

Tumor-infiltrating DCs are known to perform crucial functions, such as reinvigorating, activating, and modulating the magnitude and duration of T cell responses, and recruiting and regulating effector T cells influx to the tumor site. These functions are crucial not only for the coordination of anti-tumor T cell responses, but also for immunotherapy effectiveness. DCs achieve this by either the generation of chemokine/cytokine gradients or direct antigen presentation (11, 12, 42, 43). MoDCs can prime Th1 and cytotoxic immune responses and have been shown to play an important role in different physiological and inflammatory settings including tumors (44–47). In our co-culture system, we include and study immature and mature MoDCs, as both functional states can be found within the TME and, greatly influence the quality and pro- or anti-tumor direction of immune responses (12).

Retrieving viable DCs from the 3D co-culture system was crucial for studying tumor-induced phenotypic and functional changes. Our results corroborate the different behaviors, phenotypes, and functions of mDCs and iDCs. For instance, in an immature state DCs are more active in tumor engulfing, whereas in a mature state they are specialized in antigen presentation and T cell activation. Overall, our results suggest that the expression of co-stimulatory molecules (CD86), antigen presentation machinery (HLA-DR), and co-inhibitory molecules (PD-L1) in DCs, and their ability to activate T cells were impacted upon interaction with tumor organoids. This suggests that the tumor shifted or locked DCs in a more immature state, associated with tolerance and pro-tumorigenic effects. Future research, building on our model, can further characterize the functional consequences of tumor-induced DC dysfunction on T cell biology and dissect associated mediators and mechanisms

The observed phenotype shift with impaired maturation and T cell activation abilities is in line with previous studies investigating DCs phenotype and function in patients, and also in a study assessing the impact of tumor-derived supernatant on DC maturation (48–50). We observed a stronger tumor impact on mDCs than on iDC phenotype, this might be related to a higher basal expression of the studied markers on mDCs or perhaps due to a higher sensitivity to environmental cues. Importantly, a stronger effect on mDCs would benefit the tumor since the presence of impaired mDCs has a stronger repercussion on mounting effective anti-tumor responses.

We also found that the two PDTOs used had different impacts on iDCs and mDCs behavior, distribution, recruitment, activation, and function. Notably, our data demonstrate that DCs interacted less with and were not in as close proximity (or inside) to PDTO dense when compared with PDTO cystic. Paradoxically, it was PDTO dense that had a more pronounced effect on DC phenotype. We speculate that this PDTO's stronger immunosuppressive effect may be related to DC exclusion from the tumor surroundings. Further research including PDTO secretome profiles would be required to test this hypothesis.

Of note, the observation of morphologically distinct glandular structures, i.e., cystic versus dense, or 'solid'—that characterize CRCs and are frequently recapitulated in tumour organoids, stems from the first CRC organoid biobank reported (51). However, our methods-focused exploratory study cannot make any claim ascribing functional differences to these two phenotypes based on single representatives. Additional experiments are needed to confirm a biological difference between any type of feature - including, e.g., mutational status - that these PDTOs can represent. Nevertheless, our results do suggest that our model may be sufficiently robust and feasible for the careful classification of CRC-DC interactions using larger numbers of

organoids, or even for the assessment of patient-specific tumor-induced DC dysfunction.

Altogether, these findings support the physiological relevance of the tumor-mediated effects observed within our 3D co-culture system, indicating that the presented tool is a valuable additional approach to studying DC–CRC interactions. This model allows real-time investigation of tumor organoids modulating DCs phenotype and behavior. Importantly, getting insight into how CRC shapes DC maturation and functionality paves the way for the development of new therapies to prevent tumor-induced DC dysfunction, or restore their full anti-tumor potential. And hence, getting one step closer to promoting tumor destruction, avoiding metastasis formation, or unleashing treatment response in patients.

4.3 Future perspectives

Our study raises several additional opportunities for future research, and we view it as a promising starting point and a toolbox to be exploited and adapted for more complex and detailed studies of CRC-DC interactions within the TME. In the future, we believe that the presented co-culture system can be exploited for studies with primary DCs subsets and different tumor organoids. This can aid our understanding of (1) the individual contributions of the different DC subsets - with inherently different functional specializations; (2) and the tumor-specific mechanisms and mediators that regulate the fate of DC subset-mediated anti-tumor responses or tolerance within the TME. Furthermore, this knowledge might open doors for the (3) identification of potential targets and biomarkers for the design of DC subset-specific interventions. Finally, (4) possibly this system could be used for patient/organoid-specific studies if the physiological relevance and predictive power of the co-culture are confirmed by correlating *in vitro* outcomes with patients' parameters such as tumor T cell infiltration or response to immunotherapy. Potentially, this approach can bring us closer to making existing or new immunotherapies available for more mCRC patients.

Data availability statement

The raw data supporting the conclusions of this article will be made available by the authors, without undue reservation.

Ethics statement

The studies involving human participants were reviewed and approved by ORCHESTRA trial (NCT01792934). The patients/participants provided their written informed consent to participate in this study.

Author contributions

BS: conceived, performed the experiments, analysed the data, and wrote the manuscript. KI, DP, LB, HV: established and provided essential biological material. MG: assisted with immunohistochemistry experiments in patient samples. JC/KD/AC: assisted with experiment setup, data analysis, and interpretation. IV and DT: supervised the entire project. All authorscontributed to the article and approved the submitted version.

Funding

DT is funded by a Hypatia Tenure Track Fellowship grant from the Radboudumc and by the Dutch Research Council(NWO/ZonMW VIDI grant number 91719371). IV is funded by EU grant Oncobiome (825410) and Health Holland/SGF grant DC4Balance (LSHM18056-SGF).

Acknowledgments

We would like to thank all the members of the Cell Biology, and Tumor immunology departments (Radboudumc, Nijmegen) for the valuable discussions. We are grateful to Iris Nagtegaal from the Radboudumc pathology department for providing anonymized patient sections and helping with assessing patient histology.

Conflict of interest

The authors declare that the research was conducted in the absence of any commercial or financial relationships that could be construed as a potential conflict of interest.

Publisher's note

Supplementary material

The Supplementary Material for this article can be found online at: https://www.frontiersin.org/articles/10.3389/fimmu.2023.1105244/full#supplementary-material

References

1. Sawicki T, Ruszkowska M, Danielewicz A, Niedźwiedzka E, Arłukowicz T, Przybyłowicz KE. A review of colorectal cancer in terms of epidemiology, risk factors, development, symptoms and diagnosis. *Cancers* (2021) 13(9):2025. doi: 10.3390/cancers13092025

2. Kow AWC. Hepatic metastasis from colorectal cancer. *J Gastrointestinal Oncol* (2019) 10:1274–98. doi: 10.21037/jgo.2019.08.06

3. Van Der Jeught K, Xu HC, Li YJ, Bin L, Ji G. Drug resistance and new therapies in colorectal cancer. *World J Gastroenterol* (2018) 24:3834–48. doi: 10.3748/wjg.v24.i34.3834

4. Hanahan D, Coussens LM. Accessories to the crime: Functions of cells recruited to the tumor microenvironment. *Cancer Cell Cancer Cell* (2012) 21:309–22. doi: 10.1016/j.ccr.2012.02.022

5. Pedrosa L, Esposito F, Thomson TM, Maurel J. The tumor microenvironment in colorectal cancer therapy. *Cancers* (2019) 11(8):1172. doi: 10.3390/cancers11081172

6. Tauriello DVF, Palomo-Ponce S, Stork D, Berenguer-Llergo A, Badia-Ramentol J, Iglesias M, et al. TGFβ drives immune evasion in genetically reconstituted colon cancer metastasis. *Nature* (2018) 554(7693):538–43. doi: 10.1038/nature25492

7. Gessani S, Belardelli F. Immune dysfunctions and immunotherapy in colorectal cancer: The role of dendritic cells. *Cancers (Basel)* (2019) 11(10):1–17. doi: 10.3390/cancers11101491

8. Lin A, Schildknecht A, Nguyen LT, Ohashi PS. Dendritic cells integrate signals from the tumor microenvironment to modulate immunity and tumor growth. *Immunol Lett* (2010) 127(2):77–84. doi: 10.1016/j.imlet.2009.09.003

9. Wculek SK, Cueto FJ, Mujal AM, Melero I, Krummel MF, Sancho D. Dendritic cells in cancer immunology and immunotherapy. *Nat Rev Immunol* (2020) 20:7–24. doi: 10.1038/s41577-019-0210-z

10. Gardner A, Ruffell B. Dendritic cells and cancer immunity. *Trends Immunol* (2016) 37:855–65. doi: 10.1016/j.it.2016.09.006

11. Pfirschke C, Siwicki M, Liao HW, Pittet MJ. Tumor microenvironment: No effector T cells without dendritic cells. *Cancer Cell* (2017) 31(5):614–5. doi: 10.1016/j.ccell.2017.04.007

12. Tran Janco JM, Lamichhane P, Karyampudi L, Knutson KL. Tumor-infiltrating dendritic cells in cancer pathogenesis. *J Immunol* (2015) 194(7):2985–91. doi: 10.4049/jimmunol.1403134

13. Dudek AM, Martin S, Garg AD, Agostinis P. Immature, semi-mature, and fully mature dendritic cells: Toward a DC-cancer cells interface that augments anticancer immunity. *Front Immunol* (2013) 4. doi: 10.3389/fimmu.2013.00438

14. Kuang D-M, Zhao Q, Xu J, Yun J-P, Wu C, Zheng L. Tumor-educated tolerogenic dendritic cells induce CD3ε down-regulation and apoptosis of T cells through oxygen-dependent pathways. *J Immunol* (2008) 181(5):3089–98. doi: 10.4049/jimmunol.181.5.3089

15. Torres-Aguilar H, Aguilar-Ruiz SR, González-Pérez G, Munguía R, Bajaña S, Meraz-Ríos MA, et al. Tolerogenic dendritic cells generated with different immunosuppressive cytokines induce antigen-specific anergy and regulatory properties in memory CD4 + T cells. *J Immunol* (2010) 184(4):1765–75. doi: 10.4049/jimmunol.0902133

16. DeVito NC, Plebanek MP, Theivanthiran B, Hanks BA. Role of tumor-mediated dendritic cell tolerization in immune evasion. *Front Immunol* (2019) 10:2876. doi: 10.3389/fimmu.2019.02876

17. Subtil B, Cambi A, Tauriello DVF, de Vries IJM. The therapeutic potential of tackling tumor-induced dendritic cell dysfunction in colorectal cancer. *Front Immunol* (2021) 12, 4048. doi: 10.3389/fimmu.2021.724883

18. Murgaski A, Bardet PMR, Arnouk SM, Clappaert EJ, Laoui D. Unleashing tumour-dendritic cells to fight cancer by tackling their three a's: Abundance, activation and antigen-delivery. *Cancers (Basel)* (2019) 11(5):670. doi: 10.3390/cancers11050670

19. Nishida-Aoki N, Gujral TS. Review emerging approaches to study cell–cell interactions in tumor microenvironment. *Oncotarget Impact J LLC* (2019) 10:785–97. doi: 10.18632/oncotarget.26585

20. Rodrigues J, Heinrich MA, Teixeira LM, Prakash J. 3D *In vitro* model (R)evolution: Unveiling tumor–stroma interactions. *Trends Cancer Authors* (2021) 7:249–64. doi: 10.1016/j.trecan.2020.10.009

21. Fiorini E, Veghini L, Corbo V. Modeling cell communication in cancer with organoids: Making the complex simple. *Front Cell Dev Biol* (2020) 8:1–12. doi: 10.3389/fcell.2020.00166

22. Sebrell TA, Hashimi M, Sidar B, Wilkinson RA, Kirpotina L, Quinn MT, et al. A novel gastric spheroid Co-culture model reveals chemokine-dependent recruitment of human dendritic cells to the gastric epithelium. *Cmgh* (2019) 8(1):157–171.e3. doi: 10.1016/j.jcmgh.2019.02.010

23. Di Blasio S, van Wigcheren GF, Becker A, van Duffelen A, Gorris M, Verrijp K, et al. The tumour microenvironment shapes dendritic cell plasticity in a human organotypic melanoma culture. *Nat Commun* (2020) 11(1):1–17. doi: 10.1038/s41467-020-16583-0

24. Bakdash G, Buschow SI, Gorris MAJ, Halilovic A, Hato SV, Sköld AE, et al. Expansion of a BDCA1+ CD14+ myeloid cell population in melanoma patients may attenuate the efficacy of dendritic cell vaccines. *Cancer Res* (2016) 76(15):4332–46. doi: 10.1158/0008-5472.CAN-15-1695

25. Yuki K, Cheng N, Nakano M, Kuo CJ. Organoid models of tumor immunology. *Trends Immunol* (2020) 41(8):652–64. doi: 10.1016/j.it.2020.06.010

26. LeSavage BL, Suhar RA, Broguiere N, Lutolf MP, Heilshorn SC. Next-generation cancer organoids. *Nat Mater* (2021) 21(2):143–59. doi: 10.1038/s41563-021-01057-5

27. Neal JT, Li X, Zhu J, Giangarra V, Grzeskowiak CL, Ju J, et al. Organoid modeling of the tumor immune microenvironment. *Cell* (2018) 175(7):1972–1988.e16. doi: 10.1016/j.cell.2018.11.021

28. Linde N, Gutschalk CM, Hoffmann C, Yilmaz D, Mueller MM. Integrating macrophages into organotypic Co-cultures: A 3D in vitro model to study tumor-associated macrophages. *PloS One* (2012) 7(7):e40058. doi: 10.1371/journal.pone.0040058

29. Dijkstra KK, Cattaneo CM, Weeber F, Chalabi M, van de Haar J, Fanchi LF, et al. Generation of tumor-reactive T cells by Co-culture of peripheral blood lymphocytes and tumor organoids. *Cell* (2018) 174(6):1586–1598.e12. doi: 10.1016/j.cell.2018.07.009

30. Chakrabarti J, Koh V, So JBY, Yong WP, Zavros Y. A preclinical human-derived autologous gastric cancer Organoid/Immune cell Co-culture model to predict the efficacy of targeted therapies. *J Vis* (2021) 2021(173):e61443. doi: 10.3791/61443

31. Cherne MD, Sidar B, Sebrell TA, Sanchez HS, Heaton K, Kassama FJ, et al. A synthetic hydrogel, VitroGel® ORGANOID-3, improves immune cell-epithelial interactions in a tissue chip Co-culture model of human gastric organoids and dendritic cells. *Front Pharmacol* (2021) 12:1–16. doi: 10.3389/fphar.2021.707891

32. Koh WH, Zayats R, Lopez P, Murooka TT. Visualizing cellular dynamics and protein localization in 3D collagen. *STAR Protoc* (2020) 1(3):100203. doi: 10.1016/j.xpro.2020.100203

33. Gorris MAJ, van der Woude LL, Kroeze LI, Bol K, Verrijp K, Amir AL, et al. Paired primary and metastatic lesions of patients with ipilimumab-treated melanoma: high variation in lymphocyte infiltration and HLA-ABC expression whereas tumor mutational load is similar and correlates with clinical outcome. *J Immunother Cancer* (2022) 10(5):e004329. doi: 10.1136/jitc-2021-004329

34. Gorris MAJ, Halilovic A, Rabold K, van Duffelen A, Wickramasinghe IN, Verweij D, et al. Eight-color multiplex immunohistochemistry for simultaneous detection of multiple immune checkpoint molecules within the tumor microenvironment. *J Immunol* (2018) 200(1):347–54. doi: 10.4049/jimmunol.1701262

35. Kim J, Koo BK, Knoblich JA. Human organoids: model systems for human biology and medicine. *Nat Rev Mol Cell Biol* (2020) 21:571–84. doi: 10.1038/s41580-020-0259-3

36. Ooft SN, Weeber F, Dijkstra KK, McLean CM, Kaing S, van Werkhoven E, et al. Patient-derived organoids can predict response to chemotherapy in metastatic colorectal cancer patients. *Sci Transl Med* (2019) 11(513):eaa2574. doi: 10.1126/scitranslmed.aay2574

37. Yao Y, Xu X, Yang L, Zhu J, Wan J, Shen L, et al. Patient-derived organoids predict chemoradiation responses of locally advanced rectal cancer. *Cell Stem Cell* (2020) 26(1):17–26.e6. doi: 10.1016/j.stem.2019.10.010

38. Narasimhan V, Wright JA, Churchill M, Wang T, Rosati R, Lannagan TRM, et al. Medium-throughput drug screening of patient-derived organoids from colorectal peritoneal metastases to direct personalized therapy. *Clin Cancer Res* (2020) 26(14):3662–70. doi: 10.1158/1078-0432.CCR-20-0073

39. Koh WH, Lopez P, Ajibola O, Parvarchian R, Mohammad U, Hnatiuk R, et al. HIV-Captured DCs regulate T cell migration and cell-cell contact dynamics to enhance viral spread. *iScience* (2020) 23(8):101427. doi: 10.1016/j.isci.2020.101427

40. Yoon PS, Del Piccolo N, Shirure VS, Peng Y, Kirane A, Canter RJ, et al. Advances in modeling the immune microenvironment of colorectal cancer. *Front Immunol* (2021) 11:3876. doi: 10.3389/fimmu.2020.614300

41. Kim MK, Kim J. Properties of immature and mature dendritic cells: phenotype, morphology, phagocytosis, and migration. *RSC Adv* (2019) 9(20):11230–8. doi: 10.1039/C9RA00818G

42. Lucarini V, Melaiu O, Tempora P, D'amico S, Locatelli F, Fruci D. Dendritic cells: Behind the scenes of t-cell infiltration into the tumor microenvironment. *Cancers* (2021) 13:1–22. doi: 10.3390/cancers13030433

43. Lizée G, Gilliet M. Human dendritic cells in cancer. *Innate Immune Regul Cancer Immunother* (2022) 9409:121–45. doi: 10.1126/sciimmunol.abm9409

44. León B, Ardavín C. Monocyte-derived dendritic cells in innate and adaptive immunity. *Immunol Cell Biol* (2008) 86:320–4. doi: 10.1038/icb.2008.14

45. Nakano H, Lin KL, Yanagita M, Charbonneau C, Cook DN, Kakiuchi T, et al. Blood-derived inflammatory dendritic cells in lymph nodes stimulate acute T helper type 1 immune responses. *Nat Immunol* (2009) 10(4):394–402. doi: 10.1038/ni.1707

46. Le Borgne M, Etchart N, Goubier A, Lira SA, Sirard JC, Van Rooijen N, et al. Dendritic cells rapidly recruited into epithelial tissues *via* CCR6/CCL20 are responsible for CD8+ T cell crosspriming *in vivo*. *Immunity* (2006) 24(2):191–201. doi: 10.1016/j.immuni.2006.01.005

47. Ruffell B, Chang-Strachan D, Chan V, Rosenbusch A, Ho CMT, Pryer N, et al. Macrophage IL-10 blocks CD8+ T cell-dependent responses to chemotherapy by suppressing IL-12 expression in intratumoral dendritic cells. *Cancer Cell* (2014) 26(5):623–37. doi: 10.1016/j.ccell.2014.09.006

48. Morrissey ME, Byrne R, Nulty C, McCabe NH, Lynam-Lennon N, Butler CT, et al. The tumour microenvironment of the upper and lower gastrointestinal tract differentially influences dendritic cell maturation. *BMC Cancer* (2020) 20(1):1–13. doi: 10.1186/s12885-020-07012-y

49. Maciejewski R, Radej S, Furmaga J, Chrościcki A, Rudzki S, Roliński J, et al. Evaluation of immature monocyte-derived dendritic cels generated from patients with colorectal cancer. *Pol Prz Chir Polish J Surg* (2013) 85(12):714–20. doi: 10.2478/pjs-2013-0109

50. Onishi H, Morisaki T, Baba E, Kuga H, Kuroki H, Matsumoto K, et al. Dysfunctional and short-lived subsets in monocyte-derived dendritic cells from patients with advanced cancer. *Clin Immunol* (2002) 105(3):286–95. doi: 10.1006/clim.2002.5293

51. Van De Wetering M, Francies HE, Francis JM, Bounova G, Iorio F, Pronk A, et al. Prospective derivation of a living organoid biobank of colorectal cancer patients. *Cell* (2015) 161(4):933–45. doi: 10.1016/j.cell.2015.03.053

frontiers | Frontiers in Immunology

TYPE Mini Review
PUBLISHED 25 January 2023
DOI 10.3389/fimmu.2023.1104860

OPEN ACCESS

EDITED BY
Ling Ni,
Tsinghua University, China

REVIEWED BY
Yu Zeng,
Tongji Hospital Affiliated to Tongji University, China
Naoe Taira Nihira,
St. Marianna University School of Medicine, Japan

*CORRESPONDENCE
Xueju Wang
xueju@jlu.edu.cn

SPECIALTY SECTION
This article was submitted to Cancer Immunity and Immunotherapy, a section of the journal Frontiers in Immunology

RECEIVED 22 November 2022
ACCEPTED 04 January 2023
PUBLISHED 25 January 2023

CITATION
Zhang X, Xu Z, Dai X, Zhang X and Wang X (2023) Research progress of neoantigen-based dendritic cell vaccines in pancreatic cancer. *Front. Immunol.* 14:1104860. doi: 10.3389/fimmu.2023.1104860

Research progress of neoantigen-based dendritic cell vaccines in pancreatic cancer

Xin Zhang[1], Zheng Xu[1], Xiangpeng Dai[2,3], Xiaoling Zhang[2,3] and Xueju Wang[1*]

[1]Department of Pathology, China-Japan Union Hospital, Jilin University, Changchun, Jilin, China, [2]Key Laboratory of Organ Regeneration and Transplantation of Ministry of Education, First Hospital of Jilin University, Changchun, China, [3]National-Local Joint Engineering Laboratory of Animal Models for Human Disease, First Hospital of Jilin University, Changchun, China

The mutation of the crucial genes such as tumor suppressors or oncogenes plays an important role in the initiation and development of tumors. The non-synonymous mutations in the tumor cell genome will produce non-autologous proteins (neoantigen) to activate the immune system by activating CD4+ and CD8 + T cells. Neoantigen-based peptide vaccines have exhibited exciting therapeutic effects in treating various cancers alone or in combination with other therapeutic strategies. Furthermore, antigen-loaded DC vaccines are more powerful in inducing stronger immune responses than vaccines generated by antigens and adjuvants. Therefore, neoantigen-based dendritic cell (DC) vaccines could achieve promising effects in combating some malignant tumors. In this review, we summarized and discussed the recent research progresses of the neoantigen, neoantigen-based vaccines, and DC-based vaccine in pancreatic cancers (PCs). The combination of the neoantigen and DC-based vaccine in PC was also highlighted. Therefore, our work will provide more detailed evidence and novel opinions to promote the development of a personalized neoantigen-based DC vaccine for PC.

KEYWORDS

dendritic cell, pancreatic cancer, mutation burden, immunotherapy, cancer vaccines, neoantigen

Introduction

Cancer can be caused by the alteration of the expression of genes controlling cell growth. The mutation of the crucial genes such as tumor suppressors or oncogenes plays an important role in the initiation and development of tumors. The loss of function mutations in tumor suppressor genes are frequently found in multiple cancers that will fail to produce the protein or the protein will not function properly. Moreover, mutation, gene amplification, and chromosome rearrangements are the three main genetic mechanisms to activate oncogenes. The activation mutations of proto-oncogenes will cause structural changes in their encoded proteins and lead to uncontrolled, continuous activation of the

oncoproteins. The loss of the function mutations of tumor suppressors and the activation mutations of oncogenes will cause uncontrolled cell growth and ultimately contribute to tumorigenesis. For example, Hui Cai et al. analyzed the mutational landscape of 153 gastric cancer patients by targeted next-generation sequencing and identified 35 significantly mutated genes, and the tumor suppressor *TP53* was found to be the most frequently mutated gene (1). Moreover, Kirsten rat sarcoma viral oncogene homolog (KRAS) mutation is one of the most common gene mutations and is a frequent driver in lung cancer, colorectal cancer, and pancreatic cancer (PC). KRAS mutations drive 85%–90% of PC cases, and the high prevalence of the oncogenic mutation of the KRAS gene is the hallmark of PC that plays a crucial role in the initiation and development of PC (2).

Importantly, non-synonymous mutations of the genes in the tumor cell genome will produce non-autologous proteins that can only be found in tumor cells (3, 4). These proteins have the capability to activate the immune system and are now known as neoantigens, which own strong immunogenicity and does not express in normal cells. Neoantigens can activate CD4+ and CD8+ T cells to induce immune response, and they are current novel and important targets of cancer immunotherapy (5). Therapeutic vaccination is one of the cancer immunotherapies and could regulate immune pathways to induce or enhance the inadequate antitumor immune responses (6). Therefore, the successful development of tumor vaccines targeting neoantigens through nucleic acid, dendritic cell (DC)–based and synthetic long peptide (SLP) vaccines might benefit the currently used immunotherapeutic strategy. The safety and immunogenicity of the personalized neoantigen vaccine NEO-PV-01 in combination with PD-1 blockage was firstly investigated in the treatment of advanced melanoma, non-small cell lung cancer, or bladder cancer patients, and no adverse events of the regimen were found (7). DCs are bone marrow–derived, morphologically and functionally heterogeneous cells with the capability to activate primary immune responses by presenting the antigens to naïve CD4+ and CD8+ T cells (8). Therefore, given the critical function of DCs in modulating the innate and adaptive immune responses and their high sensitization to tumor-associated antigens (TAAs), DCs are considered crucial players for the development of immunotherapies and a major focus of cancer vaccine development (6). DC-based immunotherapies, especially the DC-based vaccination, were widely studied in recent years, and the clinical trials for different DC-based vaccinations have exhibited positive effects on the induction of antitumor responses and prolonged survival of patients with different types of tumors (6).

Given the high tumor specificity and immunogenicity of neoantigens, neoantigens were thought to be one of the ultimate targets for tumor immunotherapy. Neoantigen-based peptide vaccines have exhibited exciting therapeutic effects on the treatment of glioblastoma (9). It was reported that antigen-loaded DC vaccines are more powerful in inducing stronger immune responses than vaccines generated by antigens and adjuvants (10). Therefore, neoantigen-based DC vaccines could achieve promising effects in combating some malignant tumors (11). In this review, we summarized and discussed the recent research progresses of the neoantigens and DC-based vaccines and the potential roles of neoantigens in the generation of neoantigen-based DC vaccines in the treatment of PC.

Neoantigens of pancreatic cancer

Pancreatic ductal adenocarcinoma (PDAC), a highly aggressive cancer type, accounts for 85% of PCs with a 5% of 5-year survival rate (12). Surgical resection is the only effective approach to prolong the survival time of PDAC patients if PDAC is diagnosed. However, the surgical resection is no longer beneficial for the PDAC patients with metastasis. Moreover, chemotherapy, radiotherapy, or immunotherapy could block the development of PDAC but the survival time of treated patients can only be extended to several months. Due to the poor early detection and the specific invasiveness of PDAC, further in-depth investigations for additional therapeutic strategies with high selectivity are need to eradicate PDAC (12).

It was well known that the mutations of oncogenes and tumor suppressors are critical factors for tumorigenesis including PC. The most frequently mutated genes of PDAC are *KRAS*, *CDKN2A*, *TP53*, and SMAD family member 4 (SMAD4), which are also considered driver genes and correlated with the poor outcomes of resected PDAC patients (13). Furthermore, the other germline mutations in mismatch repair genes (MLH1, etc.), the partner and localizer of BRCA2 (PALB2), cationic trypsinogen-gene (PRSS1), serine/threonine kinase 11 (STK11), ATM serine/threonine kinase (ATM), and breast cancer 1 (BRCA1) and breast cancer 2 (BRCA2) are correlated with a high risk of PC (14–16). As early as 2008, the coding regions of more than 29,000 genes in pancreatic adenocarcinomas were sequenced and 63 genomic alterations were identified that covered a core set of 12 cellular signaling pathways. These pathways included KRAS signaling, cell cycle regulation, DNA damage, TGF-beta signaling, RNA processing, and WNT signaling (13, 17) (Table 1). Further analysis of the *KRAS* types indicated that the most frequent mutations of *KRAS* are G12VD (31%), G12V (31%), and G12R (21%). Importantly, multiple concurrent *KRAS* mutations were detected in approximately 4% of PDACs, and, interestingly, these different *KRAS* mutations could be presented in different cells of the same tumor (19). As a tumor suppressor, *TP53* is the top frequently mutated gene in multiple tumors. Based on the results of the MSK-IMPACT study and the GENIE project, *TP53* mutations have been identified in approximately 70% of PDACs (20). The missense mutations of *TP53* occurred at approximately 190 codons, and the "hotspot" mutation codons included 175, 245, 248, 249, 273, and 282 whose mutation leads to abnormal conformational changes in the DNA-binding surface of TP53 (21). The mismatch repair–deficient cancers usually generate a large amount of neoantigens that are beneficial for their sensitivity to immune checkpoint blockage (22). It was reported that those pancreatic patients with longer survival time usually have stronger T-cell activity and less immunogenic mutations (neoantigens), which implied that the quality of neoantigens is important biomarker for tumor immunotherapy (18). Moreover, in addition to the location proximity of cytotoxic T cells to cancer cells, the neoantigen number in combination with the $CD8^+$ T-cell infiltration status is correlated with the survival of patients with PDAC (23, 24). It was reported that the mis-splicing of exons and errors in microsatellite (MS) transcription could generate highly immunogenic frameshift (FS) neoantigens whose sequence could be predicted and used to build the peptide array that covers all possible FS neoantigens (25).

TABLE 1 The list of mutated genes and the related pathways in pancreatic cancer (PC).

Pathway	Mutated Gene	Global Frequency (%)
KARS	**KRAS**, MAPK4	92
Cell Cycle	**TP53**, CDKN2A	78
TGF-beta Signaling	SMAD3, TGFBR1, ACVR1B, **SMAD4**, TGFBR2, ACVR2A	47
DNA Repair	BRCA1, BRCA2, PALB2, ATM, ATF2	17
Chromatin	MLL2, MLL3, **KDM6A**, SETD2	26
SWI/SNF	ARID1A, ASD1B. PBRM1, SMARCA4	20
Notch Signaling	JAG1, BCORL1, NF2, FBXW7	10
WNT Signaling	RNF43, MARK2, TLE4	5
RNA Processing	RBM10, SF3B1, U2AF1	15
ROBO SLIT Pathway	ROBO1, ROBO2, SLIT2, MYCBP2	5

The table is modified from the paper (18). The top frequent drivers of pancreatic tumorigenesis are indicated in bold.

Given that PDACs are highly associated with several mutations of genes such as *KRAS*, *TP53*, and *CDKN2A*, the development of neoantigen-based immunotherapy might be a promising therapeutic strategy for the treatment of PDAC. There are two kinds of neoantigens: shared neoantigens and personalized neoantigens (26, 27). Shared neoantigens are common antigens that are present in different cancer patients. Wenyi Zhao et al. found that 10 neoantigens were shared by approximately 50% of pancreatic patients that can be the potential targets for off-the-shelf immunotherapy (27). Personalized neoantigens are the unique mutated antigens from other most frequently used neoantigens, and the targeting of personalized neoantigens is specific personalized therapy (28). More importantly, the hallmarks of carcinogenesis are the accumulation of genetic and epigenetic mutations that are commonly classified as a 'driver' or 'passenger' mutation according to their roles in promoting cell proliferation and invasion (29). Driver mutations have the capability to drive the cell lineage to cancer, but passenger mutations do not exhibit the proliferation-promoting benefit to cell lineage (30). Moreover, due to the large fraction of passenger mutations compared with driver mutations, the passenger genes contribute to the majority of experimentally confirmed neoantigens that showed high immunogenicity (31). More notably, PCs have a limited number of neoantigen expressions due to their markedly low mutational burden, which is highly associated with the efficiency of immunotherapy (32). In line with this finding, the KPC pancreatic mice models showed that low mutation burden is highly associated with deficient immunoediting, but the ectopic expression of a neoantigen Ovalbumin (OVA) could rescue the tumor elimination ability (33). Therefore, these findings indicated that mutation burden can be considered a potential predictive biomarker of clinical response to checkpoint inhibition therapy (34).

A comprehensive analysis was performed on the genomic profiles of 221 PDAC cases, and the results indicated that the targetable neoantigens were expressed in almost all PDAC samples. Importantly, the top promising targetable neoantigens are KRAS codon 12 mutations (35). It was reported that T-cell receptors (TCRs) that are reactive to KRAS G12V and G12D neoantigens could be isolated for the immunized HLA-A*11:01 transgenic mice. Furthermore, these TCR-transduced peripheral blood lymphocytes (PBLs) could recognize plenty of HLA-A*11:01(+) tumor cell lines expressing the KRAS G12V and G12D mutations (36). Moreover, the genetically engineered T cells ectopically expressing two allogeneic HLA-C*08:02-restricted TCRs targeting KRAS G12D neoantigens were injected into the patient with metastatic PC and regressed the visceral metastases of the patient (37).

Neoantigen-based vaccines in pancreatic cancer

In recent years, immunotherapeutic strategies including various immune-checkpoint blockage, chimeric antigen receptor T-cell therapies are well studied in the treatment of multiple cancer types including PC. Importantly, as a novel cancer immunotherapy, the development and application of the personalized vaccines based on tumor-specific neoantigens attracted increasing attention in treating diverse cancers by enhancing the endogenous repertoire of tumor-specific T cells (38). Given that the neoantigens are expressed only on the tumor cells but not normal cells and they are unique epitopes of somatic mutations, the neoantigen-based vaccines could avoid the "off-target" damage to normal cells and prevent the T-cell central tolerance caused by self-epitopes and subsequently induce the tumor-specific T-cell response (38). Early studies showed that the neoantigen-based personalized cancer vaccines proved promising outcomes in prolonging the overall survival (OS) of cancer patients. The advances of next-generation sequencing and the bioinformatics for the prediction of major histocompatibility complex class I (MHC I)–binding epitopes promote the identification of tumor-specific mutations and the generation of personalized therapeutic cancer vaccines based on neoantigens.

Notably, the feasibility, safety, and immunogenicity of neoantigen-based personalized cancer vaccines were fully measured in patients with melanoma and glioblastoma (39, 40). The effect of iNeo-Vac-P01, a personalized neoantigen-based peptide vaccine, was examined in the treatment of PC, and the iNeo-Vac-P01 could enhance the clinical efficacy of PC (41). Recently, Li L et al. combined next-generation sequencing, novel predictive modeling techniques, and computational

algorithms based on bioinformatics to build and optimize a DNA vaccine platform to target multiple neoantigens in a metastatic pancreatic neuroendocrine tumor (42). In their study, the positive effect of the optimized polyepitope neoantigen DNA vaccine on the induction of antitumor immune responses and neoantigen-specific TCRs were confirmed in preclinical and clinical trials. Moreover, their findings also suggested that the neoantigen DNA vaccine can target multiple neoantigens at the same time and the longer epitope fragments could markedly extend the immune responses. Importantly, they found that the addition of a neoantigen-tagging mutant marker on the end of the epitope could dramatically enhance the immune responses (42). A neoantigen-targeted vaccine was generated using the synthesized 20-mer peptides according to the mutation of 12 genes: Myo1g, Ace, Glb1L12, Map2k5, Rasa3, Clcn7, Notch2, Bsg, Pnpla7, Ppp2r3a, Tg, and Ttn (43). The effect of the triple immunotherapeutic strategy, the combined administration of neoantigen-targeted vaccine PancVAX, anti-PD-1, and agonist OX40 antibodies, was investigated on the treatment of xenograft mice bearing pancreatic adenocarcinoma (Panc02) cells (43). The results indicated that PancVAX led to the transient regression of the tumor by inducing markedly the tumor infiltration of neoepitope-specific T cells. The addition of anti-PD-1 and agonist OX40 antibodies decreased the exhausted T-cell number, induced a durable tumor regression, and prolonged the survival time (43). Furthermore, TG01, the first injectable antigen-specific tumor immunotherapy targeting KRAS mutations, was designed by including seven synthetic RAS peptides that covered seven KRAS common mutations that occurred in codon 12 and 13 (44). The design aimed to activate both MHC-I CD8+ and MHC-II CD4 T-cell functions because the activation of CD4+ cells plays important roles in promoting the DC- meditated cross-presentation of neoantigens and TAAs on the tumor surface and further enhances the antitumor effect of CD8+ T cells (44, 45). Moreover, the safety, immunological responses, and clinical effect for TG01 in combination with recombinant human granulocyte macrophage–colony-stimulating factor and gemcitabine (GEM) chemotherapy were firstly examined on the resected pancreatic adenocarcinoma by Daniel H. Palmer et al., and the result indicated that the vaccination strategy can be well tolerated and trigger remarkable immune responses (45).

Currently, different personalized neoantigen-based cancer vaccines for the treatment of patients with PC are in the clinical trials (Table 2). With the advanced development of tumor mutation identification tools, neoantigen-prediction algorithms, vaccine delivery platforms, novel immunogenomic tools, and other bioinformatics technologies, the more effective, long-lasting personalized neoantigen-based immunotherapeutic strategies, especially the neoantigen-based vaccines, will be explored and benefit the patients with PC.

Dendritic cell vaccines of pancreatic cancer

DC–mediated antigen presentation plays essential roles in modulating immune responses. The dysregulation of antigen processing and presentation is a critical mechanism facilitating tumor escape from the immune surveillance by the immune system. However, it was reported that DCs and other antigen-processing and -presenting molecules such as human leukocyte antigen (HLA) class I and transporter for antigen presentation (TAP) were downregulated in PCs (46). Moreover, accumulating evidence indicated that tumor antigen–based DC vaccines exhibited effectiveness to induce the T-cell-mediated adaptive cytolytic immune responses in PC (46).The development of DCs vaccines aimed to connect the DCs with TAA to present the antigen and subsequently activate cytotoxic T cells. Currently, various types of DC-based vaccines were developed and in the clinical trial stage (47).

In a phase I study, the effect of allogeneic tumor lysate–loaded autologous monocyte-derived DCs was evaluated in the treatment of resected PDAC and the vaccination treatment indicated a feasible and safe immune reactivity induction capability (48).The prophylactic DC vaccination strategy used DC vaccines generated by *ex vivo* differentiation, and the maturation of bone marrow–derived precursors was investigated in PDAC tumor mice models and exhibited a significant effect in inhibiting recurrent tumor growth and extending the survival time (49). It was well known that in PCs, the telomerase [human telomerase reverse transcriptase (hTERT)] is a promising target antigen and it mainly expresses in cancer stem cells that are difficult to eliminate by common therapeutic strategies (50). PC patients who received the vaccination of DCs transfected with hTERT full-length mRNA exhibited an induction of hTERT-specific immune responses but have not experienced serious adverse issues. This study therefore provided positive evidence for the generation of DC vaccines loaded with mRNA for a specific antigen with clinical relevance by inducing the antigen-specific immune responses (51). However, although DCs are well known for their antigen presentation function in the immune system and could induce the TCR specific to tumor antigens, the immunotherapeutic efficacy of DCs in combating PCs is still limited. Therefore, the combination immunotherapy of DC vaccines with other therapies to improve the efficacy of DC vaccination is a promising research topic. In line with this notion, the efficacy of peptide-pulsed DC vaccines in combination with the Toll-like receptor (TLR)-3 agonist poly-ICLC was tested in the murine orthotopic Panc02 cell models. The combination vaccination method showed a significant antimetastatic effect *via* CD8+ T-cell activation (52). The DC vaccines could also dramatically induce the cytotoxic T-lymphocyte (CTL) responses and block the migration of PC (53). Given that numerous antitumor strategies including checkpoint inhibitor treatments are less sensitive to PDAC, the combined therapeutic method by inducing tumor-specific T cells *via* DC vaccination and remodeling the desmoplasia of the tumor microenvironment (TME) *via* CD40-agonistic antibody administration could reduce the tolerance to PDAC. Therefore, the effect of mesothelioma-lysate loaded DCs coupled with FGK45 (CD40 agonist) was tested in immune-competent PDAC mice models and the novel approach induced a significant change in the tumor transcriptome including the inhibitory markers on CD8 +T cells and dramatically enhanced patient survival (54). Notably, the survival of patients with advanced pancreatic carcinoma who received the DC-based immunotherapy combined with GEM and/or S-1 was dramatically prolonged by the administration of lymphokine-activated killer (LAK) cell therapy. However, immunotherapy alone could increase the number of cancer antigen–specific cytotoxic T cells and reduce the regulatory T cells (55). The antitumor effect of DCs loaded with alpha-galactosylceramide (alpha-GalCer) was evaluated

10.3389/fimmu.2023.1104860

TABLE 2 Clinical trials of neoantigen-based therapies on PC.

NCT Number	Intervention/ treatment	Phase	Start date	Completion date	Enrollment	Status	Sponsor
NCT03645148	iNeo-Vac-P01 + GM-CSF	I	10/24/ 2017	04/01/2021	7	completed	Zhejiang Provincial People's Hospital
NCT05111353	Neoantigen peptide vaccine: Poly-ICLC	I	10/10/ 2022	12/31/2027	30	Recruiting	Washington University School of Medicine
NCT03122106	Personalized neoantigen DNA vaccine	I	01/05/ 2018	08/13/2022	15	Terminated	Washington University School of Medicine
NCT03956056	Neoantigen peptide vaccine: Poly-ICLC	I	02/13/ 2020	06/21/2023	12	Active, not recruiting	Washington University School of Medicine
NCT04810910	iNeo-Vac-P01 + GM-CSF	I	03/30/ 2021	03/30/2025	20	Recruiting	Zhejiang Provincial People's Hospital
NCT03558945	Personalized neoantigen vaccine	I	04/02/ 2018	04/30/2023	60	Recruiting	Changhai Hospital
NCT04799431	Neoantigen vaccine with Poly-ICLC adjuvant: retifanlimab	I	01/01/ 2023	01/01/2028	12(estimated)	Not yet recruiting	Sidney Kimmel Comprehensive Cancer Center at Johns Hopkins
NCT04161755	Personalized tumor vaccines (PCVs) + PD-L1 blocker: atezolizumab + mFOLFIRINOX	I	12/13/ 2019	11/01/2023	29	Active, not recruiting	Memorial Sloan Kettering Cancer Center
NCT03953235	GRT-C903/GRT-R904 + nivoluma/ ipilimumab	I/II	07/18/ 2019	12/00/2023	144	Recruiting	Gritstone bio, Inc.
NCT03871790	Peptide-based immunization	N/A	04/01/ 2019	11/01/2021	100 (estimated)	N/A	CENTOGENE GmbH Rostock
NCT03662815	iNeo-Vac-P01 + GM-CSF	I	02/07/ 2018	12/30/2022	30(estimated)	Active, not recruiting	Sir Run Run Shaw Hospital
NCT05013216	KRAS peptide vaccine Hiltonol® (Poly-ICLC)	I	04/11/ 2022	05/01/2026	25(estimated)	Recruiting	Sidney Kimmel Comprehensive Cancer Center at Johns Hopkins
NCT03468244	Personalized mRNA tumor vaccine	N/A	05/01/ 2018	12/31/2020	24(estimated)	N/A	Changhai Hospital
NCT05292859	Neoantigen-specific TCR-T-cell drug product	N/A	09/00/ 2022	06/00/2039	180 (estimated)	Not yet recruiting	Alaunos Therapeutics
NCT04117087	KRAS peptide vaccine, nivolumab, ipilimumab	I	05/29/ 2020	06/01/2024	30(estimated)	Recruiting	Sidney Kimmel Comprehensive Cancer Center at Johns Hopkins
NCT05194735	Neoantigen-specific TCR-T-cell drug product + aldesleukin (IL-2)	I/II	04/04/ 2022	03/00/2029	180 (estimated)	Recruiting	Alaunos Therapeutics
NCT02600949	Synthetic tumor-associated peptide vaccine: imiquimod	I	05/11/ 2016	05/31/2025	150 (estimated)	Recruiting	M.D. Anderson Cancer Center

All clinical trial data were collected from ClinicalTrials.gov by the keywords neoantigen and pancreatic cancer (https://clinicaltrials.gov/ct2).

in PC C57BL/6 mice models, and tumor growth was inhibited, which might be correlated with the increased number of IFNγ-producing NKT cells (56).

Currently, most of the efforts of DC-based vaccination were focused on MUC1, WT1, and KRAS antigens. The TAA MUC1, a glycoprotein, is ubiquitously expressed in PC cells. The effect of MUC1-DCs vaccine that was generated by transfecting the liposomal MUC1 cDNA into DCs was investigated in PC patients, and the result indicated that MUC1-DC vaccination was well tolerated and enhanced the CTL response (57). However, MUC1 peptides-loaded/pulsed DC vaccines were well tolerated in treating PCs in two separate studies but the clinical benefit is controversial, which might be caused by the different patients (58, 59). Importantly, the efficacy of triple therapy for MUC1-mRNA-transfected DCs in combination with MUC1-CTLs and GEM was examined in PCs and the addition of MUC1-DCs and MUC1-CTLs dramatically prolonged the survival time (60). The Wilms tumor gene (WT1) is overexpressed in many PCs, and WT1 peptide–pulsed DC vaccines were reported to dramatically prolong the median OS of PC patients in combination with standard chemotherapy (61).

Neoantigen-based dendritic cell vaccines in pancreatic cancer

Generally, neoantigens belong to antigens, but they are specific novel antigens to each patient's cancer and produced by random mutations in the cancer genome. Therefore, DCs still own the capability to present the neoantigens to T cells and subsequently induce a specific immune response to each patient with related

mutations. The high level of neoantigen expression is positively correlated with pathogenic TCR and PDAC progression. The dysregulation of conventional DCs (cDCs) is highly correlated with abnormal immune surveillance and hampered the response of early T_H1 and CTL to the neoantigens of PDAC (62). Moreover, the function and amount of cDCs in PDAC could be considered as a biomarker for the adaptive immune responses to tumor neoantigens in PDAC (63). Therefore, DCs may play essential roles in neoantigen presentation and inducing the neoantigen-specific TCR because the neoantigen-loaded DC vaccines can directly present neoantigens to T cells.

Due to the unclear mutational load of specific cancers, the large amount of DC vaccines was designed to induce the immune response by targeting predetermined and universal antigens. However, the neoantigen-based DC vaccine is considered a personalized DC vaccine because the patient-specific neoantigens could be identified through novel genomic sequencing technologies and bioinformatics (64). Given that PC is characteristic for lower tumor burden and a limited number of neoantigen and DCs, the effect of neoantigen-pulsed DC vaccines was firstly examined in other cancers including melanoma and lung cancer. The induction of the neoantigen-specific TCR repertoire of neoantigen-pulsed DC vaccination was firstly investigated in advanced melanoma (65). Moreover, the feasibility, safety, immunogenicity, and efficacy of a peptide vaccine targeting 20 predicted neoantigens were further investigated in melanoma patients, which provided a newly possible rationale to optimize the neoantigen-based vaccine and the development of novel therapeutic strategy in combination with commonly used immunotherapies (39). Notably, the effect of neoantigen-pulsed DC vaccines on the patients with advanced NSCLC was evaluated in a trial in 2021 (11). They generated the personalized DC vaccines based on the 13-30 peptide of the neoantigens identified in the tumor tissues of 12 patients. Upon the personalized neoantigen-pulsed DC vaccine treatment, 25% of patients responded to the vaccination and 75% of patients showed a disease inhibition, which indicated a favorable therapeutic outcome for the vaccination strategy (11). Furthermore, Changbo Sun et al. found and designed a neoantigen short peptide L82 based on the result from the whole-exome and RNA sequencing on the LLC1 cell line. This candidate neoantigen short peptide L82 can both trigger $CD8^+$ T-cell responses and suppress the LLC1 growth *in vivo*. THE L82-pulsed DC vaccination in combination with anti-CD38 antibody treatment effectively inhibited the tumor growth by reducing the tumor- infiltrated regulatory T cells (66). Furthermore, the effect of the combination of DC-loaded with MART-1 peptide vaccine with tremelimumab and the anti-CTLA-4 antibody was tested in melanoma, and the treatment strategy achieved a stronger and durable tumor response than each treatment alone (67). Moreover, the patients with metastatic gastric cancer have received the administration of neoantigen-pulsed DC (Neo-MoDC) vaccines combined with immune checkpoint inhibition (ICI). Although the Neo-MoDC vaccine alone could trigger neoantigen-specific $CD4^+$ and $CD8^+$ TCRs, the combination therapy induced a higher immune response and significant elimination of tumors (68). Notably, a phase Ib trial (CHUV-DO-0017_PC-PEPDC_2017) was also conducted on a DC vaccine pulsed with personalized neoantigen peptides (PEP-DC) coupled with the treatment of chemotherapy and the anti-PD-1 antibody. The study comprehensively evaluated the feasibility, safety, immunogenicity, and efficacy of the combination therapy of the DC vaccine in PCs (69). Therefore, these findings suggested that the neoantigen-based DC vaccine combined with other therapeutic strategies enhanced the effects of cancer treatment by inducing highly patient-specific immune responses and provided novel therapeutic opportunities for cancer treatment.

In a phase I pilot study, the feasibility and efficacy of a DC vaccine pulsed with the Wilms tumor gene-1 (WT1) peptide in combination with GEM were evaluated in the treatment of advanced PC as a first line of treatment. The WT1 peptide–pulsed DCGEM is feasible and effective in triggering the antitumor TCRs but showed less effect in treating the PC with live metastasis and elevated levels of inflammatory markers (70). Furthermore, a phase Ib trial (CHUV-DO-0017_PC-PEPDC_2017) was conducted to test the safety, immunogenicity, feasibility, and efficacy of the DC vaccine pulsed with personalized neoantigen peptides (PEP-DC) in PDAC and the efficacy of combination with aspirin, nivolumab, and adjuvant chemotherapy was further evaluated (69). NeoDisc, a novel proteogenomics antigen discovery pipeline, was used to find and optimize the candidate neoantigen in PDAC, and, furthermore, the long peptides of relative neoantigens were designed. Due to the possibility of low immunogenic capability, the p53 (TP53), mucin-1 (MUC1), prolyl endopeptidase FAP (FAP), TAA mesothelin (MSLN), outer dense fiber protein 2 (ODF2), coiled-coil domain-containing protein 110 (CCDC110), and the testis-specific protein bromodomain testis-specific protein (BRDT) were excluded in the design of the DC vaccine (69). Shikhar Mehrotra et al. generated a DC vaccine pulsed with three specific A2-restricted peptides: 1) hTERT (TERT572Y), 2) carcinoembryonic antigen (CEA; Cap1-6D), and 3) survivin (SRV.A2). The neoantigen-pulsed DC vaccine in combination with the Toll-like receptor (TLR)-3 agonist poly-ICLC was used to treat the metastatic or locally advanced unresectable PC (52). The results of the study indicated that the combination therapeutic strategy is safe and could effectively induce the tumor-specific TCR (52). Furthermore, the MUC1 peptide-pulsed DC vaccines were used to treat the advanced PC patients and the results indicated that the vaccination is safe and effective to trigger the immunological response to the tumor antigen MUC1 (58, 59).

Importantly, the effects of the mDC3/8-KRAS vaccine that included a DC vaccine loaded with KRAS mutation peptides on the resected PDAC patients is evaluated in the ongoing phase I study (NCT03592888). For each vaccine dose in the trial, all subjects will receive autologous DCs pulsed with mutant KRAS peptides corresponding to the subject's specific tumor mutation and HLA type. In addition, the inclusion criteria included pathologically confirmed KRAS(G12D-), KRAS(G12V-), KRAS(G12R-), or KRAS (G12C-mutated) PDAC who are at a high risk of relapse and have no evidence of disease (NCT03592888). A terminated phase II trial on a DC vaccine against defined neoantigens expressed by autologous cancers had been performed in patients with epithelial cancers including PDAC, but only one patient was enrolled (NCT03300843).

Therefore, given that PDAC is one of the poorly immune-responsive cancers and some currently used immunotherapies are also less effective in treating PDAC, it is urgent to develop novel therapeutic strategies including alone administration or the combinations of chemotherapy, radiation, vaccines, and ICIs and

the development of personalized neoantigen-pulsed DC vaccines to fully induce antitumor TCRs.

Conclusion and outlook

Recently, immunotherapies have proven their effectiveness in multiple types of cancers but the efficacy is limited in the treatment of PC partially due to the immune-tolerant state, lower mutational burden, and decreased amount of DC. The high tumor specificity and immunogenicity make neoantigens an exciting and promising target of tumor immunotherapy. Neoantigens, the novel and specific antigens, could also be presented by DCs. Neoantigen-based DC vaccines illustrated promising effects in multiple cancers, but few are investigated in PCs, which is possibly due to low mutation burden and limited neoantigens. Given that the feasibility, safety, immunogenicity, and efficacy of neoantigen-based DC vaccines were evaluated in various cancers, it is an urgent need to put more effort on the development of suitable neoantigen-based DC vaccines for PC and evaluate their efficacy in clinical trials, which will provide precise treatment for more PC patients. However, high costs, longer time for manufacturing, difficulty in large-scale DC cell maturation, the low efficiency of DC migration, the lack of a better method for accurate identification of immunogenic neoantigens, and a less optimized vaccine delivery platform limited the development of personalized immunotherapy, which warrants further in-depth investigation in the future (38). Fortunately, with the advances and optimization in whole exome sequencing and neoantigen-prediction algorithms, the in-depth understanding of the molecular mechanisms underlying the immune-tolerant state of pancreatic cancer, the development of neoantigen-based DC vaccines will be significantly improved. The combined immunotherapy approach using neoantigen-based DC vaccines, chemotherapy, and ICIs showed exciting therapeutic benefits to various cancer patients. Therefore, the novel therapeutic strategies including combination immunotherapy for PC should also be explored and optimized to benefit more PC patients.

Author contributions

XinZ wrote the manuscript with partial help from ZX. XD, XiaZ, and XW edited and revised the manuscript. All authors approved the final manuscript.

Funding

This work is supported by the Young Scientists Fund of the National Natural Science Foundation of China (No: 81700198), the Science and Technology Development Project of Jilin Province (No: 20190701064GH).

Acknowledgments

We thank other members of the Wang laboratory for the critical reading of the manuscript and useful discussions.

Conflict of interest

The authors declare that the research was conducted in the absence of any commercial or financial relationships that could be construed as a potential conflict of interest.

Publisher's note

References

1. Cai H, Jing C, Chang X, Ding D, Han T, Yang J, et al. Mutational landscape of gastric cancer and clinical application of genomic profiling based on target next-generation sequencing. *J Transl Med* (2019) 17(1):189. doi: 10.1186/s12967-019-1941-0

2. Luo J. KRAS mutation in pancreatic cancer. *Semin Oncol* (2021) 48(1):10–8. doi: 10.1053/j.seminoncol.2021.02.003

3. Srivastava PK. Neoepitopes of cancers: Looking back, looking ahead. *Cancer Immunol Res* (2015) 3(9):969–77. doi: 10.1158/2326-6066.CIR-15-0134

4. Nakagawa H, Fujita M. Whole genome sequencing analysis for cancer genomics and precision medicine. *Cancer Sci* (2018) 109(3):513–22. doi: 10.1111/cas.13505

5. Peng M, Mo Y, Wang Y, Wu P, Zhang Y, Xiong F, et al. Neoantigen vaccine: an emerging tumor immunotherapy. *Mol Cancer* (2019) 18(1):128. doi: 10.1186/s12943-019-1055-6

6. Filley AC, Dey M. Dendritic cell based vaccination strategy: an evolving paradigm. *J Neurooncol* (2017) 133(2):223–35. doi: 10.1007/s11060-017-2446-4

7. Ott PA, Hu-Lieskovan S, Chmielowski B, Govindan R, Naing A, Bhardwaj N, et al. A phase ib trial of personalized neoantigen therapy plus anti-PD-1 in patients with advanced melanoma, non-small cell lung cancer, or bladder cancer. *Cell* (2020) 183 (2):347–62 e24. doi: 10.1016/j.cell.2020.08.053

8. Banchereau J, Briere F, Caux C, Davoust J, Lebecque S, Liu YJ, et al. Immunobiology of dendritic cells. *Annu Rev Immunol* (2000) 18:767–811. doi: 10.1146/annurev.immunol.18.1.767

9. Keskin DB, Anandappa AJ, Sun J, Tirosh I, Mathewson ND, Li S, et al. Neoantigen vaccine generates intratumoral T cell responses in phase ib glioblastoma trial. *Nature* (2019) 565(7738):234–9. doi: 10.1038/s41586-018-0792-9

10. Dissanayake D, Murakami K, Tran MD, Elford AR, Millar DG, Ohashi PS. Peptide-pulsed dendritic cells have superior ability to induce immune-mediated tissue destruction compared to peptide with adjuvant. *PloS One* (2014) 9(3):e92380. doi: 10.1371/journal.pone.0092380

11. Ding Z, Li Q, Zhang R, Xie L, Shu Y, Gao S, et al. Personalized neoantigen pulsed dendritic cell vaccine for advanced lung cancer. *Signal Transduct Target Ther* (2021) 6 (1):26. doi: 10.1038/s41392-020-00448-5

12. Chen H, Yang G, Xiao J, Zheng L, You L, Zhang T. Neoantigen-based immunotherapy in pancreatic ductal adenocarcinoma (PDAC). *Cancer Lett* (2020) 490:12–9. doi: 10.1016/j.canlet.2020.06.011

13. Pelosi E, Castelli G, Testa U. Pancreatic cancer: Molecular characterization, clonal evolution and cancer stem cells. *Biomedicines* (2017) 5(4):65. doi: 10.3390/biomedicines5040065

14. Shindo K, Yu J, Suenaga M, Fesharakizadeh S, Cho C, Macgregor-Das A, et al. Deleterious germline mutations in patients with apparently sporadic pancreatic adenocarcinoma. *J Clin Oncol* (2017) 35(30):3382–90. doi: 10.1200/JCO.2017.72.3502

15. Childs EJ, Chaffee KG, Gallinger S, Syngal S, Schwartz AG, Cote ML, et al. Association of common susceptibility variants of pancreatic cancer in higher-risk

patients: A PACGENE study. *Cancer Epidemiol Biomarkers Prev* (2016) 25(7):1185–91. doi: 10.1158/1055-9965.EPI-15-1217

16. Roberts NJ, Norris AL, Petersen GM, Bondy ML, Brand R, Gallinger S, et al. Whole genome sequencing defines the genetic heterogeneity of familial pancreatic cancer. *Cancer Discovery* (2016) 6(2):166–75. doi: 10.1158/2159-8290.CD-15-0402

17. Jones S, Zhang X, Parsons DW, Lin JC, Leary RJ, Angenendt P, et al. Core signaling pathways in human pancreatic cancers revealed by global genomic analyses. *Science* (2008) 321(5897):1801–6. doi: 10.1126/science.1164368

18. Luksza M, Sethna ZM, Rojas LA, Lihm J, Bravi B, Elhanati Y, et al. Neoantigen quality predicts immunoediting in survivors of pancreatic cancer. *Nature* (2022) 606 (7913):389–95. doi: 10.1038/s41586-022-04735-9

19. Cancer Genome Atlas Research Network. Integrated genomic characterization of pancreatic ductal adenocarcinoma. *Cancer Cell* (2017) 32(2):185–203 e13. doi: 10.1016/j.ccell.2017.07.007

20. Voutsadakis IA. Mutations of p53 associated with pancreatic cancer and therapeutic implications. *Ann Hepatob Pancreat Surg* (2021) 25(3):315–27. doi: 10.14701/ahbps.2021.25.3.315

21. Baugh EH, Ke H, Levine AJ, Bonneau RA, Chan CS. Why are there hotspot mutations in the TP53 gene in human cancers? *Cell Death Differ* (2018) 25(1):154–60. doi: 10.1038/cdd.2017.180

22. Le DT, Durham JN, Smith KN, Wang H, Bartlett BR, Aulakh LK, et al. Mismatch repair deficiency predicts response of solid tumors to PD-1 blockade. *Science* (2017) 357 (6349):409–13. doi: 10.1126/science.aan6733

23. Balachandran VP, Luksza M, Zhao JN, Makarov V, Moral JA, Remark R, et al. Identification of unique neoantigen qualities in long-term survivors of pancreatic cancer. *Nature* (2017) 551(7681):512–6. doi: 10.1038/nature24462

24. Carstens JL, Correa de Sampaio P, Yang D, Barua S, Wang H, Rao A, et al. Spatial computation of intratumoral T cells correlates with survival of patients with pancreatic cancer. *Nat Commun* (2017) 8:15095. doi: 10.1038/ncomms15095

25. Shen L, Zhang J, Lee H, Batista MT, Johnston SA. RNA Transcription and splicing errors as a source of cancer frameshift neoantigens for vaccines. *Sci Rep* (2019) 9(1):14184. doi: 10.1038/s41598-019-50738-4

26. Sahin U, Tureci O. Personalized vaccines for cancer immunotherapy. *Science* (2018) 359(6382):1355–60. doi: 10.1126/science.aar7112

27. Zhao W, Wu J, Chen S, Zhou Z. Shared neoantigens: Ideal targets for off-the-shelf cancer immunotherapy. *Pharmacogenomics* (2020) 21(9):637–45. doi: 10.2217/pgs-2019-0184

28. Tureci O, Lower M, Schrors B, Lang M, Tadmor A, Sahin U. Challenges towards the realization of individualized cancer vaccines. *Nat BioMed Eng* (2018) 2(8):566–9. doi: 10.1038/s41551-018-0266-2

29. Bozic I, Antal T, Ohtsuki H, Carter H, Kim D, Chen S, et al. Accumulation of driver and passenger mutations during tumor progression. *Proc Natl Acad Sci U S A* (2010) 107 (43):18545–50. doi: 10.1073/pnas.1010978107

30. Vogelstein B, Papadopoulos N, Velculescu VE, Zhou S, Diaz LAJr., Kinzler KW. Cancer genome landscapes. *Science* (2013) 339(6127):1546–58. doi: 10.1126/science.1235122

31. Efremova M, Finotello F, Rieder D, Trajanoski Z. Neoantigens generated by individual mutations and their role in cancer immunity and immunotherapy. *Front Immunol* (2017) 8:1679. doi: 10.3389/fimmu.2017.01679

32. Looi CK, Chung FF, Leong CO, Wong SF, Rosli R, Mai CW. Therapeutic challenges and current immunomodulatory strategies in targeting the immunosuppressive pancreatic tumor microenvironment. *J Exp Clin Cancer Res* (2019) 38(1):162. doi: 10.1186/s13046-019-1153-8

33. Evans RA, Diamond MS, Rech AJ, Chao T, Richardson MW, Lin JH, et al. Lack of immunoediting in murine pancreatic cancer reversed with neoantigen. *JCI Insight* (2016) 1(14):e88328. doi: 10.1172/jci.insight.88328

34. Gubin MM, Schreiber RD. Cancer. the odds of immunotherapy success. *Science* (2015) 350(6257):158–9. doi: 10.1126/science.aad4140

35. Bailey P, Chang DK, Forget MA, Lucas FA, Alvarez HA, Haymaker C, et al. Exploiting the neoantigen landscape for immunotherapy of pancreatic ductal adenocarcinoma. *Sci Rep* (2016) 6:35848. doi: 10.1038/srep35848

36. Wang QJ, Yu Z, Griffith K, Hanada K, Restifo NP, Yang JC. Identification of T-cell receptors targeting KRAS-mutated human tumors. *Cancer Immunol Res* (2016) 4(3):204–14. doi: 10.1158/2326-6066.CIR-15-0188

37. Leidner R, Sanjuan Silva N, Huang H, Sprott D, Zheng C, Shih YP, et al. Neoantigen T-cell receptor gene therapy in pancreatic cancer. *N Engl J Med* (2022) 386 (22):2112–9. doi: 10.1056/NEJMoa2119662

38. Blass E, Ott PA. Advances in the development of personalized neoantigen-based therapeutic cancer vaccines. *Nat Rev Clin Oncol* (2021) 18(4):215–29. doi: 10.1038/s41571-020-00460-2

39. Ott PA, Hu Z, Keskin DB, Shukla SA, Sun J, Bozym DJ, et al. An immunogenic personal neoantigen vaccine for patients with melanoma. *Nature* (2017) 547(7662):217–21. doi: 10.1038/nature22991

40. Hilf N, Kuttruff-Coqui S, Frenzel K, Bukur V, Stevanovic S, Gouttefangeas C, et al. Actively personalized vaccination trial for newly diagnosed glioblastoma. *Nature* (2019) 565(7738):240–5. doi: 10.1038/s41586-018-0810-y

41. Chen Z, Zhang S, Han N, Jiang J, Xu Y, Ma D, et al. A neoantigen-based peptide vaccine for patients with advanced pancreatic cancer refractory to standard treatment. *Front Immunol* (2021) 12:691605. doi: 10.3389/fimmu.2021.691605

42. Li L, Zhang X, Wang X, Kim SW, Herndon JM, Becker-Hapak MK, et al. Optimized polyepitope neoantigen DNA vaccines elicit neoantigen-specific immune responses in preclinical models and in clinical translation. *Genome Med* (2021) 13 (1):56. doi: 10.1186/s13073-021-00872-4

43. Kinkead HL, Hopkins A, Lutz E, Wu AA, Yarchoan M, Cruz K, et al. Combining STING-based neoantigen-targeted vaccine with checkpoint modulators enhances antitumor immunity in murine pancreatic cancer. *JCI Insight* (2018) 3(20):e122857. doi: 10.1172/jci.insight.122857

44. Gjertsen MK, Buanes T, Rosseland AR, Bakka A, Gladhaug I, Soreide O, et al. Intradermal ras peptide vaccination with granulocyte-macrophage colony-stimulating factor as adjuvant: Clinical and immunological responses in patients with pancreatic adenocarcinoma. *Int J Cancer* (2001) 92(3):441–50. doi: 10.1002/ijc.1205

45. Palmer DH, Valle JW, Ma YT, Faluyi O, Neoptolemos JP, Jensen Gjertsen T, et al. TG01/GM-CSF and adjuvant gemcitabine in patients with resected RAS-mutant adenocarcinoma of the pancreas (CT TG01-01): a single-arm, phase 1/2 trial. *Br J Cancer* (2020) 122(7):971–7. doi: 10.1038/s41416-020-0752-7

46. Deicher A, Andersson R, Tingstedt B, Lindell G, Bauden M, Ansari D. Targeting dendritic cells in pancreatic ductal adenocarcinoma. *Cancer Cell Int* (2018) 18:85. doi: 10.1186/s12935-018-0585-0

47. Ni L. Advances in human dendritic cell-based immunotherapy against gastrointestinal cancer. *Front Immunol* (2022) 13:887189. doi: 10.3389/fimmu.2022.887189

48. Lau SP, Klaase L, Vink M, Dumas J, Bezemer K, van Krimpen A, et al. Autologous dendritic cells pulsed with allogeneic tumour cell lysate induce tumour-reactive T-cell responses in patients with pancreatic cancer: A phase I study. *Eur J Cancer* (2022) 169:20–31. doi: 10.1016/j.ejca.2022.03.015

49. Shangguan A, Shang N, Figini M, Pan L, Yang J, Ma Q, et al. Prophylactic dendritic cell vaccination controls pancreatic cancer growth in a mouse model. *Cytotherapy* (2020) 22(1):6–15. doi: 10.1016/j.jcyt.2019.12.001

50. Bhagwandin VJ, Shay JW. Pancreatic cancer stem cells: Fact or fiction? *Biochim Biophys Acta* (2009) 1792(4):248–59. doi: 10.1016/j.bbadis.2009.02.007

51. Suso EM, Dueland S, Rasmussen AM, Vetrhus T, Aamdal S, Kvalheim G, et al. hTERT mRNA dendritic cell vaccination: complete response in a pancreatic cancer patient associated with response against several hTERT epitopes. *Cancer Immunol Immunother* (2011) 60(6):809–18. doi: 10.1007/s00262-011-0991-9

52. Mehrotra S, Britten CD, Chin S, Garrett-Mayer E, Cloud CA, Li M, et al. Vaccination with poly(IC : LC) and peptide-pulsed autologous dendritic cells in patients with pancreatic cancer. *J Hematol Oncol* (2017) 10(1):82. doi: 10.1186/s13045-017-0459-2

53. Pan L, Shang N, Shangguan J, Figini M, Xing W, Wang B, et al. Magnetic resonance imaging monitoring therapeutic response to dendritic cell vaccine in murine orthotopic pancreatic cancer models. *Am J Cancer Res* (2019) 9(3):562–73.

54. Lau SP, van Montfoort N, Kinderman P, Lukkes M, Klaase L, van Nimwegen M, et al. Dendritic cell vaccination and CD40-agonist combination therapy licenses T cell-dependent antitumor immunity in a pancreatic carcinoma murine model. *J Immunother Cancer* (2020) 8(2):e000772. doi: 10.1136/jitc-2020-000772

55. Kimura Y, Tsukada J, Tomoda T, Takahashi H, Imai K, Shimamura K, et al. Clinical and immunologic evaluation of dendritic cell-based immunotherapy in combination with gemcitabine and/or s-1 in patients with advanced pancreatic carcinoma. *Pancreas* (2012) 41(2):195–205. doi: 10.1097/MPA.0b013e31822398c6

56. Nagaraj S, Ziske C, Strehl J, Messmer D, Sauerbruch T, Schmidt-Wolf IG. Dendritic cells pulsed with alpha-galactosylceramide induce anti-tumor immunity against pancreatic cancer in vivo. *Int Immunol* (2006) 18(8):1279–83. doi: 10.1093/intimm/dxl059

57. Pecher G, Haring A, Kaiser L, Thiel E. Mucin gene (MUC1) transfected dendritic cells as vaccine: results of a phase I/II clinical trial. *Cancer Immunol Immunother* (2002) 51(11-12):669–73. doi: 10.1007/s00262-002-0317-z

58. Lepisto AJ, Moser AJ, Zeh H, Lee K, Bartlett D, McKolanis JR, et al. A phase I/II study of a MUC1 peptide pulsed autologous dendritic cell vaccine as adjuvant therapy in patients with resected pancreatic and biliary tumors. *Cancer Ther* (2008) 6(B):955–64.

59. Rong Y, Qin X, Jin D, Lou W, Wu L, Wang D, et al. A phase I pilot trial of MUC1-peptide-pulsed dendritic cells in the treatment of advanced pancreatic cancer. *Clin Exp Med* (2012) 12(3):173–80. doi: 10.1007/s10238-011-0159-0

60. Shindo Y, Hazama S, Maeda Y, Matsui H, Iida M, Suzuki N, et al. Adoptive immunotherapy with MUC1-mRNA transfected dendritic cells and cytotoxic lymphocytes plus gemcitabine for unresectable pancreatic cancer. *J Transl Med* (2014) 12:175. doi: 10.1186/1479-5876-12-175

61. Okamoto M, Kobayashi M, Yonemitsu Y, Koido S, Homma S. Dendritic cell-based vaccine for pancreatic cancer in Japan. *World J Gastrointest Pharmacol Ther* (2016) 7 (1):133–8. doi: 10.4292/wjgpt.v7.i1.133

62. Hegde S, Krisnawan VE, Herzog BH, Zuo C, Breden MA, Knolhoff BL, et al. Dendritic cell paucity leads to dysfunctional immune surveillance in pancreatic cancer. *Cancer Cell* (2020) 37(3):289–307 e9. doi: 10.1016/j.ccell.2020.02.008

63. Bordon Y. DC Deployment in pancreatic cancer. *Nat Rev Immunol* (2020) 20 (5):276–7. doi: 10.1038/s41577-020-0298-1

64. Cannon MJ, Block MS, Morehead LC, Knutson KL. The evolving clinical landscape for dendritic cell vaccines and cancer immunotherapy. *Immunotherapy* (2019) 11(2):75–9. doi: 10.2217/imt-2018-0129

65. Carreno BM, Magrini V, Becker-Hapak M, Kaabinejadian S, Hundal J, Petti AA, et al. Cancer immunotherapy. A dendritic cell vaccine increases the breadth and diversity of melanoma neoantigen-specific T cells. *Science* (2015) 348(6236):803–8. doi: 10.1126/science.aaa3828

66. Sun C, Nagaoka K, Kobayashi Y, Nakagawa H, Kakimi K, Nakajima J. Neoantigen dendritic cell vaccination combined with anti-CD38 and CpG elicits anti-tumor immunity against the immune checkpoint therapy-resistant murine lung cancer cell line LLC1. *Cancers (Basel)* (2021) 13(21):5508. doi: 10.3390/cancers13215508

67. De Plaen E, Lurquin C, Van Pel A, Mariame B, Szikora JP, Wolfel T, et al. Immunogenic (tum-) variants of mouse tumor P815: cloning of the gene of tum- antigen P91A and identification of the tum- mutation. *Proc Natl Acad Sci U S A* (1988) 85 (7):2274–8. doi: 10.1073/pnas.85.7.2274

68. Guo Z, Yuan Y, Chen C, Lin J, Ma Q, Liu G, et al. Durable complete response to neoantigen-loaded dendritic-cell vaccine following anti-PD-1 therapy in metastatic gastric cancer. *NPJ Precis Oncol* (2022) 6(1):34. doi: 10.1038/s41698-022-00279-3

69. Bassani-Sternberg M, Digklia A, Huber F, Wagner D, Sempoux C, Stevenson BJ, et al. A phase ib study of the combination of personalized autologous dendritic cell vaccine, aspirin, and standard of care adjuvant chemotherapy followed by nivolumab for resected pancreatic adenocarcinoma-a proof of antigen discovery feasibility in three patients. *Front Immunol* (2019) 10:1832. doi: 10.3389/fimmu.2019.01832

70. Mayanagi S, Kitago M, Sakurai T, Matsuda T, Fujita T, Higuchi H, et al. Phase I pilot study of wilms tumor gene 1 peptide-pulsed dendritic cell vaccination combined with gemcitabine in pancreatic cancer. *Cancer Sci* (2015) 106(4):397–406. doi: 10.1111/cas.12621

Frontiers in Immunology

Explores novel approaches and diagnoses to treat immune disorders.

The official journal of the International Union of Immunological Societies (IUIS) and the most cited in its field, leading the way for research across basic, translational and clinical immunology.

Discover the latest Research Topics

See more →

Frontiers

Avenue du Tribunal-Fédéral 34
1005 Lausanne, Switzerland
frontiersin.org

Contact us

+41 (0)21 510 17 00
frontiersin.org/about/contact